



University
of Glasgow

Vudhironarit, Thishnapha (2019) *Evaluation of gene-therapy as an alternative to pharmacological based approaches in mouse models of Rett syndrome*. PhD thesis.

<http://theses.gla.ac.uk/76745/>

Copyright and moral rights for this work are retained by the author

A copy can be downloaded for personal non-commercial research or study, without prior permission or charge

This work cannot be reproduced or quoted extensively from without first obtaining permission in writing from the author

The content must not be changed in any way or sold commercially in any format or medium without the formal permission of the author

When referring to this work, full bibliographic details including the author, title, awarding institution and date of the thesis must be given

Enlighten: Theses

<https://theses.gla.ac.uk/>
research-enlighten@glasgow.ac.uk

Evaluation of gene-therapy as an alternative to pharmacological based approaches in mouse models of Rett syndrome

Thishnapha Vudhironarit

BSc (Medical technology), MSc (Pharmacology)

Thesis submitted in fulfilment of the requirements for the degree of Doctor of Philosophy

Institute of Neuroscience and Psychology
College of Medical, Veterinary and Life Science
University of Glasgow
Glasgow, G12 8QQ
UK

November 2019

© Thishnapha Vudhironarit 2019

Abstract

Rett syndrome (RTT) is a neurological disorder characterized by severe impairment of motor and cognitive functions, caused in >95 % of patients by *de novo* mutations in the X-linked gene, methyl-CpG-binding protein 2 (*MECP2*) gene. The protein product of this gene, MeCP2, is widely expressed but especially abundant in postmitotic neurons of the central nervous system (CNS). However, there remains a fundamental lack of knowledge about the downstream pathways involved in gene function. Both *Mecp2* knock-out and knock-in mutant mice present many of the overt neurological features seen in RTT patients. Both provide a very useful model for testing potential therapeutic applications. The current lack of effective therapies together with the monogenicity of the disorder and established reversibility of the phenotype in mice suggest that replacement of the *MECP2* gene is a potential therapeutic option worthy of exploration, mainly using viral based delivery of *MECP2*-based gene constructs. Significant challenges remain, both in the efficiency of delivery of gene constructs to target cells and controlling construct-derived toxicity.

In this study, I have explored the potential for augmentation gene therapy in RTT mice. First, I determine the best RTT mouse model and modify behavioral tests for RTT mice in preparation for the experiment testing therapeutic agents. Second, I assessed escalating doses of viral vector containing human *MECP2_e1* isoform coding sequences cloned into an AAV2 vector backbone with AAV9 capsid (scAAV9) under control of the murine *Mecp2* endogenous core promoter (MeP229), a first generation vector, to ascertain the dose that has greater efficacy and lower toxicity after delivery to young adult *Mecp2* knockout male mice. Third, I assess the safety and effectiveness of a new AAV vector construct design aiming to reduce the toxicity observed with the first-generation vector. This was carried out by direct brain injection in male neonates proving the efficacy of this vector.

In the mouse behavioural studies, symptomatic hemizygous male and heterozygous female mice were used for assessment the two mouse models. The results demonstrated that in males, the *Mecp2* knockout mouse model differed

significantly from their wild-type cage mates in terms of survival, body weight and a range of behavioural tests, while the T158M *Mecp2* knock-in model presents with a somewhat milder phenotype. In contrast, in females, the knockout and knock-in heterozygotes show the same severity of the RTT-like phenotype in the behavioural tests. A notable finding was that in the RTT mouse models motor ability is improved by the addition of their own bedding into the testing arena (distance moved in open field arena with bedding increased around 60% in male knockout mice). Locomotor activity assessment in openfield test demonstrated that male knockout mice have significantly lower locomotor ability than the knock-in and WT, both in males and females, whereas the treadmill motor challenge test rotarod test demonstrated significantly different results in each group. In the novel object recognition test, a test of memory, the RTT mouse model showed differences from WT, while there was some learning capability shown on rotarod motor learning skills. The social interaction test in a reduced-size three chamber arena demonstrated that the RTT mouse did not engage in any interaction with a stranger mouse. Both anxiety tests administered, a light-dark test and a splash test, demonstrated that the RTT mouse models do not present with anxiety. The breathing test for apnoeas using the whole-body plethysmography apparatus demonstrated a significantly different level of breathing abnormality in knockout and knock-in mice.

In the second phase of experiments, I showed that AAV-mediated delivery of *MECP2* to *Mecp2* null mice by systemic administration, and utilizing a minimal endogenous promoter, was associated with a narrow therapeutic window and resulted in liver toxicity at higher doses. Lower doses of this vector significantly extended the survival of mice lacking MeCP2 or expressing a mutant T158M allele but had no impact on RTT-like neurological phenotypes. Modifying vector design by incorporating an extended *Mecp2* promoter and additional regulatory 3'-UTR elements significantly reduced hepatic toxicity after systemic administration. Moreover, direct cerebroventricular injection of this vector into neonatal *Mecp2*-null mice resulted in high brain transduction efficiency, increased survival and body weight, and an amelioration of RTT-like phenotypes. My results show that controlling levels of MeCP2 expression in the liver is achievable through modification of the expression cassette. However, it also

highlights the importance of achieving high brain transduction to impact the RTT-like phenotypes.

In summary, I have shown that the male *Mecp2* knockout model is appropriate for use in screening studies for the treatment of RTT, while the female T158M *Mecp2* knock-in model is suitable for long-term studies. I demonstrated that tests involving motor function in RTT mouse models should add the mouse's own bedding into the arena to increase spontaneous mobility. An applicable test for mobility and motor defects is the rotarod test, and for learning, social interaction, and anxiety is the novel object recognition test using a resized three-chamber arena and splash test, respectively.

I showed that the first-generation vector at an intermediate dose (10^{12} vg/mouse) presents some therapeutic benefits in terms of extending survival and improving bodyweight, however it also causes liver toxicity. I discovered that newer cassette design vectors scAAV9/JeT/MECP2, scAAV9/sPA (sPA), and scAAV9.47/MECP2 (9.47) are no better in terms of efficiency and toxicity than the first-generation vector. I have demonstrated the successful application of a second-generation vector to deliver exogenous *MECP2* to RTT mouse models with the same efficacy as with the first-generation vector, but with reduced liver pathology. I have also shown that without the physical barrier to the delivery of the viral vector to brain, the second-generation vector is likely to be useful for RTT therapy as it shows limited spread of the virus outside the brain and was able to significantly decrease the aggregate RTT-like severity score.

Table of Contents

Abstract	2
List of Tables	10
List of Figures	11
Acknowledgement.....	16
Author's Declaration	17
Publications.....	18
Abbreviations	19
Chapter 1 Introduction	22
1.1 General introduction.....	22
1.2 Clinical manifestations of RTT	23
1.3 Genetic basis of RTT	24
1.3.1 Rett Syndrome and <i>MECP2</i>	24
1.3.2 <i>MECP2</i> structure	25
1.3.3 MeCP2 Functions	27
1.4 Animal models of Rett syndrome	29
1.5 Behavioural tests in the mouse model	30
1.6 Reversibility of the RTT phenotype and treatment strategies.....	32
1.6.1 Treatment strategies for RTT.....	32
1.6.2 Gene therapy approaches	32
1.7 Adeno-associated virus (AAV) as a potential gene therapy vector	35
1.7.1 AAV-based vectors and mammalian cell transduction	35
1.7.2 Self-complementary AAV	36
1.7.3 AAV capsid.....	38
1.7.4 Clinical application and potential in RTT	39
1.8 Design of gene therapy approaches	40
1.8.1 choice of regulatory elements & vector	40
1.8.2 Optimal time for gene therapy interventions	42
1.8.3 Local or global <i>MECP2</i> delivery.....	43

1.8.3 To target specific types of cells in the brain: astrocytes or neurons?	46
1.8.4 Other gene-targeted strategies in RTT	47
1.9 Summary and aim	50
Chapter 2 Material and Methods	52
2.1 General molecular biology materials	52
2.2 General solutions	54
2.3 Mouse models of RTT	55
2.3.1 source of the <i>Mecp2</i> -KO mouse and <i>Mecp2</i> T158M knock-in models	56
2.3.2 Breeding strategy of <i>Mecp2</i> -KO and <i>Mecp2</i> T158M knock-in mice	56
2.3.3 Ethic and husbandry	57
2.3.4 Genotyping	57
2.3.3.1 DNA extraction and PCR genotyping	57
2.3.3.2 Agarose gel electrophoresis	59
2.3.5 Allocating animals to experimental groups and blinding system	59
2.3.6 Phenotypic severity scoring and weight measurement	60
2.4 Behavioural tests	60
2.4.1 Open field test	63
2.4.2 Novel object recognition test	63
2.4.3 Rotarod performance test	64
2.4.4 Treadmill motor challenge test (Exercise tolerance)	65
2.4.5 Social interaction test	65
2.4.6 Light/Dark box test	66
2.4.7 Splash test	67
2.4.8 Breathing test (Whole body plethysmograph)	68
2.5 Adeno-associated viral vectors and Vector administration	69
2.5.1 Vector preparation	69
2.5.2 Vector injection	70

2.5.2.1 Tail vein injection	70
2.5.2.2 Cerebroventricular injection into neonatal mice	70
2.6 Immunohistochemistry (IHC).....	71
2.7 Image analysis	72
2.8 Statistical analysis	73
Chapter 3 Validation of behavioural tests in RTT mouse models.....	74
3.1 Introduction	74
3.2 Study aims.....	75
3.3 Method	76
3.4 Results	81
3.4.1 RTT model genotyping by PCR.....	81
3.4.2 Phenotype severity assessment in KO and KI mice	82
3.4.2.1 Male	82
3.4.2.2 Female	84
3.4.3 Establishment and validation of detailed behavioural tests in the male RTT mouse models	85
3.4.3.1 Open field test.....	85
3.4.3.2 Novel object recognition test.....	87
3.4.3.3 Rotarod test	88
3.4.3.4 Motor learning.....	89
3.4.3.5 Treadmill motor challenge test	90
3.4.3.6 Social interaction test	91
3.4.3.7 Light-dark box test	92
3.4.3.8 Splash test	93
3.4.3.9 Breathing test	94
3.4.4 Establishment and validation of detailed behavioural tests in female RTT mouse models	95
3.4.4.1 Open field test	95

3.4.4.2 Novel object recognition test.....	96
3.4.4.3 Rotarod test	97
3.4.4.4 Motor learning.....	98
3.4.4.5 Treadmill motor challenge test	99
3.4.4.6 Social interaction test	100
3.4.4.7 Light-dark box test	101
3.4.4.8 Splash test	102
3.4.4.9 Breathing test	103
3.5 Discussion.....	104
Chapter 4 Assessment of safety and efficacy of vector-derived <i>MeCP2</i> on the progression of the RTT-like phenotype in a dose escalation study.....	111
4.1 Introduction	111
4.2 Aims	112
4.3 Methods.....	112
4.4 Results	113
4.4.1 1 st generation vector safety and efficacy at different doses by IV delivery in the <i>Mecp2</i> KO mouse model of RTT	113
4.4.2 1 st generation vector transduction efficiency and level of vector-derived MeCP2 in the brain in <i>Mecp2</i> KO mice	117
4.4.3 1 st generation vector transduction efficiency and level of vector-derived MeCP2 in the liver in <i>Mecp2</i> KO mice.....	119
4.4.4 Effect of IV delivery of 1 st generation vector on survival, bodyweight and phenotype severity score in <i>Mecp2</i> ^{T158M/y} mice	124
4.4.5 The expression of 1 st generation vector in <i>Mecp2</i> ^{T158M/y} brain	126
4.5 Discussion.....	126
Chapter 5 Development of a novel MECP2 expression cassette with enhanced safety features.....	129
5.1 Introduction	129
5.2 Study aims.....	130

5.3 Methods.....	130
5.4 Results	132
5.4.1 The efficacy and safety of SpA, JeT and 9.47 vectors in the KO mouse model, dosing at 10^{12} vg/mouse by IV injection.....	132
5.4.2 Development of a Second-Generation Vector that Reduced Liver Toxicity after Systemic Administration.....	136
5.4.3 Neonatal Cerebroventricular Injection of the Second-Generation Vector Improved the RTT-like Aggregate Severity Score	141
5.4 Discussion.....	144
Chapter 6 General discussion	148
6.1 Major findings.....	148
6.1.1 Phenotypic characteristics and behavioural test results in the RTT mouse models.	150
6.1.2 Dose escalation with AAV/MECP2 revealed a narrow therapeutic window following systemic administration and resulted in liver toxicity ...	151
6.1.3 Development of a second-generation vector that reduced liver toxicity after systemic administration and the efficiency of the second-generation vector improved the RTT-like aggregate severity score via neonatal cerebroventricular injection.....	153
6.2 Technical considerations.....	153
6.3 Significance of this study.....	155
6.4 Future studies.....	157
6.5 Summary.....	160
References.....	162

List of Tables

Table 1-1. Summary of behavioural tests of published studies in RTT mouse models.....	31
Table 1-2. Summary of experimental design and outcomes of published studies of gene therapy interventions in Rett syndrome mouse models.....	41
Table 2-1 General molecular biology reagents.....	52
Table 2-2 Primer sequences and sizes of amplified PCR products for <i>Mecp2</i> ^{+/-} and <i>Mecp2</i> ^{+/^{T158M}} genotyping.....	52
Table 2-3 List of AAV vectors.....	53
Table 2.4 - General molecular biology solutions.....	54
Table 2-5 Breeding scheme for <i>Mecp2</i> -KO and <i>Mecp2</i> T158M knock-in mice	56
Table 2-6 Setting of PCR reaction for genotyping of <i>Mecp2</i> -null mice, <i>Mecp2</i> T158M mice and their WT littermates.....	58
Table 2-7 The conditions of thermocycling for genotyping	58
Table 2-8 phenotyping score.....	61
Table 3-1 Order of behavioural experiments performed for each mouse in behavioural tests in male RTT mouse models.....	77
Table 3-2 Order of behavioural experiments performed for each mouse in behavioural tests in female RTT mouse models.....	80

List of Figures

Figure 1.1 Clinical manifestations of Rett syndrome Representative diagram showing the characteristic RTT clinical presentation.....	24
Figure 1.2 Composition and splicing pattern of <i>MECP2</i> gene.....	26
Figure 1.3 MeCP2 protein structure.....	28
Figure 1.4 Therapeutic targets and potential pharmacological strategies currently being explored in animal models for the treatment of Rett syndrome.....	33
Figure 1.5 Summary of current challenges for RTT gene therapy.....	34
Figure 1.6 AAV-based vector transduction.....	37
Figure 2.1 the open field arena which is recorded by IR camera	63
Figure 2.2 Novel object test phase and recognition training.....	64
Figure 2.3 Setting up of Arena for social interaction test.....	66
Figure 2.4 Two-compartment arena used in the light-dark box test.....	67
Figure 2.5 This experiment is a test of mouse stress by observing the grooming behaviour in its home cage	68
Figure 2.6 Images of the whole-body plethysmograph used for assessment of the breathing phenotype.....	69
Figure 2.7 Cerebroventricular injection in neonatal mice	71
Figure 3.1 Results of PCR genotyping of wild-type, hemizygous and heterozygous mice from both lines; <i>Mecp2</i> KO and <i>Mecp2</i> ^{T158M}	81
Figure 3.2 Composite body weight measurements and severity score in wild-type, <i>Mecp2</i> ^{-/y} and <i>Mecp2</i> ^{T158M/y} mice.....	83
Figure 3.3 Composite body weight measurements and severity score in wild-type, <i>Mecp2</i> ^{+/-} and <i>Mecp2</i> ^{+/T158M} female mice (6-8 months old).....	84
Figure 3.4 The comparison of locomotor assessment in wild-type and <i>Mecp2</i> ^{-/y} male mice in open field arena with and without bedding.....	86

Figure 3.5 The general locomotor assessment in WT, <i>Mecp2</i> ^{-/y} and <i>Mecp2</i> ^{T158M/y} male mice.....	86
Figure 3.6 Discrimination index for learning and cognition baseline in novel object recognition test in WT, <i>Mecp2</i> ^{-/y} and <i>Mecp2</i> ^{T158M/y} male mice in 15 minutes.....	87
Figure 3.7 Rotarod performance of WT, <i>Mecp2</i> ^{-/y} and <i>Mecp2</i> ^{T158M/y} male mice using rotarod machine.....	88
Figure 3.8 Motor learning curve of WT, <i>Mecp2</i> ^{-/y} and <i>Mecp2</i> ^{T158M/y} male mice using rotarod machine over 3 days.....	89
Figure 3.9 Treadmill motor test of WT, <i>Mecp2</i> ^{-/y} and <i>Mecp2</i> ^{T158M/y} male mice...	90
Figure 3.10 Social interaction test in WT, <i>Mecp2</i> ^{-/y} and <i>Mecp2</i> ^{T158M/y} male mice.....	91
Figure 3.11 Exploration and anxiety-related measures of the light-dark test in WT, <i>Mecp2</i> ^{-/y} and <i>Mecp2</i> ^{T158M/y} in male mice.....	92
Figure 3.12 Anxiety assessment of wild-type, <i>Mecp2</i> ^{-/y} and <i>Mecp2</i> ^{T158M/y} male mice by splash test.....	93
Figure 3.13 Persistent breathing phenotype in WT, <i>Mecp2</i> ^{-/y} , <i>Mecp2</i> ^{T158M/y} male mice.....	94
Figure 3.14 The general locomotor assessment in WT, <i>Mecp2</i> ^{+/-} , <i>Mecp2</i> ^{+/T158M} female mice.....	95
Figure 3.15 Discrimination index of learning and cognition baseline in novel object recognition test in WT, <i>Mecp2</i> ^{+/-} , <i>Mecp2</i> ^{+/T158M} female mice in 15 minutes.....	96
Figure 3.16 Motor deficit test of WT, <i>Mecp2</i> ^{+/-} , <i>Mecp2</i> ^{+/T158M} female mice using rotarod machine.....	97
Figure 3.17 Motor learning curve of WT, <i>Mecp2</i> ^{+/-} , <i>Mecp2</i> ^{+/T158M} female mice using rotarod machine over 3 days.....	98
Figure 3.18 Motor function and locomotion assessment in WT, <i>Mecp2</i> ^{+/-} , <i>Mecp2</i> ^{+/T158M} female mice.....	99

Figure 3.19 Social interaction test in WT, <i>Mecp2</i> ^{+/-} , <i>Mecp2</i> ^{+/T158M} female mice.....	100
Figure 3.20 Exploration and anxiety related measures of the light-dark test in WT, <i>Mecp2</i> ^{+/-} , <i>Mecp2</i> ^{+/T158M} female mice.....	101
Figure 3.21 Anxiety assessment of WT, <i>Mecp2</i> ^{+/-} , <i>Mecp2</i> ^{+/T158M} female mice by splash test.....	102
Figure 3.22 Persistent breathing phenotype in WT, <i>Mecp2</i> ^{+/-} , <i>Mecp2</i> ^{+/T158M} female mice.....	103
Figure 4.1 <i>MECP2_e1</i> /Myc fusion constructs were cloned into AAV2 backbones under a MeP promoter.....	113
Figure 4.2 Survival plot of <i>Mecp2</i> KO mice treated with 3 different doses of scAAV9/MeP/ <i>MECP2</i>	114
Figure 4.3 Graph showing the average body weight of wild-type and <i>Mecp2</i> ^{-/y} treated with vehicle and <i>Mecp2</i> ^{-/y} treated with 10 ¹² vg/mouse dose.....	115
Figure 4.4 RTT-like severity score of wild-type and <i>Mecp2</i> ^{-/y} treated with vehicle and <i>Mecp2</i> ^{-/y} treated with 10 ¹² vg/mouse dose.....	116
Figure 4.5 Flattened confocal stack images of the CA1 region of the hippocampus taken from <i>Mecp2</i> ^{-/y} mice treated intravenously with different doses of the 1 st generation vector.....	117
Figure 4.6 Dose-dependent transduction efficiency (Mycpositive nuclei as a proportion of DAPI-positive nuclei) across different brain regions.....	118
Figure 4.7 Intravenous injection of AAV9/h <i>MECP2</i> into wild-type mice resulted in toxicity at the high dose.....	119
Figure 4.8 Vector biodistribution analysis of mice injected intravenously with 10 ¹² vg/mouse showing high transduction efficiency in the liver and heart and low transduction efficiency in the CNS.....	120
Figure 4.9 Intravenous injection of 1 st generation vector resulted in high level of vector-derived MeCP2 expression in the liver.....	121
Figure 4.10 Toxicity issues revealed after systemic administration of high vector dosage.....	122

Figure 4.11 Diagram Showing AAV vector constructs.....	123
Figure 4.12 Comparison of liver toxicity between 1 st generation <i>Mecp2</i> vector treatment and the GFP vector treatment in <i>Mecp2</i> KO mice injected with 10 ¹³ vg/mouse.....	123
Figure 4.13 The comparison between WT, KO and treated <i>Mecp2</i> ^{T158M/y} cohort in different parameter.....	124
Figure 4.14 Survival plot, bodyweight measurements and bodyweight measurements of WT and <i>Mecp2</i> ^{T158M/y} KI mice treated vehicle and <i>Mecp2</i> ^{T158M/y} KI mice treated with the moderate dose of 1 st generation vector.....	125
Figure 4.15 Transduction efficiency in the brain of treated mice.....	126
Figure 5.1 Diagram showing AAV vector constructs of vectors.....	131
Figure 5.2 Survival of <i>Mecp2</i> KO mice treated with SpA containing vector, vector utilising JeT, and vector utilising AAV9.47 capsid.....	132
Figure 5.3 Body weight measurement of <i>Mecp2</i> KO mice treated with SpA containing vector, vector utilising JeT, and vector utilising AAV9.47 capsid.....	133
Figure 5.4 of Rett-like phenotype severity score of <i>Mecp2</i> KO mice treated with spA containing vector, vector utilising JeT, and vector utilising AAV9.47 capsid.....	134
Figure 5.5 summary of Novel vector design features and efficacy.....	135
Figure 5.6 Comparison of liver toxicity between 1 st generation vector treatment and the novel vectors treatment (10 ¹² vg/mouse; for 30 days) in WT mice aged 35 days).....	135
Figure 5.7 Design of the 2 nd generation vector construct.....	137
Figure 5.8 Therapeutic Efficacy of Second-Generation Vector after Systemic Delivery to <i>Mecp2</i> ^{-y} Mice.....	138
Figure 5.9 Expression of vector-derived MeCP2 in the livers of mice treated with second-generation vector compared with first-generation vector.....	139

Figure 5.10 Comparison of liver toxicity between 1 st generation vector treatment and the novel vectors treatment (10^{12} vg/mouse; for 30 days) in WT mice aged 35 days).....	140
Figure 5.11 Survival plot, bodyweight measurements and bodyweight measurements of <i>Mecp2</i> ^{-y} and WT neonatal mice treated with the 426-vector 1×10^{11} vg/ mouse and <i>Mecp2</i> ^{-y} and WT mice treated with vehicle by direct brain injection.....	142
Figure 5.12 Direct Brain Delivery of Second-Generation Vector to Neonatal <i>Mecp2</i> ^{-y} Mice Revealed Therapeutic Efficacy.....	143
Figure 5.13 Distribution analysis of 2 nd generation vector delivered MeCP2 in mouse brain by direct brain injection method.....	144
Figure 6.1 Mechanism of action of CRISPR/Cas system.....	160

Acknowledgements

The completion of this thesis was made possible by the financial support of a PhD scholarship awarded by, Ministry of Science and Technology, Thailand. I would like to thank them for this support throughout the PhD program.

I am eternally grateful to a number of people for their help and support throughout my studies. In particular to my supervisors Dr Stuart Cobb and Dr Mark Bailey for giving me this great opportunity to undertake a fascinating and challenging project, and for their continuous guidance, advice and constructive criticism.

I would like to thank my assessors Dr Deborah Dewar and Dr Leanne McKay for their advice and suggestions during the course of my PhD.

It is a pleasure to thank those whose contributions made this thesis possible especially Dr Kamal Gadalla, Dr Lieve Desbonnet and Dr Alex Surget.

I am grateful also to Dr Steven Gray, Prof Brian Morris and Dr John Riddell for their technical assistance and fruitful collaboration.

I have been fortunate to work with some fantastic people over the past few years. Special thanks go to Dr Bushra Kamal, Dr Paul Ross, Dr Rebecca Openshaw, Dr Daniela Minchella, Dr Elaine Hunter, Dr Noha Bahey, Dr Ralph Hector and John Craig for their kind help and support during my PhD.

I owe my deepest gratitude to the University of Glasgow Senate and Disability service especially Ms Shona Robertson, Ms Fiona Gray and Ms Lesley-Anne Morrison who provided a great deal of support during a difficult time when I had a severe eye problem through the last year of my PhD.

Finally, I would like to thank my family who gave me mental support, especially my beloved grandma and John.

Author's Declaration

I declare that, except where explicit reference is made to the contribution of others, this thesis is the result of my own work and has not been submitted for any other degree at the University of Glasgow or any other institution.

Signature:

Thishnapha Vudhironarit 2019

Publications

Some of the work contained in this thesis has been published in part:

Manuscripts

Gadalla, K. K. E., T. Vudhironarit, R. D. Hector, S. Sinnett, N. G. Bahey, M. E. S. Bailey, S. J. Gray, and S. R. Cobb, 2017, Development of a Novel AAV Gene Therapy Cassette with Improved Safety Features and Efficacy in a Mouse Model of Rett Syndrome: *Mol Ther Methods Clin Dev*, v. 5, p. 180-190.

Oral presentation

“AAV-mediated MECP2 Gene Delivery in Mouse Models of Rett Syndrome.” at “The 13th Asia Pacific Federation of Pharmacologist (APFP) Meeting” on February 2016

Abbreviations

AAV	Adeno-associated virus
ANOVA	Analysis of variance
BBB	Blood brain barrier
Bp	Base pair
Cas	CRISPR-associated
CNS	Central nervous system
CMV	Cytomegalovirus promoter
CpG	Cytosine-guanine dinucleotide
CO ₂	Carbon dioxide
CRISPR	clustered regularly interspaced short palindromic repeats
CTD	C-terminal domain
DAPI	4',6-diamidino-2-phenylindole
DNA	Deoxyribonucleic acid
FO	Familiar object
GFAP	Glial fibrillary acidic protein
GFP	Green fluorescent protein
HEMI	Hemizygous
HET	Heterozygous
Hp1	Heterochromatin protein 1
IC	Intracranial
ICM	intra-cisterna magna
IV	Intravenous
IU	Infection unit
IT	intratracheal injection
ITR	Inverted terminal repeat
JET	scAAV9/JeT/MECP2 or Jet promoter vector
KI	Knock in
KO	Knockout
LTP	Long term potentiation
LTR	Long terminal repeat
MAP2	Microtubule associated protein
MBD	Methyl-CpG-binding domain

<i>MECP2</i>	Human Methyl-CpG-binding protein 2 gene
<i>Mecp2</i>	Mouse Methyl-CpG-binding protein 2 gene
MeCP2	Human Methyl-CpG-binding protein 2 protein
<i>Mecp2</i>	Mouse Methyl-CpG-binding protein 2 protein
<i>MECP2_e1</i>	Methyl-CpG-binding protein 2 isoform e1
<i>MECP2_e2</i>	Methyl-CpG-binding protein 2 isoform e2
ME1	<i>Mecp2_e1</i>
MeP <i>Mecp2</i>	endogenous core promoter
N	Number
MiR	microRNA
NeuN	Neuron nuclear antigen rbfox3
NHEJ	Non-homologous end joining
NLS	Nuclear localisation signal
NO	Novel object
NOR	Novel object recognition test
NTD	N-terminal domain
ORF	open reading frames
PB	Phosphate buffer
PBS	Phosphate buffer saline
PCR	Polymerase chain reaction
PEI	Polyethylenimine
PSC	Premature stop codon
RE	Regulatory elements
RefSeq	Reference Sequence
Rep	Replication
scAAV	self-complementary Adeno-associated virus
SD	Standard deviation
SEM	Standard error of mean
SMA	Spinal muscular atrophy
SpA	scAAV9/sPA or short polyA vector
ssAAV	Single-stranded Adeno-associated virus
Syn1	Synapsin1 promoter
TFIIB	Transcription factor IIB
RNA	Ribonucleic acid

rpm	revolutions per minute
RTT	Rett syndrome
TRD	Transcription repression domain
vg	vector genome
WT	Wild-type
YB1	Y box binding protein

Chapter 1 Introduction

1.1 General introduction

RTT (Rett syndrome) is a paediatric neurological disorder with postnatal onset. RTT is the leading cause of severe mental retardation in females after Down Syndrome. It was first described by Andreas Rett (Rett, 1966). After this, it was re-described in 1983 by Bengt Hagberg (Hagberg et al., 1983). In 1999, it was shown that RTT was caused primarily by mutations in an X-linked gene, *MECP2* (Amir et al., 1999). After this, *Mecp2* knockout mouse models were developed by a number of groups (Chen et al., 2001) and there have been many attempts made to apply therapeutic interventions to prevent or delay the onset of the RTT-like phenotype or reverse the signs after onset. The initial successes reported have demonstrated the tractability of the problem of ameliorating several aspects of the phenotype and have highlighted the potential to treat RTT patients by addressing the pathogenetic pathway's early stages and going beyond mere amelioration of downstream consequences.

In this thesis, *Mecp2* knockout mice have been used in evaluating a therapeutic approach based on viral vector-mediated delivery of a wild-type copy of *MECP2* to cells that lack this protein. Delivery of exogenous *MECP2* to the brain is a challenging approach not only due to the obstacles inherent in delivering substances to the CNS, but also due to the impediments to transducing large numbers of cells and in maintenance of exogenous levels of MeCP2 within the limits of physiology to prevent toxicity relating to overexpression. The evaluation of outcomes pertaining to these experiments should provide information about drawbacks, benefits, challenges and prospects of application of gene therapy in the treatment of Rett syndrome.

1.2 Clinical manifestations of RTT

RTT (OMIM 312750) has traditionally been considered a neurodevelopmental disorder and is a primary cause of severe mental retardation in girls, with an incidence of around 1 in 10,000 female births (Neul et al., 2010).

The characteristics of RTT include the fact that it occurs exclusively in females and a constellation of clinical features (Neul et al., 2010). The features that distinguish RTT from autism spectrum disorders, which RTT has often been co-classified with, include apparent normal growth in the initial 6-18-month period. However, reduced head circumference and birth weight are also observed (Leonard and Bower, 1998), after which there ensues a period of developmental regression, with the patients displaying deficits in social interaction (features being similar to autism, figure 1-1), impaired speech and mobility, loss of hand skills and development of stereotypical movements of the hands (repetitive and continuous twisting, wringing, clapping hand automatism when awake). This phase of regression is followed by a stationary or recovery phase lasting for years, with some patients regaining the lost skills partially. Nonetheless, a phase of late motor deterioration generally takes place thereafter with features of motor disabilities of a severe nature (Hagberg, 2002).

One of the common characteristics of RTT is epilepsy. Onset occurs primarily during the stationary phase (Hagberg, 2002). However, after the age of 20 years, there is usually a decrease in severity. Other characteristics include abnormalities which are musculoskeletal in nature in the form of scoliosis, which often has onset during school ages, subtle distal deformity of bones of the lower limbs is also observed in many patients (Hagberg, 2002). There is a high frequency of autistic like features during regression in RTT and this includes unresponsiveness to social prompts, indifference to the surrounding environment, hypersensitivity to sound and expressionless facial features (Chahrour and Zoghbi, 2007).

RTT's autonomic features include frequent apnoea when awake, breath holding, and episodic hyperventilation. Among RTT patients, intestinal distention and constipation, gastro-oesophageal reflux, and swallowing dysfunction are

observed as well (Hagberg, 2002). Most features mentioned above result directly from the primary CNS deficits; however, several can also be influenced by peripheral effects.

The severity and the clinical presentation of RTT vary widely. Certain features must be present in patients for the diagnosis of typical RTT, or there may be differences enabling their assignment to one of a range of atypical RTT diagnoses (Neul et al., 2010).

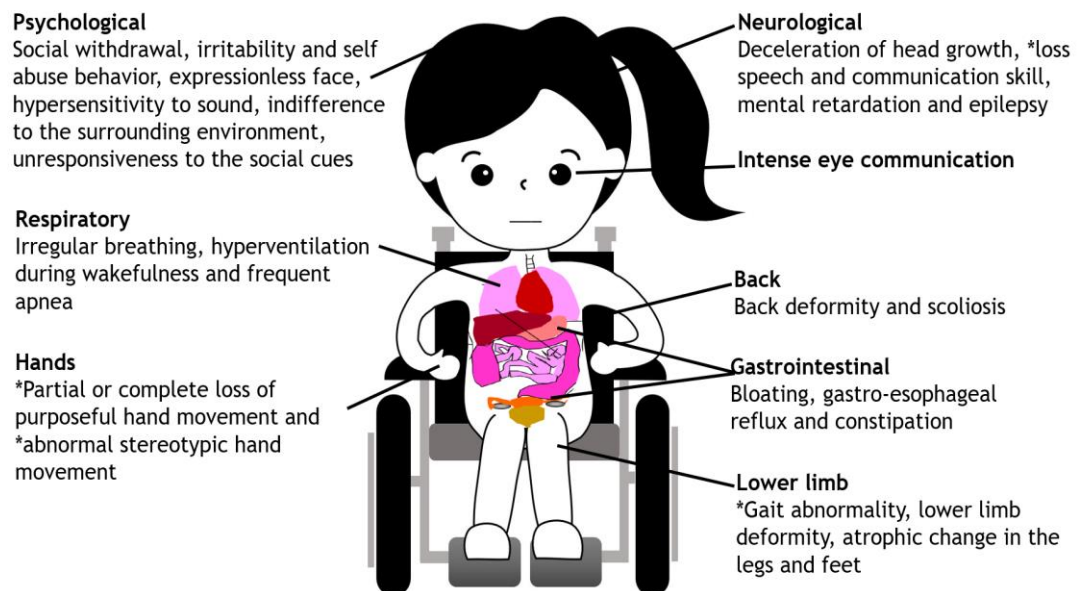


Figure 1.1 Clinical manifestations of Rett syndrome Representative diagram showing the characteristic RTT clinical presentation.* indicates main criteria essential for typical RTT diagnosis.

1.3 Genetic basis of RTT

1.3.1 Rett Syndrome and *MECP2*

Cases of RTT are generally a result of dominantly-acting *de novo* mutations (Chen et al., 2001) in *MECP2*, which encodes a protein product known as MeCP2. There have been reports of over 600 pathogenic *MECP2* mutations (RettBase: <http://mecp2.chw.edu.au/>), including frameshift, nonsense and missense mutations, as well as large deletions. Pathogenic mutations in *MECP2* mostly cause RTT in heterozygous females, although *MECP2* mutations have an

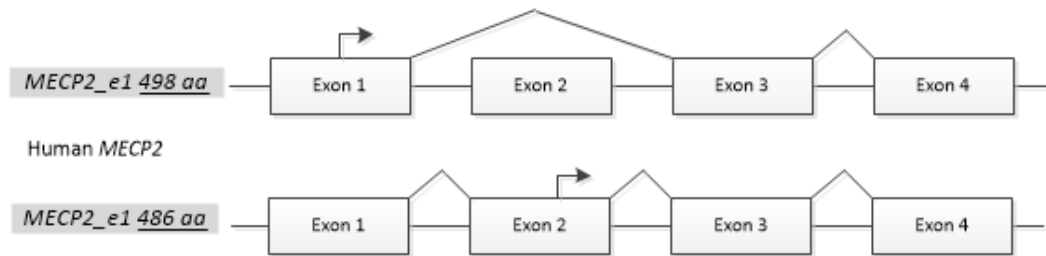
association with other phenotypic outcomes (Bienvenu and Chelly, 2006), including milder forms of learning disability and, in rare cases, autism (Moretti et al., 2006). Boys who inherit a mutant *MECP2* allele that would cause typical RTT in a heterozygous female are more severely affected, presenting with infantile encephalopathy and generally not surviving infancy. The differences existing between the female and the male phenotypes exists as a result of the cell proportions in the nervous system that express the mutant allele. All cells expressing MeCP2 will express the mutant allele only in hemizygous males. However, in the brains of the females, because of X chromosome inactivation (XCI), there is development of a mosaic cellular network at the level of expression with some cells expressing the normal allele and others expressing the mutant allele. This way, the pathology that is associated with the mutant allele has undergone dilution (at the level of the network) in the brains of the females, at least for the actions that pertain to mutations' direct cell-autonomous effects.

1.3.2 *MECP2* structure

MeCP2 is a nuclear protein predominantly and was first discovered through its affinity for DNA sequences that contain methylated 5'-CpG-3' dinucleotides. It belongs to the MBD (methylated DNA binding domain) protein family, several of whose members can act as repressors of transcription (Klose and Bird, 2006). The *MECP2* gene is located within chromosome Xq28, is approx. 68kbp in length and comprises four exons (Dragich et al., 2000). There are two encoded proteins translated from two major transcripts. The two main transcript splice isoforms are *MECP2_e1* and *MECP2_e2*, encoding proteins of 498 and 486 amino acids, respectively, which differ only at the N-terminus (Figure 1.2) (Mnatzakanian et al., 2004). *MECP2_e2* uses a translational start site within exon 2 whereas *MECP2_e1* does not include exon 2 (figure 1.2A). Both isoforms are considered to have two primary functional domains (figure 1-3), an Me-CpG binding domain (MBD; 85 amino acids) and a transcriptional repressor domain (TRD; 104 amino acids in length). The coding sequence for the MBD is split between exons 3 and 4, while the TRD, amino acids 207 to 310, is encoded by exon 4 (Nan et al., 1997). Exon 4 also encodes the 3' UTR which in the human gene is up to 8.5 kb

long, depending on which of two major polyadenylation signals are used. MeCP2 is expressed widely throughout the body, including in postnatal neurons, where there is specifically high expression (LaSalle et al., 2001). MeCP2 is quite strongly conserved in mammals - MeCP2_e2 shows 95% identity at the amino acid level between human and mouse, while there is 100 per cent identity between these species across the MBD (Nan et al., 1996).

A)



B)

```

MECP2_e1      MAAAAAAPSGGGGGEEERLEEKSEDLQGLKDKP LKFKKVKKDKKEEKEGKHEPVQP 60
MECP2_e2      MVAGMLGLREEKSEDLQGLKDKP LKFKKVKKDKKEEKEGKHEPVQP 48
                *****

MECP2_e1      SAHHSAPAEAGKAET SEGSGSAPAVPEASASPQRRSI I RDRGPMYDDPT LPEGWTRKL 120
MECP2_e2      SAHHSAPAEAGKAET SEGSGSAPAVPEASASPQRRSI I RDRGPMYDDPT LPEGWTRKL 108
                *****

MECP2_e1      KQRKSGRSAGKYDVYLLINPQGKAFRSKVELIAYFEKVGDTSLDPNDFDFTVTGRGSPSRR 180
MECP2_e2      KQRKSGRSAGKYDVYLLINPQGKAFRSKVELIAYFEKVGDTSLDPNDFDFTVTGRGSPSRR 168
                *****

MECP2_e1      EQKPPKKPKSPKAPGTGRGRGRPKSGTTRPKAATSEGVQKRVLEKSPGKLLVKMPFQT 240
MECP2_e2      EQKPPKKPKSPKAPGTGRGRGRPKSGTTRPKAATSEGVQKRVLEKSPGKLLVKMPFQT 228
                *****

MECP2_e1      SPGGKAEGGGATTSTQVMVIRKPRGRKRKAEADPQAIPKKRGRKPGSVVAAAAAEAKKAV 300
MECP2_e2      SPGGKAEGGGATTSTQVMVIRKPRGRKRKAEADPQAIPKKRGRKPGSVVAAAAAEAKKAV 288
                *****

MECP2_e1      KESSIRSVQETVLPICKRKTRETVSIEVKEVVKPLLSTLGEKSGKGLKTKCKSPGRKSKE 360
MECP2_e2      KESSIRSVQETVLPICKRKTRETVSIEVKEVVKPLLSTLGEKSGKGLKTKCKSPGRKSKE 348
                *****

MECP2_e1      SSPKGRSSASPPPKKEHHHHHHHSESPKAPVPLLPPLP PPPPEPESSEDPTSPPEPQDL 420
MECP2_e2      SSPKGRSSASPPPKKEHHHHHHHSESPKAPVPLLPPLP PPPPEPESSEDPTSPPEPQDL 408
                *****

MECP2_e1      SSSVCKEEKMPRGGLES DGCPKEPAKTQPAVATAATAAEKYKHRGEGGERKDIVSSSMR 480
MECP2_e2      SSSVCKEEKMPRGGLES DGCPKEPAKTQPAVATAATAAEKYKHRGEGGERKDIVSSSMR 468
                *****

MECP2_e1      PNREEPVDSRTPVTERVS 498
MECP2_e2      PNREEPVDSRTPVTERVS 486

```

Figure 1.2 Composition and splicing pattern of MECP2 gene (A) Representative figure showing the splicing patterns of the *MECP2* gene. Two mRNA isoforms are generated; *MECP2_e1* and *MECP2_e2*. The two isoforms generate two protein isoforms of MeCP2 with differing N-termini due to the use of alternative translation start sites (bent arrows) (B) Alignment of the _e1 (GenBank accession no. NM_001110792.1) and _e2 (GenBank accession no. NM_004992.3) isoforms of MeCP2, showing the different N-termini (yellow and green highlights).

MeCP2_e2 shows 95% identity at the amino acid level between human and mouse, while there is 100 per cent identity between these species across the MBD (Nan et al., 1996).

Mecp2_e1 is a plentiful isoform in the brain (Mnatzakanian et al., 2004) and is translated with higher efficiency *in vivo* (Kriaucionis and Bird, 2004). Mutations in exon 1 are sufficient to produce neurological manifestations. In contrast, no specific exon 2 mutations associated with RTT have been observed thus far (Mnatzakanian et al., 2004). A report recently showed that during neuron-induced toxicity, MeCP2_e2 is upregulated and its driven overexpression in healthy neurons enhanced apoptosis. Moreover, it has been found to be neuroprotective (Dastidar et al., 2012). Another study in which MeCP2_e2 was knocked down demonstrated the dispensability of this isoform. Nonetheless, further analysis has shown that *Mecp2_e2* allele mutations have association with survival disadvantage and placental defects.

1.3.3 MeCP2 Functions

The functions of MeCP2 are mediated primarily by the two primary functional domains, the MBD and TRD. These domains interact with histone deacetylase and the Sin3a repressor complex among other proteins (Nan et al., 1997; 1998). MeCP2 protein has two NLS (nuclear localization signals) responsible for nuclear targeting of *Mecp2* (Nan et al., 1996) and a C-terminal segment that helps it bind to the core of the nucleosome. MeCP2 is expressed in neuronal stem cells in *Xenopus* (Jung et al., 2003). However, in mammals *Mecp2* is not expressed in neural precursors, indicating that it is unlikely that *Mecp2* is involved in neuronal differentiation or early cell fate decisions, but rather is involved in maintenance and neuronal maturation (Kishi and Macklis, 2004). During development, expression of MeCP2 is absent or very low in immature neurons and increases during neuronal maturation, reaching its highest level in postmitotic neurons and remaining high through adult life (Kishi and Macklis, 2004). *Mecp2* knocked out in the adult brain of the mice results in very similar motor and neurological deficits to those observed in germline knockout mice which suggests MeCP2's necessary role in maintaining neuronal function (McGraw et al., 2011).

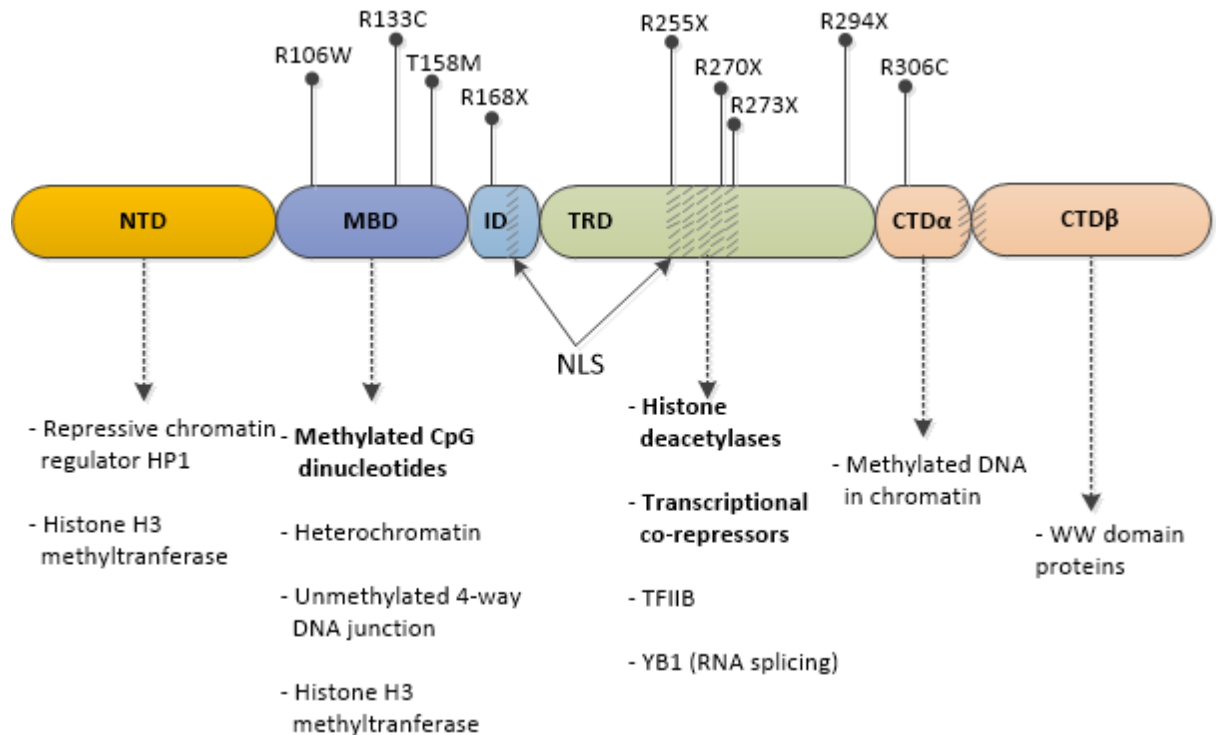


Figure 1.3 MeCP2 protein structure.

Representative figure showing the distinct functional domains of MeCP2. Apart from the N-terminus, both MeCP2 isoforms are identical and contain several functionally distinct domains: NTD, N-terminal domain; MBD, methyl binding domain; ID, inter domain; TRD, transcription repression domain; CTD, C-terminal domain; NLS; nuclear localisation signals. Locations of 9 of the most common point mutations in RTT are indicated (●). Below each domain are indicated major (bold) and other (grey) interactors and functions). HP1; heterochromatin protein 1, TFIIB; transcription factor IIB, YB1; Y box binding protein 1. This figure was adapted from Gadalla et al., 2011 and Xu et al., 2013.

Biophysical studies have probed the specificity of MeCP2 binding and have reported on the interaction (through hydration within the main groove) with methylated DNA and the interaction with nucleosomes (Yang et al., 2011). Despite this knowledge, the precise biological function of MeCP2 remains unclear. Alternative or additional functions proposed include selective activation/enhancement of gene expression, processing of RNA (Young et al., 2005), and regulation of chromatin (Nikitina et al., 2007). It was established that the distribution of MeCP2 across the genome is largely in parallel with the density of methylation and occurs, in neurons at least, to the exclusion of histone H1. The data suggests MeCP2 plays a major role in suppressing

transcription through large-scale actions genome wide, perhaps via global dampening of transcriptional noise.

1.4 Animal models of Rett syndrome

The status of RTT is that of a relatively common monogenic disorder that has created enough interest to further investigate the underlying pathology. The interest has largely emanated from the need to develop rational therapies for patients. However, fuller understanding of neuronal dysfunction and the underlying pathology in RTT may also provide insight into the pathophysiology of neurodevelopmental disorders more generally (Neul and Zoghbi, 2004). As *MECP2* mutations lead to RTT via loss of function effects, modelling of RTT has been conducted using *Mecp2* knockout mice. Due to the high levels of conservation of this protein in mammals (see 1.3.2), studying the effects of mutations of *Mecp2* in mice has been suggested to be appropriate in order to understand further the RTT phenotype and potential therapeutic avenues.

There are many models that have successfully recapitulated several of the cardinal traits which characterise RTT in humans, albeit there are key variations. An early RTT animal model was generated by deleting exon 3 (encoding 116 amino acids, the majority of which comprise portions of the MBD) (Chen et al., 2001). An *Mecp2*^{-/y} male mouse, where *Mecp2* was knocked out either specifically in the central nervous system, or globally, appears to be normal for the first few weeks of life. However, as the disease progresses, the mice display hypoactivity, a decrease in bodyweight, an increase in trembling, and end with premature death around the age of 10 weeks. Contrastingly, heterozygous females (*Mecp2*^{+/-}) have a mosaic network at the cellular level (due to XCI) and comprise a mixture of cells expressing the WT and mutant *Mecp2* alleles. This has similarity with RTT patients, with apparent normal growth in the initial four-month period followed by gait and ataxia abnormalities, reduction of activity, and weight-gain.

After discovering that the *MECP2* gene is a cause of 96% of typical RTT cases, (Amir et al., 1999; Chahrour and Zoghbi, 2007), the RTT mouse models were created (Chen et al., 2001; Guy et al., 2001; Shahbazian et al., 2002). The first

generation of RTT mouse models involved deletion of exons 3 and/or 4 (Chen et al., 2001; Guy et al., 2001). Subsequently, RTT mouse models were constructed to have the most common mutations seen in RTT patients (Brown et al., 2016; Chen et al., 2001; Pelka et al., 2006; Shahbazian et al., 2002).

1.5 Behavioural tests in the mouse model

After the creation of the RTT mouse models, there were further dramatic improvements in investigative techniques with regards to RTT disease progression (Goffin et al., 2011; Guy et al., 2001) and possible reversibility (Robinson et al., 2012). To investigate this more intensively, behavioural tests are required to characterise the RTT mouse models, especially to clarify the baseline of each systemic impairment before instigating treatment.

The *Mecp2* null mouse is the first line to study the characteristics in the RTT mouse model (Chen et al., 2001; Guy et al., 2001). Most of the studies recorded body weight and aggregate phenotype severity RTT score which originated in studies carried out by Guy et al. in 2007 as a standard to report the condition of the RTT mice, with some papers reporting on breathing abnormality tests.

Following this, the *Mecp2* knock-in lines that mimic the most prevalent *MECP2* mutations in humans were created. The research showed characteristics compared with the *Mecp2* knock-out mice in terms of the basic behavioural tests (body weight, aggregate phenotype severity RTT score and breathing) including additional behavioural tests for example, mobility, anxiety and learning tests.

Recent studies have focussed on the treatment of RTT using these *Mecp2* knock-in lines. Several reports show comparisons between the treatment in *Mecp2* knock-in and knock-out mice with several additional behavioural tests (table 1-1).

Table 1-1. Summary of behavioural tests of published studies in RTT mouse models.

Tests of mouse behaviour	Experimental paradigm	References
Test for mobility and motor function	Open field	(Zhou et al., 2017), (Chin et al., 2018), (Vigli et al., 2018), (Vogel Ciernia et al., 2017), (Mantis et al., 2009), (Matagne et al., 2013) (Matagne et al., 2017), (Zhong et al., 2016), (Gadalla et al., 2013) (McGill et al., 2006)
	Home cage spontaneous activity	(Vigli et al., 2018), (Ross et al., 2016), (Garg et al., 2013)
	Forelimb grip strength	(Zhong et al., 2016), (Zhou et al., 2017), (Johnson et al., 2016)
	Balance beam	(Ross et al., 2016), (Robinson et al., 2012)
	Accelerating rotarod	(Ross et al., 2016), (Vogel Ciernia et al., 2017), (Robinson et al., 2012), (Matagne et al., 2017)
	Treadmill	(Ross et al., 2016), (Gadalla et al., 2013)
	Grid walking	(Zhong et al., 2016), (Johnson et al., 2016)
Breathing activity	Plethysmography	(Johnson et al., 2016), (Zhong et al., 2016), (Ross et al., 2016) (Gadalla et al., 2013), (Robinson et al., 2012), (Matagne et al., 2017)
Test for memory	Novel object recognition test	(Gogliotti et al., 2016), (Schaevitz et al., 2013), (De Filippis et al., 2012) (Matagne et al., 2013)
	Y-maze test	(Vigli et al., 2018)
	Fear conditioning	(Gandaglia et al., 2018) (Gogliotti et al., 2016),
Test for anxiety	Light-dark exploration	(Vogel Ciernia et al., 2017) (McGill et al., 2006)
	Elevated plus-maze	(Matagne et al., 2017) (Matagne et al., 2013), (McGill et al., 2006)
	Elevated zero maze	(Matagne et al., 2013), (De Filippis et al., 2012)
Social approach	Three-chamber social test	(Gogliotti et al., 2016), (Vogel Ciernia et al., 2017), (Vigli et al., 2018), (Zhou et al., 2017), (Zhong et al., 2016)

There are many behavioural paradigms for testing each behavioural phenotype, but the most appropriate paradigm for behavioural testing in the RTT mouse has not been greatly documented due to its many physical limitations. It is often not possible to use the standard behavioural tests. Therefore, it is necessary to study and improve detailed behavioural testing for it to be suitable for experimental RTT model animals in standardized research in biomedical research.

1.6 Reversibility of the RTT phenotype and treatment strategies.

1.6.1 Treatment strategies for RTT

In the last decade, the preclinical studies on mice including behavioural and neurological, which resulted from abnormal development of the brain have been potentially reversible across an array of neurodevelopmental disorders models (Costa et al., 2002). The *Mecp2* knockout phenotype's reversibility demonstrated in mice (Guy et al., 2007) has stimulated various groups to explore therapeutic approaches designed to reverse the RTT-like dysfunction or to ameliorate, delay or prevent its onset. Two major intervention approaches have been suggested: to target the primarily underlying cause (i.e. a loss in *MECP2*'s function mutation) or to target processes further downstream in the pathogenetic pathway (Figure 1.4).

1.6.2 Gene therapy approaches

For disorders resulting from loss of function mutations, the primary gene therapy approach involves gene augmentation. In the case of RTT, this involves delivering a construct that contains the WT copy of the coding regions of *MECP2* to the cells affected (i.e. brain neurons predominantly) to restore to those cells the functions of the gene, and, in turn, to establish improvement in functions at the cellular, molecular network, regional, and whole animal level. The challenges to these approaches (Figure 1.5) include finding an appropriate method of controlling exogenously derived gene expression and ensure high transduction efficiency in appropriate cells while minimizing transduction of inappropriate cells. MeCP2 level regulation within transduced cells is an issue that is particularly challenging as dosage sensitivity is found with MeCP2 and in the brain cells of both mice and humans - MeCP2 overexpression can lead to a severe phenotype (del Gaudio et al., 2006). Additionally, in females, gene therapy for X-linked dominant disorders must accommodate the fact that because of XCI (X chromosome inactivation), around half of the transduced cells already express WT MeCP2 at normal levels.

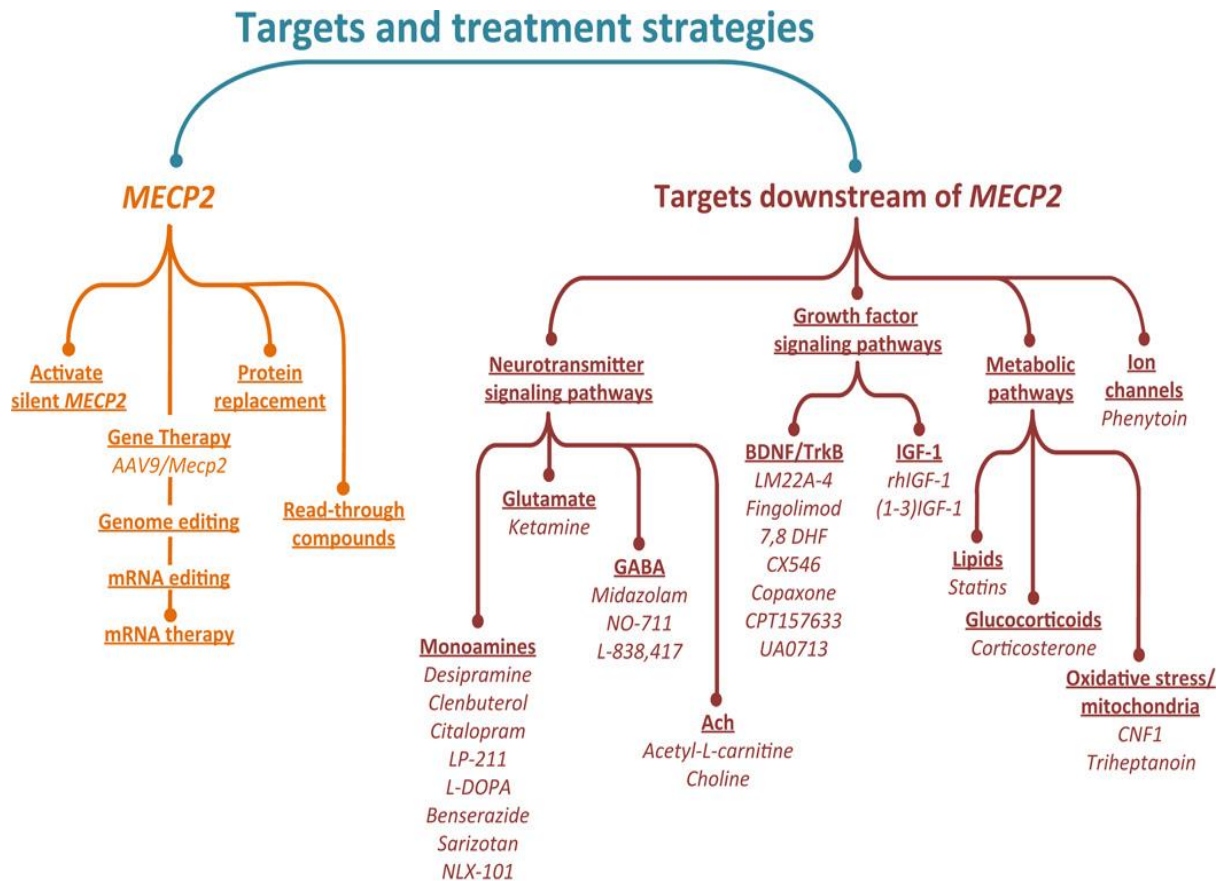


Figure 1.4 Therapeutic targets and potential pharmacological strategies currently being explored in animal models for the treatment of Rett syndrome

Underlined headings indicate therapeutic targets; compounds that have been reported in the literature to be effective in improving behavioural outcome measures or physiological function in vivo are shown in italics. Taken from (Katz et al., 2016).

AAV vectors are an attractive vector of choice for targeting disorders of the nervous system (see 1.7 below). The strategies based on AAV for gene therapy have been applied for both periphery and CNS (Wagner et al., 1998). Some of these are in an advanced preclinical stage or in phase 1/2 clinical trials, for example, for Parkinson's disease and haemophilia B (Samulski and Muzyczka, 2014). The construction of AAV vectors with serotype 9 capsid (AAV9) show some promise in achieving high efficiency in CNS transduction after systemic administration (Foust et al., 2009).

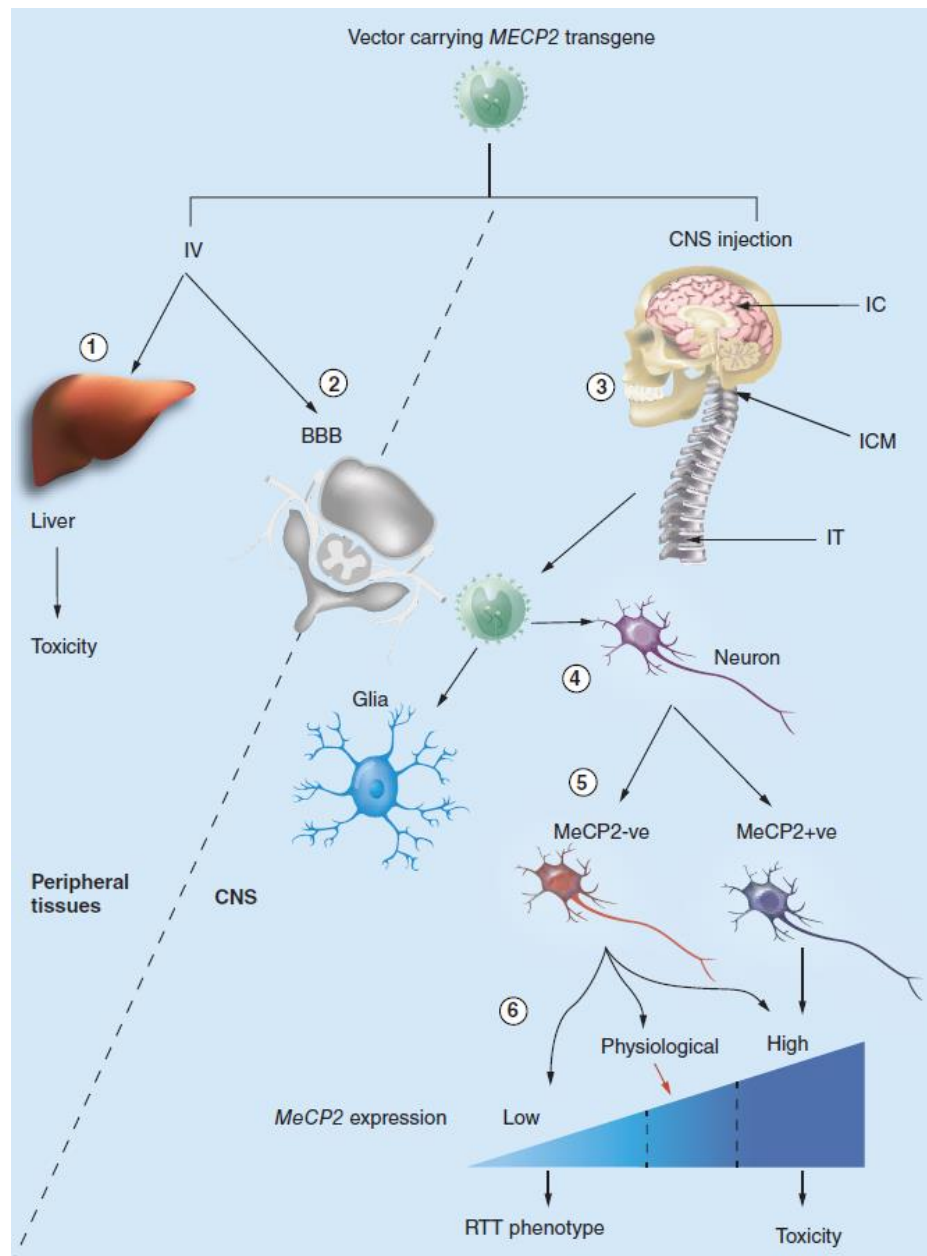


Figure 1.5 Summary of current challenges for RTT gene therapy. Intravenous (IV) injection of vector is likely to produce high peripheral expression, particularly in the liver (1), with potential accompanying toxicity. The BBB (2) presents a challenge that prevents many types of vector from accessing the CNS. This problem can be overcome by direct CNS injection (3) using an IC route or routes that target the cerebrospinal fluid: ICM or IT injection. In the brain it is very important to transduce as many neurons as possible (4) to achieve maximal therapeutic effect. Among neurons, only neurons expressing the mutant allele and thus lacking functional MeCP2 should be targeted, ideally (5). In the transduced neurons the level of exogenous MeCP2 expression needs to be maintained at physiological levels (6) to avoid overexpression-related toxicity. BBB: Blood-brain barrier; IC: Intracranial; ICM: Intra-cisterna magna; IT: Intrathecal. This figure was adapted from (Gadalla et al., 2015).

1.7 Adeno-associated virus (AAV) as a potential gene therapy vector

AAV, a non-enveloped virus 22-25nm in length, is a member of the parvoviridae family and requires a helper virus in order to replicate, hence, it is classified as a dependovirus (Daya and Berns, 2008). Most humans are seropositive for AAV infection; however, in most of the infections are latent in the absence of the helper virus, with latency involving site-specific integration into a locus within chromosome 19q13.4 (Kotin et al., 1992). Effectiveness of AAV as a vehicle for gene therapy is derived from (1) its ability to transduce dividing and non-dividing cells; (2) a wide cellular tropism; (3) low immunogenicity; (4) stable transgene expression; and (5) absence of disease production in humans (McCarty et al., 2004).

AAV2 is the most widely studied AAV serotype and, as a result, AAV vectors developed to date are based on the AAV2 genome backbone comprised of a linear, single stranded DNA of 4.7kb (Srivastava et al., 1983). The genome is composed of two inverted terminal repeats (ITRs) which flank two open reading frames (ORF) (figure 1-6a). ITRs act as priming sites for the synthesis of the complementary strand by DNA polymerase. In addition, they are involved in AAV genome packaging, transcription and site-specific integration (Daya and Berns, 2008). The left ORF houses the Rep (replication) gene that encodes four Rep proteins. Rep78 and Rep68 are produced under control of the P5 promoter, act as regulatory proteins and are critical for virus replication (Pereira and Muzyczka, 1997). Rep52 and Rep40 are produced under control of the P19 promoter and account for the accumulation of single-strand viral DNA used for packing inside capsids. The right ORF contains the Cap gene (figure 1-6a). This encodes three capsid proteins (VP1, VP2 and VP3 in 1:1:10 molar ratio) and is produced under the P40 promoter (Grieger and Samulski, 2005).

1.7.1 AAV-based vectors and mammalian cell transduction

Recent AAV based vectors have the Cap and Rep genes replaced by the transgene cassette and are flanked by the two ITRs that provide the *cis* signal

vital for packaging and priming for the creation of the second strand (Samulski et al., 1982), (Schnepp et al., 2005). Also included in controlling transgene expression are other post transcriptional regulators. Additional plasmids required for packaging and supply encoding sequences for Rep and Cap genes, the adenovirus helper genes (E4, VA and E2A) respectively.

Either *de novo* synthesis of the second strand or strand annealing (SA) of complementary strands from two infecting viruses contribute to the generation of the second strand of DNA (figure 1-7); (Nakai et al., 2001). AAV packages the plus or minus DNA strands with equal efficiency (Berns, 1990). However, impeding the SA pathway (by packaging the vector solely with either the positive or negative strands) did not impact transduction efficiency of ssAAV. This indicates that *de novo* synthesis has a major role in second strand synthesis during transduction (Zhong et al., 2008). The rAAV genome requires synthesis of the complementary strand inside the nucleus to start gene expression. Failure to achieve transgenic expression is generally due to incapacity to generate complementary strands and should therefore be considered a rate-limiting step in the vector transduction process (Miao et al., 2000).

1.7.2 Self-complementary AAV

Viral genome trafficking to the nucleus and second strand generation are the most vital steps in the rAAV transduction process (Ferrari et al., 1996). Completion of the second strand shows a transitory period of genome instability that can compromise gene expression (Wang et al., 2007). Two of these crucial steps can be bypassed by packaging AAV with both sense and non-sense strands together to form self-complementary AAV (scAAV), enabling the complementary strands to produce a dimeric inverted repeat genome (Carter and Rose, 1972). scAAV vectors increase transduction efficiency and rapid onset of transgene expression compared to ssAAV vectors (McCarty et al., 2001). Low transduction in ssAAV can result from a lack of competency in generating the second strand, vital for gene expression. Contrastingly, for scAAV, the formation of the second strand is independent of host cell-directed DNA synthesis (McCarty et al., 2001). Rapid onset and an estimated 15-fold increase in transgene expression is also displayed by the scAAV vector when compared to the ssAAV (Ren et al., 2005). However, the reduction of the cloning capacity to roughly half that of the

ssAAV vector limits extensive applications of scAAV in gene therapy. Nevertheless, scAAV can still be useful in several applications and its limitation can be partially overcome via reduction/optimization of the size of the promoter and transcription regulatory elements (Li et al., 2008). The use of AAV capsids can also facilitate larger genome size insertion for example, capsid 5 (Grieger and Samulski, 2005).

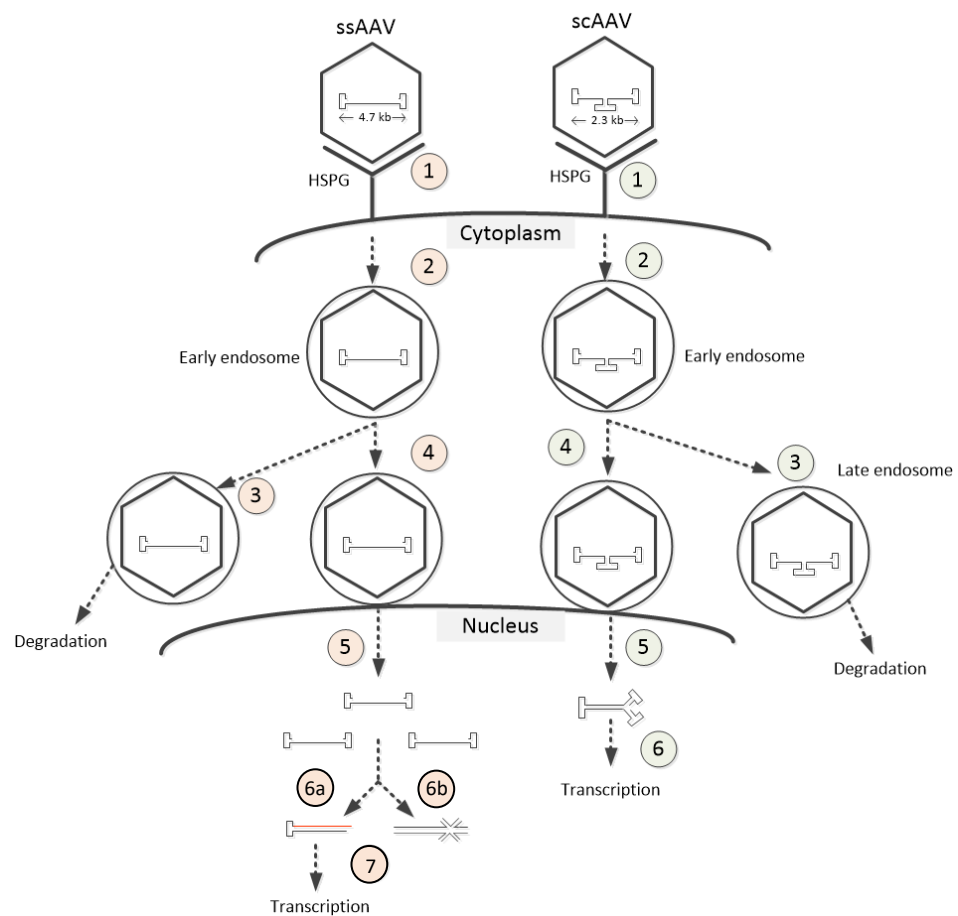


Figure 1.6 AAV-based vector transduction.

Representative diagram showing the transduction of AAV-based vector; (1) virus binding to heparin sulphate proteoglycan, (2) virus endocytosis to the early endosome followed either by (3) maturation to late endosome and degradation or (4) escape early endosome and (5) translocation to the nucleus. (6) in the case of ssAAV (green circles), the single stranded DNA must be converted to double stranded DNA either by de novo synthesis (6a) or strand annealing between plus and minus strands (6b) followed by (7) transcription of the transgene. Whereas, in the case of scAAV (red circles), once inside the nucleus it can bypass the 2nd strand synthesis via intramolecular annealing and start transcription faster than the ssAAV vector. HSPG; heparin sulphate proteoglycan, ssAAV; single-stranded Adeno-associated virus, scAAV; self-complementary Adeno-associated virus.

1.7.3 AAV capsid

Despite the presence in infected individuals of AAV2 capsid in tissues and cells, certain cells show resistance to infection with AAV2 (Gigout et al., 2005). Using differing AAV serotypes in a pseudo-typing approach allows for extended tissue tropism. Analysing the difference in transduction efficiency and expression levels between capsids 1-9 indicated that AAV virus pseudo-typed with capsids 7 and 9 respectively, presented the highest expression levels, with the most rapid onset being that of capsids 1, 6, 7, 8 and 9. Subsequently, capsid 9 showed optimal viral genome distribution and the greatest protein levels (Zincarelli et al., 2008). Further studies indicate high transduction efficiency of capsids 8 and 9 in liver, skeletal muscle and the pancreas post IV injection with high cardiac tropism for AAV9 virus (Inagaki et al., 2006).

The BBB challenges gene delivery as it impedes the passing of large drug molecules, proteins and viruses. As a result, it is a vital factor in protecting the brain from pathogens and toxins. Virus based gene delivery applications are prevented from entering the brain. However, gene delivery into the brain in animal and human studies has been achieved by direct brain injection to the target area via the vector. This approach however presents challenges and can require multiple injections to induce the therapeutic effect. To add to this, the short-lived disruption of the BBB using hyperosmotic drugs for example, mannitol, can permit gene delivery to the brain using small-sized vectors (McCarty et al., 2009). Studies of AAV9 have demonstrated its ability to act as a potential vector for gene delivery to the brain following a peripheral injection. This negates the need to disrupt the BBB (Duque et al., 2009; Foust et al., 2009). Generating the scAAV9 vector further improved the ability to transduce the CNS with a 10-100 times more efficacy than ssAAV9 (Gray et al., 2011b). As a result, scAAV9 is the focus in numerous studies to determine transduction efficiency and cell type specific tropism following differing means of administration.

Foust et al. (2009) indicated that due to the BBB, age-dependent differential cell tropism was a factor, while Saunders et al. (2009) disagreed, indicating the

BBB is fully functional in neonatal mice. Gray et al. (2011b), however, indicated that adult peripheral injection of scAAV9 could produce high neuronal transduction, 2X glial transduction. Interestingly, the same study indicated that peripheral injection of scAAV9 in non-human primates resulted in limited brain transduction and decreased neuronal transduction. However, it is unknown whether reduced transduction efficiency in the brain is dose-dependent, if so, whether it can be altered by dose modification.

1.7.4 Clinical application and potential in RTT

Advances in vector/capsid design of adeno-associated virus-based vectors have led to an extensive preclinical and phase 1 clinical study to implement these vectors in the treatment of human diseases (Warrington and Herzog, 2006). Data has shown that AAV vectors produce significant therapeutic effects when treating cystic fibrosis (Wagner et al., 1998), (Moss et al., 2004) and haemophilia B (Kay et al., 2000); (Manno et al., 2003). Many CNS disorders are being tested for potential AAV mediated gene therapy, some of which include amyotrophic lateral sclerosis (Azzouz et al., 2000); (Kaspar et al., 2005), spinal muscular atrophy (SMA) (Valori et al., 2010), Huntington's disease (McBride et al., 2003), (Kells et al., 2004), lysosomal storage disorders (Sferra et al., 2004), Parkinson's disease (Eslamboli et al., 2005), (Feigin et al., 2007) and Canavan's disease (Klugmann et al., 2005). In the case of RTT therapy, AAV is encouraging as it can cross the BBB when pseudo-typed with AAV9 capsid (Foust et al., 2009), can infect neurons efficiently, mediate long-term transgene expression (Herzog et al., 1997), (Arruda et al., 2005), (Jiang et al., 2006) and does not integrate sporadically into host chromosomes (Duan and Kollman, 1998); (Nakai et al., 2001). Recently, *MECP2* gene therapy publications have set the scene for plans for clinical trials using AAV9, generating hope for caregivers of RTT patients (Coenraads et al., 2017); (Gadalla et al., 2017), (Matagne et al., 2017), (Sinnott and Gray, 2017); (Tillotson et al., 2017).

1.8 Design of gene therapy approaches

1.8.1 choice of regulatory elements & vector

The RTT phenotype is mainly the result of effects on the central nervous system's postmitotic and long lived neurons (Chen et al., 2001); it is clear that *ex vivo* strategies involving cells' removal from the patient and subsequent replacement would not be viable, and thus, *in vivo* delivery of the therapeutic transgene into the brain is required. The current use of vectors for gene therapy has generally been based on retroviruses, and lentivirus (Kay et al., 2001) or an AAV (adeno-associated virus). Lentiviral vectors can transduce non-dividing cells and drive long-term, stable expression in neurons (Scherr et al., 2001). These vectors cannot cross the BBB (blood-brain barrier), however, even following the disruption with mannitol (McIntyre et al., 2008), and must be delivered by injection directly into the brain parenchyma. In addition to this, they show a very limited capacity of spreading beyond the injection site (Brooks et al., 2002). Safety issues are also inevitable around potentially causing insertional mutagenesis, although non-integrating versions have been developed (Nightingale et al., 2006). The demonstration of potential delivery for the lentiviral transgene was carried out by Rastegar and colleagues in improving the *Mecp2* phenotype - derivation of *Mecp2*-null neurons from neuronal stem cells in culture. Lenti-treated neurons displayed more branching than unaffected controls; and dendritic growth (Rastegar et al., 2009). Lentiviral approaches have gone towards specific neurological disorders clinical development targets, brain nuclei or regions. The ubiquitous nature of MeCP2 expression across the nervous system can render lentiviral technologies in RTT insert, unless the aim is targeting limited range of specific traits, for example, targeting brainstem nuclei to correct problems related to breathing (Julu et al., 2001). AAV9 displays promise in relation to RTT gene therapy and has the potential to cross the blood-brain barrier, efficiently infecting neurons and mediating transgene expression in the long term (Herzog et al., 1997).

For delivery of WT *MECP2* in ssAAV9 vectors to neonatal mice by direct brain injection, the initial choice of promoter was chicken β -actin, which results in a high efficiency of brain transduction (Table 1-2). Transgene expression occurred

mostly in neurons and generated MeCP2 levels similar to those seen endogenously. Further, the treated mice showed improvement of the RTT-like phenotype trajectory in term of the prolonged survival and amelioration of severity score and locomotion (Gadalla et al., 2013).

Table 1-2. Summary of experimental design and outcomes of published studies of gene therapy interventions in Rett syndrome mouse models.

Route of administration	Age/Sex	Virus/promoter	Dose/mice (vg)	Transduction efficiency	Result	Reference
Intracranial	Neonate / male	ssAAV9/CBA	9.3×10^9	~40%	<ul style="list-style-type: none"> ↑ Prolonged survival ↓ Reduced phenotype severity ↓ Rescued nuclear volume Rescued soma size ↑ Improved locomotion 	(Gadalla et al., 2013)
Intracranial	Neonate / male	scAAV9/ MeP (426 bp)	1×10^{11}	~40%	<ul style="list-style-type: none"> ↑ Improved survival ↓ Reduced phenotype severity ↓ Reverse neurological symptoms 	(Tillotson et al., 2017)
Intravenous	Young adult/ male	scAAV9/MeP (229 bp)	5×10^{11}	~2-4% of neurons	<ul style="list-style-type: none"> ↑ Improved survival ✓ Normalization of phenotype GABA level 	(Gadalla et al., 2013)
Intravenous	Adult/ male	scAAV9/ MeP (730 bp)	3×10^{12}	~25%	<ul style="list-style-type: none"> ↑ Prolonged survival ↓ Reduced phenotype severity ↓ Rescued soma size 	(Garg et al., 2013)
Intravenous	Adult/ female	scAAV9/ MeP (730 bp)	3×10^{12}	N/A	<ul style="list-style-type: none"> ✓ Stabilization of phenotype 	(Garg et al., 2013)
Intravenous	Adult/ male	scAAV9/ MeP (223 bp)	1×10^{11}	~10-20%	<ul style="list-style-type: none"> ↑ increased body weight ↓ Delayed phenotype severity ↑ increased tyrosine hydroxylase levels in the A1C1 and A2C2 ↑ increased MeCP2 expression found in midbrain 	(Matagne et al., 2017)

In the same study, expression of WT *MECP2* delivered systemically in an scAAV9 vector was driven by a small, 229bp fragment of the endogenous *Mecp2* promoter. The result of this was a lower efficiency of transduction in the brain, although it was associated with improvement in survival of male *Mecp2* null mice. Reports from another study indicate identical findings in male mice and stabilization of the phenotype in heterozygous female mice (Garg et al., 2013).

For optimal safety and efficacy in the applications of gene therapy, there are two primary considerations - the target cell proportion being transduced, and the transgene products levels in each transduced cell. In a STOP-Cre mouse model of RTT, genetic reversal experiments demonstrated a strong correlation between degree of amelioration of the phenotype and the proportion of cells that express MeCP2 after reversal. (Guy et al., 2007) However, in AAV9 studies (Gadalla et al., 2013), significant amelioration of the phenotype was linked with transgene expression in around 25-40% of brain cells.

However, the transduction efficiencies achieved thus far have not been able to completely rescue the RTT-like phenotype to the level of wild type, requiring higher efficiency of transduction. Where levels of MeCP2 are concerned, there is significant evidence suggesting that a reduced level of functional MeCP2 would lead to RTT-like phenotypes, whereas overexpression of MeCP2 or *Mecp2* duplication would result in other neurological effects (Collins et al., 2004). The level of transgenic protein is likely to be influenced mainly by the promoter used in the construct. In an early study comparing two promoters, the endogenous core promoter of murine *Mecp2* and the well-characterised chicken β -actin promoter (Gray et al., 2011a), results showed that both promoters can drive exogenous MeCP2 expression at approximately physiological levels.

1.8.2 Optimal time for gene therapy interventions

RTT is considered to result from a lack of neuronal maturation and MeCP2 playing a key role in both maintenance and neuronal development processes. Early restoration of *Mecp2* expression found in pre-symptomatic mice led to apparently normal development (Guy et al., 2007). Delayed re-activation of *Mecp2* in symptomatic mice can normalize lifespan and phenotypic recovery (Guy et al., 2007). In another study, brain-specific expression of *Mecp2* early in life showed neuronal size normalization, motor activity improvement, development of delayed phenotype, and prolonged lifespan. These are reduced typically in the *Mecp2*-null mouse (Chen et al., 2001). From the literature related to the preclinical gene therapy published to date, *MECP2* delivery either

in adult mice or in mouse neonates can produce phenotype and survival benefits. This indicates that across a wide array of ages, therapeutic interventions can be effective.

However, there is no clarity yet as to whether there is a critical time window during which *Mecp2* delivery will be producing improvements which are more robust, as systematic testing has not yet been conducted. This may be of direct relevance to clinical considerations as improvements in early diagnostic testing are made. The appearance of the RTT phenotype several months postnatally (generally eight to eighteen months) could present a window that is particularly effective for intervention prior to the onset of overt RTT features if diagnosis of early pre-symptomatic molecular in nature were to become cost effective and practical. During infancy, such early treatment would also dramatically reduce the viral vector amount required (if peripherally required) for treatment. However, the extent of phenotypic amelioration after treating adult mice would predict that administration carried out later to older adults or girls with RTT Syndrome would also be effective (Guy et al., 2007). Irrespective of the intervention time, an important requirement is that there should be longevity of transgene expression as *Mecp2* deletion from neurons that are mature is deleterious (McGraw et al., 2011). There have been several reports of AAV-mediated transgenes that persist for long periods that includes reports pertaining to continued expression of greater than six years following delivery in primates and following greater than eight years in dogs (Stieger et al., 2009). Further, a gene therapy clinical trial conducted recently has shown gene expression persistently for at least 10 years following gene delivery of AAV mediated in the human brain (Leone et al., 2012).

1.8.3 Local or global *MECP2* delivery

RTT modelling in mice has played a pivotal role in studying the requirement for MeCP2 in different areas of the brain, in different types of cells in brain (Chao et al., 2010) and at various development stages, in addition to testing the reversibility of RTT-like phenotypes (Guy et al., 2007). The brain is the most important contributor to RTT pathology as brain-specific *Mecp2* knockout leads to development of the RTT-like phenotype, while peripheral knockout leads to a phenotype very similar to wild-type in almost all respects (Ross et al., 2016). It

could be the case that the effect of a lack of MeCP2 in the peripheral tissue is masked by the profound phenotype related to its lack in the CNS. Clinical and mouse model data, however, do suggest that several aspects of the KO phenotype, particularly affecting lung, liver and bone, may originate in peripheral effects (De Felice et al., 2014; Ross et al., 2016).

Direct delivery of exogenous *MECP2* to the brain using ssAAV9 (Gadalla et al., 2013) emphasizes the brain's crucial role in ameliorating most of the phenotype's gross aspects. Failure in correcting certain features resembling RTT, such as abnormalities in breathing, may reflect cells' insufficient transduction in areas of the brain pertaining to those phenotypes or lacking expression in the peripheral tissues which may contribute to the given phenotype. Independent studies suggest that systemic delivery of *MECP2* vectors (Table 1.2) using scAAV9 confers extended survival despite low numbers of transduced cells in the brain. The first report shows the transduced neurons at around 2-4% with peripheral tissues taking up majority of the virus particles, especially the liver. In another study, the dose was increased six-fold (Garg et al., 2013), leading to brain transduction being increased and greater phenotypic improvement in null male mice and stabilization of the phenotype in female heterozygous mice. These studies show how important it is to achieve an appropriate therapeutic dose. A high viral titer is essential for getting good coverage. Detection of transduction, on the other hand, may depend on vector construct overexpression, which is undesirable.

The restoration of MeCP2 in the brain is described as achieving improvement of the RTT-like phenotype. Two methods can be used in delivering therapeutic constructs into the CNS: systemic delivery (for example, intravenous injection) which results in passing through the blood brain barrier and direct delivery routes into the CNS. Both approaches are approved for clinical trials using AAV in other neurological disorders. The reactivation experiments of *Mecp2* demonstrate a strong correlation between the magnitude of phenotypic rescue and the proportion of brain cells that express MeCP2 (Robinson et al., 2012). Systemic administration of vector, while more desirable from the standpoint of clinical translation, results in limited transduction of cells in the CNS and

restricts the vector choice options to those which can cross the BBB (Yang et al., 2014; Zhang et al., 2011).

Further, attempting to increase the dose in order to achieve higher expression in the CNS will have an accompanying increase in expression level in peripheral tissues, especially in the liver (Figure 1.5). As several peripheral tissues usually express low MeCP2 levels relative to neurons, this could lead to toxicity (Gadalla et al., 2013). Modification of vector constructs to de-target the liver, minimizing off target effects and enhancing CNS expression, may be critical if systemic delivery is to be feasible.

The level of exogenous *MECP2* varies according to the promoter used; a weak promoter produced near physiological levels of exogenous MeCP2 (80% of the WT levels) whereas a stronger promoter, such as PGK promoter (Owens et al., 2002) produced relatively high cellular levels (200% of the WT levels). This is particularly important when considering the danger of MeCP2 overexpression-induced toxicity in humans as patients with *MECP2* duplication show overt neurological deficit (Meins et al., 2005), (Friez et al., 2006). In addition, the *Mecp2* overexpression model shows the phenotype severity increasing as *MeCP2* increased beyond normal levels (Chao and Zoghbi, 2012) with the worst phenotype observed with 2-3 fold increase of *MeCP2* levels (Luikenhuis et al., 2004).

Previous studies using a self-complementary AAV9/MeP229-hMECP2-myc-BGHpA vector (first generation vector), extended the survival of *Mecp2*^{y/-} male mice when injected intravenously (IV) between post-natal day 28 and 2nd at day 35 (Gadalla et al., 2013). This IV gene therapy resulted in high transgene expression in the liver as well as significantly increased levels of alanine aminotransferase (ALT), an indicator of liver toxicity. (Gadalla et al., 2013). After IV treatment with 1×10^{11} viral genomes (vg) of the first generation vector, the level of total MeCP2 expression (measured by PCR technique) in WT liver, was around six times that observed within the brain (Gadalla et al., 2013). This liver tropism and hepatic transgene expression observed after IV treatment can be attributed to the AAV capsid (Gray et al., 2013) and the use of a small endogenous *Mecp2* promoter fragment (MeP229), (Gadalla et al., 2013), (Gray et al., 2011b)

respectively. In conclusion, the first generation presents possible efficiency, however, vector design and administration route would need to be optimized before being used in humans. Increasing severity of hindlimb claspings and abnormal gait were unexpected side effects in previous publications of MeCP2 gene transfer studies. (Garg et al., 2013; Matagne et al., 2017)

To consider the availability of current vector technology, achieving high efficiency of transduction in the brain following systemic administration is challenging. Therefore, direct CNS delivery is necessary in achieving CNS transduction as appropriate. The widespread action of MeCP2 throughout the nervous system indicates that strategies of gene augmentation should be targeting the whole brain rather than selectively targeting crucial regions of the brain. To achieve widespread coverage of the brain, while avoiding overexpression within the brain has been a challenge and requires appropriate regulatory/promoter elements development in gaining a level of control over levels of overexpression.

1.8.3 To target specific types of cells in the brain: astrocytes or neurons?

MeCP2 expression has been recognized in numerous tissues (LaSalle et al., 2001), but is particularly plentiful in postmitotic neurons. The disorder's key neurological manifestations are indicative of a more severe effect on the neurons compared to other cell types. However, recognition is increasing regarding glial cells' possible role in phenotype development and its recovery (Lioy et al., 2011).

It has been found that mice only lacking MeCP2 in neurons have shown overt RTT-like symptoms, while mice which express MeCP2 in neurons have shown an apparent normal phenotype (Luikenhuis et al., 2004). This bulk of observable knockout phenotypes come from a loss of function by *Mecp2* in neurons (Ross et al., 2016). The improvements which are phenotypic after delivery mediated by AAV9 of *MECP2* in young adult mice and neonatal, has mainly been due to its expression in neurons (Gadalla et al., 2013).

Further complications arise with many reports showing greater importance of MeCP2 expression in some neuronal subpopulations. For instance, if *Mecp2* is

specifically silenced in inhibitory GABAergic cells, a subtle range of neuropsychiatric phenotypes that are RTT-like are revealed which include repetitive, autistic-like behaviours. Another study shows the silencing of *Mecp2* in neurons containing tyrosine hydroxylase. It was found that mice display breathing problems and motor abnormalities which include an increase in the incidences of apnoeas which suggest that dysfunction of aminergic systems may be responsible for breathing phenotypes in RTT (Samaco et al., 2009). Interestingly, preservation of MeCP2 expression in some subtypes of neuron in genetically engineered mice was associated with reduced phenotype severity and extended survival (Goffin et al., 2014). Direct delivery of the gene to cells with the use of cell type-specific promoters is an alternative option in treating specific aspects of the RTT phenotype at the gene level.

1.8.4 Other gene-targeted strategies in RTT

Considering the challenges of gene therapy in RTT - the need to regulate and maintain the levels of MeCP2 expression in a physiological manner - provisional need by an ideal therapy of MeCP2 derived exogenously could be avoided, although it can result in endogenous WT MeCP2 expression under its regulatory control which are normal and endogenous. One viable approach when the cause of RTT is a nonsense mutation in the final exon is translational read-through delivered via pharmacotherapy.

In this approach, mRNA produced from the mutant allele undergoes translation under conditions where the premature stop codon is skipped. Therefore, it produces a protein that is WT at all residues except that translated from the mutant codon itself. Early truncating mutations account for around 40% of typical RTT patients. This can be treated with the use of gentamycin and the compounds related to it, inducing ribosomal read-through of premature stop codons (Manuvakhova et al., 2000).

In vitro experiments have demonstrated the production of full-length MeCP2, produced in cell lines that harbour various nonsense mutations following gentamycin treatment, although with a rather lower level of process efficiency, which ranges between 17-32% depending on the effective concentration of

gentamycin and the identity of the mutation (Brendel et al., 2009). This low efficiency of production of full-length MeCP2 after aminoglycoside treatment, along with the well-known aminoglycoside toxicity (ototoxicity and nephrotoxicity) suggests that this approach may not be ideally translational. In the search for translationally beneficial approaches, other compounds with improved safety profiles are instead being tested. New generation aminoglycosides, such as NB84, NB54 and PTC12, are being trialled; these have lower toxicity and greater efficacy compared to gentamycin (Welch et al., 2007). Not much is known about these compounds ability to cross the BBB and therefore, their likeliness and efficiency to treat CNS disorders including RTT remains unknown.

Another approach consists of reactivating the previously inactive *MECP2* gene on the X chromosome. XCI is a random process resulting in around 50:50 cell mixture of each type (mutant and normal), albeit there is variation of the XCI ratio between individuals and tissues. In the process of brain development, mutant and normal cells are closely intermingled in a mosaic pattern of a fine scale with some clustering tendency (Guy et al., 2007).

The therapeutic strategy, which involves reactivation of the inactive X, may need to target only mutant cells depending on whether biallelic expression results in dominant negative effects of the mutant allele or not. A recent publication suggests that there is no occurrence of such effects, at least for some mutations (Pitcher et al., 2015).

Activation of X-linked genes is possible by reducing the levels of genomic methylation by using 5-azacytidine - this has been tried in cell culture (Mohandas et al., 1981). However, this type of approach is a blunt instrument and has a low chance of being of therapeutic utility. A study conducted recently used small molecules to inhibit X-chromosome inactivation factors. Expression of MeCP2 from the inactive X in cultured fibroblasts from RTT patients was demonstrated (Bhatnagar et al., 2014). Pharmacological activation of the inactive X is reversible, and thus reactivation needs the continued presence of the drug.

For inactive X reactivation to work effectively as RTT's therapeutic strategy, many key hurdles must be surmounted. Firstly, in cells currently expressing the normal allele, the silent X's reactivation will lead to potentially detrimental effects of the mutant allele. However, recent evidence suggests that the disruptive interactions are unlikely between mutant domains and wild type of MeCP2 and when in the same cells, they are co-expressed.

Secondly, the safety and the properties of CNS bioavailability of the potentially small molecule activators of the X-chromosomes would need to be within acceptable limits. Thirdly, the dependency of expression and efficacy on dose and on prior proportion of cells already expressing the normal MeCP2 allele are presently unknown and would require assessment in detail.

Finally, a major potential problem with this approach is that it involves reactivation of the entire inactive X, with the additional potential for problems arising from gene dosage imbalances and pathological overexpression of many genes on the X (which X-inactivation evolved to combat). However, female mice that lack STC1, a primary X-inactivation factor, results in expression of genes from both X chromosomes and is associated with normal phenotype, so there may be previously unknown compensatory mechanisms (Bhatnagar et al., 2014). There is no knowledge so far as to whether similar compensatory mechanisms operate in humans. However, as the reactivation process of X-chromosome that is pharmacologically-induced is reversible, there are safety benefits with other interventions that are based on the gene.

The discussed possible solutions so far are associated with the challenge that the mutant allele's continuous presence in cells poses. The most attractive conceptually, but potentially challenging technically, is an approach that is gene-based which, at the genomic level would be to edit the mutation and turn it into a WT allele. The WT allele would perform, and the cell would function normally for the remainder of its life.

1.9 Summary and aim

Rett syndrome (RTT) is an uncommon neurodevelopmental disorder which occurs mainly in girls and is characterised by neurological, motor and social disabilities. *MECP2* gene mutations are responsible for > 95% of typical RTT cases. Mouse models of RTT have been helpful tools to assess RTT at the molecular and cellular levels and help to estimate the efficacy of possible therapeutic interventions. A previous study demonstrated the reversibility of the phenotype in mouse models after reactivation of endogenous *Mecp2*, which provides evidence that it may be possible to treat and or prevent RTT in patients. Behavioural testing in RTT mouse models has mostly focussed on the overt RTT-like phenotype while specific in-depth behavioural tests in RTT mouse models are relatively still lacking. A curative treatment for RTT has not yet been achieved, while the exact function of MeCP2 protein and its downstream effects are not clear. Therapeutic intervention at the *Mecp2* gene level either by reactivation of the inactive X chromosome, which contains a normal *Mecp2* allele or by viral-mediated delivery of exogenous copy of normal *Mecp2* offer attractive possible strategies. There are some studies that suggest AAV9-based delivery systems have potential for delivery of transgenes to the CNS and suggest a possible application for these vectors in exogenous delivery as a first step to developing gene therapy strategies in RTT models.

The main aim of this thesis was to investigate the effectiveness of gene therapy in mice modelling Rett syndrome by investigating AAV9-mediated delivery of *MECP2* in genetic mouse models of RTT. Specific goals were as follows:

1. To establish a battery of behavioural tests for mouse models of RTT encompassing cognition and memory, social activity, anxiety, and motor function specific in RTT mouse models.
2. To investigate dose escalation of scAAV/*MECP2* by systemic delivery in knock-in and knockout *Mecp2* mouse models. To further examine the transduction efficiency, pattern and levels of transgenic *Mecp2* expression and to ascertain the phenotypic consequences that result.
3. To explore the potential for overexpression-related toxicity and identify the tolerated threshold of MeCP2 overexpression.

4. To develop and test second-generation scAAV/*MECP2* vectors that reduce the toxicity and target neurons in the brain more efficiently than the first generation vectors.

5 To identify the best vector to use in long-term studies in female *Mecp2*^{+/-} mice.

The overall objective of my thesis research was thus to take the next step in developing a gene therapy-based approach in Rett syndrome.

Chapter 2 Material and Methods

2.1 General molecular biology materials

Table 2-1 General molecular biology reagents

Reagents	Supplier
DNAreleasey™	Anachem Ltd
Nuclease Free Water	Qiagen Cat.no 129115
Maxima Hot Start Green PCR Master mix (2X) Water	Thermo Scientific Part No. K1062
1kb DNA ladder	NEB Cat.no N3232
Rabbit anti-Myc	Abcam Cat.no ab9106
Mouse monoclonal anti-MeCP2	Sigma Cat.no WH0004204M1
Chicken anti-GFP	Abcam, Cat.no ab13970
Alexa Fluor 488 goat anti-mouse/rabbit (1/500)	Invitrogen Cat.no A-11029, A-11008
Alexa Fluor 546 goat anti-mouse/rabbit (Invitrogen; 1/500)	Invitrogen Cat.no A-11003, A-11010
Alexa Fluor 647, goat anti-mouse	Jackson ImmunoResearch Laboratories Cat.no 112-495-003JIR
DAPI nuclear stain (1/1,000)	Sigma Cat.no D9542

Table 2-2 Primer sequences and sizes of amplified PCR products for *Mecp2*^{+/-} and *Mecp2*^{+/-T158M} genotyping

Primer name	Nucleotide Sequence 5'-3'	Supplier
New P5	TGGTAAAGACCCATGTGACCCAAG	IDT
P7 WT REV	GGCTTGCCACATGACAAGAC	IDT
New P6 KO REV	TCCACCTAGCCTGCCTGTACTTTG	IDT
Ex4 Fwd A	GTTAGCTGACTTTACATAG	IDT
GFP Fwd 3A	GGACGAGCTGTACAAGTAA	IDT
Me2 UTR1	CGGGAAGCTTTGTCAGAGC	IDT

Table 2.3 List of AAV vectors

All the vectors listed below are viral vectors based on an AAV2 backbone. The encoded product of the vectors is human MeCP2_e1 protein. The vectors were manufactured and supplied by Dr Steven Gray, University of North Carolina (UNC), USA.

Name	Capsid	Promoter	Coding seq.	Tag	pA	Reference
1st generation	AAV9	MeP 229	<i>hMECP2_e1</i>	Myc	bGH	(Gadalla et al., 2013; Gray et al., 2011a)
Jet promoter	AAV9	Jet	<i>hMECP2_e1</i>	Myc	bGH	(Tornøe et al., 2002)
Short synthetic polyA	AAV9	MeP 229	<i>hMECP2_e1</i>	Myc	Short polyA	(Levitt et al., 1989)
Liver de-targeted	AAV9.47	MeP 229	<i>hMECP2_e1</i>	Myc	bGH	(Karumuthil-Melethil et al., 2016; Pulicherla et al., 2011)
426 promoter-RDH	AAV9	MeP 426	<i>hMECP2_e1</i>	Myc	Micro RNA binding	(Gadalla et al., 2017; Sinnott and Gray, 2017)

2.2 General solutions

Table 2.4 - General molecular biology solutions

Solution	Composition
5x DNA loading dye	SDS 0.5% (w/v), Xylene cyanol 0.25% (w/v), Bromophenol blue 0.25% (w/v) and FicollR 400 1.5% (w/v) in 3x TBE.
Ethidium Bromide	Stock solution: 10 mg/ml in H ₂ O (Sigma, E-1510)
0.5x TBE buffer	108 g Tris base, 55 g Boric acid, and 40 ml 0.5 M EDTA pH 8.0. then add H ₂ O to 2 L. Place the flask on a magnetic stirrer until completely dissolved
0.2 M Phosphate buffer (PB)	8.740 g of Sodium dihydrogen Phosphate (NaH ₂ PO ₄) in 1000 ml H ₂ O Add 20.442 g of diSodium Hydrogen Phosphate (Na ₂ HPO ₄) and mix well. Adjust pH to 7.4 with 1N NaOH
50% Ethanol	500 ml of 100% ethanol, 500 ml of distilled water
0.1 M PB	Made from a dilution of 0.2 M PB
0.3M Phosphate Buffered Saline Triton X-100 (PBST)	17.532 g of Sodium Chloride, 0.2M Phosphate Buffer 100 ml, 3ml of Triton X-100 and mix well.
10mM Sodium Citrate pH6.0	2.941 g of Trisodium Citrate, Adjust pH to 6.0 with 1N HCL

2.3 Mouse models of RTT

The Rett syndrome mouse models used in this research were *Mecp2* null (KO), which does not produce MeCP2 protein (Guy et al., 2001), and a knock-in model, *Mecp2*^{T158M} (T158M mice), which produces mutant MeCP2 carrying the p.T158M substitution (Brown et al., 2016). Both sexes were investigated.

In terms of KO line, these comprised of male WT (*Mecp2*^{+/y}), female WT (*Mecp2*^{+/+}) male hemizygous KO (*Mecp2*^{-/y}) and female heterozygous (*Mecp2*^{+/-}) mice. The generation of mutant mice in this line involved the cre-lox mediated excision of exon 3 (Guy et al., 2001). Hemizygous male KO mice develop a severe phenotype from about 4-6 weeks after birth. The body of this line also less than the WT at the same age (around 8-11 g at five weeks). Therefore, they need more taken care after the phenotypes start (around five-week of age). KO mouse model is suitable for short-term screening studies to enable the rapid assessment of the effects of putative therapeutic interventions on RTT-like phenotypes. In contrast to the hemizygous male mice, heterozygous female KO mice display RTT-like phenotypes with a later onset and more gradual progression. (Garg et al., 2013) The phenotype in female KO mice is milder and slow progress when compared with male KO mice, however, obviously opposite from the male is the bodyweight. The mostly of KO female mouse has overweight (>30 g at 8 weeks) when compared with the WT female (around 25 g). These KO female mice are a more accurate genetic model of RTT in females, most assessments have been conducted in male KO mice.

There are a number of common mutations causing Rett syndrome including missense mutations (p.R106W, p.R133C, p.T158M, and p.R306C) and nonsense mutations p.R168X, p.R255X, p.R270X, and p.R294X (Neul et al., 2008). In addition to using the *Mecp2*-KO line, experiments were also conducted using a *Mecp2*^{T158M} knock-in (KI) mouse, which models the most common mutation in RTT patients (Neul et al., 2008). This generates defective MeCP2 protein, harbouring the substitution of methionine for threonine at amino acid position 158 (T158M) in exon 4, which affects the DNA binding domain (MBD). This allele has GFP fused downstream of the mutant MeCP2 protein. The T158M hemizygous male mice show early-onset and severe RTT phenotypes as same as the KO male line, but the phenotype and the bodyweight is less severity than KO males (more

than 11 g at five weeks) (Brown et al., 2016). However, the close husbandry also is needed in this line. The heterozygous female T158M mice show the progression of the RTT-like phenotypes and overweight after 6-8 months as same as in the female KO mice (Brown et al., 2016).

2.3.1 source of the *Mecp2*-KO mouse and *Mecp2* T158M knock-in models

Both the *Mecp2* knock-out and the *Mecp2*-T158M knock-in mouse lines were created and supplied by Professor Adrian Bird's laboratory at the University of Edinburgh, UK.

2.3.2 Breeding strategy of *Mecp2*-KO and *Mecp2* T158M knock-in mice

At the University of Glasgow, the local *Mecp2*-KO line of was established and maintained by mating heterozygous female with WT males (C57BL/6 background) purchased from Harlan laboratories (Shardlow, UK). A similar strategy was adopted for the knock-in line by mating *Mecp2*^{+ / T158M} (C57BL/6 background) and WT males (C57BL/6). Mice were backcrossed onto a C57BL/6 background (>8 generations) and maintained on an inbred C57BL/6 background. The mice generated for experimental cohorts consisted of hemizygous *Mecp2*^{- / y} or *Mecp2*^{T158M / y} males and heterozygous *Mecp2*^{+ / -} or *Mecp2*^{+ / T158M} females together with their WT littermates as controls. Genders and genotypes of offspring from the *Mecp2*^{+ / -} or *Mecp2*^{+ / T158M} females mating with WT males are provided in table 2-5.

Table 2-5 Breeding scheme for *Mecp2*-KO and *Mecp2* T158M knock-in mice

lines	KO	T158M
Parents	Male WT <i>Mecp2</i> ^{+ / y} + Female <i>Mecp2</i> ^{+ / -}	Male WT <i>Mecp2</i> ^{+ / y} + Female <i>Mecp2</i> ^{+ / T158M}
Offspring	(1) Male WT <i>Mecp2</i> ^{+ / y} (2) Male Hemizygous <i>Mecp2</i> ^{- / y} (3) Female WT <i>Mecp2</i> ^{+ / +} (4) Female Heterozygous <i>Mecp2</i> ^{+ / -}	(1) Male WT <i>Mecp2</i> ^{+ / y} (2) Male Hemizygous <i>Mecp2</i> ^{T158M / y} (3) Female WT <i>Mecp2</i> ^{+ / +} (4) Female Heterozygous <i>Mecp2</i> ^{+ / T158M}

2.3.3 Ethic and husbandry

All work was conducted in accordance with the standards of the European Communities Council Directive (86/609/EEC) and under the authority of a project license under the UK Animals (Scientific Procedures) Act (1986). Mice were bred and housed at the University of Glasgow Biological Services main campus facilities. After weaning, all experimental mice of the same sex and parentage were caged together as litter mates (2-5 mice per cage). Bedding was changed twice a week. The mice were maintained on a 12-hour dark/light cycle and at 25 degree Celsius with free access to distilled water and standard rodent diet.

In some cases, symptomatic mice were provided with a supplement of soft diet (moistened rodent pellet) and baby food (Carnation®) if required.

2.3.4 Genotyping

2.3.3.1 DNA extraction and PCR genotyping

Ear punches were used to identify individual mice at weaning (3 weeks) and resultant ear punch biopsies were used for genotyping.

To extract DNA, each ear sample was placed into 20µl of DNA releasy (Anachem Ltd) for 5 minutes at 75°C in the PCR machine and then the temperature setting increased to 96°C for 2 minutes. Then hold this sample at 20°C.

PCR amplification for genotyping was carried in out in a GeneAmp thermal cycler (Applied Biosystems, UK; PCR system 9700) using reaction mixes and conditions given in Tables 2-6 and 2.7. For the KO line, primers P7 and P5 were employed to amplify the WT allele while primers-P6 and P5 were used to amplify the KO *Mecp2* allele. For the T158M line, primers Ex4 Fwd A and Me2 UTR1 were used to amplify the WT allele and primers GFP Fwd 3A and Me2 UTR1 were used for the *Mecp2* T158M allele. For the KO line, the PCR products produced by the P5/P7 primers (WT allele) are 416bp, and PCR products of the P5/P6 primer set (*Mecp2*-KO allele) are 470bp. For the *Mecp2*T158M line the PCR products are 107bp for the GFP Fwd 3A/ Me2 UTR1 primer set (WT allele), and 300bp for the Ex4 Fwd A / Me2 UTR1 primer set (*Mecp2*-T158M allele).

Table 2-6 PCR reaction setup for genotyping of *Mecp2*-null mice, *Mecp2*T158M mice and their WT littermates

Lines	KO	T158M
i. Extracting DNA	1 μ l	1 μ l
ii. Maxima Hot Start Green Master mix	13 μ l	13 μ l
iii. Nuclease Free Water	8 μ l	8 μ l
iv. Forward Primer	P5 1 μ l (0.4 μ M)	Ex4 Fwd A (0.4 μ M) for WT GFP Fwd 3A (0.4 μ M) for T158M
v. Reverse Primer	- P7 1 μ l (0.4 μ M) for WT	Me2 UTR1 (0.4 μ M)
	- P6 1 μ l (0.4 μ M) for KO	
Final Volume	24 μ l	24 μ l
Final Product (base pair)	WT allele: 416bp Mecp2-KO allele: 470bp	WT allele: 107bp Mecp2-T158M allele: 300bp

Table 2-7 Thermocycling conditions for genotyping

Step	Temperature (°C)	Time (seconds)
1) Initial Denaturation	95	240 (4 minutes)
2) Denaturation	95	30
3) Annealing	61	30
4) Extension	72	45
Repeat steps 2) to 4)	35 cycles	
5) Final extension	72	600 (10 minutes)
6) Hold	4	∞

2.3.3.2 Agarose gel electrophoresis

DNA molecules were separated by 1-2% agarose gel electrophoresis in 0.5 TBE. Agarose was dissolved by boiling and subsequent cooling down (~40°C). A final concentration of 200 ng/ml of ethidium bromide was added. Gels were then poured in a gel tray and allowed to set at room temperature for one hour. After PCR, products were loaded with 5X DNA loading dye and electrophoresed for one hour at 100-120 volts. An aliquot of a 100bp DNA ladder (1.5-2 µg) was also electrophoresed and used as a marker. Gels were imaged using a UV transilluminator (UV-TM-40; Upland, USA; wavelength 254nm) and photographed using a Canon digital camera (PC1192; Japan).

2.3.5 Allocating animals to experimental groups and blinding system

After genotyping each mouse, numbers of WT and mutant mice in each cage of littermates were balanced by humanely euthanizing excess WT mice at random. All the experimental mice used in the behavioural tests were identified uniquely (within each cage) via ear notches and given a new ID code by Biological Services staff, while any birth IDs were not visible thereafter. Experimenters were thus as blind to the genotype of each mouse in a cage of littermates as it was possible to be (mutant mice are often smaller and affected in somewhat obvious ways, but efforts were made to ignore any such signs). Original and new IDs for each mouse were sent by Biological Services staff to my supervisor, and unblinding for genotype was only carried out after all major data polishing steps had been completed and just before analyses.

For the gene therapy experiments, the blinding system were applied after the viral delivery in young adult mice. The experimenters did not know genotype and the treatment at the time of weekly weight and score the mice (moreover, for neonatal delivery, mice were sexed but genotype was unknown; unique ID codes were assigned at weaning and experimenters kept blind to genotype). When they died or an experimental end-point was reached, and tissues were collected and data processed before unblinding.

2.3.6 Phenotypic severity scoring and weight measurement

All the experimental mice (and stock mutant mice) underwent weekly observational phenotyping from weaning (postnatal day 33-35) onwards using an established scoring system for mice modelling Rett syndrome (Guy et al., 2007). There are six cardinal features that are recorded as RTT-like phenotypes and which can be used to monitor the disease trajectory in a semi-quantitative manner. These features are: breathing abnormality, bodily tremors, hind limb clasp, gait, mobility and general appearance. Each of these traits scores 2 for severe phenotype, 1 for mild phenotype and 0 for phenotype indistinguishable from WT **Table 2-8**. An aggregate severity score can be created from the total score of the above features which varies from 0-12. The breathing and tremors are observed whilst the mouse is standing still. Hind limb clasp is tested by suspending the mouse by the base of the tail with its forelimbs on a hard surface. (Gadalla et al., 2013; Garg et al., 2013; Guy et al., 2007; Robinson et al., 2012). Scoring was conducted blind to genotype. The score was also used to trigger humane endpoints, with animals culled due to severe breathing problems, severe overall condition or if the mice showed a 20% loss in bodyweight relative to peak bodyweight. At these end points, the mouse was euthanized humanely.

2.4 Behavioural tests

All scoring and behavioural tests were conducted, where possible, at the same time of day (range 10:00-16:00). All behavioural tests were conducted in the same dedicated procedure room. Multiple tests were conducted on individual mice; however, the mice were given one day of rest between each test. To eliminate potential residual odours and potential contaminants, 70 % ethanol was used to clean the apparatus.

Table 2-8 phenotyping score

Test Location	Phenotype	Score		
		0	+1	+2
On hand 	Tremor: Mouse observed while standing on the flat palm of the hand.	no tremor	intermittent mild tremor	continuous tremor or intermittent violent tremor
	Breathing: Movement of flanks observed while mouse is standing still.	normal breathing	periods of regular breathing interspersed with short periods of more rapid breathing or with pauses in breathing	very irregular breathing - gasping or panting
	General condition: Mouse observed for indicators of general well-being such as coat condition, eyes, body stance.	clean, shiny coat, clear eyes, normal stance	eyes dull, coat dull/ungroomed, somewhat hunched stance	eyes crusted or narrowed, piloerection, hunched posture

<p>On table</p> 	<p>Hindlimb clasp</p>	<p>legs splayed outwards</p>	<p>hindlimbs are drawn towards each other (without touching) or one leg is drawn in to the body</p>	<p>both legs are pulled in tightly, either touching each other or touching the body</p>
<p>In arena</p> 	<p>Mobility</p>	<p>as wild-type</p>	<p>reduced movement when compared to wild-type: extended freezing period when first placed on bench and longer periods spent immobile</p>	<p>no spontaneous movement when placed on the bench; mouse can move in response to a gentle prod or a food pellet placed nearby</p>
	<p>Gait abnormality</p>	<p>as wild-type</p>	<p>hind legs are spread wider than wild-type when walking or running with reduced pelvic elevation, resulting in a “waddling” gait</p>	<p>more severe abnormalities : tremor when feet are lifted, walks backwards or 'bunny hops' by lifting both rear feet at once</p>

2.4.1 Open field test

The open field test is an established measure of anxiety and motor function (Briellmaier et al., 2012; Choleric et al., 2001). The arena is an infra-red transparent Perspex box (40x40cm), where the mice were placed in the centre (in low but even light level) and recorded for 15 minutes while exploring the arena. During the test, the experimenter could not be seen by the mice. The activity of the mouse in the arena was continually monitored using an overhead digital infrared camera and tracked using Ethovision XT tracking software (Noldus, USA). The digital tracks produced by the mouse were subjected to off-line analysis using the software. The distance moved by each mouse over 15 mins was calculated.

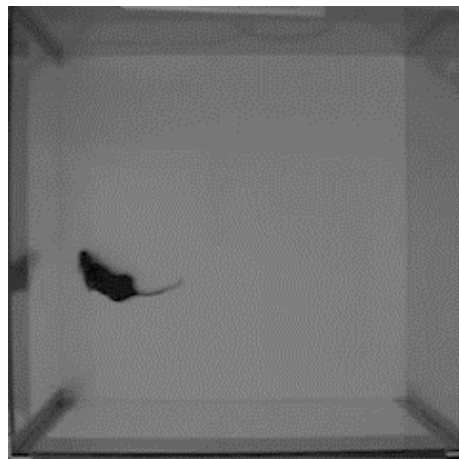


Figure 2.1 the open field arena which is recorded by IR camera. The arena is a square sized 40 cm x 40 cm and made from IR transparent black material

2.4.2 Novel object recognition test

The novel object recognition test was used to evaluate recognition memory in mice (Antunes and Biala, 2012; Li et al., 2012; Vogel-Ciernia et al., 2013; Vogel-Ciernia and Wood, 2014). Mice were placed in a 40cm x 40cm arena with new bedding and were allowed 10 minutes to habituate with the environment. The next day, mice were placed in the first arena with two objects that were identical (either two plastic figurines or two bottles) and permitted 10 minutes to explore the objects, enabling familiarity with them. Following a waiting period of an hour, the mouse was reintroduced into the area where one of the

objects had been replaced with a novel object that was unfamiliar to the mouse. Mouse exploratory activity and time spent sniffing were tracked using Ethovision XT tracking software (Noldus, USA). Latency to reach each object and time spent at respective objects were analysed offline. Time spent exploring each object was scored by an experimenter, blind to all conditions. A discrimination index was calculated as follows: (time exploring the novel object - time exploring familiar object)/total object exploration time *100.

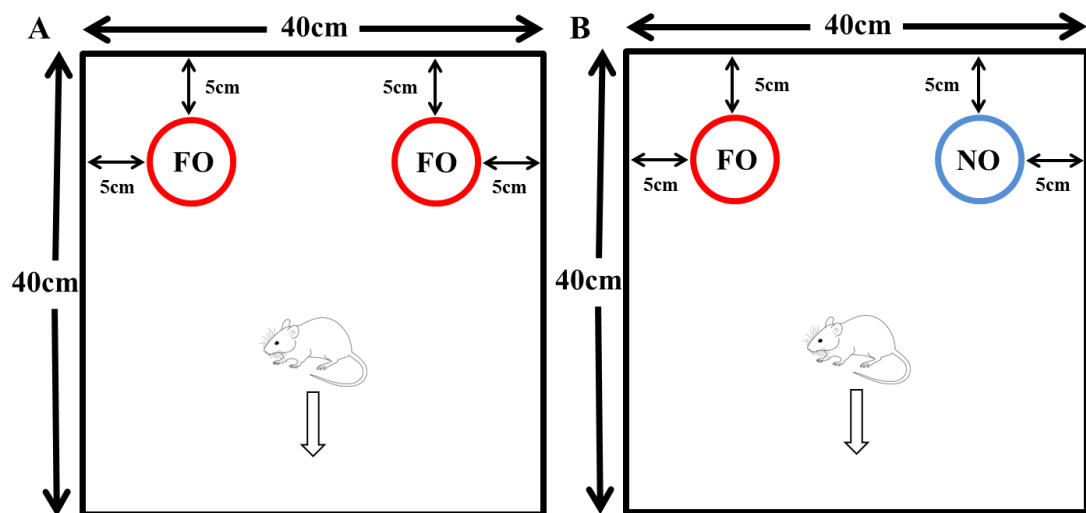


Figure 2.2 Novel object test phase and recognition training. (A) Mice were placed in the arena with two identical objects 5cm from each edge; mice explored for 10 minutes so that novel objects would become familiar objects (FO). (B) After a delay of one hour, the mice were placed in the arena with one object that is familiar from one novel object (NO) and the last trial (FO), placement of both were in the arena corners of 5cm x 5cm and was allowed 10 minutes for exploring. In both trials, the mice were placed facing away from the objects to avoid development of biased preference based on initial positioning relative to the objects.

2.4.3 Rotarod performance test

Motor learning and coordination were measured over three consecutive days using a rotarod device. On each day, each mouse was subjected to three experimental sessions separated by rest periods of 15 minutes. During each session, the rotating rod (Jones and Roberts Accelerating Rotarod 7650; Ugo Basile, Varese, Italy) was gradually accelerated over a time period of five minutes from 4 to 40 rpm (Briemaier et al., 2012). Mice were assessed by the time spent on the rotarod until falling, passively rotating or a maximum of 300 s had elapsed (Briemaier et al., 2012; Yang et al., 2012).

To evaluate motor skill learning, a steep learning curve was deployed, with assays conducted over 3 consecutive days, with 3 consecutive tests on each day. The results from the first day of testing were not included as this was a training session. The data from the two subsequent days were collected, and the mean of six trials (3 per day) was used as the data point for each mouse. These datapoints were compared between groups statistically.

2.4.4 Treadmill motor challenge test (Exercise tolerance)

Exercise endurance and fatigue were tested using a treadmill. Exercise capacity was investigated with the use of an accelerating elevated treadmill (Kemi et al., 2004). At the treadmill's base, an electrified grid provides a mild aversive stimulus (electric shock) when stood upon, acting as a deterrent in preventing mice from stopping for reasons that are motivational, to ensure the measurement of the true exercise capacity. The treadmill test was applied to the mice after two days of training on the treadmill. Treadmill speed was initially 10 cm/s with speed increasing every two minutes by 2 cm/s till it becomes impossible for mice to cope with the speed and they allow themselves passively to be subject to shock on the grid without returning to the treadmill. At this point, the trial was terminated, and the time was recorded.

2.4.5 Social interaction test

Mice were assessed for memory and social affiliation. Mice were placed in a three-chamber arena made from darkened plastic, as indicated in Figure 2.3. The subject mouse's bedding from its home cage was added to each arena in order to familiarize the mouse to the chamber and it was allowed 10 minutes exploring and interacting with the stranger and the familiar mice. An overhead digital camera was used in filming the analysis and the experiment with the use of Ethovision XT software. Zones were defined around the stranger and familiar mice and the time spent sniffing the other mice in their zone was collected (Moy et al., 2007; Nadler et al., 2004; Yang et al., 2012; Yang et al., 2011). A social novelty test was performed by introducing a new stranger mouse in the chamber and switching the familiar littermate to the other chamber. The time spent in each side chamber was analysed subsequently (Samaco et al., 2012).

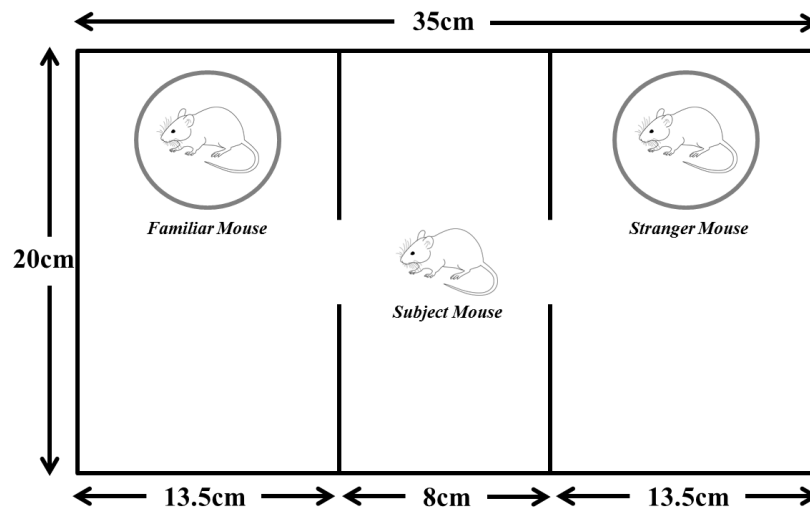


Figure 2.3 Setting up of Arena for social interaction test. Mice were placed in a three-chamber arena. The subject mouse was placed in the central chamber (8cm x 20cm). The chamber on the left (13.5cm x 20cm) housed a mouse that is a cage mate and is familiar to the subject. A stranger mouse was also housed in an adjacent chamber (13.5cm x 20cm) on the right. Both mice were contained in an aluminium mesh cylinder. The programme detected the mouse when it moved within 1cm of either stranger or familiar mouse cage. The arena in total was 35cm x 20cm.

2.4.6 Light/Dark box test

As a further test of anxiety levels, mice were subjected to a dark/light box test. This test relies on the mouse's natural tendency to avoid areas that are brightly lit; but also, its inner desire to explore new areas (Bourin and Hascoët, 2003; Brielmaier et al., 2012; Campos et al., 2013). Mice were maintained in the darkened test room for one hour prior to being transferred to the two-compartment test box (Figure 2.4). Mice were placed in the darkened third of the box that makes up a dark compartment. This was attached to the second compartment which is illuminated by an application on iPhone named "Photon Beard highlight" at 400 lux. The door connecting the two compartments was removed and the activity recorded for 10 minutes using an overhead digital camera (Panasonic CCTV camera, Model WV-BP334) and Ethovision XT tracking software. In the resulting video file, the dark and the light compartment were marked as separate zones and software was set up to calculate and track the transitions between the zones, the time point at which mice entered the light area and spent time in each zone.

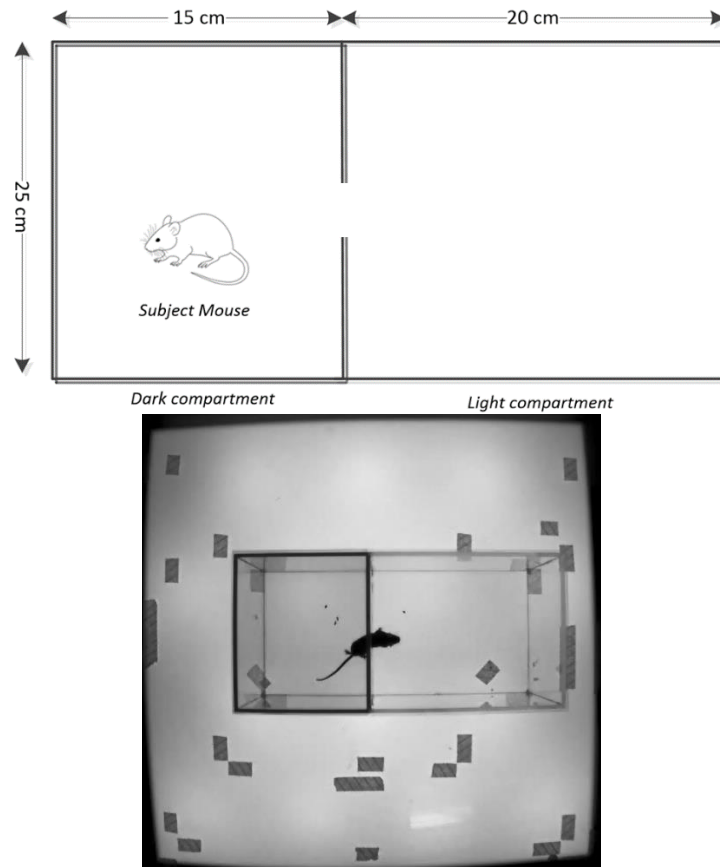


Figure 2.4 Two-compartment arena used in the light-dark box test. The arena consists of two IR, transparent compartments with a small 5cm x 7 cm channel which is connected to allow mice to move freely between them. The dark compartment with its lid, 20 cm x 25 cm x 25 cm, is made from IR transparent black plexiglass, and the light compartment diameter is 20 cm x 25 cm x 25 cm and it is made from clear material. Arrow indicates other experimental arena markers which the mouse cannot see. Mice usually explore when they are in an unfamiliar environment, but if the mouse is stressed, it always stays in the dark environment and has minimal movement.

2.4.7 Splash test

A final test for anxiety in the mice was to artificially stimulate grooming behaviour using the splash test (Piato et al., 2008; Yalcin et al., 2005; Yalcin et al., 2007). Each mouse was quickly sprayed twice until its coat was damp with a sucrose solution (10%) and then put back in its cage where it was then observed for grooming behaviour (Figure 2.5). Behaviour was recorded for 15 minutes using a Nikon D5200 camera. The performance of each mouse in terms of the observed behaviours was manually counted. Specific behaviours were measured after recording by a point system or counting scale every time the mouse shook itself, scratched, licked its hair, groomed its face, or dug into the bedding.



10% sucrose

Figure 2.5 This experiment is a test of mouse stress by observing the grooming behaviour in its home cage. A mouse was sprayed with a 10% sucrose solution that made the mouse feel discomforted which will provoke grooming behaviour in an unstressed mouse. In contrast if the experimental mouse is stressed it will not groom. The photo shows the mouse grooming itself in its own cage after being sprayed with sucrose solution.

2.4.8 Breathing test (Whole body plethysmograph)

Respiratory phenotypes were evaluated in conscious and unrestrained mice with a whole-body plethysmography apparatus (EMMS, Bordon, U.K.). Mice were placed in a Plexiglas chamber and left for 20 minutes to become familiar with the environment, and then their breathing was monitored for 30 minutes. To analyse differences in movement and grooming levels between groups, data was recorded while mice remained at quiet rest. A continuous bias airflow supply allowed the mouse to be kept in the chamber for extended periods of time.



Figure 2.6 Images of the whole-body plethysmograph used for assessment of the breathing phenotype. Mice were placed in plexiglass chambers with a source for air supply. Pressure changes were detected and analysed by a pressure transducer (EMMS, Bordon, U.K.) software.

The temperature and humidity of the air result in pressure changes as air enters and leaves the mice's lungs. The breathing pattern of the mouse was detected by a pressure transducer and was represented using a respiratory waveform. Then, breathing frequency, frequency variability (using the coefficient of variability of the waveforms) and the frequency of apnoeas (expiratory pauses more than three respiratory cycles in length) of the waveform pattern were analysed using pClamp 10.2 (Molecular Devices Inc., California, USA).

2.5 Adeno-associated viral vectors and Vector administration

2.5.1 Vector preparation

All recombinant AAV vectors were generated at the University of North Carolina (UNC) Gene Therapy Centre Vector Core facility ([website](#)). The vectors were of the self-complementary design (scAAV) which is scAAV2 ITR [inverted terminal repeat]-flanked genomes packaged into AAV9 or AAV9.47 serotype capsids (Clément and Grieger, 2016). Viral particle preps were produced from suspension HEK293 cells using proprietary methods developed by the UNC Gene

Therapy Vector Core. All MeCP2-expressing constructs utilized the human *MECP2_e1* coding region with a C-terminal Myc epitope tag unless stated otherwise. Viral particle preps were prepared in a final formulation of high-salt PBS (containing 350 mmol/L total NaCl) supplemented with 5% sorbitol. These were stored at -80° C.

Before each injection, the frozen scAAV9 viral particle aliquots were thawed and diluted to 100 µL in PBS/350 mm NaCl containing 5% sorbitol. Control injections were made using the same diluent lacking vector (“vehicle control”).

2.5.2 Vector injection

2.5.2.1 Tail vein injection

Tail vein injections were carried out by a member of biological services staff in biological services facilities. For injection into unanaesthetised young adult male mice, injections were made via the tail vein at 4-5 weeks of age. The mice were placed in a heating device to produce venodilatation and then were locked in a restraining device that allowed only the tail to protrude. 70% alcohol was applied to the tail and a 0.3ml Insulin syringe with a 30 g needle (MICRO-FINE PLUS U100 SYRINGE 0.3ml 30G) was used to deliver the viral vectors into the mouse tail vein. The maximum volume delivered was 100 µL. A member of Biological Services staff administered the tail vein injections.

2.5.2.2 Cerebroventricular injection into neonatal mice

For delivery of viral vectors to neonatal mice, unanaesthetised male littermates were sexed (0-3 days postnatally) and bilateral injections were made directly through the skin and into the brain. Bilateral injections of viral particle preps (~3 µL/site) were given using a 10 µL Hamilton syringe and 33 g needle (Finescience Instruments, Germany) connected via an ultra-narrow gauge silicone tube. Two people were required for the neonatal brain injection. Dr. Kamal Gadalla held the pup’s head in place and inserted the needle into the brain. I then slowly administered the viral vector by injection. The sites of brain injection were over the temporal cortex, ~1-2 mm lateral to the midline, ~1-2 mm anterior to lambda and at a depth of ~2mm, approximately coinciding with

the lateral ventricle. The injected pups were returned quickly to their home cage containing their mother and non-injected female littermates.

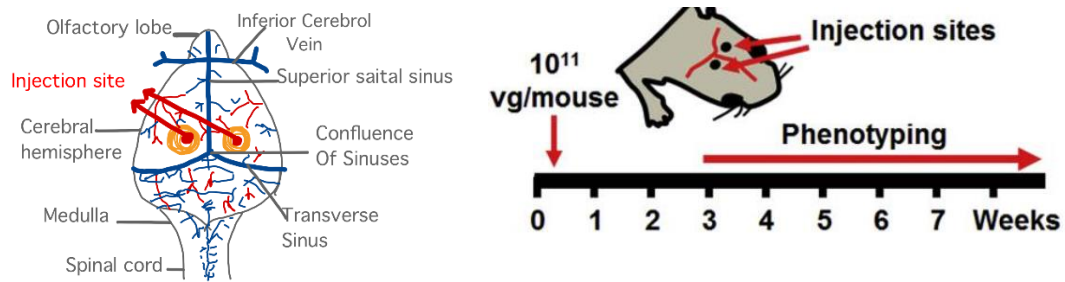


Figure 2.7 Cerebroventricular injection in neonatal mice (a) Neonatal injection site (b) Experimental design of direct brain injection to neonatal mice.

2.6 Immunohistochemistry (IHC)

After behavioral phenotyping was completed, mice were administered a non-recovery intraperitoneal injection of pentobarbitone (Euthatal 50 mg). On deep anaesthesia and absence of sensory reflexes, mice were transcardially perfused with 4% paraformaldehyde (0.1 mol/L PBS, pH=7.4). After 10 minutes (~50ml perfusion), brain and other tissues were removed and post-fixed in the same fixative for ~4 hours before being stored in PBS. Thereafter, 80 μ m sagittal sections of brain, spinal cord, and liver were obtained by using a vibrating microtome (Leica VT1200).

After that, the 80 μ m sections were incubated in 50% (v/v) ethanol in distilled water for 30 minutes and were washed three times in 0.3 mol/L PBS, followed by incubation in 10 mM sodium citrate (pH 6, 85°C, 30 minutes) for antigen retrieval. Sections were incubated in the blocking solution (5% normal goat serum in 0.3mol/L PBS with 0.3% Triton X-100) for 1 hour at room temperature. Samples were then incubated for 48 hours on a shaker at 4°C with the following primary antibodies: rabbit anti-Myc (Abcam, ab9106), mouse monoclonal anti-MeCP2 (Sigma, WH0004204M1), and chicken anti-GFP (Abcam, ab13970).

The primary antibodies were washed off (3 \times 0.3 mol/L PBST), and secondary antibodies were applied to the sections overnight at 4°C: Alexa Fluor 488 goat anti-mouse/rabbit (Invitrogen; 1/500), Alexa Fluor 546 goat anti-mouse/rabbit (Invitrogen; 1/500), Alexa Fluor 649, goat anti-mouse (Jackson ImmunoResearch

Laboratories, 112-495-003JIR). Finally, sections were incubated with DAPI nuclear stain (Sigma; 1/1,000) for 30 minutes at room temperature before mounting into standard glass microscope slides using Vectashield (Vector Laboratories)

2.7 Image analysis

Image stacks were captured using a Zeiss LSM710 or Zeiss Axiovert LSM510 laser confocal microscope (Zeiss) and were used to analyse expression patterns, transduction efficiency, and quantification of vector-derived MeCP2 levels within nuclei.

The z series were collected at 1 μm intervals through the section of interest using a 40 \times objective. To guard against biases due to limited antibody penetration, stack images were taken close to the surface of sections to a maximum depth of 20 μm . To evaluate transduction efficiency, images were captured as described earlier, and the proportion of DAPI-stained nuclei that were also Myc-immunopositive was calculated for random fields (n = 12 images per region: minimum of 4 images from each of a minimum of three mice) from sections of hippocampus (CA1 region), layer 5 of primary motor cortex, thalamus, hypothalamus, brain stem, and striatum.

The levels of vector-derived MeCP2 per nucleus in WT mice were quantified in confocal stacks (20 μm thick).

To calculate the percentage of transgenic expression in neurons, anti-Myc antibodies were used to identify the transduced cells, and the proportion of NeuN-immunopositive cells that were also Myc-immunopositive was determined. Anti-Mecp2 immunofluorescence was used for intensity measures of the cellular Mecp2 level. ImageJ software (<http://rsbweb.nih.gov/ij/>) was used to determine mean MeCP2-channel fluorescence intensity within transduced (Myc +ve) and non-transduced (Myc -ve) cells. Fluorescence in the DAPI channel was used to define the nuclear boundary.

2.8 Statistical analysis

GraphPad PRISM (GraphPad Software[®]) was used for statistical analysis as well as for graph presentation. To test differences between treatment groups, General linear models, One-way ANOVA, Two-way ANOVA, Student's t-test, and the Mantel-Cox test (for survival curves) were used as appropriate. $p < 0.05$ was used to define statistical significance. In multi-group post-hoc comparisons, multiple testing correction for pairwise tests among groups was applied using Tukey's post hoc analysis.

Some behavioural tests carried out on the viral-vector-treated mice in Ch.4 and Ch.5 involved measurements of individual mice on different occasions. Within-subject analyses could not be carried out for these as group size differed across time points as mice died or were humanely euthanized. For tests with multiple timepoints where group size remained the same across the timepoints, general linear model statistics were used to analyse all predictor variables including time.

Chapter 3 Validation of behavioural tests in RTT mouse models

3.1 Introduction

RTT mouse models have been an important tool in pre-clinical studies, assessing putative pharmacotherapies and genetic therapies in RTT syndrome, caused by mutations in the *MECP2* (methyl-CpG-binding protein 2) gene. Ever since it was first described in the 1960s by Andreas Rett (Rett, 1966) and after that by Bengt Hagberg in 1983 (Hagberg et al., 1983), there has been no effective treatment for RTT.

In vivo experiments in animal models, are a first, important and essential step to evaluate effectiveness and safety of putative therapies, to build up information about a possible drug, or other therapy, before moving onto the clinical phase. In RTT, human and mouse MeCP2 proteins are orthologs with 95% amino acid sequence identity. Loss of MeCP2 function in knock-out mice gives a comparable, although somewhat less severe, RTT like phenotype when compared to human patients (Brown et al., 2016; Guy et al., 2001). Hemizygous male mice with RTT do not show fatality at birth but show overt signs of neurological deficits from 3-8 weeks of age. Typically, the RTT-like phenotype in male mice is characterised by gait and motor impairments, breathing difficulties, tremor and severe regression leading to a premature death at 50-60 days of age. In comparison to hemizygous males, heterozygous female mice exhibit milder phenotype characterised by weight-gain, reduced activity and gait impairments. In addition, the RTT-like phenotype appears to progress at a slower rate in females than in males, with onset of overt signs at approximately 6 months of age, which is then followed by phenotypic stabilization and a normally non-altered lifespan (Chen et al., 2001; Guy et al., 2001).

Recently, a new knock-in (KI) model of RTT has been developed to test hypotheses about mutant MeCP2 function that cannot be tested using a KO model. Missense mutations in RTT vary in severity and there is evidence that the severity correlates between human and mouse models - for example, mutations that cause milder forms of RTT in human cases also seem to cause less severe

RTT-like phenotypes in mice (Brown et al., 2016). RTT-associated missense mutations localizing to the MBD, including p.T158M, the most common human *MECP2* missense mutation, have been shown to reduce DNA binding affinity and overall MeCP2 protein stability offering an explanation for the clinical phenotype (Ballestar et al., 2000; Brown et al., 2016; Neul et al., 2008; Yusufzai and Wolffe, 2000). The T158M mutation occurs in 12% of typical RTT cases and causes a methionine for threonine change at amino acid position 158 (Neul et al., 2008). The generated *Mecp2*^{T158M} mouse model mimics the human missense mutation and exhibits typical RTT-like features, offering a suitable model system in which to study the T158M mutation effects on RTT phenotype (Brown et al., 2016).

However, due to the RTT mouse model being recently generated, the line has only undergone basic phenotyping which has not been validated or extended in another laboratory. There is therefore a need to carry out additional behavioural tests in the KO and KI RTT mouse model using data on physical disability and validate the KI model for RTT. It is also of interest to provide baseline data for evaluation of potential treatments for preclinical efficacy. (Antunes and Biala, 2012; Grayson et al., 2015; Yang et al., 2015).

3.2 Study aims

The overall aim of the work in this chapter was to conduct a detailed characterisation of phenotypes and identify specific behavioural tests in both male and female RTT mouse models as a prerequisite for downstream testing of therapeutic interventions. This included testing the newly developed T158M line modelling the most common RTT-causing variant. The specific objectives of this chapter are:

- (1) To determine the characteristic baseline RTT-like phenotypes in male and female mice of different genotypes.
- (2) To modify behavioural tests for the RTT mouse to render them less sensitive to impaired mobility.

3.3 Method

To study the characteristics of RTT phenotypes, wild-type (WT), *Mecp2* knock-out (KO) and *Mecp2* T158M knock-in (KI) lines which were born during the same time period were examined. After weaning at three weeks, WT and mutant individual littermates of the same sex were caged together. Mice were weighed and scored for RTT-like phenotypes weekly (see section 2.3.4); however, during the experiments, if I found a mouse that had reached a severe condition, I applied the approved humane termination procedures. The results for each behavioral test were calculated from mice of the same genotype.

To carry out additional behavioural tests, mice whose total RTT-like score was more than three were used because they completely present the RTT-like phenotype. Males were used at approximately 5-6 weeks while females were tested from six months onwards. More than ten mice per genotype were used repeatedly in each behavioral test. Moreover, I attempted to include treat/reward for some of the initially planned experiments that it was needed in, for example, T-maze or touch screen (Arime and Akiyama, 2017; Kim et al., 2015; Leach and Crawley, 2018; Nichols et al., 2017; Sakai et al., 2016; Zeleznikow-Johnston et al., 2018). But, after fasting for 8 hours, the KI and KO mice did not eat any food during the test, thus precluding conclusions being drawn from these experiments. I had to remove tests from my initial plan that depended on the treat/reward mechanism.

In this chapter, the behavioural tests have been grouped under five categories: mobility and function, learning and cognitive processes, social interaction, stress, and breathing (see Chapter 2, Section 2.4). These were applied in a particular order. The mice were given at least one day's break before the next test. For the testing in male mice, initiation of testing for each mouse took place when it reached six weeks of age. Although the overall order of tests was standardised, different mice could enter the programme of tests at different points, as they were introduced into the programme whenever they reached the correct age and batches of mice were tested in the same way in the same week for reasons of efficiency. The order of tests for each mouse is given in table 3.1. For the female mice, every mouse had the range of tests administered in the same order, although some mice were not used in some tests as they did not

meet criteria for inclusion - details are given in table 3.2. Most of the behavioral tests were video recorded and analysed by Ethovision X program, except the breathing test which was recorded as a graph on the computer and the rotarod test which I recorded manually (with assistance from students I was supervising, after which we compared and confirmed our results with each other). I did not carry out a power calculation initially (see Section 2.3 for group size justification), but I did run post-hoc power calculations based on the group differences and variances observed (see Section 3.4.3.1 and Figure 3.5). For both the open-field and rotarod tests in male mice of the KO line (vs WT), I would have been able to see the observed difference at an alpha of $p < 0.05$ with 80% power at $n = 9$ per group. For the open field test in female heterozygotes, I would have had 80% power to detect the observed difference with $n = 21$ per group, but for the rotarod test, I would have been able to see the observed difference at an alpha of $p < 0.05$ with 100% power at $n = 13-15$ per group, as was in fact used. Thus, the results from this chapter are reliable due to the number of mice used and because the same conditions were applied in each experiment, as I mentioned above.

Table 3-1. Order of behavioural experiments performed for each mouse in behavioural tests in male RTT mouse models * means the mice were exclude from the experiment because its own condition.

Genotype	number	open field w/0 bedding	open field with bedding	NOR	Rotarod	Motor learning	treadmill	Social interaction	Light-dark	Splash test	breathing
WT	L590	1			2	3	4	5	age >7W		
WT	L619	1					2	3	4	5	age >7W
WT	L621	1					2	3	4	5	6
WT	L625	5			age >7W			1	2	3	4
WT	L630	5			age >7W			1	2	3	4
WT	L631	5			age >7W			1	2	3	4
WT	L633	5			age >7W			1	2	3	4
WT	L649	3			age >7W					1	2
WT	L656	3			age >7W					1	2
WT	L740				1	2	3	4	5	6	age >7W
WT	L742		1	2	3	4	5	6	7	8	age >7W
WT	L777	8			1	2	3	4	5	6	7
WT	T221		1	2	3	4	5	6	7	age >7W	
WT	T222		1	2	3	4	5	6	7	age >7W	
WT	T224		1	2	3	4	5	6	7	age >7W	

Genotype	number	open field w/0 bedding	open field with bedding	NOR	Rotarod	Motor learning	treadmill	Social interaction	Light-dark	Splash test	breathing
WT	T248		age >7W		1	2	3	4	5	6	7
WT	T249		age >7W		1	2	3	4	5	6	7
WT	T250		3	4	5	6	age >7W			1	2
WT	T251		3	4	age >7W					1	2
WT	T260		2	3	age >7W						1
WT	T261		1	2	age >7W						
WT	T262		1	2	age >7W						
WT	T263		1	2	age >7W						
WT	T295		1	2	age >7W						
WT	T302			1	age >7W						
WT	T306			1	age >7W						
WT	T307			1	age >7W						
WT	T310			1	age >7W						
	Total	10	11	15	10	10	11	15	14	15	13
Mecp2 ^{-/-}	L588	1			2	3	4	5	dead		
Mecp2 ^{-/-}	L589	1			2	3	4	5	age >7W		
Mecp2 ^{-/-}	L595	1			2	3	4	5	6	age >7W	
Mecp2 ^{-/-}	L596	1			2	3	4	5	6	age >7W	
Mecp2 ^{-/-}	L603						1	2	3	4	age >7W
Mecp2 ^{-/-}	L620						1	2	3	4	age >7W
Mecp2 ^{-/-}	L660		4	5	age >7W				1	2	3
Mecp2 ^{-/-}	L666		4	5	age >7W				1	2	3
Mecp2 ^{-/-}	L667		4	5	age >7W				1	2	3
Mecp2 ^{-/-}	L668		4	5	age >7W				1	2	3
Mecp2 ^{-/-}	L739		1	2	dead						
Mecp2 ^{-/-}	L741	7			1	2	3	4	5	video not record	6
Mecp2 ^{-/-}	L745	8			1	2	3	4	5	6	7
Mecp2 ^{-/-}	L746	8			1	2	3	4	5	6	7
Mecp2 ^{-/-}	L756	2						1			
Mecp2 ^{-/-}	L757	1						2	x	x	3
Mecp2 ^{-/-}	L776	2			3	4	dead				1
Mecp2 ^{-/-}	L778	2			3	4	5	6			1
Mecp2 ^{-/-}	L779		video not rec	1							
Mecp2 ^{-/-}	L781		1	2							
Mecp2 ^{-/-}	L782		1	2							
Mecp2 ^{-/-}	L788		1	2							
Mecp2 ^{-/-}	L790		1	2							
Mecp2 ^{-/-}	L792		1	2							
Mecp2 ^{-/-}	L793		1	2							
Mecp2 ^{-/-}	L640						1	2	3	dead	
Mecp2 ^{-/-}	L641						1	2	dead		
Mecp2 ^{-/-}	L650	dead						1	2	3	4
Mecp2 ^{-/-}	L651		4	5	age >7W				1	2	3

Genotype	Mouse number	openfield w/0 bedding	openfield with bedding	NOR	Rotarod	Motor learning	treadmill	Social interaction	Light-dark	Splash test	breathing
Mecp2 ^{-/-}	L657		4	5	age >7W				1	2	3
Mecp2 ^{-/-}	L659		4	5	age >7W				1	2	3
	Total	11	14	15	9	9	12	15	16	12	14
Mecp2 ^{T158M/y}	T223	1		x	2	3	4	age >7W			
Mecp2 ^{T158M/y}	T252	1		x	2	3	4	5	age >7W		
Mecp2 ^{T158M/y}	T256	1		x	2	3	4	5	age >7W		
Mecp2 ^{T158M/y}	T257	1		x	2	3	4	5	age >7W		
Mecp2 ^{T158M/y}	T264	1		x	2	3	4	5	age >7W		
Mecp2 ^{T158M/y}	T271	1		x	2	3	4	5	6	7	8
Mecp2 ^{T158M/y}	T274		age >7W				1	2	3	4	5
Mecp2 ^{T158M/y}	T292		age >7W				1	2	3	4	5
Mecp2 ^{T158M/y}	T293		age >7W				1	2	3	4	5
Mecp2 ^{T158M/y}	T296		age >7W				1	2	3	4	5
Mecp2 ^{T158M/y}	T301		5	6	age >7W			1	2	3	4
Mecp2 ^{T158M/y}	T308		5	6	age >7W			1	2	3	4
Mecp2 ^{T158M/y}	T309		5	6	age >7W			1	2	3	4
Mecp2 ^{T158M/y}	T323		3	4	5	6	age >7W			1	2
Mecp2 ^{T158M/y}	T324		3	4	5	6	age >7W			1	2
Mecp2 ^{T158M/y}	T327		3	4	5	6	age >7W			1	2
Mecp2 ^{T158M/y}	T329		x	3	4	5	age >7W			1	2
Mecp2 ^{T158M/y}	T332		x	3	4	5	age >7W			1	2
Mecp2 ^{T158M/y}	T333		x	3	age >7W					1	2
Mecp2 ^{T158M/y}	T337		x	3	age >7W					1	2
Mecp2 ^{T158M/y}	T339		x	3	age >7W					1	2
Mecp2 ^{T158M/y}	T343		x	2	age >7W						1
	Total		6	12	11	11	12	12	8	16	17

Table 3-2. Order of behavioural experiments performed for each mouse in behavioural tests in female RTT mouse models - * means the mice were humanely euthanized to collect tissue.

genotype	Mouse number	Open field	NOR	Rotarod	Motor learning	treadmill	Social interaction	Light-dark	Splash test	breathing
WT	L610	1	2	3	4	5	6	7	8	9
WT	L611	1	2	3	4	5	6	7	8	9
WT	L624	1	2	3	4	5	6	7	8	9
WT	L627	1	2	3	4	play behaviour	6	7	8	9
WT	L642	1	2	3	4	5	6	7	8	9
WT	T268	1	2	3	4	5	6	7	8	9
WT	T272	1	2	3	4	5	6	7	8	9
WT	T280	1	2	3	4	5	6	7	8	9
WT	T337	1	2	3	4	5	6	7	8	9
WT	T390	1	2	3	4	play behaviour	6	7	8	9
WT	T393	1	2	3	4	5	6	7	8	9
WT	T407	1	2	3	4	5	6	7	8	9
WT	T409	1	2	3	4	5	6	7	8	9
Total		13	13	13	13	11	13	13	13	13
Mecp2 ^{+/-}	L102	1	2	3	4	Overweight, did not move	6	*	*	*
Mecp2 ^{+/-}	L607	1	2	3	4	5	6	*	*	*
Mecp2 ^{+/-}	L609	1	2	3	4	Overweight not move	6	*	*	*
Mecp2 ^{+/-}	L613	1	2	3	4	Overweight not move	6	*	*	*
Mecp2 ^{+/-}	L623	1	2	3	4	5	6	*	*	*
Mecp2 ^{+/-}	L628	1	2	3	4	Overweight not move	6	7	8	9
Mecp2 ^{+/-}	L643	1	2	3	4	5	6	7	8	9
Mecp2 ^{+/-}	L644	1	2	3	4	5	6	7	8	9
Mecp2 ^{+/-}	L646	1	2	3	4	5	6	7	8	9
Mecp2 ^{+/-}	L678	1	2	3	4	5	6	7	8	9
Mecp2 ^{+/-}	L679	1	2	3	4	Overweight not move	6	7	8	9
Mecp2 ^{+/-}	L84	1	2	3	4	5	6	7	8	9
Mecp2 ^{+/-}	L85	1	2	3	4	5	6	7	8	9
Mecp2 ^{+/-}	L89	1	2	3	4	5	6	7	8	9
Mecp2 ^{+/-}	L98	1	2	3	4	5	6	7	8	9
Total		15	15	15	15	10	15	10	10	10
Mecp2 ^{+/-} /T158M	T253	1	2	3	4	5	6	7	not used	8
Mecp2 ^{+/-} /T158M	T254	1	2	3	4	5	6	7	not used	8
Mecp2 ^{+/-} /T158M	T255	1	2	3	4	5	6	7	not used	8
Mecp2 ^{+/-} /T158M	T267	1	2	3	4	5	6	7	not used	8
Mecp2 ^{+/-} /T158M	T273	1	2	3	4	Overweight not move	6	7	not used	8
Mecp2 ^{+/-} /T158M	T279	1	2	3	4	5	6	7	8	9
Mecp2 ^{+/-} /T158M	T323	1	2	3	4	5	6	7	8	9
Mecp2 ^{+/-} /T158M	T325	1	2	3	4	Overweight not move	6	7	8	9
Mecp2 ^{+/-} /T158M	T334	1	2	3	4	Overweight not move	6	7	8	9
Mecp2 ^{+/-} /T158M	T335	1	2	3	4	5	6	7	8	9
Mecp2 ^{+/-} /T158M	T336	1	2	3	4	5	6	7	8	9
Mecp2 ^{+/-} /T158M	T352	1	2	3	4	5	6	7	8	9
Mecp2 ^{+/-} /T158M	T391	1	2	3	4	5	6	7	8	9
Mecp2 ^{+/-} /T158M	T392	1	2	3	4	5	6	7	8	9
Mecp2 ^{+/-} /T158M	T408	1	2	3	4	5	6	7	8	9
Total		15	15	15	15	12	15	15	10	15

3.4 Results

3.4.1 RTT model genotyping by PCR

To achieve an adequate number of mice in each experimental cohort two colonies of mice representing KO and KI RTT mouse models were established by crossing heterozygous female mice (*Mecp2*^{+/-} and *Mecp2*^{+/*T158M*}) with WT male mice (both on a C57BL/6 background). PCR genotyping was carried out after offspring were weaned and separated into cages. The results of an example of a genotyping experiment as shown in Figure. 3.1, demonstrating hemizygous, heterozygous and WT individuals in both lines.

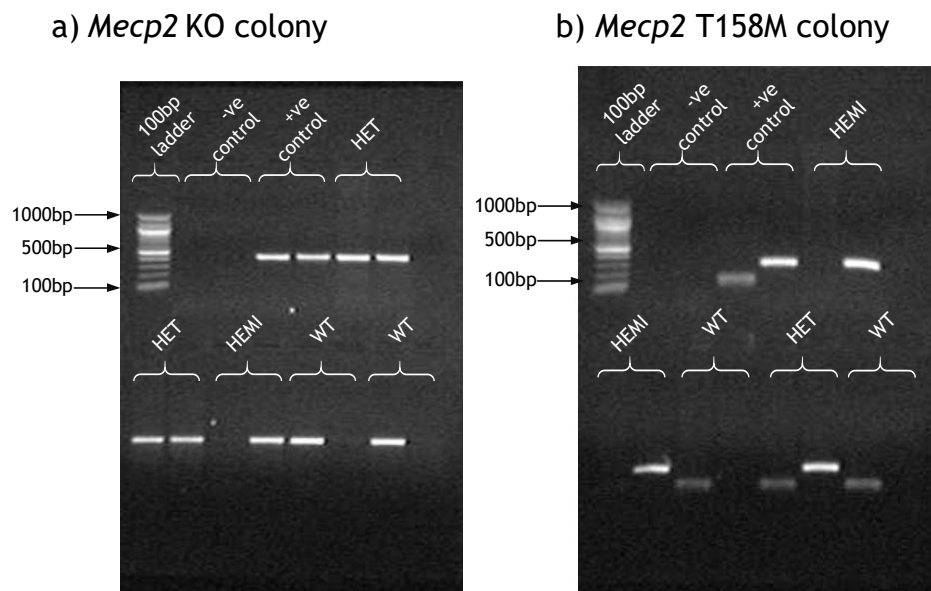


Figure 3.1 Results of PCR genotyping of wild-type, hemizygous and heterozygous mice from both lines; *Mecp2* KO and *Mecp2*^{T158M}. Genotype for each individual is represented in two neighboring gel lanes indicated by brackets. Genomic DNA of known heterozygous female mouse was used in a PCR as a positive control and nuclease-free water instead of DNA was used in a PCR as a negative control. (A) Genotyping results for the *Mecp2* KO line. Common forward primer, and wild-type and mutant reverse primers were used to amplify DNA fragments from the wild-type *Mecp2* allele (416bp) and the *Mecp2* KO allele (470bp). (B) Genotyping results for the *Mecp2* T158M line. WT and mutant forward primers and a common reverse primer were used to amplify DNA fragments from wild-type *Mecp2* allele (107bp) and *Mecp2*^{T158M} allele (300bp). Genotypes of selected individuals are indicated above the brackets; WT - wild-type, HEMI - hemizygous male, and HET - heterozygous female.

3.4.2 Phenotype severity assessment in KO and KI mice

All the experimental mice, both mutant and WT, were assessed using a standardised and widely adopted phenotype scoring system (Brown et al., 2016; Derecki et al., 2012; Gadalla et al., 2013; Gadalla et al., 2017; Guy et al., 2007) weekly from the age of four weeks in males and six months in females.

Hemizygous and heterozygous mice of each line exhibited RTT-like characteristics, mostly reduced mobility and gait abnormalities and, in rare cases, breathing difficulties and tremor. Some wild-type mice showed stop/start movements and therefore scored 1 for mobility. The aggregate severity score, as shown in Figure 3.2, was significantly different in mutant and wild-type individuals.

Due to the different age of onset and severity of progression of the RTT-like phenotype by sex, I separated the mice in the main analysis into male and female. In both male and female mice, I compared the characteristics of male WT with male KO and male KI. All symptomatic (scoring more than 2) and WT male mice at age 6-8 weeks were compared. Symptomatic female mice were compared with WT in the same way when RTT-like phenotypes were present after 6 months.

3.4.2.1 Male

In males, the RTT-like phenotype is observable from 4-5 weeks (Brown et al., 2016; Guy et al., 2001). In this experiment I used symptomatic mice, aged 6-7 weeks. In males, phenotype severity score differed significantly between KO, WT and KI (Aggregate severity score; WT 0.14 ± 0.36 ; *Mecp2*^{T158M/y} 2.06 ± 1.05 ; *Mecp2*^{-/y} 0.69 ± 0.85 ; **** = P<0.0001; Figure 3.2a). *Mecp2*^{T158M/y} and *Mecp2*^{-/y} also showed significantly different body weights from each other (Average body weight; WT 21.68 ± 2.33 ; *Mecp2*^{T158M/y} 17.85 ± 2.83 ; *Mecp2*^{-/y} 14.98 ± 2.11 ; **** = P<0.0001; Figure 3.2b). *Mecp2*^{-/y} is more severe than KI.

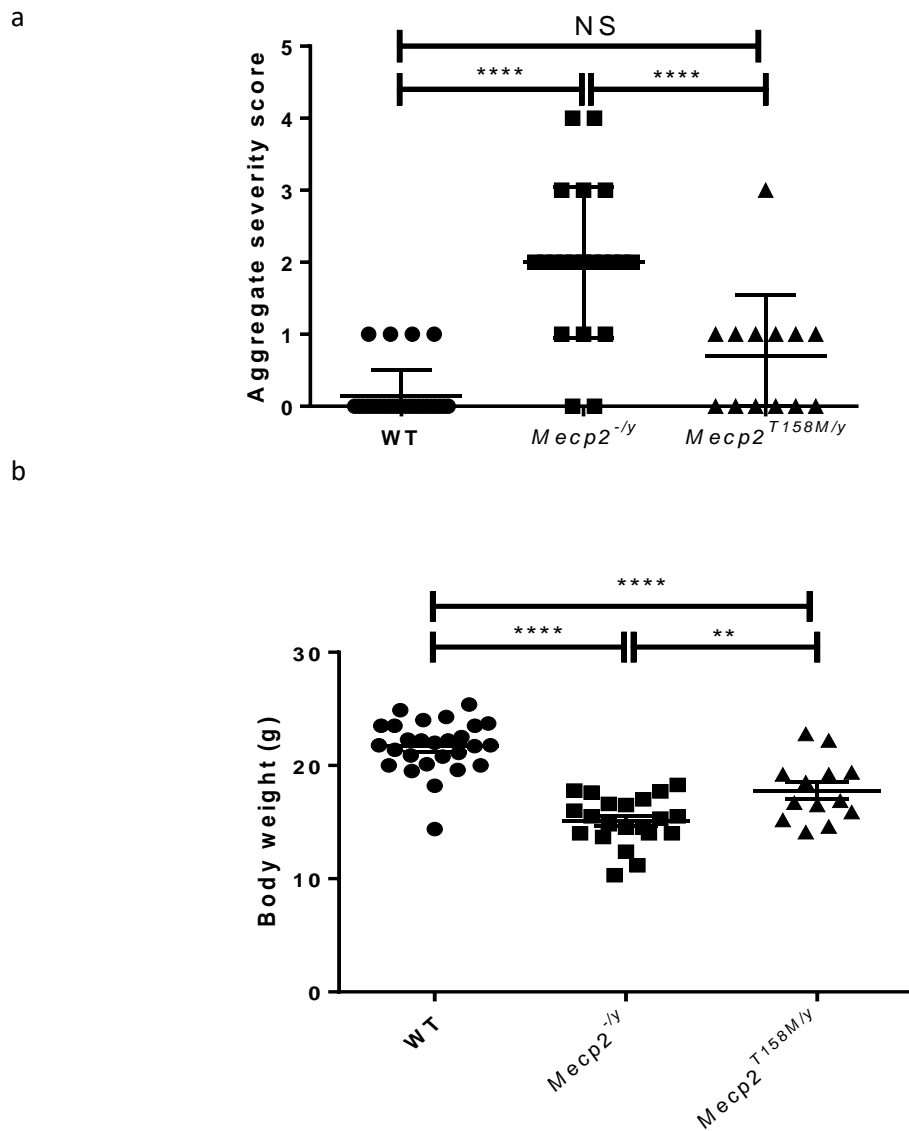


Figure 3.2 Composite body weight measurements and severity score in wild-type, $Mecp2^{-/-}$ and $Mecp2^{T158M/y}$ mice (a) Graph showing the RTT-like phenotype severity score comparisons the age at 6 weeks. (b) Graph showing bodyweight comparisons the age at 6 weeks. WT (n=26), $Mecp2^{-/-}$ (n=20), and $Mecp2^{T158M/y}$ (n=13). Data presented as mean \pm SEM. Statistical test results: (a) ANOVA test, $F(2, 58) = 34.99$, $p < 0.0001$ (b) ANOVA test, $F(2, 58) = 47.64$, $p < 0.0001$ Tukey's post-hoc tests: **** = $P < 0.0001$; ** = $p < 0.01$, ns = non-significant.

3.4.2.2 Female

In females, the onset of RTT starts at 6-8 months with the age range in this group being much wider than that in the males.

For the aggregate severity score in my experimental symptomatic mice aged between 6-8 months, both *Mecp2*^{+/-} and *Mecp2*^{+/*T158M*} mice present significantly higher than the WT (Aggregate severity score; WT 0.00 ± 0.00; *Mecp2*^{+/*T158M*} 2.06 ± 1.16; *Mecp2*^{+/-} 2.06 ± 0.96; **** = P<0.0001; Figure 3.3a). The trend in body weight differences between genotype does not mirror that of the males. WT body weight is significantly lower than both mutants (Average body weight; WT 24.34 ± 2.86; *Mecp2*^{+/*T158M*} 29.00 ± 4.38; *Mecp2*^{+/-} 29.19 ± 4.29; ** = P<0.01; Figure 3.3b).

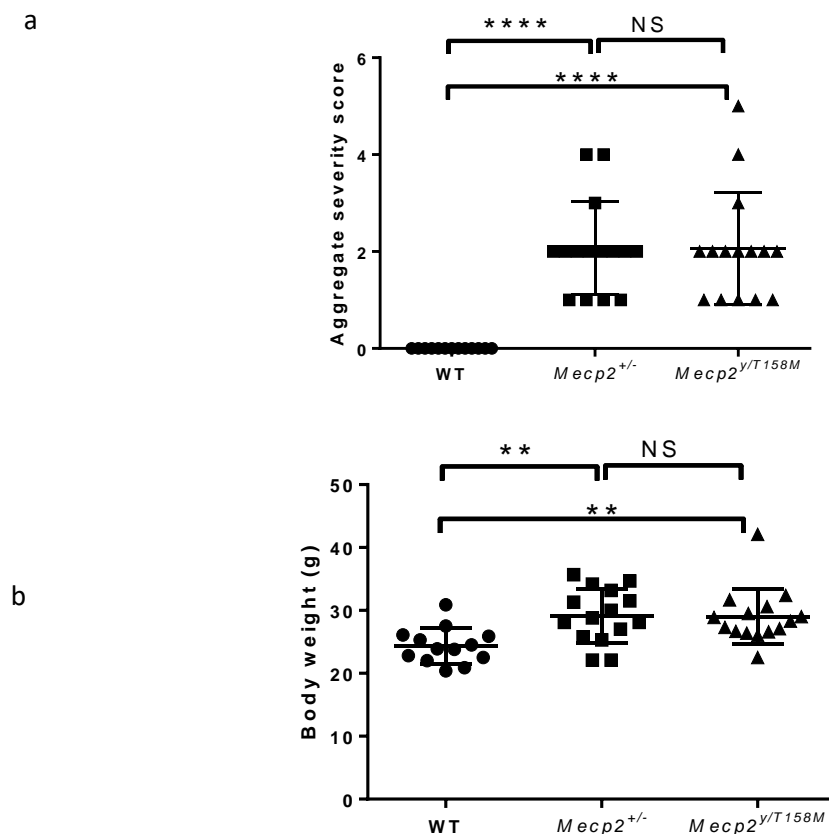


Figure 3.3 Composite body weight measurements and severity score in wild-type, *Mecp2*^{+/-} and *Mecp2*^{+/*T158M*} female mice (6-8 months old). (a) Graphs showing RTT-like phenotype severity score; (b) Graph showing bodyweight. WT (n=13), *MeCP2*^{+/-} (n=15) and *MeCP2*^{+/*T158M*} (n=15). Data presented as means ± SEM. Statistical test results: (a) ANOVA test, F (2, 40) = 24.31, p < 0.0001 (b) ANOVA test, F (2, 40) = 6.549, p = 0.0035 Tukey's post-hoc tests: ** = p<0.01, **** = p<0.0001 ns = non-significant.

3.4.3 Establishment and validation of detailed behavioural tests in the male RTT mouse models

To optimize additional behavioural tests I used WT, KO and KI male mice to characterise the baseline of each genotype and to validate the experiment and to indicate the robustness of the genotypes.

Before testing I weighed the mice and scored them for RTT-like aggregate severity. Mice with complete mobility impairment (scoring 2 for mobility) were excluded from these experiments. All animals had a one-day recovery period between phenotyping experiments.

3.4.3.1 Open field test

Mice were placed into the centre of the 40x40cm arena and allowed to move freely and explore for 15 minutes. To examine movement and mobility, compiled recorded footage was analysed using Ethovision XT10. Figure 3.4 shows distance moved for the WT and KO mice in the presence and absence of bedding.

The *Mecp2*^{-/y} mobility was very impaired in the open-field arena. However when I placed bedding from the mouse homecage into the arena, the mobility of *Mecp2*^{-/y} increased (distance moved ; no bedding 939.70 ± 560.79 cm; with bedding 1494.03 ± 571.75 cm; * = p<0.05; figure 4.5a), whereas the wild-type did not change significantly (distance moved; no bedding 2259.68 ± 609.24 cm; with bedding 2861.66 ± 780.08 cm; figure 4.5b) Because of this result, I incorporated bedding in to other tests to counter the effect of reduced mobility of KO and KI mice performance.

The result of the locomotor activity test between the genotypes in the open-field arena with bedding shows that there were no significant differences found in the other pairwise comparisons. (Distance moved; WT 2861.65 ± 780.08 cm; *Mecp2*^{T158M/y} 2263.17 ± 1039.88 cm; *Mecp2*^{-/y} 1494.03 ± 571.75 cm; *** = P<0.001; Figure 3.5)

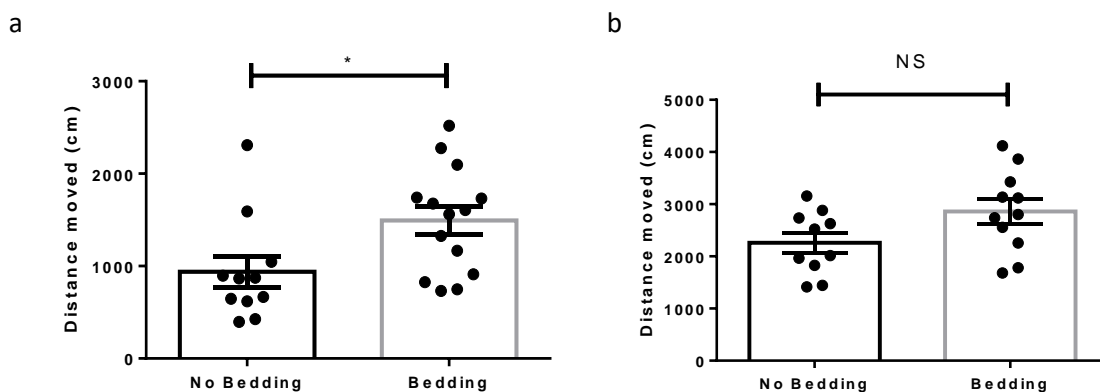


Figure 3.4 The comparison of locomotor assessment in wild-type and *Mecp2*^{-/-} male mice in open field arena with and without bedding. Column plot showing average group values (mean \pm SEM) for distance moved in *Mecp2*^{-/-} (a) and WT (b). *Mecp2*^{-/-} without bedding (n=11) and *Mecp2*^{-/-} with bedding (n=14). WT without bedding (n=10), WT with bedding (n=11). Data presented as mean \pm SEM. Statistical test results: (a) *t*-test, $t=2.432$, $DF=21.81$ * = $p<0.05$ (b) *t*-test, $t=1.980$ $DF=18.6$; NS = not significant

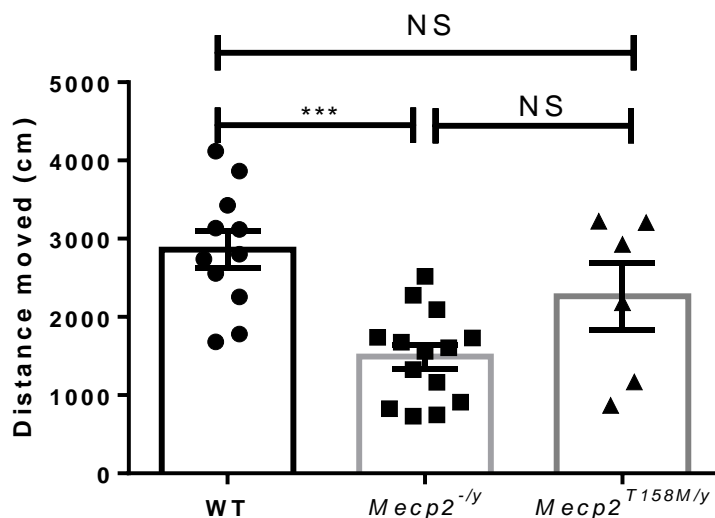


Figure 3.5 The general locomotor assessment in WT, *Mecp2*^{-/-} and *Mecp2*^{T158M/y} male mice. Column plot showing average group values (mean \pm SEM) for distance moved with bedding in WT, *Mecp2*^{-/-} *Mecp2*^{T158M/y}. WT (n=11) *Mecp2*^{-/-} (n=14) and *Mecp2*^{T158M/y} (n=6); Data presented as mean \pm SEM. Statistical test results: One-way ANOVA test, $F(2, 28) = 10.37$, $p=0.0004$ Tukey's post hoc test: *** = $p<0.001$

3.4.3.2 Novel object recognition test

To examine the learning and memory of the mice, I conducted the novel object recognition test as shown in chapter 2. However, I modified the test by extending the time allowed for the mice to explore the test section and the added objects. After analyzing the data for the exploration time in the test period between 10 and 15 minutes, RTT mice benefitted from the additional 5 minutes that the 15-minute period allowed for exploration due to their mobility problems.

The results were expressed as a discrimination index. WT mice spent a significantly greater proportion of their time exploring the novel object than the *Mecp2*^{-/y} mice. While the *Mecp2*^{T158M/y} mice showed no difference in time spent with the novel object compared with the other lines (% of time spent with novel object; WT 25.02 ± 19.24; *Mecp2*^{T158M/y} 3.60 ± 25.83; *Mecp2*^{-/y} 0.53 ± 30.85; * = P<0.05; Figure 3.6)

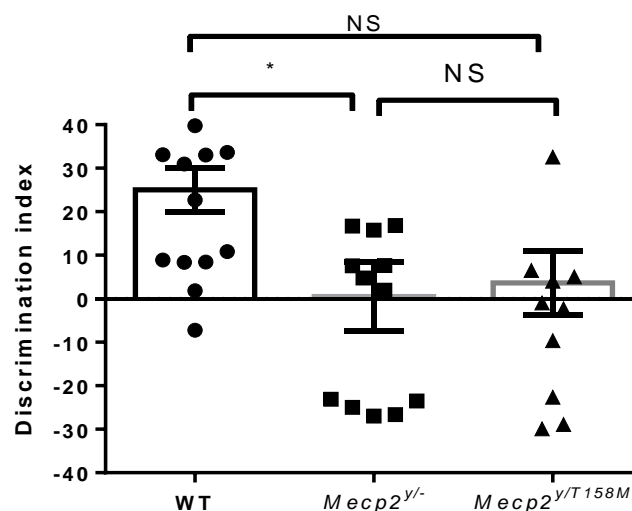


Figure 3.6 Discrimination index for learning and cognition baseline in novel object recognition test in WT, *Mecp2*^{-/y} and *Mecp2*^{T158M/y} male mice in 15 minutes. Column plot shows group average (mean ± SEM) for the proportion of time spent with the novel object compared with the familiar object. WT (n=15), *Mecp2*^{-/y} (n=15) and *Mecp2*^{T158M/y} (n=12). Data presented as mean ± SEM. Statistical test results: One-way ANOVA test, F (2, 39) = 3.936, ANOVA p=0.027; Tukey's post hoc test: * = p<0.05

3.4.3.3 Rotarod test

Rotarod tests were used to measure motor function and balance. The average time on the rod was compared between groups. The end of the experiment occurred when the mouse dropped off or rolled with the rod.

The results showed that the wild-type mice stayed on the rod significantly longer than both *Mecp2^{-/y}* and *Mecp2^{T158M/y}* (Time on rod; WT 247.83 ± 45.76 sec; *Mecp2^{T158M/y}* 132.14 ± 42.83 sec; *Mecp2^{-/y}* 122.87 ± 42.87; **** = P<0.0001; Figure 3.7). However, there is no difference of motor function between mutant lines in this experiment (figure 3.7). Most of WT male mice generally showed good performance, however a small number in the WT group refused to run and instead jumped off the rod.

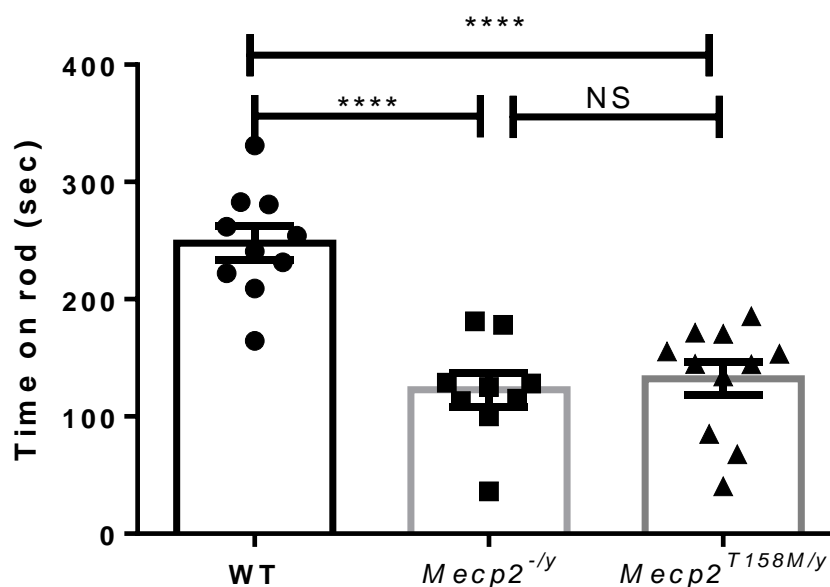


Figure 3.7 Rotarod performance of WT, *Mecp2^{-/y}* and *Mecp2^{T158M/y}* male mice using rotarod machine. Column plot showing average group values (mean ± SEM) of duration on a rod. WT (n=10), *Mecp2^{-/y}* (n=9) and *Mecp2^{T158M/y}* (n=11). Data presented as mean ± SEM. Statistical test results: One-way ANOVA test, F (2, 27) = 23.41, ANOVA p < 0.0001. Tukey's post hoc test: **** = P<0.0001

3.4.3.4 Motor learning

To evaluate motor learning skills, the average time spent on the rod on each day were compared. There were significant differences in the rotarod performance between WT, *Mecp2*^{-/y} and *Mecp2*^{T158M/y}. Only WT showed motor learning, as demonstrated by increased time on the rod from days one to three (Average time on rod WT: day one 214.83 ± 55.28.04 sec; day two 223.42 ± 60.82 sec; day three 257.89 ± 94.94 sec Figure 3.8) while *Mecp2*^{-/y} and *Mecp2*^{T158M/y} showed similar performance with no significant improvement in their motor learning, (Average time on rod *Mecp2*^{-/y}: day one 104.5 ± 33.91 sec; day two 117.50 ± 36.14 sec; day three 134.57 ± 54.68 sec Figure 3.8); (Average time on rod *Mecp2*^{T158M/y}; day one 123.5 ± 51.07 sec; day two 134.0 ± 55.54 sec; day three 130.4 ± 54.78 sec Figure 3.8). *Mecp2*^{-/y} mice remained on the rod for a shorter time than both the other lines.

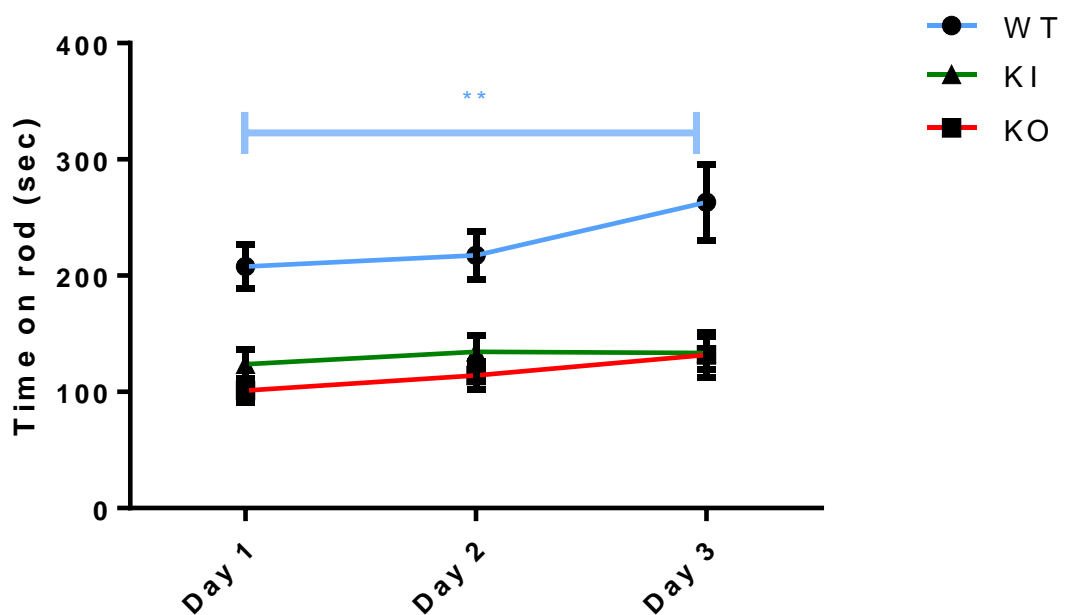


Figure 3.8 Motor learning curve of WT, *Mecp2*^{-/y} and *Mecp2*^{T158M/y} male mice using rotarod machine over 3 days. Line plot showing daily average group values (mean ± SEM) of duration on a rod WT (n=17), *Mecp2*^{-/y} (n=9) and *Mecp2*^{T158M/y}; Data presented as mean ± SEM. Statistical test results: General Linear model, F(2) = 15.248, P = <0.001; Paired Samples Test (WT Day1-Day3 ** = P<0.01

3.4.3.5 Treadmill motor challenge test

To investigate potential differences in exercise fatigue between phenotypes, the treadmill motor challenge test was used. The time was recorded until the mouse was unable to maintain locomotor activity on the treadmill. Results show that the mean time on the treadmill for WT mice was significantly greater than for both mutant groups. (Time spent on treadmill; WT 1077.93 ± 268.14 sec; *Mecp2*^{T158M/y} 843.62 ± 176.00 sec; *Mecp2*^{-/y} 479.70 ± 165.63 sec; **** = $P < 0.0001$; Figure 3.9). This equated to a 56% and 25% reduction from the WT levels of performance in the KO and KI line respectively. The KO line was more severely affected than the KI.

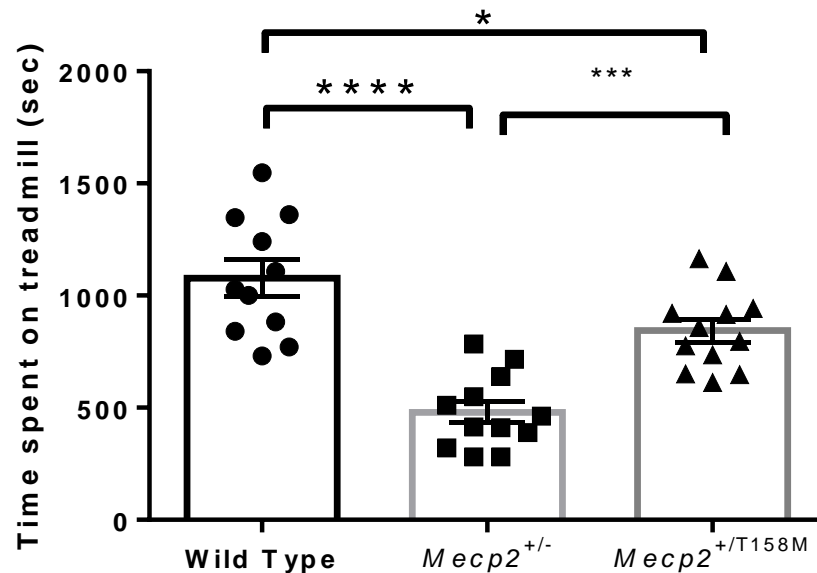


Figure 3.9 Treadmill motor test of WT, *Mecp2*^{-/y} and *Mecp2*^{T158M/y} male mice. WT (n=11), *MeCP2*^{+/-} (n=12) and *MeCP2*^{+/T158M} (n=12). Data presented as mean \pm SEM. Statistical test results: One-way ANOVA test, $F(2, 32) = 24.70$, $p < 0.0001$. Tukey's post hoc test: * = $p < 0.05$; *** = $p < 0.001$, **** = $P < 0.0001$.

3.4.3.6 Social interaction test

Tests of social novelty preference provide robust and quantifiable measures of social withdrawal and social cognition deficits analogous to that observed in intellectual disability (Schaevitz et al., 2010). To gain further access to the social interactions of the mouse, the freely accessible, 3-chamber arena, smaller than a standard arena, with bedding from home cages included, was used in this experiment. The cage-mate and another mouse that the test mouse had had no prior interaction with were placed in a small cage on the other side of the arena. Generally, WT mice showed an interest in the unfamiliar mouse (Time WT spent with stranger; Stranger 1 (familiar) 53.35 ± 23.58 sec; Stranger 2 (unfamiliar) 146.47 ± 65.49 sec; $*** = p < 0.001$; Figure 3.10). The results clearly show that both mutants showed significantly less interaction with the unfamiliar mouse than the WT.

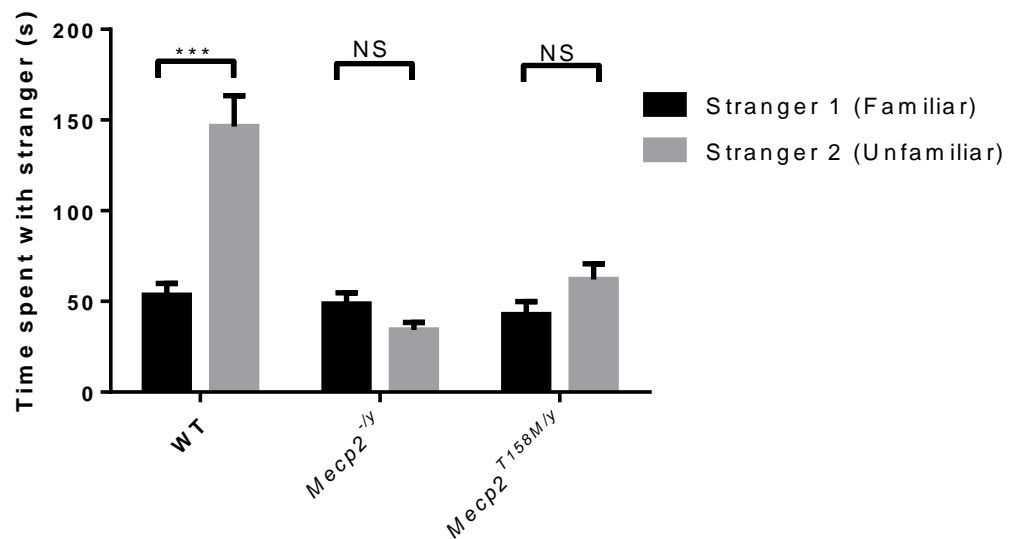


Figure 3.10 Social interaction test in WT, *Mecp2*^{-/-} and *Mecp2*^{T158M/y} male mice. The graph shows average group values (mean \pm SEM) of time spent with their cage-mate and unknown mouse. WT (n=15), *Mecp2*^{-/-} (n=15), *Mecp2*^{T158M/y} (n=12). Statistical test results: Stratified t-tests were carried out for each genotype separately. For WT, $t=4.554$, $DF=24$, $*** = p < 0.001$ between Stranger 1 (Familiar) and Stranger 2 (Unfamiliar); For both mutant lines, there was no significant difference in time spent with each stranger mouse.

3.4.3.7 Light-dark box test

To estimate anxiety levels, the standard light-dark test (Bourin and Hascoët, 2003; Brielmaier et al., 2012; Campos et al., 2013; Li et al., 2015) was applied in this experiment. The mouse was placed in the dark chamber that had free access to the light chamber (20 x 13.5, 50 lumen). The video tracking data were analyzed by Ethovision XT10 programme. The normal mice explored the new arena, while the mice experiencing anxiety stayed in the dark. The results show that WT were more enthusiastic to explore the light chamber than both mutants. (Latency to enter the light area; WT 38.16 ± 34.12 ; *Mecp2*^{T158M/y} 83.84 ± 113.35 ; *Mecp2*^{-/y} 102.22 ± 67.52 ; * = P<0.05; Figure 3.11a). There is no significant difference between all groups in time spent in the dark (Time spent in the dark; WT 233.56 ± 16.43 ; *Mecp2*^{T158M/y} 207.60 ± 57.48 ; *Mecp2*^{-/y} 196.94 ± 65.49 ; Figure 3.11b).

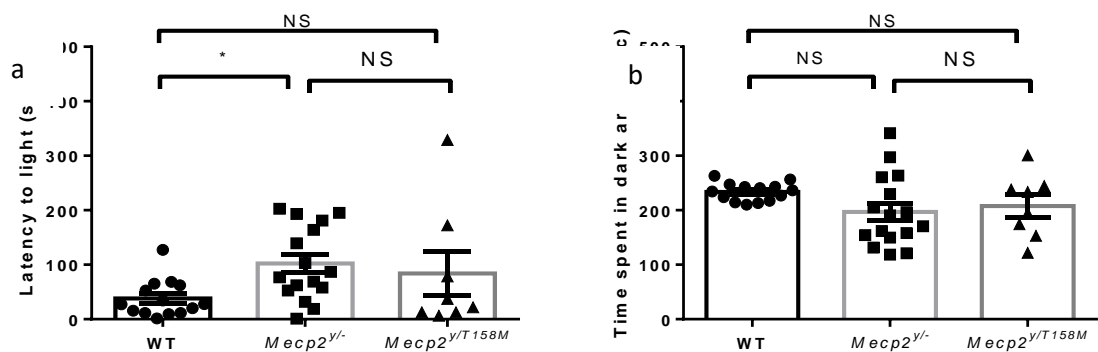


Figure 3.11 Exploration and anxiety-related measures of the light-dark test in WT, *Mecp2*^{-/y} and *Mecp2*^{T158M/y} in male mice. Column plot shows average group values (mean ± SEM) for the (a) latency to enter the light area and (b) time spent in dark area. WT (n=14), *Mecp2*^{-/y} (n=16), *Mecp2*^{T158M/y} (n=8). Statistical test results: (a) One-way ANOVA test, $F(2, 35) = 3.175$, $p = 0.0541$, Tukey's multiple comparison test. * = $p < 0.05$ in WT vs. *Mecp2*^{-/y}; (b) One-way ANOVA test, $F(2, 35) = 1.976$, ANOVA $p = 0.1538$.

3.4.3.8 Splash test

A splash test was also used to measure anxiety. Anxiety levels can be observed without the mobility factor which impedes the RTT mice in previous tests. In the test, there was no difference in grooming time between each group. (Grooming count; WT 168.73 ± 61.78 ; *Mecp2*^{T158M/y} 217.62 ± 72.26 ; *Mecp2*^{-/y} 220.08 ± 61.96 ; Figure 3.12).

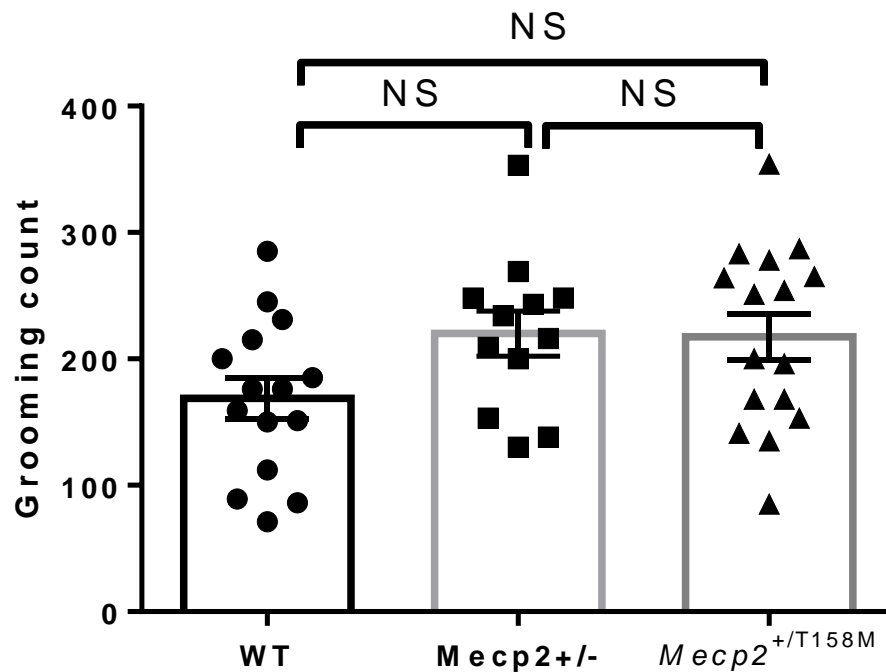


Figure 3.12 Anxiety assessment of wild-type, *Mecp2*^{-/y} and *Mecp2*^{T158M/y} male mice by splash test. Column plot shows average group values (mean \pm SEM) for time grooming. WT (n=15), *Mecp2*^{-/y} (n=12), *Mecp2*^{T158M/y} (n=16). Statistical test results: One-way ANOVA test(2, 40), $F(2, 40) = 2.805$, $p=0.0724$.

3.4.3.9 Breathing test

Abnormal breathing patterns and apneas were investigated using the whole-body plethysmography apparatus (EMMS, Bordon, UK) in 8-week-old male mice.

Mecp2^{-/y} and *Mecp2*^{T158M/y} mice presented with apneas, a characteristic of an erratic breathing pattern (figure 3.13a), in contrast to the regular breathing pattern in WT. The number of apneas in *Mecp2*^{-/y} was significantly higher than WT and KI. (Apneas; WT 0.00 ± 0.00; *Mecp2*^{T158M/y} 0.36 ± 0.51; *Mecp2*^{-/y} 1.19 ± 0.69; **** = P<0.0001; Figure 3.13b).

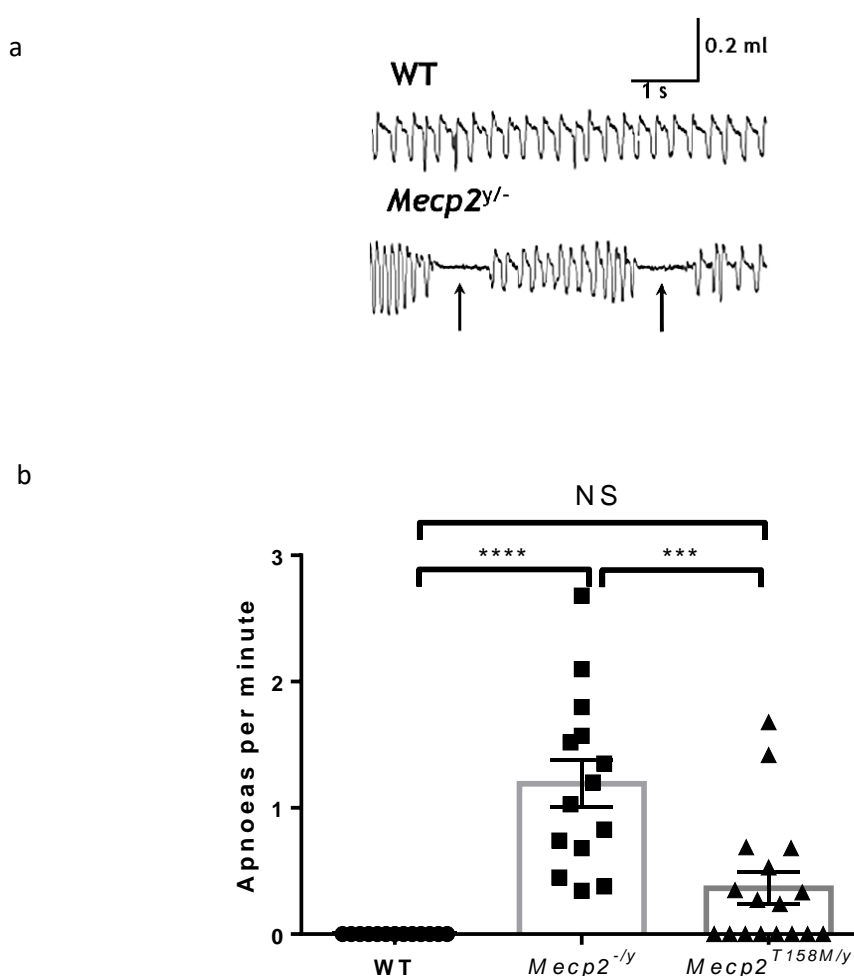


Figure 3.13 Persistent breathing phenotype in WT, *Mecp2*^{-/y}, *Mecp2*^{T158M/y} male mice. (a) Representative whole-body plethysmograph traces showing regular and erratic breathing patterns/apneas (arrows) in WT and null mouse respectively. (b) apnoeas per minute. WT (n=13), *Mecp2*^{-/y} (n=14), *Mecp2*^{T158M/y} (n=17). Data presented as mean ± SEM. Statistical test results: One-way ANOVA F (2, 41) = 20.17, p<0.0001, Tukey's post hoc comparison: **** = p<0.0001 (WT vs *Mecp2*^{-/y}), *** = p<0.001 (*Mecp2*^{-/y} vs *Mecp2*^{T158M/y}),.

3.4.4 Establishment and validation of detailed behavioural tests in female RTT mouse models

To investigate this set of behavioural tests in female mice, I used 6-month-old, symptomatic heterozygous *Mecp2*^{+/-} and *Mecp2*^{+/*T158M*} mice and their WT cage-mates, as previously conducted with the male mice. (3.4.3) Before testing, I weighed and scored the mice for RTT-like aggregate severity. It should be considered that the increased body weight phenotype in heterozygous females that may affect mobility in some tests.

3.4.4.1 Open field test

The mobility tests started with an open field test over 10 minutes, which showed the mobility of the *Mecp2*^{+/-} mice was significantly lower than that of the WT mice. However, the *Mecp2*^{+/*T158M*} line showed no significant difference in the distance moved compared to both the other lines. (Distance moved; WT 3835.01 ± 1287.53 cm; *Mecp2*^{+/*T158M*} 2630.00 ± 1129.58 cm; *Mecp2*^{-/*y*} 2593.34 ± 1509.10 cm; * = P<0.05; Figure 3.14)

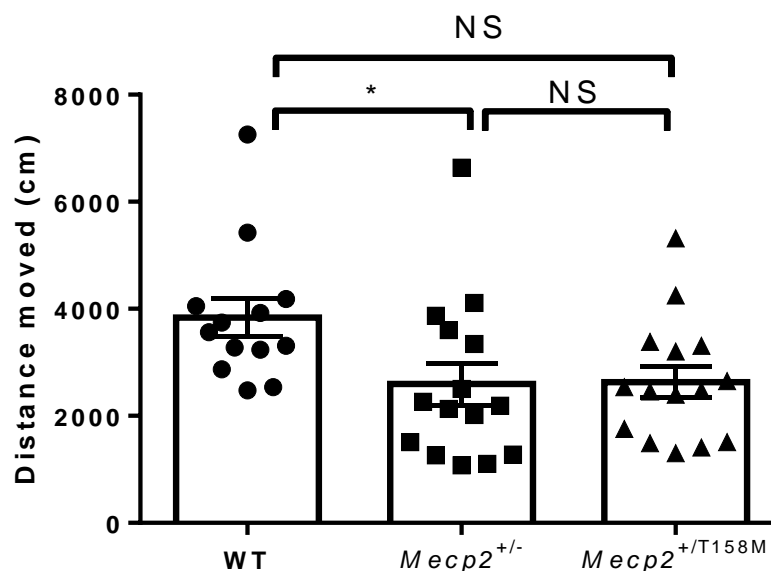


Figure 3.14 The general locomotor assessment in WT, *Mecp2*^{+/-}, *Mecp2*^{+/*T158M*} female mice. Column plot showing average group values (mean ± SEM) for distance move in WT, *Mecp2*^{+/-} and *Mecp2*^{+/*T158M*}. WT (n=13), *Mecp2*^{+/-} (n=15) and *MeCP2*^{+/*T158M*} (n=15); Statistical test results: One-way ANOVA test F (2, 40) = 3.901, p=0.0283, Tukey's post hoc comparison: * = p<0.05.

3.4.4.2 Novel object recognition test

The novel object recognition test data were analyzed using the discrimination index. The results showed that the WT could significantly recognize the familiar object and spent more time exploring the novel object than the *Mecp2*^{+/-} and *Mecp2*^{+/^{T158M}} (% of time spent with novel object; WT 24.19 ± 6.71; *Mecp2*^{+/^{T158M}} 3.12 ± 8.24; *Mecp2*^{+/-} -2.12 ± 14.11; **** = P<0.0001; Figure 3.15).

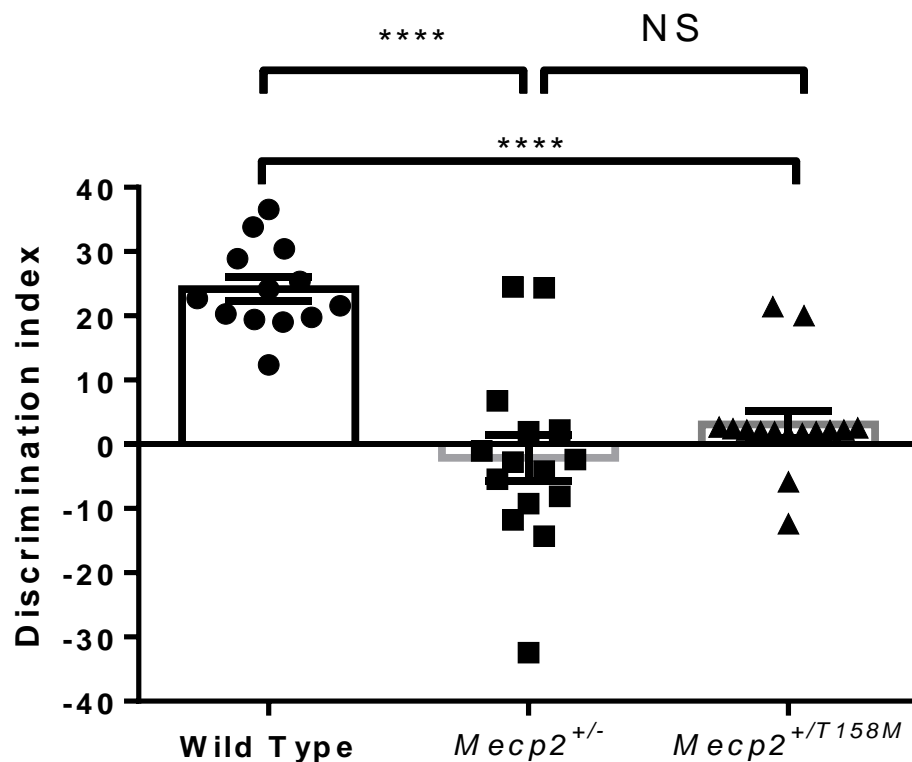


Figure 3.15 Discrimination index of learning and cognition baseline in novel object recognition test in WT, *Mecp2*^{+/-}, *Mecp2*^{+/^{T158M}} female mice in 15 minutes. Column plot shows group average (mean ±SEM) for the proportion of spending time with the novel object comparing with the familiar object. WT (n=13), *Mecp2*^{+/-} (n=15) and *Mecp2*^{+/^{T158M}} (n=15). Statistical test results: One-way ANOVA test, F (2, 40) = 24.74, p<0.0001, Tukey's post hoc comparison **** = p<0.0001 (WT vs *Mecp2*^{+/-} and *Mecp2*^{+/-} vs *Mecp2*^{+/^{T158M}}).

3.4.4.3 Rotarod test

To further study the motor functions and balance in female RTT mice, the rotarod test was used.

The results clearly show that both the *Mecp2*^{+/-} and *Mecp2*^{+/^{T158M}} lines displayed a phenotype. Time on the rod of *Mecp2*^{+/-} and *Mecp2*^{+/^{T158M}} mice was significantly lower than the WT (Time on the rod; WT 243.07.25 ± 48.78 sec; *Mecp2*^{+/^{T158M}} 129.46 ± 56.59 sec; *Mecp2*^{+/-} 116.67 ± 37.03 sec; **** = P<0.0001; Figure 3.16). The mutant groups were not significantly different from each other.

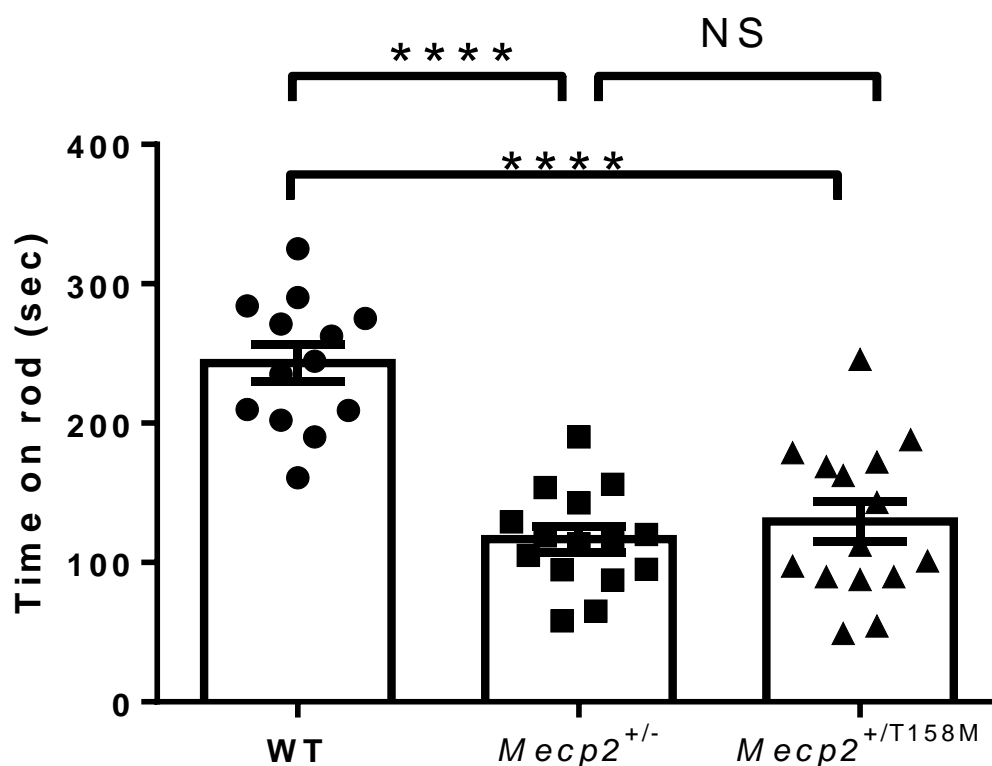


Figure 3.16 Motor deficit test of WT, *Mecp2*^{+/-}, *Mecp2*^{+/^{T158M}} female mice using rotarod machine. Column plot showing average group values (mean ±SEM) of duration on a rod. WT (n=13), *Mecp2*^{+/-} (n=15) and *Mecp2*^{+/^{T158M}} (n=15). Statistical test results: One-way ANOVA test, F (2, 40) = 30.44, p<0.0001 Tukey's post hoc comparison :**** = p<0.0001 (WT vs *Mecp2*^{+/-} and *Mecp2*^{+/-} vs *Mecp2*^{+/^{T158M}}).

3.4.4.4 Motor learning

Motor learning skills were tested in females using the rotarod. Mice of all three genotypes, particularly WT mice, showed some ability to learn, with improvement between Day 1 and Day 3. (Average time on rod WT; day one 224.85 ± 49.25 sec; day two 249.83 ± 54.72 sec; day three 254.52 ± 39.53 sec, Figure 3.17). *Mecp2^{T158M/y}* also showed similar improvement (average time on rod *Mecp2^{+/T158M}*; day one 117.96 ± 56.21 sec; day two 131.06 ± 62.46 sec; day three 139.36 ± 52.48 sec Figure 3.17). Moreover, *Mecp2^{+/-}* mice generate an improvement in their motor skills between day 1 and day 2. (average time on rod *Mecp2^{+/-}*; day one 108.99 ± 36.81 sec; day two 121.1 ± 40.90 sec; day three 119.91 ± 34.44 sec Figure 3.17)

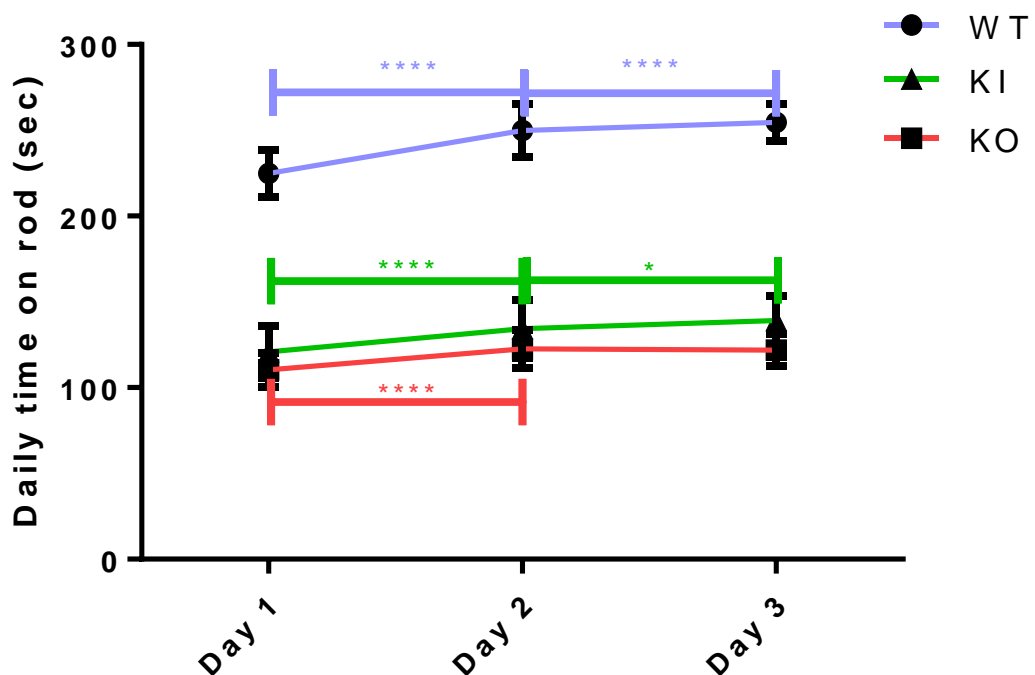


Figure 3.17 Motor learning curve of WT, *Mecp2^{+/-}*, *Mecp2^{+/T158M}* female mice using rotarod machine over 3 days. Line plot showing average group values (mean ± SEM) of duration on a rod. WT (n=13), *Mecp2^{+/-}* (n=15) and *Mecp2^{+/T158M}* (n=15). Data presented as mean ± SEM. Statistical test results: General Linear model, $F(2) = 27.919$, $P < 0.001$; Paired Samples Test **** = $P < 0.0001$ (WT Day1-Day3 and Day1-Day3, KI Day1-Day2, and KO Day1-Day2), * = $P < 0.01$ (WT Day1-Day2)

3.4.4.5 Treadmill motor challenge test

The other test for mobility in female mice was the treadmill motor challenge test. The result presented the same pattern as shown in the rotarod test. The *Mecp2*^{+/-} and *Mecp2*^{+/^{T158M}} have a significantly lower level of exercise capacity from the WT (Time spent on treadmill; WT 857.45 ± 231.33 sec; *Mecp2*^{+/^{T158M}} 341.08 ± 228.67 sec; *Mecp2*^{+/-} 158.7 ± 70.79 sec; **** = P<0.0001; Figure 3.18). Although the results from the *Mecp2*^{+/-} clearly show that most of them have a very low exercise capacity the results in the *Mecp2*^{+/^{T158M}} are more variable than those for the KO heterozygotes. Moreover, KO and KI heterozygous mice present more severe motor deficit compared with the male at the age tested.

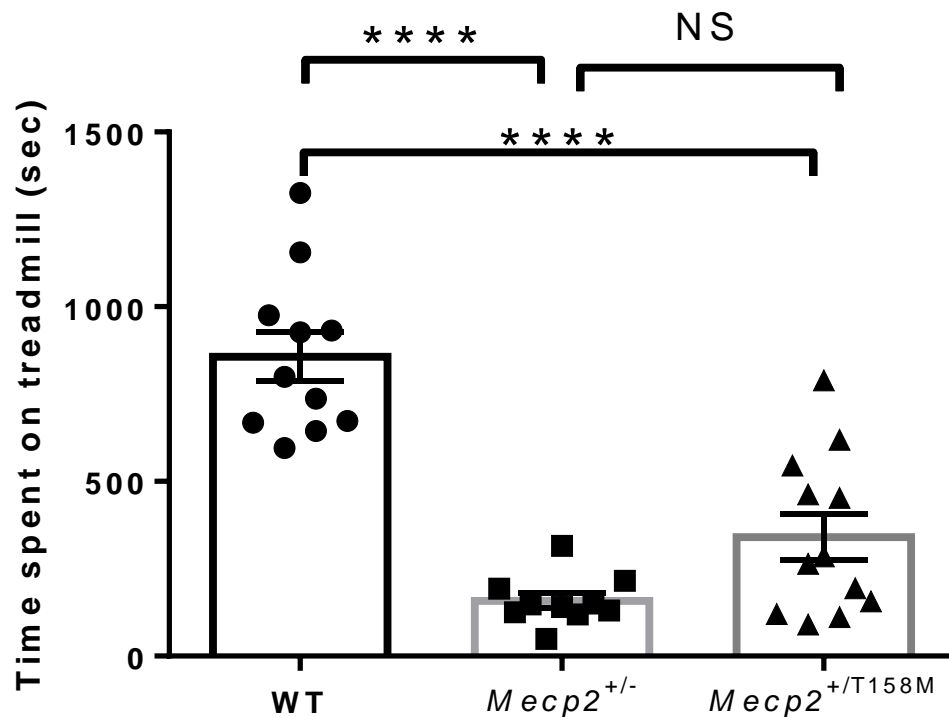


Figure 3.18 Motor function and locomotion assessment in WT, *Mecp2*^{+/-}, *Mecp2*^{+/^{T158M}} female mice. Plot showing the proportion of mice that were able to perform at an acceleration speed on treadmill. WT (n=11), *Mecp2*^{+/-} (n=10) and *Mecp2*^{+/^{T158M}} (n=12). Data presented as mean ± SEM. Statistical test results: One-way ANOVA test, F (2, 30) = 36.54, p<0.0001. Tukey's post-hoc tests: **** = p<0.0001 (WT vs *Mecp2*^{+/-} and *Mecp2*^{+/-} vs *Mecp2*^{+/^{T158M}})

3.4.4.6 Social interaction test

To examine the social interaction of the female mice in the three-chamber arena, the percentage of the time the mouse spends with its cage-mate was compared to that spent with a WT female mouse that they had never seen before. The results show that the WT spent more time with the unfamiliar mouse than their cage-mate. (Time WT spent with stranger; Stranger 1 (familiar) 39.95 ± 8.24 sec; Stranger 2 (unfamiliar) 60.04 ± 8.24 sec; *** = $p < 0.001$; Figure 3.19).

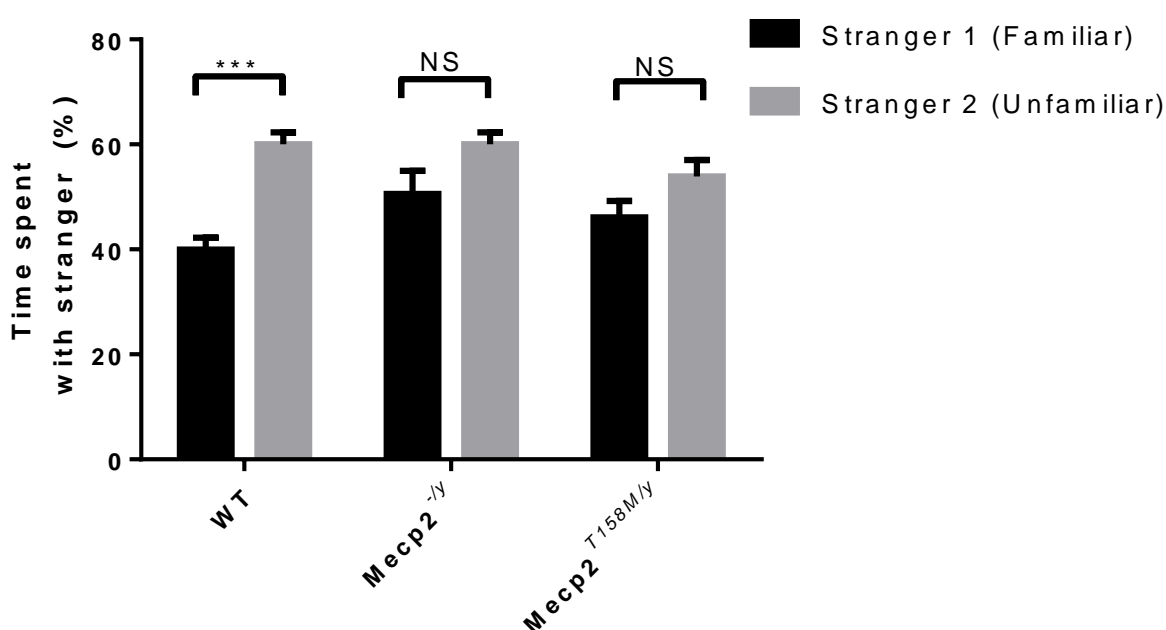


Figure 3.19 Social interaction test in WT, *Mecp2*^{+/-}, *Mecp2*^{+T158M} female mice. Graph shows average group values (mean \pm SEM) of time spent with their cage-mate and unknown mouse. WT (n=13), *Mecp2*^{+/-} (n=15) and *Mecp2*^{+T158M} (n=15); Statistical test results: Stratified t-tests were carried out for each genotype separately. For WT, $t=6.211$ DF=24, *** = $p < 0.001$ in WT: Stranger 1 (Familiar) vs. WT: Stranger 2 (Unfamiliar); For both mutant lines, there was no significant difference in time spent with each stranger mouse.

3.4.4.7 Light-dark box test

To examine anxiety levels, the time in the light chamber was analyzed in all groups. (Latency to enter the light area; WT 32.70 ± 30.98 sec; *Mecp2*^{+/*T158M*} 67.43 ± 112.57 sec; *Mecp2*^{+/-} 104.76 ± 66.52 sec; Figure 3.20a). (Time spent in the dark; WT 381.89 ± 80.94 sec; *Mecp2*^{+/*T158M*} 379.41 ± 137.11 sec; *Mecp2*^{+/-} 477.40 ± 57.83 sec; Figure 3.20b).

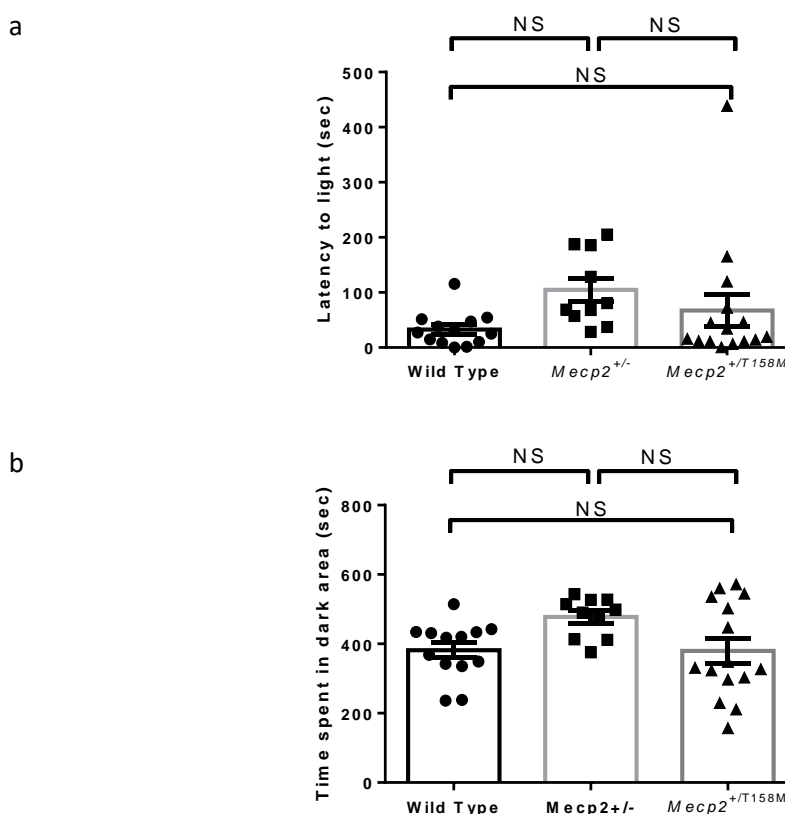


Figure 3.20 Exploration and anxiety related measures of the light-dark test in WT, *Mecp2*^{+/-}, *Mecp2*^{+/*T158M*} female mice. Column plot shows average group value (mean \pm SEM) for the (a) latency to enter the light area and (b) time spent in dark area. WT (n=13), *Mecp2*^{+/-} (n=10) and *Mecp2*^{+/*T158M*} (n=15). Statistical test results: (a) One-way ANOVA test, $F(2, 35) = 2.253$, $p = 0.1201$. (b) One-way ANOVA $F(2, 35) = 3.253$, $p = 0.0506$.

3.4.4.8 Splash test

To further analyze anxiety, the time mice spent grooming after splashing of the fur with a sugar solution was counted and recorded. Results showed that all groups spent up to 15 minutes grooming and cleaning. There were no significant differences between the groups in this test (Grooming count; WT 168.31 ± 66.56 ; *Mecp2*^{+/^{T158M} 214.53 \pm 60.12; *Mecp2*^{+/-} 206.20 \pm 47.07; Figure 3.21).}

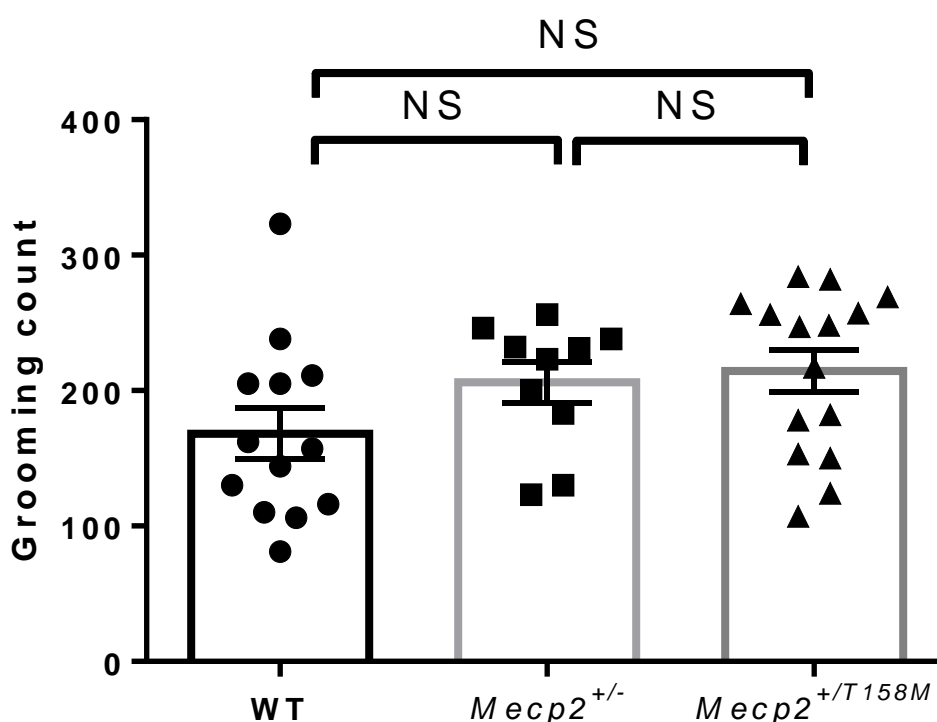


Figure 3.21 Anxiety assessment of WT, *Mecp2*^{+/-}, *Mecp2*^{+/^{T158M} female mice by splash test. Column plot shows average group values (mean \pm SEM) for time grooming. WT (n=13), *Mecp2*^{+/-} (n=10) and *Mecp2*^{+/^{T158M} (n=15). Statistical test results: One-way ANOVA test, F (2, 35) = 2.285, p=0.1168.}}

3.4.4.9 Breathing test

Apneas and abnormal breathing patterns were investigated in the same way as for the male mice in the plethysmography chamber. The results showed that the *Mecp2*^{+/-} mice presented a significantly higher number of apneas than the WT and *Mecp2*^{+/*T158M*} mice. The KI mice presented fewer apneas but statistically, was not that different from the WT (Apneas; WT 0.00 ± 0.00; *Mecp2*^{+/*T158M*} 0.34 ± 0.54; *Mecp2*^{+/-} 2.00 ± 2.79; ** = P<0.01; Figure 3.22).

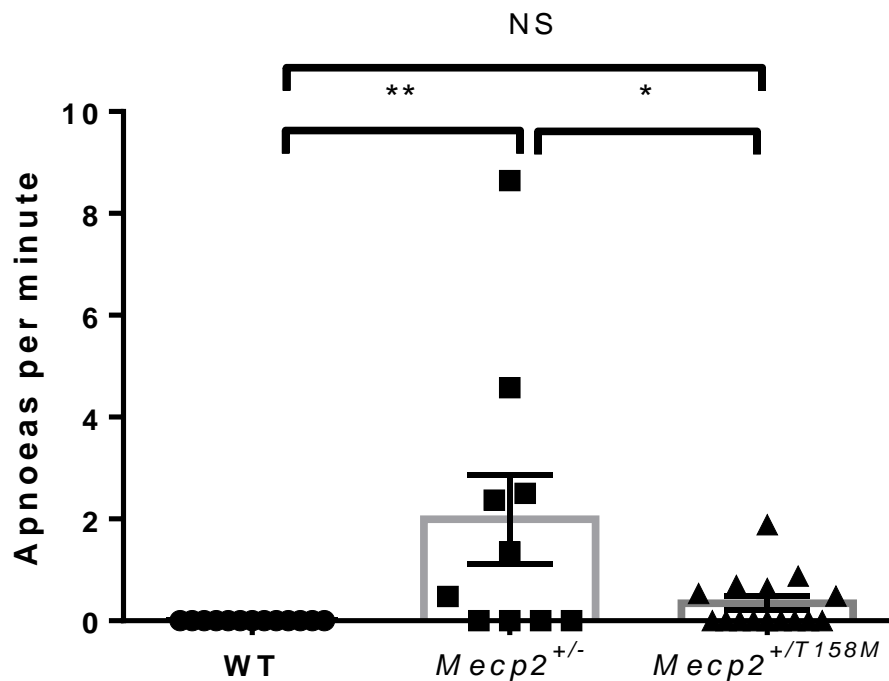


Figure 3.22 Persistent breathing phenotype in WT, *Mecp2*^{+/-}, *Mecp2*^{+/*T158M*} female mice. Column plot shows average group values (mean ± SEM) for the breathing frequency. WT (n=13), *Mecp2*^{+/-}(n=10) and *Mecp2*^{+/*T158M*} (n=15). Statistical test results: One-way ANOVA test, F (2, 35) = 5.897, p=0.0062, Tukey's post hoc comparison: * = p<0.05 (WT vs *Mecp2*^{+/*T158M*}) and ** = p<0.01 (WT vs *Mecp2*^{+/-}).

3.5 Discussion

Recently, RTT mouse models have been used widely in researching gene-based therapies (Gadalla et al., 2017; Garg et al., 2013; Matagne et al., 2017; Sinnott et al., 2017). The *Mecp2* KO model models the situation in RTT in terms of loss of function of *Mecp2* (Chen et al., 2001; Guy et al., 2001). The KO mouse has a severe phenotype including movement disability, breathing abnormalities and learning deficits. The new KI model models the human disease as closely as possible (Brown et al., 2016). In this study, I have investigated a range of behavioural phenotypes in these two models of RTT, comparing genotype effects on mobility performance, learning, cognition, social interaction, anxiety-like behavior and breathing tests in hemizygous male *Mecp2*^{-/y} and *Mecp2*^{T158M/y} mice and heterozygous female *Mecp2*^{+/-} and *Mecp2*^{+/T158M} mice with an aim to better characterise the RTT-related phenotype in the KO and T158M lines and identify the best line to use in order to evaluate the treatment for RTT symptoms in the future.

After the creation of the *Mecp2* KO mouse model in 2001 (Chen et al., 2001; Guy et al., 2001), there have been numerous reports of studies using these models, e.g. (Gadalla et al., 2013; Matagne et al., 2013; Matagne et al., 2017; Robinson et al., 2012; Ross et al., 2016; Sztainberg et al., 2015). In addition to full KO mouse models, KI models of some of the most common human RTT mutations have also been developed (Brown et al., 2016; Goffin et al., 2012; Lyst et al., 2013; Shahbazian et al., 2002). T158M is the most common missense mutation, its molecular consequence is to moderately reduce binding specificity for methylated DNA. Male hemizygous KI mice with this mutation present severe hypoactivity, gait impairment, weight loss and breathing irregularities from roughly 6 weeks of age and subsequently die between 12-14 weeks of age (Brown et al., 2016; Goffin et al., 2012) while showing a similar breathing pattern to that of the *Mecp2* null mice. In comparison, female heterozygous *Mecp2* T158M KI mice show minimal phenotypes with only minor tremor and hindlimb claspings detected, (Brown et al., 2016). However, when this mutation was modelled on a different genetic background, female *Mecp2* T158M KI mice showed a reduction in bodyweight and breathing abnormalities which, at least in the females highlighted the effects of the background strain on the phenotype. It is clear that the absence of *Mecp2* from the brain only leads to a severe phenotype,

resulting in early death in male KO mice, however, these studies have not carried out rigorous phenotyping and have instead relied on gross markers of disease such as reduced brain size and weight loss (Chen et al., 2001; Giacometti et al., 2007; Guy et al., 2001).

In agreement with (Guy et al., 2001) and (Brown et al., 2016), phenotype severity assessment in my study shows that hemizygous *MeCP2*^{+/-} and *Mecp2*^{T158M/y} male mice present the RTT-like phenotype early and severely with onset at 6-8 weeks of age. Their mobility and body weight were also reduced when compared with the WT. The total phenotype scoring in KI were counted from gait abnormality and mobility disorders, while the total score of the KO includes the score from tremor and breathing abnormality alongside gait and mobility. Heterozygous *Mecp2*^{+/-} and *Mecp2*^{+/T158M} female mice, were symptomatic for the RTT-like phenotype, exhibiting reduced locomotion, gait abnormalities and an increase in body mass, which is also normally associated with the RTT-related phenotype in female mice. (Garg et al., 2013). The *Mecp2*^{T158M} KI female model shows the same severity with the KO as observed by the aggregate severity score at the time point of 6-8 months old. However, comparison of survival between *Mecp2*^{-/y} and *Mecp2*^{T158M/y} male mice in this study and in more detail in Chapter 4 (section 4.4.1) showed that the lifespan of *Mecp2*^{T158M/y} males was significantly longer. Reduction of binding capacity of the MeCP2 T158M mutant protein to heterochromatin implies that it is not a complete loss of function mutation (Lamonica et al., 2017).

The major aspect of the RTT-like phenotype stems from mobility impairments. Many studies have observed movement patterns and mobility in the *Mecp2* mouse model in the open field test (Gadalla et al., 2013; Matagne et al., 2013; Matagne et al., 2017; Ross et al., 2016; Sztainberg et al., 2015), rotarod test (Matagne et al., 2017; Ross et al., 2016; Sztainberg et al., 2015), gait analysis (Gadalla et al., 2014; Ross et al., 2016), the balance beam (Ross et al., 2016), and exercise tolerance (Ross et al., 2016). All studies agree that the male KO is the most severe phenotype with regards to movement compared with that of the KI and WT. In addition to this, the (Lamonica et al., 2017) reports that the movement performance in females when comparing KI and KO indicates similar results. The general locomotion assessment was tested in a 15-minute-long,

open field test, without forcing the performance. Hemizygous male mice, *Mecp2*^{-/y} and *Mecp2*^{T158M/y} demonstrated less movement than the WT. An idea to add in the mouse's own bedding to ease adaptation was adopted. It was expected that this would encourage the mouse to move about more freely like it does in its own cage. This is supported by the previous report indicating that *Mecp2*^{-/y} mobility is affected by the surface of the floor, not only due to intrinsic mobility impairment. (Orefice et al., 2016). The result of mobility in the mutant male mice showed that they moved better in the arena with the bedding than without. However, the overall result shows that the hemizygous male mice still spent less time moving than wild-type individuals. This result presents with the same trend as that of the female heterozygous mice.

In addition, rotarod and treadmill tests were analyzed for motor deficits, showing that hemizygous male mice and heterozygous female mice demonstrated poor motor performance with weak co-ordination and balance on a rotarod and reduced exercise endurance on the treadmill. The performance of heterozygous females on the rod and on the treadmill was significantly different from the WT. However, although the mutant presents a lower motor ability than the WT, the *Mecp2*^{T158M/y} and *Mecp2*^{+/-T158M} demonstrated that they had better performance than the *Mecp2*^{-/y} and *Mecp2*^{+/-} respectively.

To evaluate motor learning skills, the rotarod test was administered over three consecutive days. Comparing with the previous study which used four consecutive days (Brown et al., 2016; Shiotsuki et al., 2010), the trend of the time on the rod between day one to day three showed improvement. The trend in my experiment only showed significant improvement in both male and female WT and slight improvement in female KI on day three. The learning curve can imply that the WT has better learning skills than both mutants. Results using males of each line agreed with findings of a previous study (Brown et al., 2016). This test is not suitable to see the differences between the mutant lines because there was limited learning over the three days, so it was not possible to demonstrate impairment of learning.

It is possible that the reduction of activity might be a result of anxiety-like behavior since when its own bedding was scattered in the arena, all mutant mice appeared to be more active than they were without the bedding. However, the activity of the mutants was still significantly different to that of the WT. It was most likely due to either motor deficits or reduced motivation.

Non-anxiety-based reduction in exploratory activity has previously been reported in the *Mecp2*^{+/-} mice (Guy et al., 2001) but the exact cause for such behavior has not been determined yet. Interestingly, observation results showed that the average speed of hemizygous *Mecp2*^{-/y} and *Mecp2*^{T158M/y} male mice individually with and without its own bedding was not that different from the speed exhibited by the wild-type mouse (not shown). This was also observed in the heterozygous *Mecp2*^{+/-} and *Mecp2*^{+/T158M} female mice. Therefore, it is possible that the reduction in mobility in *Mecp2*^{+/-} and *Mecp2*^{+/T158M} mice with and without bedding comes from an unwillingness to move rather than motor deficits.

Motor performance and locomotion tests that we carried out did not provide evidence for any significant differences between the KO and KI models. Both phenotypes in hemizygous *Mecp2*^{-/y} and *Mecp2*^{T158M/y} male mice and heterozygous *Mecp2*^{+/-} and *Mecp2*^{+/T158M} female mice, suggest that differences in the genotypes' specific effects are too subtle to be detected by such current tests.

Another major aspect of the RTT like phenotype is breathing abnormalities which, in RTT mouse models, generally present as disturbed breathing patterns including apnoea and irregular breathing frequency (Ogier et al., 2007; Ramirez et al., 2013; Voituron et al., 2010) as can also be seen in human RTT patients (Neul et al., 2010). Global reactivation of *Mecp2* expression in mice can reverse these issues and the breathing phenotype is therefore is a viable therapeutic target. Previous research reported that GABAergic and serotonergic control of the brain respiratory network is the main contributing factor to breathing and apnoea that characterise RTT in human patients and RTT mouse models (Abdala et al., 2010; Chao et al., 2010; Viemari et al., 2005; Voituron and Hilaire, 2011). In agreement with previous studies (Elian and Rudolf, 1991; Julu et al., 2001; Julu and Witt Engerström, 2005; Marcus et al., 1994; Weese-Mayer et al., 2008; Weese-Mayer et al., 2006) the male KO mouse presents the most severe case of breathing abnormality in terms of apnoea with some KI mice also presenting apnoea at around the age of 6-8 weeks. Most KO female mice at the age of 6-8 months present apnoea, as do some of the KI also, in agreement with previous research (Lamonica et al., 2017).

Other RTT characteristics in humans are resistance to learning new things, restricted interests and social isolation (Schaevitz et al., 2010). These characteristics also appear in previous studies in hemizygous KO mice, heterozygous KO mice (Schaevitz et al., 2010; Stearns et al., 2007), *Mecp2*^{tm1.1Meg} knock-in mice (Cohen et al., 2011) and *Mecp2*^{T158A} knock-in mice (Goffin et al., 2012), previous studies of KO and KI RTT mouse models have presented this. Earlier studies on learning in the RTT mouse model have indicated an impact of motor and mobility deficits on learning and social interaction. However, including a mouse's own bedding in the arena during the NOR test, gave more credible and more reliable memory test results and reduced the level of doubt about the effect of movement-related factors. My results demonstrate that learning in KO and KI in both males and females was very similar; however, when compared to the WT, their ability to learn was very poor, apart from male KI, who scored similarly to WT. The results I achieved are consistent with previous papers on the NOR test in the RTT mouse.

In terms of the learning tests, I suggest including the motor learning test as a standard in evaluating both males and females as they indicate clearly the differences between WT, KO and KI. However, in male mice, there are learning ability differences between WT and RTT mouse models.

Previous studies on the social interaction tests used the standard size of the three-chamber arena; however, to minimize any mobility issues, I used a half size of the arena from the standard reducing the distance to each stranger mouse. My results on KI and KO in both males and females are consistent with the reduction in social responsiveness reported in RTT and in RTT mouse studies carried out before. One study presents the KO preferring to interact with the stranger while the WT does not (Schaevitz et al., 2010) in contrast with my result and another report on the RTT mouse (Moretti et al., 2006) showing the RTT mouse model spending significantly more time away from the stranger. The different types of *Mecp2* KI mice have differing genetics effect *Mecp2* expression in the amygdala which, in turn, affects their learning levels and abilities (Gemelli et al., 2006; Moretti et al., 2005). This is clearly shown in the social interaction test in the three-chamber arena which is an ideal test to ascertain social abilities.

Likewise, anxiety analysis depends on the genetic background and experimental model. In my experiment, both light-dark box and splash test suggest that the KO and KI mouse do not have any anxiety. The result from light-dark test consistent with the other experiments in KO mice (Castro et al., 2014; Samaco et al., 2013). Many previous reports on anxiety in RTT mouse model required movement ability. The anxiety test using an open field where mice ambulate between the center of the arena and the edge of the field (more anxious behaviour), male *Mecp2^{tm1Hzo}* mutants and heterozygous female *Mecp2^{tm1.1Jae}* seem more anxious than wild types (De Filippis et al., 2010; Lonetti et al., 2010). However, the result might be affected by the severe motor impairments of RTT mouse. Other anxiety studies using the elevated plus and zero mazes present that male Nulls and *Mecp2^{tm1.1Joz}* mutants seem less anxious than wild types (Goffin et al., 2012; Kerr et al., 2012; Pelka et al., 2006; Stearns et al., 2007). However, some studies have reported that male *Mecp2^{tm1Hzo}* mutant mice display reduced anxiety compared to WT (De Filippis et al., 2010; McGill et al., 2006). Those other studies did not add the home cage bedding.

Furthermore, anxiety measures with a splash test do not require RTT mouse to ambulate. Thus, the splash test is the best test to examine anxiety in the mice because the outcome from this test is more accurate than other tests that require mobility from the mice.

On concluding my experiment, my conclusion is that the current phenotype scoring system is not suitable for the RTT mouse due to the scale not fully representing the symptoms of the mice. For example, more levels of movement should be added, for example, movement after prodding the mice. This can be recognized in WT, which will stop moving but will immediately move again if they are prodded. On the other hand, the RTT mouse who present hypoactivity doesn't move when it is gently encouraged to do so. A new better has now been developed and is in use in my lab group (Gadalla et al., unpublished). In addition, additional scoring levels need to be added to breathing levels, apnea and tremor in order to fully monitor the severity of the RTT phenotype. One surprising issue on finding a suitable object for the NOR is that some male KO mice that do not move at all in the open field test can move towards and climb onto the test object and then play with it. (I didn't use that object on my NOR

experiment due to not wanting the mice to play with the object, only learn and recognize the familiar object). This indicates that some mice that do not move don't in fact have impaired mobility. Both tests work for KO and KI lines.

From the reliable result above, I suggest that the following tests be used to demonstrate improvement in mouse models of RTT open field with bedding to test for mobility, motor learning test on the rotarod to test for learning, 3-chamber arena with reducing the arena size to test for social interaction and the splash test to test anxiety.

In conclusion the male KO mice may still be the best line for screening the improvement of the phenotype after treatment as the phenotype exhibits a rapid progression and shows clear and significant differences from the WT. I went on to use the KO for screening for vector optimization on the next chapter because it clearly indicates the onset and symptoms of RTT in KO and is reliable for screening for the best vector treatment. Some RTT-like symptoms are reversible (Guy et al., 2007; Liou et al., 2011; Robinson et al., 2012) and RTT features most likely come from dysfunction of neurons rather than neurodegeneration (Guy et al., 2007). Then, the progression of the treatment on the KO can be clearly seen.

In long-term studies, I suggest that the female heterozygous T158M be used to examine the result of treatments because the phenotype expressed in this line is milder than the KO female but still presents a significant difference from WT (Brown et al., 2016).

Chapter 4 Assessment of safety and efficacy of vector-derived *MeCP2* on the progression of the RTT-like phenotype in a dose escalation study

4.1 Introduction

Previous studies indicate that RTT has the possibility of being treated, as I have highlighted above. The justification for this is firstly that RTT is caused by mutations in a single gene, *MECP2*, (Amir et al., 1999; Gadalla et al., 2011; Lyst and Bird, 2015); secondly, that features are due to dysfunction of neurons and supporting cells, rather than neural degeneration (Armstrong, 2002); thirdly, that there are several excellent mouse models in which many of the somatic, behavioural and physiological changes observed in individuals with RTT are reproduced; and finally, that phenotypic reversibility has been reported in mouse models following reactivation of *Mecp2* (Guy et al., 2007; Liroy et al., 2011; Robinson et al., 2012).

Previous attempts at *MECP2* gene transfer using AAV9 vectors were confounded by limited brain transduction efficiency and toxicity (Gadalla et al., 2013; Matagne et al., 2016), while efficacy in other studies using self-complementary AAV (scAAV) (Garg et al., 2013) may have been compromised by use of a construct exceeding the packaging capacity of the vector.

To explore the relationship between vector dose and therapeutic benefits, *Mecp2* KO mice were assigned into experimental cohorts. A dose escalation experiment was conducted using an scAAV2/9 vector (called 1st generation vector after this) and was used to deliver a Myc-tagged human *MECP2_e1* cDNA under the control of a short, 229bp region of the murine *Mecp2* endogenous core promoter (MeP229) (Gadalla et al., 2013; Gray et al., 2011a).

The main purpose of the work described in this chapter was to address issues of vector dose and relate this to therapeutic efficacy, adverse effects and brain transduction and MeCP2 expression levels. For this, I focused on using our 'first generation' scAAV9/MeP229/MECP2 vector (a self-complementary AAV9 using a

229 base pair fragment of the endogenous *Mecp2* promoter to drive expression of the human e1 isoform of MeCP2) delivered systemically via intravenous injection.

4.2 Aims

The overall aim of the work described in this chapter was to assess the importance of vector dosage for AAV9/MECP2 gene transfer in RTT. In particular, I wanted to assess the effective and safe limits of the 1st generation vector (scAAV9/MeP229/MECP2) in male mice modelling RTT.

The specific objectives of this chapter are:

- (1) To investigate the effect of peripherally-delivered scAAV9/MeP229/MECP2 on RTT-like phenotypes in a dose-escalation experiment.
- (2) To identify potential adverse effects in response to dose escalation.
- (3) To investigate the relationship between phenotypic observations or toxicity and patterns and levels of MeCP2 expression in the brain and peripheral tissues.
- (4) To provide a baseline in terms of efficacy and safety against which next generation cassette designs can be assessed.
- (5) To investigate the efficiency and toxicity of 1st generation vector in MeCP2 knock-in mice that express endogenous mutant MeCP2 protein.

4.3 Methods

The vector I used in this chapter is the same vector that a member of staff in my lab group, Dr. Kamal Gadalla, reported previously (Gadalla et al., 2013). This vector construct consists of human *MECP2_e1* isoform coding sequences carrying a C-terminal Myc-tag fusion which was cloned into scAAV2 vector with backbone (to be packaged in AAV9 capsid particles) under the control of murine *Mecp2* endogenous core promoter (MeP, 229bp). This construct (scAAV9/MeP-hMECP2, henceforth referred to as scAAV9/MeP229/MECP2 or the 1st generation vector), is summarised in figure 4.1.

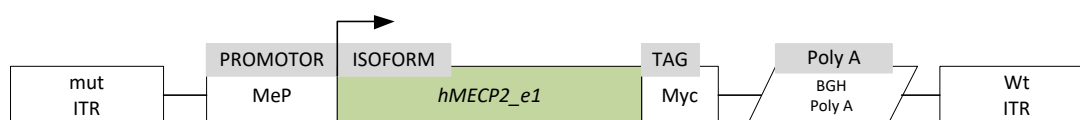


Figure 4.1 $MECP2_{-e1/Myc}$ fusion constructs were cloned into AAV2 backbones under a MeP promoter (LORRAINE - I have edited the diagram to delete 'tail' as the 'PolyA' referred to is the 3'-UTR and polyadenylation signal)

To evaluate the efficiency of the 1st generation vector, hemizygous *Mecp2*^{-/y} mice and their WT littermates were genotyped (see section 2.2.3) and then weighed and scored weekly for the RTT-like severity on mobility, gait abnormality, hind limb claspings, tremor, breathing and general condition using the standard phenotype scoring system (Guy et al., 2001; see section 2.2.5) to follow the condition of mouse closely throughout the experimental time. Mice that weighed more than 9 grams at the age of ~35 days were included in the experiment. To globally administer viral vector, the male KO, KI and WT littermate mice were carefully injected with the 1st generation vector at the following different doses: 1×10^{11} , 1×10^{12} and 1×10^{13} vg/mouse (referred to henceforth as low dose, moderate dose and high dose, respectively) diluted in PBS in a total volume of 100 μ l (see on section 2.5.1) through the tail vein using sterile technique (see on section 2.5.2.1). The control groups were the *Mecp2*^{-/y} and WT littermates treated with PBS solution.

The survival data was recorded when the mouse was found dead, lost more than 20% of the peak bodyweight or lived for more than a year. In the last two cases, the mouse was euthanized humanely and brain, spinal cord and other tissues collected for immunohistochemistry (see section 2.6) to analyse expression patterns, transduction efficiency, and quantification of vector-derived MeCP2 levels within cell nuclei.

4.4 Results

4.4.1 1st generation vector safety and efficacy at different doses by IV delivery in the *Mecp2* KO mouse model of RTT

Previous studies have demonstrated that a therapeutic dose can increase mouse survival (Gadalla et al., 2013; Matagne et al., 2013). However, in my experiments, the highest dose (10^{13} vg/mouse) showed lethality shortly after

treatment within 3-8 days after injection in KO *Mecp2*^{-/-} mice (median survival = 6.14 ± 0.23 weeks), as shown in Figure 4.2. Similarly, this dose was also associated with lethality in WT mice (median survival = 7.62 ± 0.21 weeks, n = 3; not shown). Contrastingly, vehicle treated WT showed 100% survival over the trial. On the other hand, KO *Mecp2*^{-/-} mice treated with the moderate dose (1×10^{12} vg/mouse) showed significantly increased survival (median survival = 27.3 ± 6.93 weeks compared to the to the KO treated with vehicle (median survival = 11.6 ± 4.09 weeks) while the low-dose (10^{11} vg/mouse) showed no survival advantages over the KO vehicle control (median survival = 9.36 ± 4.06 weeks).

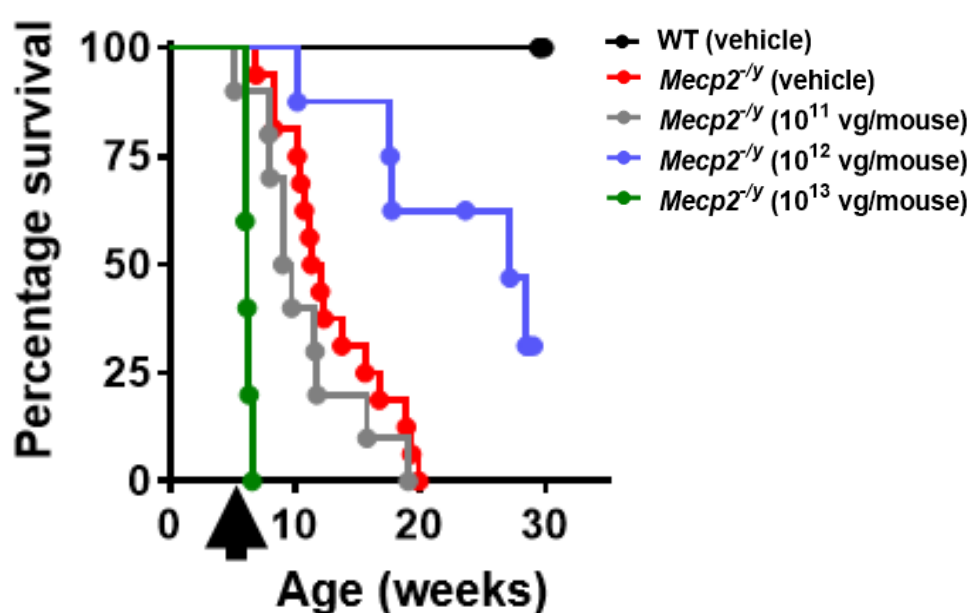


Figure 4.2 Survival plot of *Mecp2* KO mice treated with 3 different doses of scAAV9/MeP/MECP2. The plot shows the median survival of KO mice compared to the KO treated with vehicle (median survival 11.6 weeks), and with the low-dose (median survival = 9.36 weeks; p = 0.2, Mantel-Cox test, n = 9), moderate dose (median survival = 27.3 weeks, p = 0.001, Mantel-Cox test, n = 7) and high dose (median survival = 6.14 days, p= 0.004, Mantel-Cox test, n = 5); mice given the high dose showed high mortality shortly after treatment. Arrow indicates age at injection.

I focus on the group receiving the moderate dose showing a mild increase in difference of bodyweight at 11 weeks (mean \pm SEM bodyweight measured at 11 weeks of age = 19.52 ± 3.8 g, Figure 4.3) compared to vehicle-treated mice (mean bodyweight = 13.93 ± 2.46 g). However, the average bodyweight of this group remained lower than WT controls (mean bodyweight = 25.24 ± 2.16 g).

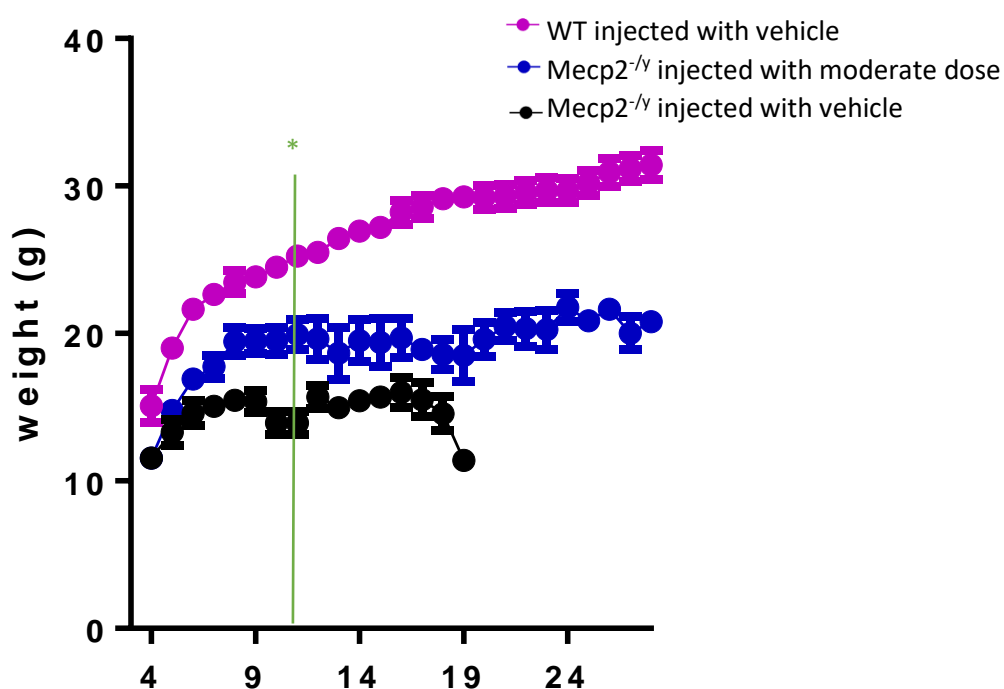


Figure 4.3 Graph showing the average body weight of wild-type and *Mecp2*^{-/-} treated with vehicle and *Mecp2*^{-/-} treated with 10¹² vg/mouse dose. WT treated with vehicle (n = 9) *Mecp2*^{-/-} (treated with vehicle n = 10) and *Mecp2*^{-/-} treated with 10¹² vg/mouse dose (n = 7) Data presented as mean \pm SEM. * means treated *Mecp2*^{-/-} mice were significantly different from the vehicle control group at the age of 11 weeks. One-way ANOVA F (2, 33) = 35.51, p < 0.0001; Tukey's post hoc comparison: ** = p < 0.01 (*Mecp2*^{-/-} injected with moderate dose vs *Mecp2*^{-/-} injected with vehicle and WT injected with vehicle vs *Mecp2*^{-/-} injected with moderate dose), ***** = p < 0.0001 (WT injected with vehicle vs *Mecp2*^{-/-} injected with vehicle).

I then evaluated the performance of AAV-mediated gene delivery of *MECP2* in improving/preventing the RTT-like phenotype. WT and KO mice were compared in terms of the standard observational scoring system (Guy et al., 2001; Lioy et al., 2011; Weng et al., 2011). The result showed that the vehicle-treated *Mecp2*-null group developed the characteristic appearance of RTT-like signs from 4 weeks, which then increased in severity over the following weeks as described

previously. The group treated with the moderate dose of vector showed an identical phenotype trajectory indicating the absence of any treatment effect (mean aggregate severity score at 11 weeks in *Mecp2*^{-/-} treated with 10¹² vg/mouse dose = 5.18 ± 0.96, *Mecp2*^{-/-} treated with vehicle = 5.35 ± 1.14, and WT treated with vehicle = 0.83 ± 0.5).

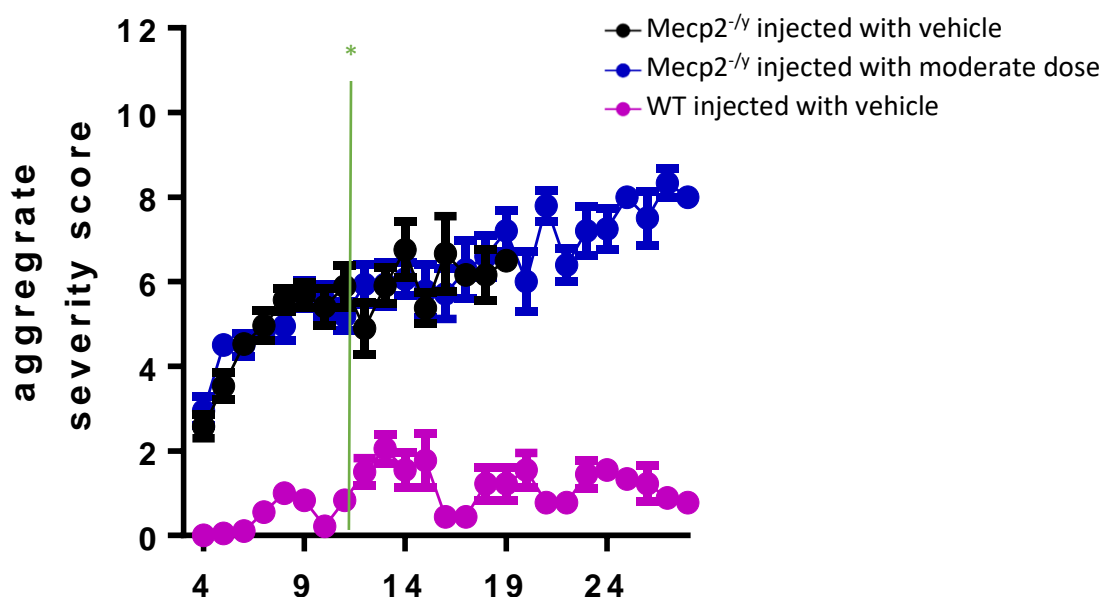


Figure 4.4 RTT-like severity score of wild-type and *Mecp2*^{-/-} treated with vehicle and *Mecp2*^{-/-} treated with 10¹² vg/mouse dose. WT treated with vehicle (n = 9) *Mecp2*^{-/-} treated with vehicle (n = 8) and *Mecp2*^{-/-} treated with 10¹² vg/mouse dose (n = 9). Data presented as mean ± SEM. One-way ANOVA F (2, 24) = 78.78, Tukey's post hoc comparison: **** = p < 0.0001 (WT injected with vehicle vs *Mecp2*^{-/-} injected with vehicle and WT injected with vehicle vs *Mecp2*^{-/-} injected with moderate dose). * means treated *Mecp2*^{-/-} mice were significantly different from the vehicle control group at the age of 11 weeks.

From the data presented above, it is apparent that peripheral (IV) delivery of the first-generation vector at a tolerated dose of 10¹² viral genome/mouse (1x10¹⁴vg/kg) resulted in enhanced survival, a modest effect on bodyweight, but no impact on RTT-like phenotypes based on observational scoring. Moreover, the cohort receiving the highest dose showed acute toxicity and lethality at 3-8 days post-injection.

4.4.2 1st generation vector transduction efficiency and level of vector-derived MeCP2 in the brain in *Mecp2* KO mice

Patterns of transduction within CNS in treated *Mecp2*^{-/-} mice were measured using anti-myc (detecting the tag on the vector-derived MeCP2), anti-MeCP2 (for total MeCP2), anti-NeuN (neuronal marker) and antibody immunofluorescence labelling (figure 4.5) to evaluate distribution and level of vector-derived MeCP2 in different tissues.

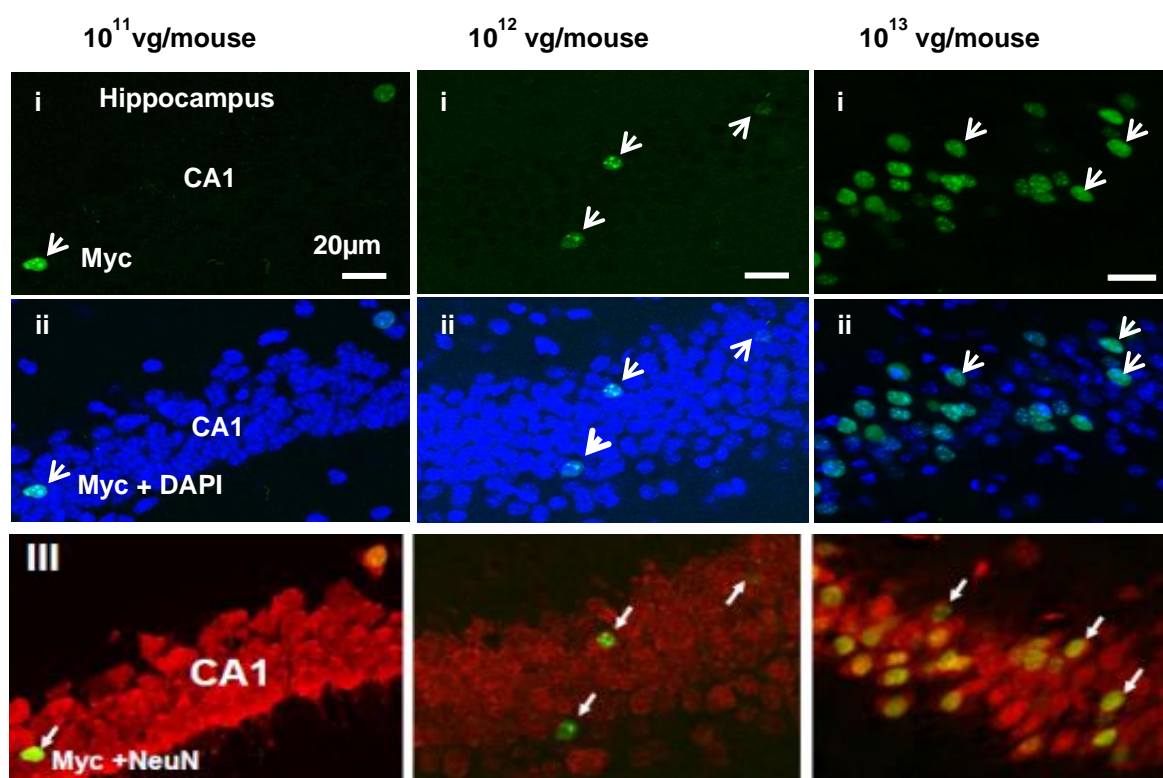


Figure 4.5 Flattened confocal stack images of the CA1 region of the hippocampus taken from *Mecp2*^{-/-} mice treated intravenously with different doses of the 1st generation vector. (i) shows anti-Myc immunostaining, (ii) shows merge with DAPI nuclear stain, and (iii) shows merge with anti-NeuN stain. Arrows denote transduced cells.

In addition, vector-derived MeCP2 protein expression distributed in a punctate pattern within the nuclei corresponding to previously observed results for endogenous MeCP2 in WT mice revealed very low levels of brain transduction. Samples from the low dose cohort revealed low transduction efficiencies across brain regions of 0.5 to 1% (Figure 4.6). The moderate dose resulted in ~3-5%

transduction efficiency, whereas the high dose reached significantly higher transduction efficiencies (~10-20% of cells).

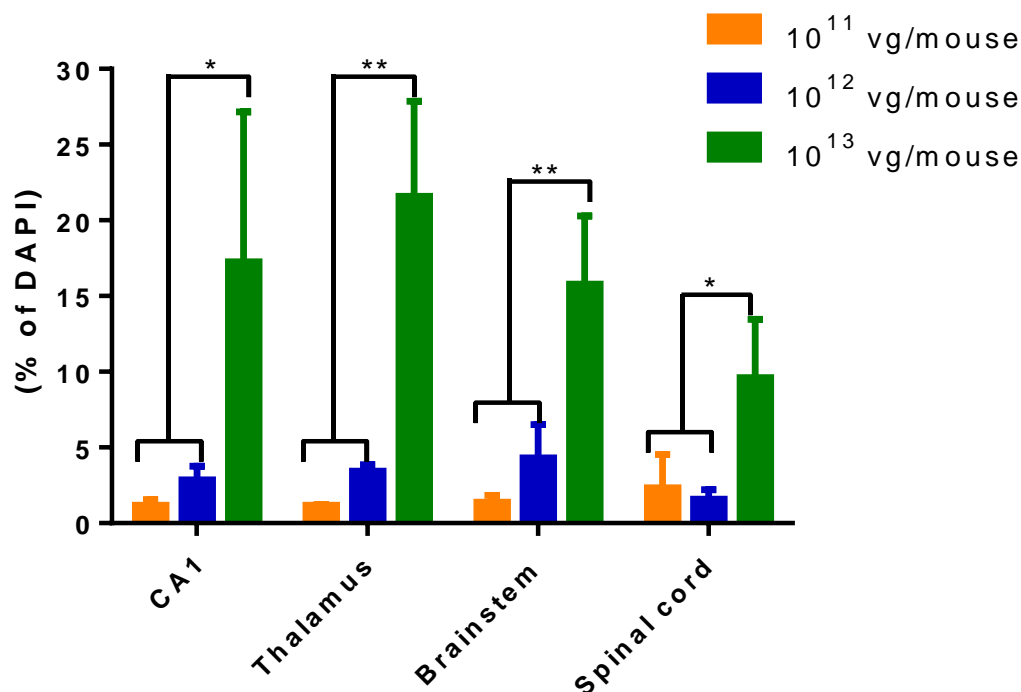


Figure 4.6 Dose-dependent transduction efficiency (Mycpositive nuclei as a proportion of DAPI-positive nuclei) across different brain regions. Data is presented as mean \pm SEM ($n = 3$ mice per group). CA1 indicates hippocampal region. Data presented as means \pm SD. Two-way ANOVA $F(6, 24) = 1.660$, $P = 0.1742$; Tukey's post hoc comparisons: * means p value is < 0.05 . ** means p value is < 0.01 .

In order to measure cellular levels of vector-derived MeCP2 relative to native levels, WT mice were treated with the 1st generation vector. The low and moderate doses were tolerated and had no observable effect on bodyweight or the phenotype severity score (Figure 4.2). However, WT mice treated with the high dose exhibited the acute toxicity and rapid lethality observed in the knockout mice (Figure 4.2). This result agrees with quantification of cellular levels of MeCP2 in mice given this high dose, which revealed that transduced hippocampal pyramidal cells expressed vector-derived MeCP2 at a mean level equivalent to 120% of the endogenous level, which results in total cellular levels of MeCP2 just over two-fold higher than normal for these cells (Figure 4.7).

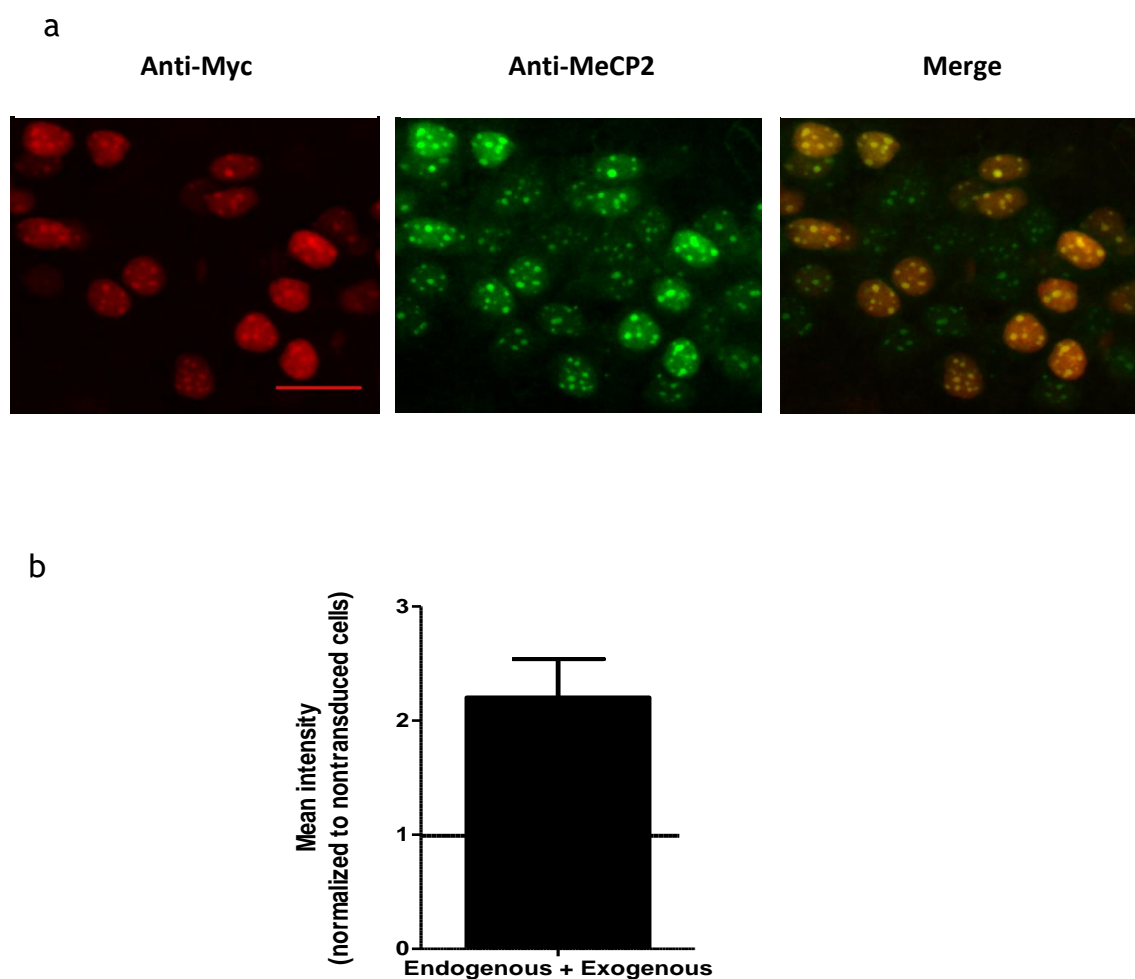


Figure 4.7 Intravenous injection of AAV9/hMECP2 into wild-type mice resulted in toxicity at the high dose. (a) Flattened confocal stack image taken from CA1 region of the hippocampus of wild type mice injected with the high dose. Tissues were immunostained with anti-Myc and anti-MeCP2 antibodies. Arrows indicate transduced cells whilst arrowheads indicate non transduced cells. (b) Relative quantity of cellular MeCP2 in the transduced cells (standardised to non-transduced cells) in the CA1 region of the hippocampus in wild type mice (N=2), data presented as means \pm SD.

4.4.3 1st generation vector transduction efficiency and level of vector-derived MeCP2 in the liver in *Mecp2* KO mice

To further investigate toxic effects encountered after systemic injection of the 1st generation vector at high doses, levels of vector-derived MeCP2 expression were tested in a range of peripheral tissues. A bio-distribution estimate of the levels of vector genome in the liver was high (Figure 4.8).

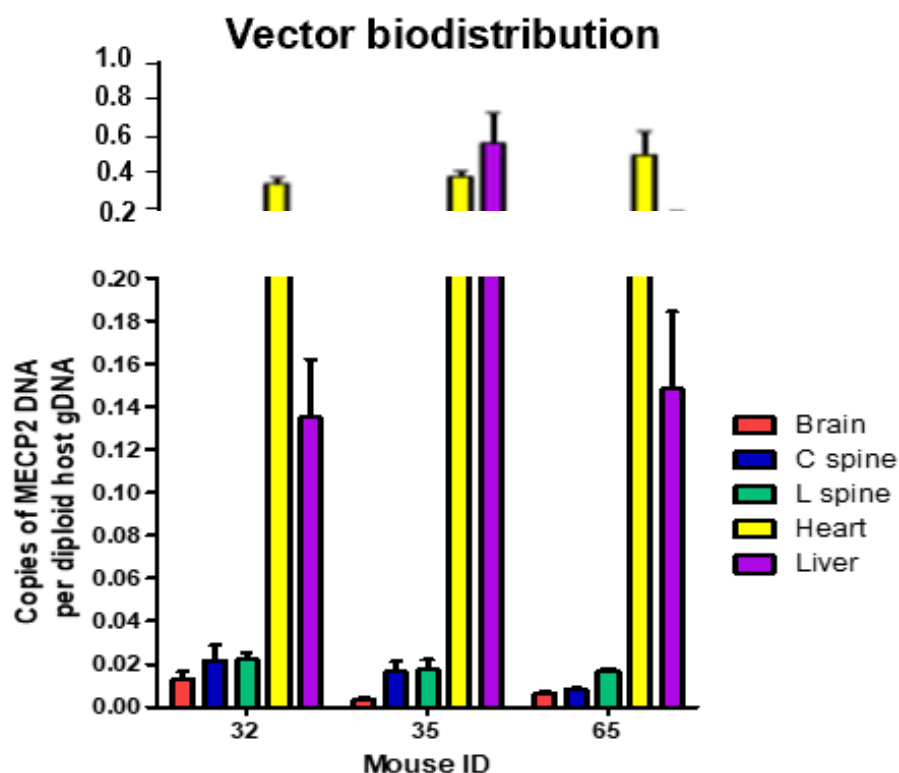


Figure 4.8 Vector biodistribution analysis of mice injected intravenously with 1012 vg/mouse showing high transduction efficiency in the liver and heart and low transduction efficiency in the CNS. Data are presented as mean \pm SEM (n = 3 mice per group).

Abnormal pathology was observed in liver (Figure 4.9B), caused presumably because endogenous MeCP2 levels are much lower in liver cells than in brain neurons (Ross et al., 2016; Skene et al., 2010). Issues are typically below detection threshold for immunohistochemistry using available antibodies. However, vector-derived MeCP2 levels in a subset of liver cells (using anti-Myc-immunolabelling) of treated WT mice were found to be higher than MeCP2 levels seen in neurons (Figure 4.9b) and were thus around 20 times higher than levels found endogenously in such cells.

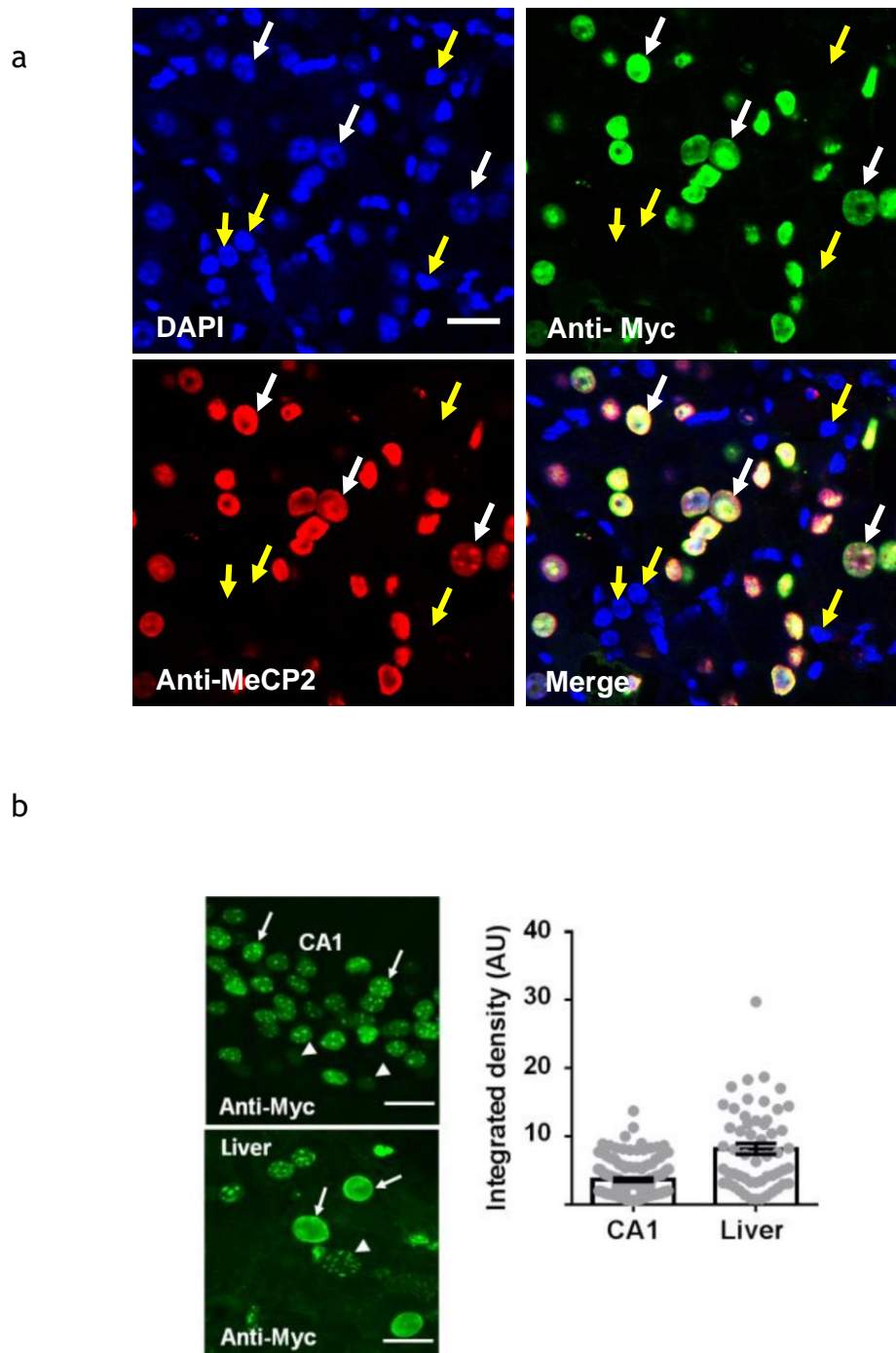


Figure 4.9 Intravenous injection of 1st generation vector resulted in high level of vector-derived MeCP2 expression in the liver. a) Representative confocal images of liver taken from WT mice injected intravenously with 1st generation vector at the dose of 10^{13} vg/mouse. Sections were immunostained with anti-Myc (green), anti-MeCP2 (red) and DAPI nuclear stain (blue). White arrows indicate transduced cells, whereas yellow arrows indicate non-transduced cells. Scale bars indicate $20\ \mu\text{m}$. B) Representative confocal images of liver taken from mice that were injected intravenously with 1×10^{13} vg/mouse using the same confocal settings. Arrows indicate nuclei with a high level of vector-derived MeCP2 expression (based on fluorescence intensity of the anti-Myc antibody) and arrowheads indicate nuclei with low expression levels. Scale bar in (a) & (b) = $20\ \mu\text{m}$.

Histological investigation of liver sections from mice injected with vehicle or low dose of the vector showed largely normal liver structure with occasional areas of mononuclear infiltration (figure 4.10 a-b). In contrast, mice injected with higher doses of the vector showed a dose-dependent increase in pathological features including cellular destruction and vacuolation, loss of hepatocytes and mononuclear cell infiltration (figure 4.11 c-d).

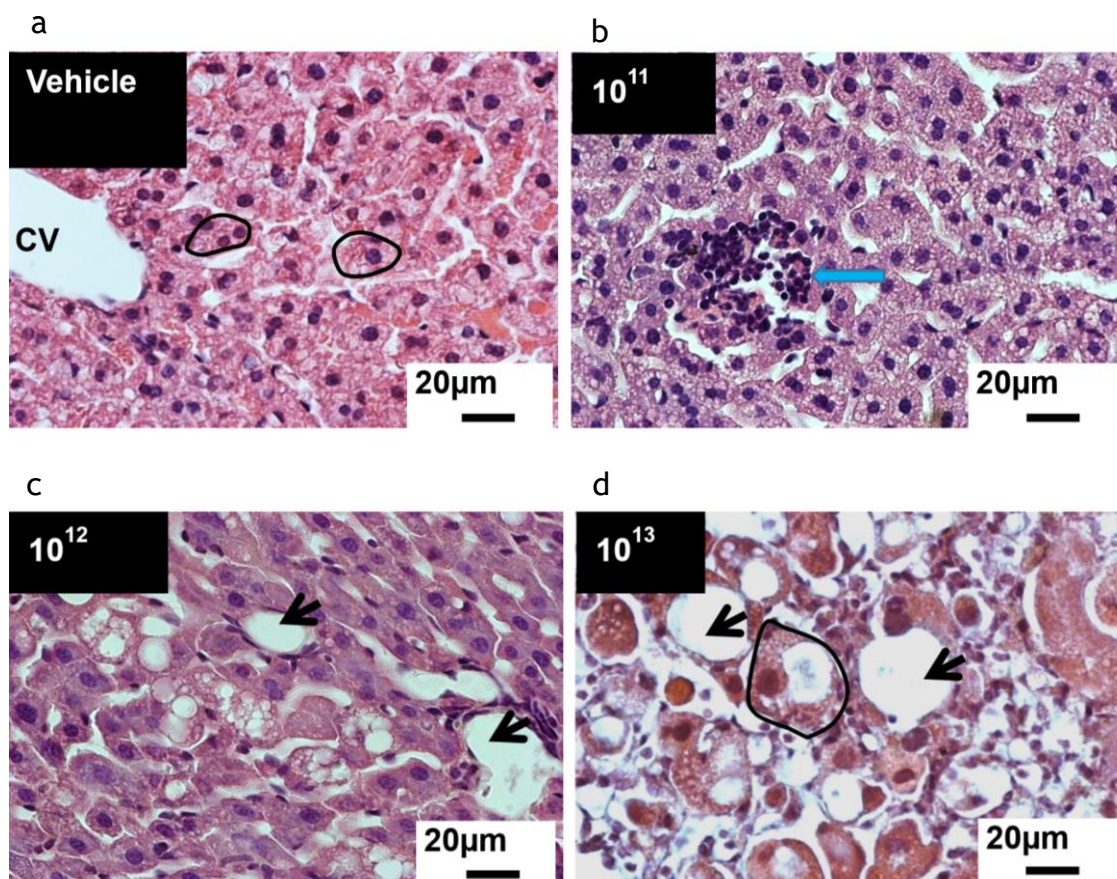


Figure 4.10 Toxicity issues revealed after systemic administration of high vector dosage. (a) mice treated with different doses of sCAA9/MeP/MECP2 vector (b)-(d) stained with H&E. Note disorganization of normal hepatocellular cord with swelling (circle), vacuolation and loss of hepatocytes (arrows). Mononuclear cell infiltration (thick blue arrow) is also evident.

In summary, IV injection of 1st generation vector provides low efficiency of the transduction in the brain, whereas very high transduction in the liver.

To assess whether the observed lethality and liver pathology was due to overexpression of the vector-derived MeCP2 or due to the vector. I tested the delivery of a high dose of AAV9 vector (10^{13} vg/mouse) but with a different cargo. For this I chose a GFP reporter construct using an identical promoter

(figure 4.11). The results revealed no noticeable effect on gross observations of the animals (no clinical signs or lethality over an 8-week period, n = 3 mice). When liver samples from mice dosed with the scAAV9/GFP were assessed by anti-GFP immunolabelling, results revealed widespread expression of GFP but, when viewed by hematoxylin and eosin labelling, showed the absence of any pathological markers observed in the *MECP2* vector-treated mice (figure 4.12). These results suggest that the acute liver toxicity was indeed due to overexpression of vector-derived MeCP2 in liver cells, which ordinarily express very low levels of the native protein.

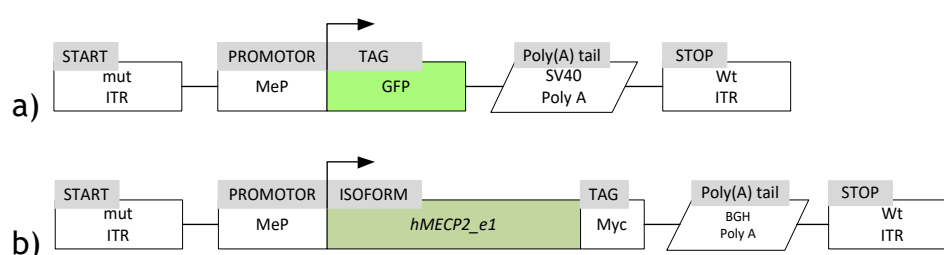


Figure 4.11 Diagram Showing AAV vector constructs (a) Construct of scAAV9/MeP229/GFP-SV40pA (control vector without *MeCP2*) (b) Construct of 1st generation vector

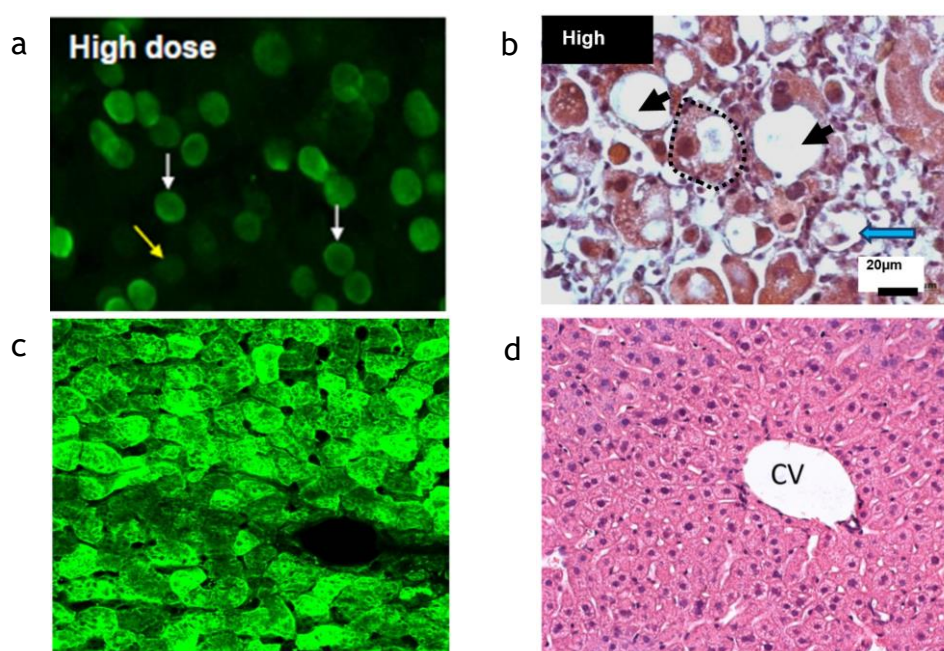


Figure 4.12 Comparison of liver toxicity between 1st generation *Mecp2* vector treatment and the GFP vector treatment in *Mecp2* KO mice injected with 1013 vg/mouse. Figure (a) and (b) show an overexpression of *mecp2* and liver damage in mice treated by scAAV9/*Mecp2* Figure (c) and (d) present no liver toxicity in liver sections in mice that were injected with a high dose of scAAV9/GFP. CV; central vein.

4.4.4 Effect of IV delivery of 1st generation vector on survival, bodyweight and phenotype severity score in *Mecp2*^{T158M/y} mice

From the above information, I concluded that the moderate dose (1×10^{12} vg/mouse) is the only dose that led to some treatment benefits in *Mecp2* KO mice. The next question was whether the presence of endogenous mutant *MeCP2* might reduce the therapeutic effect of vector-derived *MeCP2*. Male mice expressing native *MeCP2* tagged with GFP as a fusion protein and harbouring the common RTT-causing p.T158M mutation, *Mecp2*^{T158M/y} (Brown et al., 2016), display a phenotype very similar to that of *Mecp2* KO mice (Figure 4.13 a-c) but with somewhat enhanced survival (median survival of 20.3 weeks in *Mecp2*^{T158M/y} KI mice and 12.4 weeks in *Mecp2* KO mice, $p = 0.0016$, Mantel-Cox test).

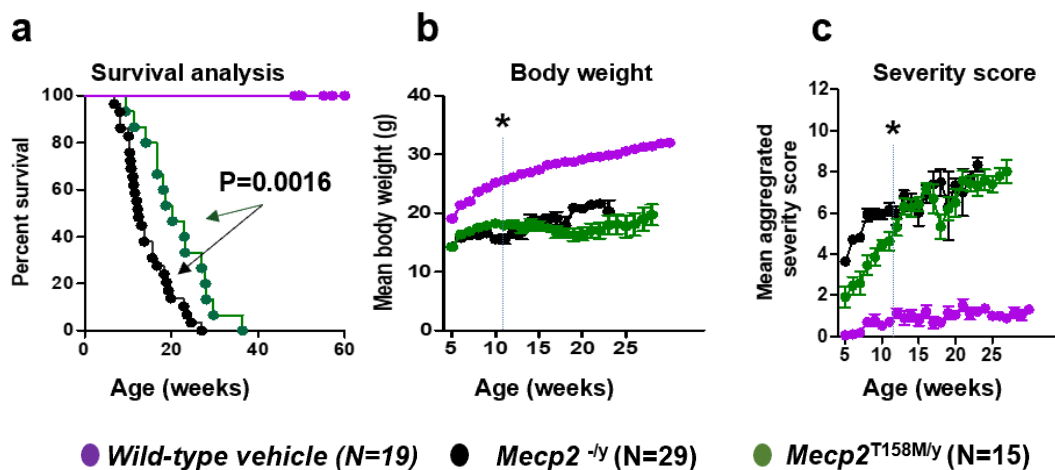


Figure 4.13 The comparison between WT, KO and treated *Mecp2*^{T158M/y} cohort in different parameter (a) Survival plot of *Mecp2*^{T158M/y} treated mice compare with vehicle control (b) Graph showing bodyweight of *Mecp2*^{T158M/y} mice treated with the vector and groups treated with the vehicle (*Mecp2*^{T158M/y} and WT) mice. * means treated *Mecp2*^{-/y} mice were significantly different from the vehicle control group at the age of 11 weeks. One-way ANOVA $F(2, 33) = 41.16$, $p < 0.0001$, Tukey's post hoc comparison. * = $p < 0.05$ (WT injected with vehicle vs *Mecp2*^{T158M/y} injected with moderate dose), ***** = $p < 0.0001$ (WT injected with vehicle vs *Mecp2*^{-/y} injected with vehicle), ** = $p < 0.01$ (*Mecp2*^{T158M/y} injected with moderate dose vs *Mecp2*^{-/y} injected with vehicle) (c) Graph showing the mean aggregate severity between groups. Data presented as means \pm SEM. At 11 weeks One-way ANOVA $F(2, 25) = 19.24$, $p < 0.0001$, Tukey's post hoc comparison. ** = $p < 0.05$ (WT injected with vehicle vs *Mecp2*^{T158M/y} injected with moderate dose), ***** = $p < 0.0001$ (WT injected with vehicle vs *Mecp2*^{-/y} injected with vehicle).

Intravenous delivery of a moderate dose (1×10^{12} vg/mouse) of the 1st generation vector to 4-5-week-old *Mecp2*^{T158M/y} mice resulted in significantly increased survival (figure 4.14a; median survival = 38.3 weeks in vector-treated mice vs

20.3 weeks in vehicle-treated mice; $p = 0.0019$, Mantel-Cox test, $n = 8-15$ per group). There was a modest increase in bodyweight in the vector-treated cohort (figure 4.14b; $p < 0.05$, one-way ANOVA using data at 20 weeks of age). However, there was no difference in the RTT-like aggregate severity score between groups (figure 4.14c), consistent with a low brain transduction efficiency ($\sim 2-4\%$) as revealed by anti-Myc labelling (not shown).

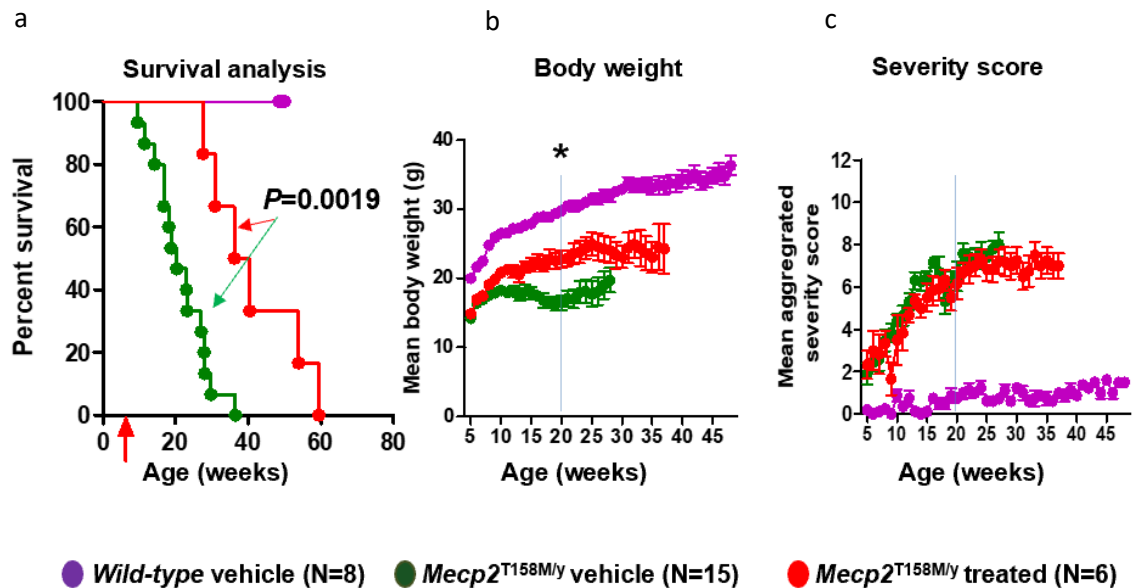


Figure 4.14 Survival plot, bodyweight measurements and bodyweight measurements of WT and Mecp2^{T158M/y} KI mice treated vehicle and Mecp2^{T158M/y} KI mice treated with the moderate dose of 1st generation vector (a) Survival plot of Mecp2^{T158M/y} treated mice (median survival 38.3 week) compared to the vehicle control (median survival 20.3 week). Red arrow indicates time of injection. One-way ANOVA $F(2, 28) = 35.56$, $p < 0.0001$, Tukey's post hoc comparison. ** = $p < 0.01$ (WT injected with vehicle vs Mecp2^{T158M/y} injected with moderate dose and Mecp2^{T158M/y} injected with moderate dose vs Mecp2^{T158M/y} injected with vehicle), **** = $p < 0.0001$ (WT injected with vehicle vs Mecp2^{T158M/y} injected with vehicle) (b) Graph showing bodyweight measurements of Mecp2^{T158M/y} mice treated by AAV9/hMECP2 vector and groups treated by vehicle (Mecp2^{T158M/y} and wild-type) mice across the experimental time. One-way ANOVA $F(2, 38) = 45.98$, $p < 0.0001$, Tukey's post hoc comparison. **** = $p < 0.0001$ (WT injected with vehicle vs Mecp2^{T158M/y} injected with moderate dose and WT injected with vehicle vs Mecp2^{T158M/y} injected with vehicle) (c) Graph showing the average aggregated severity score of the RTT-like phenotype between groups.

4.4.5 The expression of 1st generation vector in *Mecp2*^{T158M/y} brain

To explain the transduction efficiency of vector-derived MeCP2 in *Mecp2*^{T158M/y} brain, the p.T158M mutation affects the chromatin binding capacity of MeCP2, leading to loss of the punctate element of MeCP2 labelling in the nucleus (Brown et al., 2016). Immunolabelling of hippocampal neurons from treated *Mecp2*^{T158M/y} mice showed WT patterns of MeCP2 expression, with restored localization to DAPI bright spots (not shown), with a transduction efficiency of ~2%-4%, as revealed by Myc-positive cells (figure 4.15). This is consistent with vector-derived MeCP2 being able to localize normally to heterochromatin, despite the presence of mutant endogenous MeCP2 protein within the same nucleus.

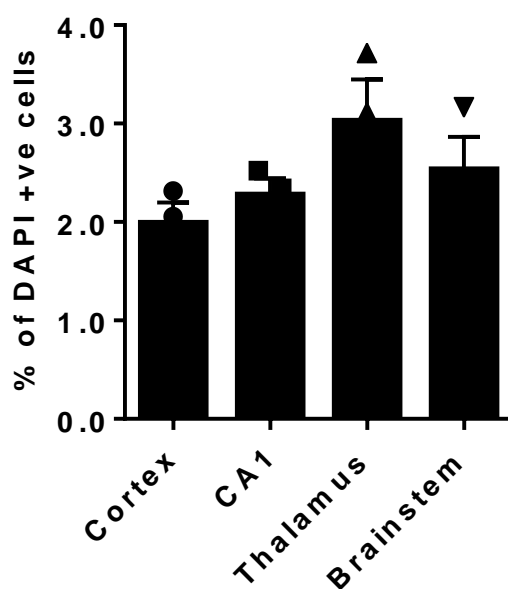


Figure 4.15 Transduction efficiency in the brain of treated mice (Myc-positive nuclei as a proportion of DAPI-positive nuclei; n = 3 mice).

4.5 Discussion

Previous studies suggested the therapeutic strategies aiming to reduce RTT-like phenotypes in mice model of RTT, however, we still lack sufficient information about safety and effectiveness of cassette design and other variables including viral production, dosing protocol and phenotype measures. In my study, I used a vector previously designed by our lab group which mainly consists of the human *MECP2_e1* gene and the MeP229 core promoter fragment to generate more

information about the safety and efficiency based on dose effect and the toxicology that was reported before (Gadalla et al., 2013).

The dose escalation results with AAV/*MECP2* revealed a narrow therapeutic window following systemic administration. Moreover, the RTT-like phenotype severity score was not improved across the range of doses tested. This issue is not due to such phenotypes being inherently resistant to reversal of phenotypes (Guy et al., 2007; Robinson et al., 2012) but can be explained by the low levels of brain transduction afforded by IV administration in my study.

In contrast, there was an effect of vector-derived *MeCP2* on extending survival and increasing body weight at the moderate dose, shown at 11 weeks (the median survival time for the control vehicle treated *Mecp2*^{-/-} mice). Survival rates did improve between the low dose group (10¹¹ vg/mouse) and moderate dose group (10¹² vg/mouse) without significant change in mean bodyweight (Figure 4.3). This indicates that the increase in survival and bodyweight is caused by either sufficient transduction level in critical brain regions, or maybe by expression in sufficient cells of peripheral tissues relevant to mortality. This is in agreement with the recent study which suggests that the level of MeCP2 in peripheral organs can impact bodyweight (Ross et al., 2016). The possible explanation that this issue may indirectly effect the survival measure that I used, 20% bodyweight loss as an endpoint criterion. Another explanation is that I may have underestimated the transduction efficiency due to the sensitivity of the immunohistochemistry assay. However, the last hypothesis can be explained by the result of biodistribution validation using qPCR that I sent to confirm with another lab group, which confirmed that my result is correct. The highest virus dose leads to significantly greater transduction efficiency in the brain (10-20%) compared to moderate and low doses and would be expected to lead to greater survival. However, mice injected with this dose showed markedly reduced lifespan and presented with severe liver pathology and lethality. Usually the expression of MeCP2 is at a much lower level in liver cells compared to neurons (Ross et al., 2016). In this study, I also present the hepatotoxicity in the moderate and low dose. The 1st generation vector resulted in liver toxicity.

This issue, as confirmed by the experiment of delivery of a similar dose of only GFP tag vector to identify the reason for this toxicity that comes from vector backbone or excessive MeCP2 expression. So, the dose dependent liver pathology can likely be attributed to the overexpression of exogenous MeCP2.

The previous RTT gene therapy studies (Gadalla et al., 2013; Garg et al., 2013; Matagne et al., 2017) used *Mecp2* knockout mice to examine the result of improvement in terms of efficiency and toxicity of viral vector. In fact RTT patient cells contain mutant MeCP2 protein that might be active and be the cause of disturbance in the action of vector-derived MeCP2 by quasi-dominant negative action. In this study, although *Mecp2*^{T158M/y} knock-in mice (Brown et al., 2016; Gadalla et al., 2017) presents RTT-like scores in the same trend with *Mecp2*^{-/y}, it also has prolonged survival. This shows that the mutant allele may produce MeCP2 with some remaining function. A notable finding is that AAV-mediated systemic delivery of *MECP2* to the knock-in line leads to a similar therapeutic effect as *Mecp2*^{-/y} treated with the same vector. Accordingly, the conclusion seems to be that the mutant MeCP2 does not interfere with vector-derived WT MeCP2. This conclusion indicates the potential of gene therapy in human patients with missense *MECP2* mutations.

These results from the delivery of the first-generation vector are very important in identifying the most suitable dose of the viral vector. We can look to use the 10¹² vg/mouse dose when optimising viral vectors in further experiments. However, this dose of the first generation viral vector is not therapeutic regarding phenotype. In the high-dose treated group, the result of transduction efficiency shows that the toxicity might involve the overexpression of MeCP2 in the liver and this could be a cause of hepatotoxicity. This result correlates with a previous paper that links AAV9 with hepatotoxicity (Gadalla et al., 2013).

Chapter 5 Development of a novel MECP2 expression cassette with enhanced safety features

5.1 Introduction

In the previous chapter (Chapter 4), I found that relatively high doses of my 1st generation vector were required in order to achieve therapeutically relevant levels of brain transduction after systemic delivery. This entailed the delivery of very high viral titers to the systemic circulation when the primary target for gene therapy in Rett syndrome is likely to be the nervous system (Ross et al., 2016). Indeed, the high dose of the peripherally delivered vector was problematic and the mice treated in the high-dose group presented signs of hepatotoxicity and high mortality after IV delivery. According to the liver section examination, there is a relationship between overexpression of vector-derived MeCP2 in liver cells and liver cell damage. Peripheral genotoxicity is a known issue with gene therapy approaches (Gadalla et al., 2013; Matagne et al., 2017) and several strategies have been developed to mitigate against such effects (Gadalla et al., 2013)

Recent studies reported new modifications to the expression cassette and capsid that were predicted to result in lower peripheral cellular expression levels and reduced liver tropism. This included the use of expression cassettes utilizing (1) an alternative, compact, and presumably weaker, JeT promoter (Tornøe et al., 2002), (2) a short synthetic 3'-UTR and polyadenylation signal (SpA) which is predicted to general lower expression levels (Levitt et al., 1989), and (3) the original 1st generation expression cassette packaged in a scAAV9.47 capsid, which emerged from an *in vivo* screen for liver de-targeted capsid sequences relative to AAV9 (Karumuthil-Melethil et al., 2016; Pulicherla et al., 2011). In addition, my lab colleague, Dr Ralph Hector, designed a new modified cassette, hereafter referred to as the 426 vector, combining various aspects of endogenous and artificial MeCP2 expression controls. The 426 vector construct includes putative regulatory elements (RE) in the extended mMeP426 promoter and endogenous distal 3'-UTR (see figure 5.1 below). The extent of the mMeP229 promoter (used in the 1st generation vector) is indicated by the dashed line. Two non-endogenous cytosine nucleotides precede the ATG start codon. The RDH1pA 3'-UTR consists of several exogenous microRNA (miR) binding sites incorporated

as a ‘binding panel’ adjacent to a portion of the distal endogenous *MECP2* 3’-UTR, including the distal polyadenylation signal and its accompanying regulatory elements.

5.2 Study aims

The main aim of the work described in this chapter was to find the most effective vector from a series of new cassette designs developed from 1st generation vector attempting to improve MeCP2 expression within the physiological limit, without producing overt overexpression-related liver toxicity and to improve RTT-like aggregate severity score. The specific objectives of this study were:

- To assess the safety and effectiveness of new cassette design vectors on RTT-like phenotypes after systemic administration
- To assess the effect of new cassette design vectors on cellular expression levels of MeCP2.
- To improve the RTT-like aggregate severity score by increasing the proportion of MeCP2-expressing cells in the brain by direct cerebroventricular injection in neonatal mouse

5.3 Methods

In this chapter, I tested four new cassette design vectors developed from the 1st generation vector (chapter 4) aiming to reduce the toxicity from MeCP2 overexpression. The vectors I used in this study are:

- 1) scAAV9/JeT/MECP2 (JET) aiming to reduce the overexpression with a small synthetic promoter that is predicted to drive low expression (Figure 5.1a).
- 2) scAAV9/SpA (SpA) aiming to reduce the overexpression using short synthetic polyA makes the mRNA unstable (Figure 5.1b).
- 3) scAAV9.47/MECP2 (9.47) aiming to de-target to the liver and thereby potentially increasing the brain transduction by using the scAAV9.47 capsid which is selected for its relatively low transduction of liver cells (Figure 5.1c).
- 4) scAAV9/MeP426 (MEP426) aiming to reduce overexpression using a longer segment of the endogenous mMeCP2 promoter and exogenous microRNA (miR) binding sites in the 3’-UTR (Figure 5.1d).

To evaluate the efficiency of all vectors, I used the same method that I applied on the 1st generation vector (chapter 4), with the IV tail injection with moderate dose (10^{12} vg per mouse), and on the same line and age of mouse model (*Mecp2* KO male mice with their WT littermates), age of 4-5 weeks). I also recorded bodyweight and RTT-like aggregate severity score weekly and analysed the expression patterns, transduction efficiency, and quantification of vector-derived MeCP2 levels in brain and spinal cord.

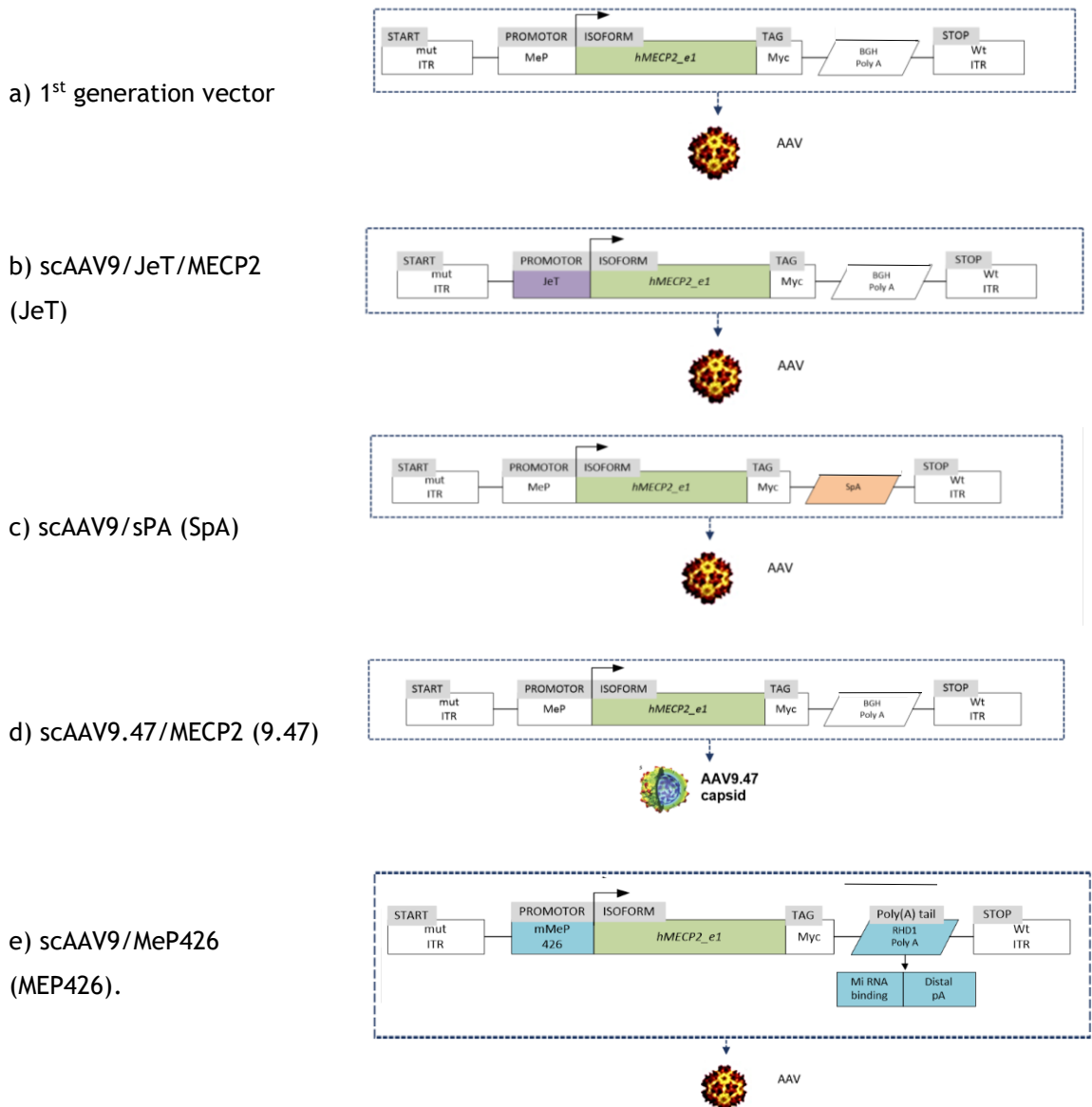


Figure 5.1 Diagram showing AAV vector constructs of vectors a) 1st generation vector b-e) a range of modifications to the expression cassette and capsid modifying from the 1st generation vector b) a synthetic and presumably weaker promoter, JeT promoter c) a short synthetic polyadenylation (SpA) signal d) the original 1st generation vector packaged in a scAAV9.47 capsid, which emerged from an in vivo screen for liver de-targeted capsid sequences relative to AAV9. e) 2nd generation vector incorporating an extended *Mecp2* promoter and additional 3' UTR regulatory elements

5.4 Results

5.4.1 The efficacy and safety of SpA, JeT and 9.47 vectors in the KO mouse model, dosing at 10^{12} vg/mouse by IV injection.

Aiming to reduce the toxicity from MeCP2 overexpression occurring with the 1st generation vector, I tested three newly developed cassette design vectors that were predicted to result in lower cellular expression levels and/or reduce liver toxicity in *Mecp2*^{-/-} KO mice. This included 1) JeT promoter vector, 2) short synthetic 3'-UTR/polyA signal (SpA) vector, and 3) the scAAV9.47 capsid.

The result with the JeT promoter, short synthetic polyA and scAAV9.47 vectors shows significantly extended survival (median survival = 24.71 ± 9.99 weeks, 32.53 ± 9.34 , and 27.45 ± 9.49 weeks) compared to the KO treated with vehicle (median survival = 11.6 ± 4.09 weeks). However, there is not much difference from the result with the 1st generation vector. (Figure 5.2)

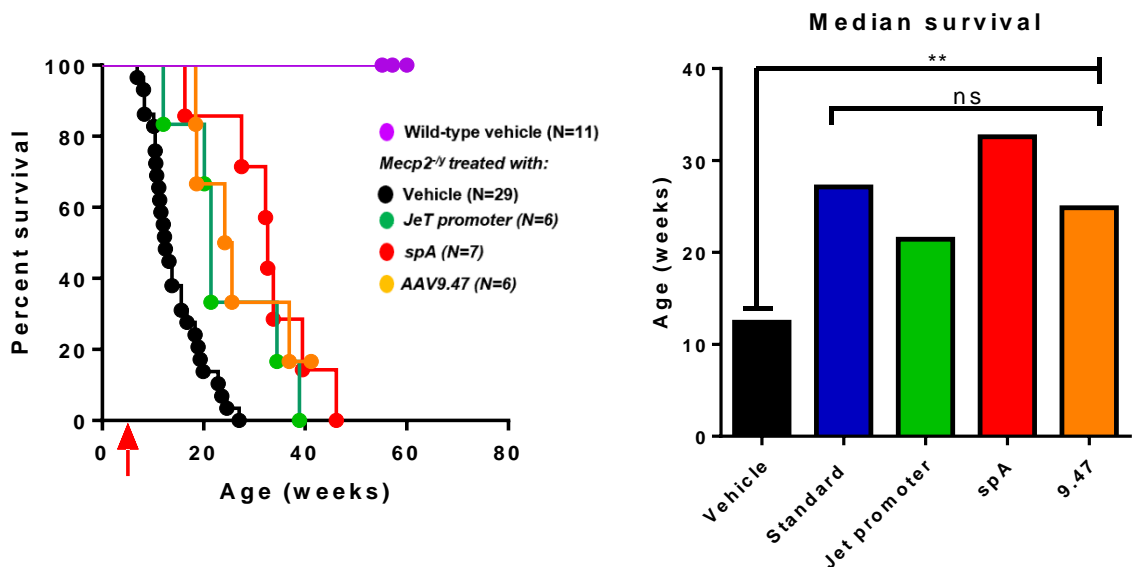


Figure 5.2 Survival of *Mecp2* KO mice treated with SpA containing vector, vector utilising JeT, and vector utilising AAV9.47 capsid (a) Survival plot of *Mecp2*^{-/-} mice treated with promoter compared to vehicle-treated *Mecp2*^{-/-} mice. The plots show the median survival of KO mice compared to the KO treated with vehicle (median survival 11.6 weeks). The red arrow indicates the time of injection. (b) Column plot showing the mean survival of *Mecp2*^{-/-} mice treated with promoter compared to vehicle-treated *Mecp2*^{-/-} mice. Data presented as mean \pm SEM. One-way ANOVA $F(2, 33) = 35.51$, $p < 0.0001$, Tukey's multiple comparison tests; ** = $p < 0.01$

There is the same trend in body weight measurement for *Mecp2*^{-/-} mice treated with the JeT promoter, short synthetic polyA and scAAV9.47. The result shows significant improvement on body weight measurement (body weight in JeT promoter group = 20.84 ± 1.11 g, SpA group = 20.84 ± 1.11 g, and 9.47 group = 20.84 ± 1.11 g, respectively) at 11 weeks of age compared to the KO treated with vehicle (median survival = 15.62 ± 3.40 g weeks). However, the average body weight of all *Mecp2*^{-/-} treated group continued lower than WT controls (mean body weight = 25.24 ± 2.16 g). Figure 5.3

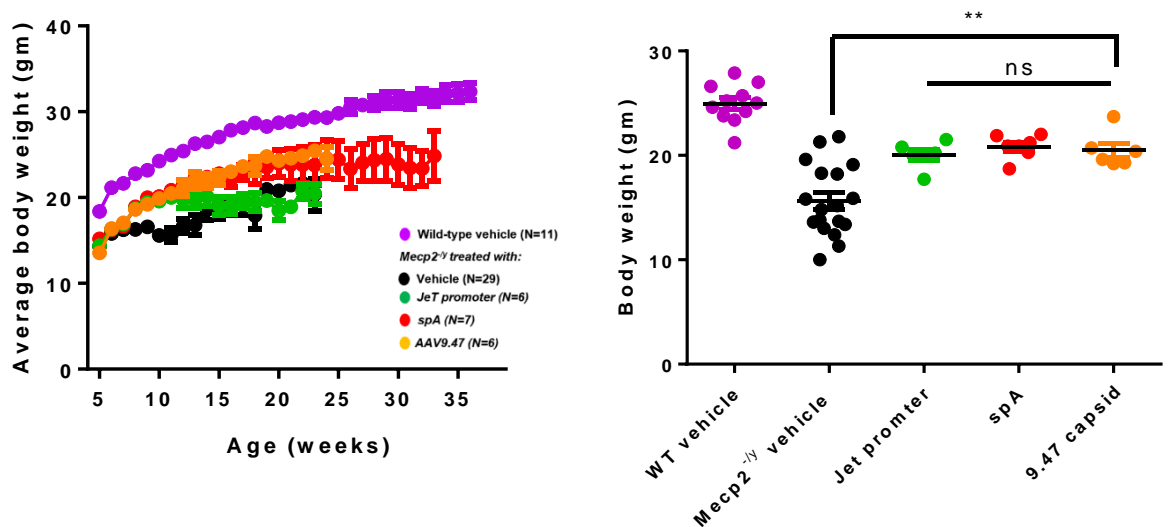


Figure 5.3 Body weight measurement of *Mecp2* KO mice treated with SpA containing vector, vector utilising JeT, and vector utilising AAV9.47 capsid. (a) bodyweight measurements across the experimental time and (b) body weight comparison at 11 weeks old. Data presented as mean \pm SEM. Statistical test results: ANOVA test, $F(5, 49) = 19.64$, $p < 0.0001$, Tukey post hoc comparison test; ** = p -value < 0.01 , between *Mecp2*^{-/-} treated with and *Mecp2*^{-/-} treated with each viral vector)

In contrast, treatment of *Mecp2*^{-/-} mice with new cassette vectors had no impact on the RTT-like phenotype severity score at the age of 11 weeks. The mean aggregated severity score in *Mecp2*^{-/-} treated with JET = 6.66 ± 0.81 , *Mecp2*^{-/-} treated with SpA = 6.71 ± 1.11 , *Mecp2*^{-/-} treated with 9.47 = 6.42 ± 0.97 , *Mecp2*^{-/-} treated with vehicle = 5.35 ± 1.14 , and WT treated with vehicle = 0.83 ± 0.5 . Figure 5.4.

These results are summarized in Figure 5.5; although the new modification vector showed the improvement from the vehicle-treated group, none of them resulted in any improvement from the 1st generation vector (Figure 5.5).

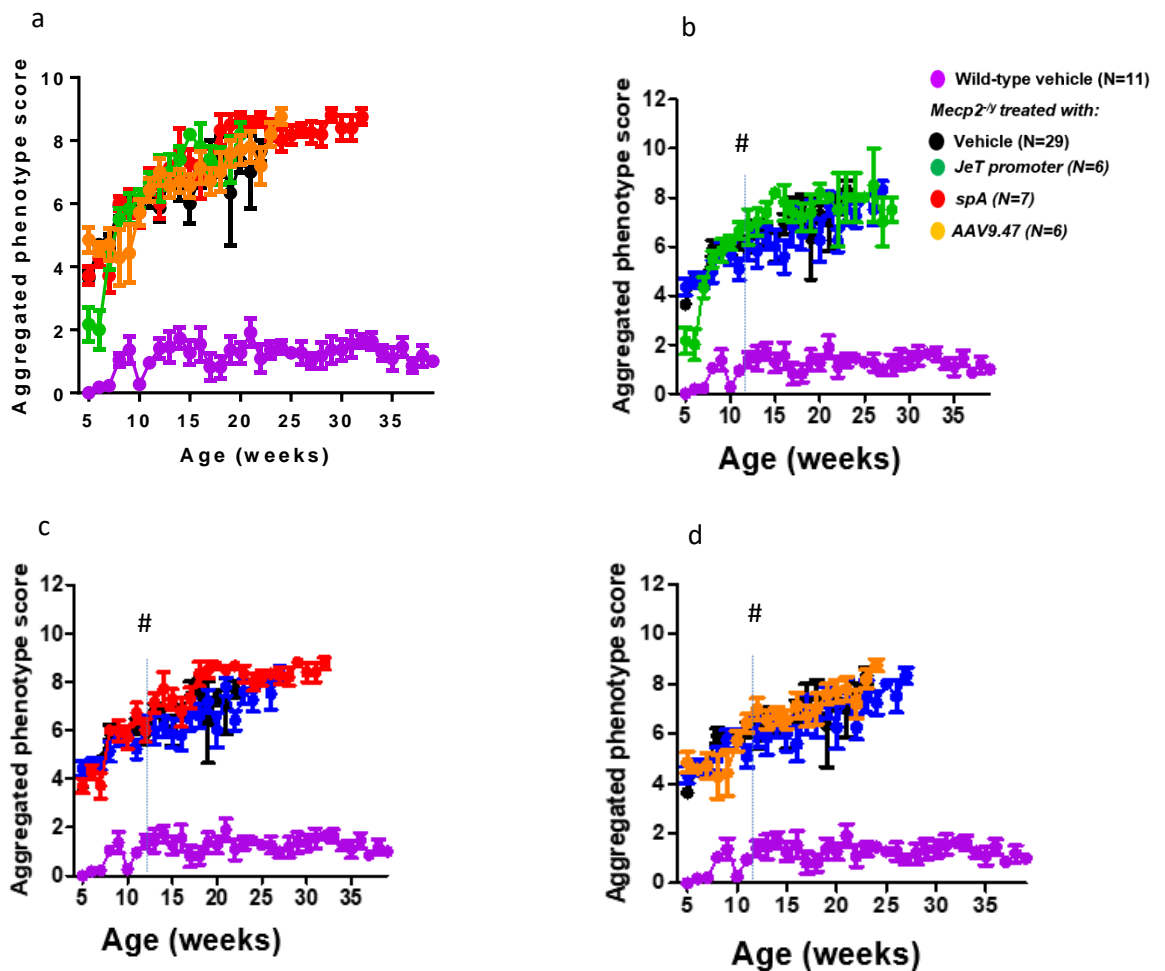


Figure 5.4 of Rett-like phenotype severity score of *Mecp2* KO mice treated with SpA containing vector, vector utilising JeT, and vector utilising AAV9.47 capsid. Graph showing the progress of Rett-like phenotype severity score in (a) all new cassette design compare to control groups (b) JET group compared to control groups, and (c) SpA group compared to control groups, and (d) 9.47 group compared to control groups across the experimental. #. # Means end of experiments at 11 weeks. Statistical test results: ANOVA test, $F(5, 48) = 48.87$, $p < 0.0001$. Tukey post hoc comparison test; ** = p -value < 0.01 , between WT and all *Mecp2*^{-/-} treated in every groups.

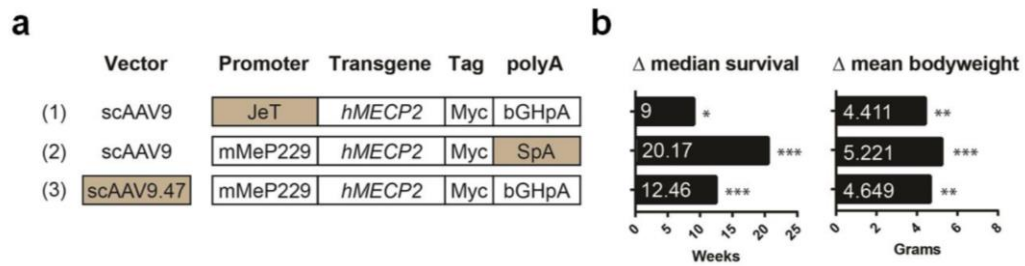


Figure 5.5 summary of Novel vector design features and efficacy. (a) A summary of the design differences for three of the novel vectors described in the text. (b) Efficacy of these three novel vectors after intravenous injection of 1×10^{12} vg/mouse to 4-5 weeks old *Mecp2*^{-/-} mice, expressed as increase in median survival relative to the vehicle controls (left; compared using Mantel-Cox test) and mean body weight at the age of 11 weeks (right) relative to the vehicle controls (one-way ANOVA with Tukey's post-hoc pairwise comparisons); * $p < 0.05$, ** $p < 0.01$, *** $p < 0.001$.

In relation to the liver toxicity that occurred in *Mecp2*^{-/-} mice injected with the 1st generation vector, the result of histological investigations of liver sections in JeT, SpA and 9.47 treated groups (3 mice in each group) also revealed vacuolation of hepatocytes (Figure 5.6). This result confirmed that these modified vectors cause the development of liver pathology and were unable to reduce the toxicity as had been predicted.

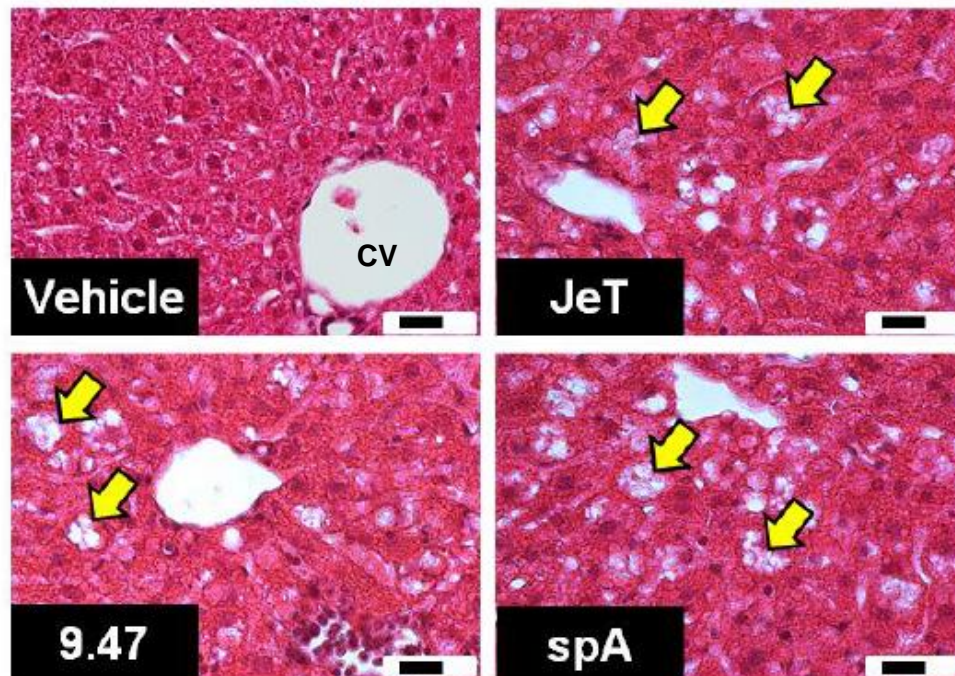


Figure 5.6 Comparison of liver toxicity between 1st generation vector treatment and the novel vectors treatment (10^{12} vg/mouse; for 30 days) in WT mice aged 35 days). Representative liver sections from mice injected with JeT, 9.47 or SpA vectors. Arrows indicate examples of vacuolation of hepatocytes that were not seen in vehicle-treated samples; scale bar indicates 20 μ m. CV; central vein

5.4.2 Development of a Second-Generation Vector that Reduced Liver Toxicity after Systemic Administration

In order to reduce toxic levels of exogenous MeCP2 expression and liver tropism, the knowledge about the relationship between *Mecp2* expression in transduction cells and the vector backbone, which were obtained from my experiment in the 1st generation vector and the novel cassette vector in *Mecp2* KO mice were used to modify the second-generation vector (426 vector).

This 2nd generation vector was designed by my lab colleague, Dr Ralph Hector, based on two main modifications of the vector backbone both aiming to control the endogenous vector-derived MeCP2 level in transduced cells. The first modification is an extension of an endogenous *Mecp2* core promoter fragment (MeP229) using in the 1st generation vector which had been shown largely to recapitulate the endogenous tissue-level pattern of MeCP2 expression (Gray et al., 2011a). The previous study (Gadalla et al., 2013) and my study showed that this core promoter fragment is missing a number of predicted upstream regulatory elements that may be important in cell-type-specific regulation of MeCP2 expression. (Adachi et al., 2005; Liu and Francke, 2006; Liyanage et al., 2013; Lyst et al., 2013). Figure 5.7. In addition to the extended promoter, another modification of a novel 3' UTR, consisting of a fragment of the endogenous MECP2 3' UTR and a selected panel of binding sites for microRNAs (miRNAs) known to be involved in regulation of *Mecp2* (Feng et al., 2014; Jovicic et al., 2013; Klein et al., 2007) (Figure 5.7). These elements were incorporated into the second-generation cassette design to build in as many intrinsic regulatory elements as possible.

To test the therapeutic efficacy of the 2nd generation vector, a moderate dose (1×10^{12} vg/mouse) was delivered intravenously into 4-5-week-old *Mecp2*^{-y} mice via tail vein injection as I applied to the previous experiment. There was a significant extension of survival in the vector-treated mice compared to the vehicle-treated mice (median survival = 29.9 ± 9.00 weeks and 11.6 ± 4.09 weeks, respectively; $p < 0.0001$, Mantel-Cox, Figure 5.8a). There was also a significant improvement in body weight at the age of 11 weeks (426 group BW = 21.72 ± 3.34 kg; vehicle-treated group = 13.93 ± 2.46 kg; $p < 0.05$, one-way ANOVA, with Tukey's post-hoc pairwise comparison test, Figure 5.8b). In

contrast, there was no effect on RTT-like aggregate severity score (Figure 5.8c). Mean aggregated severity score in *Mecp2*^{-/-} treated with 2nd generation, *Mecp2*^{-/-} treated with 1st generation, *Mecp2*^{-/-} treated with vehicle, and WT treated with vehicle are 5.11 ± 1.26 , 5.18 ± 0.96 , 5.35 ± 1.14 , and 0.83 ± 0.5 , respectively). The 426-vector thus showed no therapeutic advantages over the 1st generation vector after systemic delivery (Figure 5.8a-c) in terms of extending survival or improving the Rett-phenotypic score.

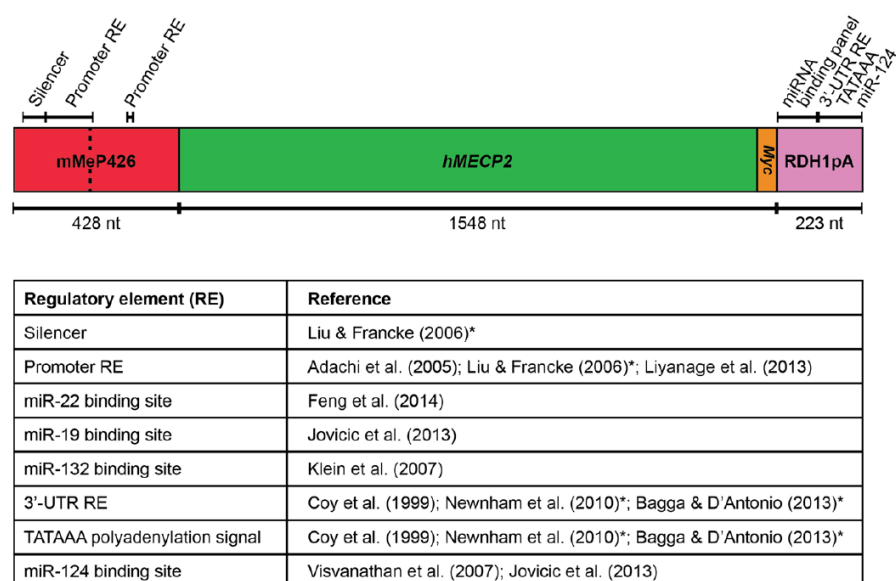


Figure 5.7 Design of the 2nd generation vector construct. Putative regulatory elements (RE) in the extended mMeP426 promoter and endogenous distal 3'-UTR are indicated. The extent of the mMeP229 promoter (used in the 1st generation vector) is indicated by the dashed line. Two non-endogenous cytosine nucleotides precede the ATG start codon. The RDH1pA 3'-UTR consists of several exogenous microRNA (miR) binding sites incorporated as a 'binding panel' adjacent to a portion of the distal endogenous *MECP2* polyadenylation signal and its accompanying regulatory elements. References with an asterisk indicate human *in vitro* studies, not rodent studies.

In addition, to compare of liver safety from exogenous endogenous vector-derived MeCP2 overexpression between 2nd generation vector and the 1st generation vector regarding liver safety, three 35-day-old male WT mice were injected intravenously with either 2nd generation vector and the 1st generation vector at a dose of 1×10^{12} vg/mouse and were sacrificed after 30 days. The liver tissues were examined for vector-derived MeCP2 expression (using anti-Myc tag antibody) and signs of liver pathology (Figure 5.9). There was no significant difference in transduction efficiency between vector constructs (Figure 5.9b),

but cellular levels of vector-derived MeCP2 (anti-Myc) in mice treated with 1st generation vector were significantly higher than those in mice treated with 426-vector (figure 5.9c; $p < 0.001$, unpaired t -test). Analysis of the distribution of cellular MeCP2 expression levels in transduced cells showed that MeCP2 expression is higher in mice injected with the first-generation vector (with fewer cells exhibiting very high expression levels) than the second-generation. We can conclude from this that second generation vector is capable of controlling the degree of MeCP2 overexpression better than the 1st generation vector.

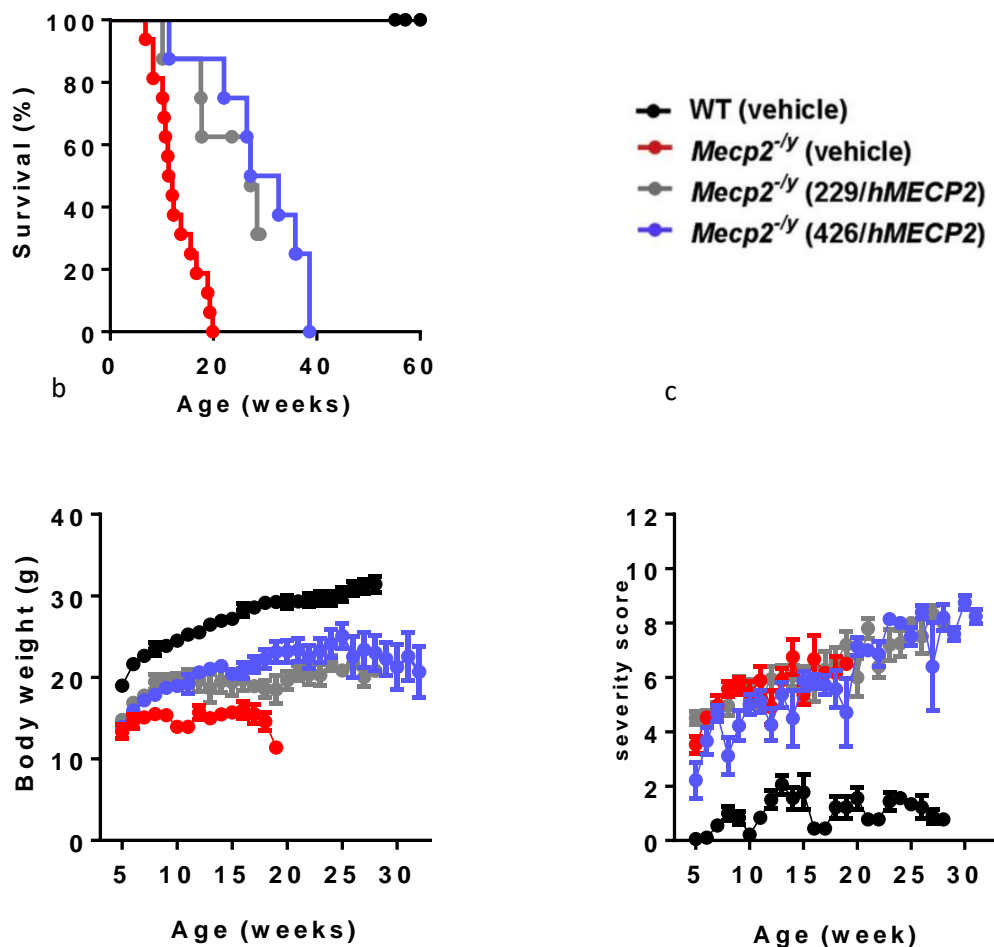


Figure 5.8 Therapeutic Efficacy of Second-Generation Vector after Systemic Delivery to *Mecp2*^{-/-} Mice. (a) Survival plot for *Mecp2*^{-/-} mice treated intravenously with 1×10^{12} vg per mouse of the second-generation vector (median survival = 29.9 weeks) or an identical dose of first-generation vector (median survival = 27.1 weeks) or vehicle (median survival = 13.93 weeks). Arrow indicates age at injection. (b) Plots showing mean body weight. At 11 weeks, Statistical test results: ANOVA test, $F(3, 41) = 21.95$, $p < 0.0001$ Tukey's post-hoc tests: * = $P < 0.05$; between *Mecp2*^{-/-} injected with vehicle vs. *Mecp2*^{-/-} injected with 426 (c) aggregate severity scores. Statistical test results: ANOVA test, $F(3, 39) = 53.75$, $p < 0.0001$ Tukey's post-hoc tests: .**** = p -value < 0.0001 , between WT and all *Mecp2*^{-/-} treated in every groups.

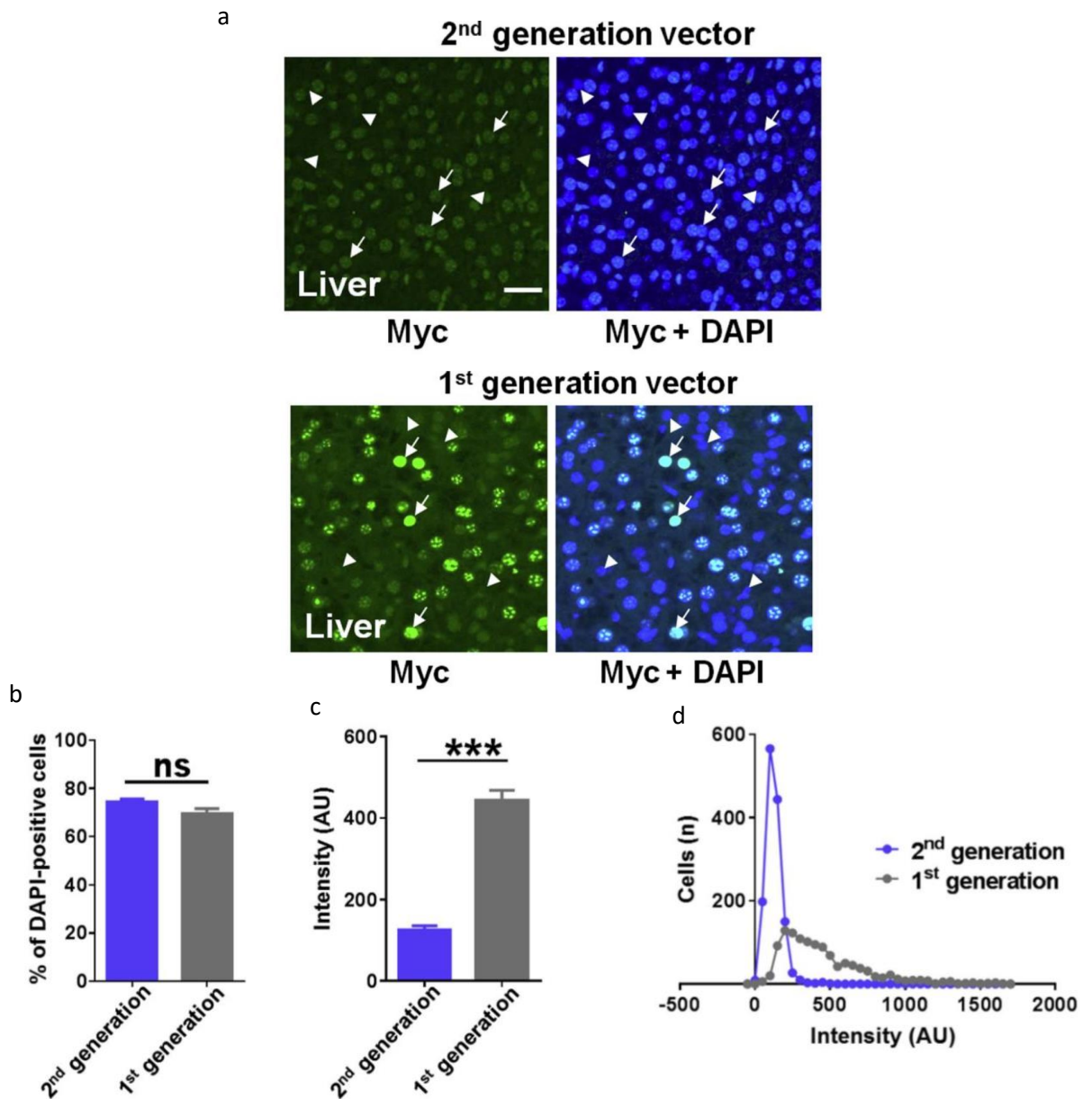


Figure 5.9 Expression of vector-derived MeCP2 in the livers of mice treated with second-generation vector compared with first-generation vector (a) Flattened confocal stack images from livers of mice 1 month after being injected intravenously at 5 weeks of age with the second-generation vector or first-generation vector at 1×10^{12} vg per mouse; confocal settings were the same in each case. Tissues were immunolabeled with anti-Myc and DAPI nuclear stain. Arrows indicate transduced cells (Myc-positive), and arrowheads indicate non-transduced cells. Scale bar indicates 20 μ m. (b) Transduction efficiencies in the liver for both vectors. Mann-whiney test $p = 0.1000$ (c) Quantification of cellular levels of vector-derived MeCP2 measured as anti-Myc immunofluorescence in transduced cells in the liver t-test $t=12.29$ $df=4$, $p = 0.0003$ ($n = 3$ mice, 1,400 transduced cells). Data are presented as mean \pm SEM. (d) Frequency distribution of cellular levels of vector-derived MeCP2 in the liver, measured as in (c).

To estimate the degree of toxicity in the liver, liver samples from three mice of each treated group were analysed for signs of liver pathology. There was none of the disrupted hepatic architecture or vacuolation previously observed with the 1st generation vector (Figure 5.10a). The density of inflammatory foci was significantly higher in liver samples from mice injected with 1st generation vector than those injected with 426-vector (Figure 5.10b).

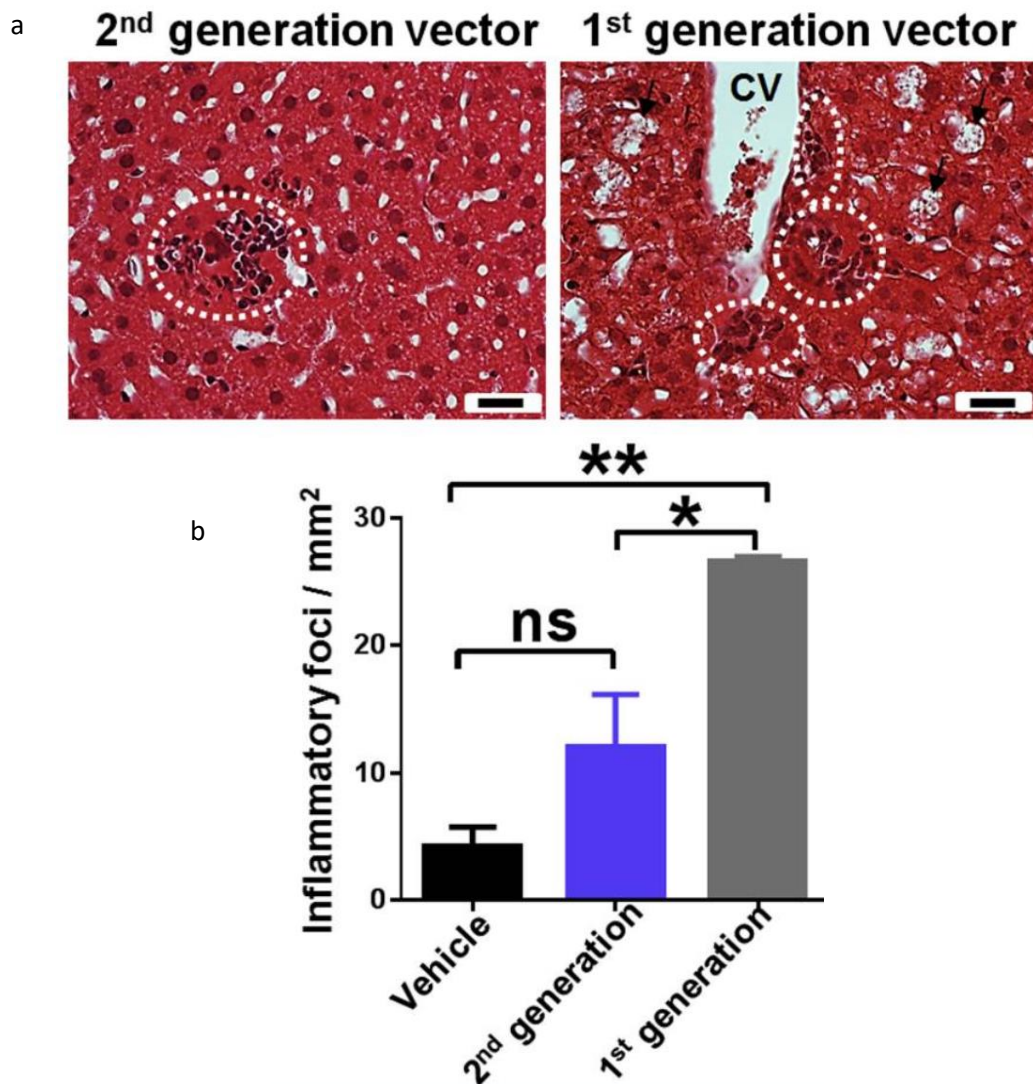


Figure 5.10 Comparison of liver toxicity between 1st generation vector treatment and the novel vectors treatment (1012 vg/mouse; for 30 days) in WT mice aged 35 days). (a) Representative liver sections showing vacuolation of hepatocytes (arrows) and sites of mononuclear cell infiltration (dashed circles). CV, central vein. White scale bar indicates 20 μ m. (b) Reduced Expression of Vector-Derived MeCP2 in the Livers of Mice Treated with Second-Generation Vector Quantification of the density of inflammatory foci in the livers of treated mice (n = 3 per group). Data are presented as mean \pm SEM. Statistical test results: (a) ANOVA test, F (2, 6) = 19.63, p = 0.0023. Tukey's post-hoc tests: * = p < 0.05; ** = p < 0.01; * = p < 0.001; ns, no = t significant.**

In summary, the 2nd generation vector seems to have a clearly beneficial effect of reducing liver toxicity while the brain transduction efficiency does not present a significant difference in RTT-like phenotype score compared with the 1st generation vector.

5.4.3 Neonatal Cerebroventricular Injection of the Second-Generation Vector Improved the RTT-like Aggregate Severity Score

From the previous set of experiments delivered 2nd generation vector by systemic administration to young adult male mice, it is apparent that the 2nd generation 426 vector demonstrate an improvement of the safety profile when compared to the original 229 construct. However, the 2nd generation vector still showed a relative lack of efficacy in relation to the RTT-like neurological phenotypes, consistent with the low brain transduction efficiencies observed in my study. This agrees with the previous study showed that phenotype severity and degree of improvement after gene restoration correlate with the proportion of MeCP2-re-expressing cells in the brain (Robinson et al., 2012). Thus, I decided to test the 2nd generation vector delivered by direct brain injection in neonatal male KO and WT mice (0-3 days postnatally) aiming to afford widespread transgene expression (Gadalla et al., 2013). The mice were delivered 2nd generation vector by cerebroventricular injection at a dose of 1×10^{11} vg/ mouse (see section 2.5.2.2).

The results show that there was a pronounced enhancement of survival of *Mecp2*^{-/-} mice treated with the 426-vector in comparison to vehicle-treated mice (median survival = 38.5 ± 11.39 and 12.4 ± 5.37 weeks, respectively; $p < 0.0001$, Mantel-Cox test, Figure 5.11a), while there was only a minor effect of vector on bodyweight. The mean bodyweight of *Mecp2*^{-/-} mice treated with the 426-vector at 11 weeks was 19.05 ± 1.85 , while *Mecp2*^{-/-} mice treated with vehicle had a mean bodyweight of 15.62 ± 3.40 kg. (Figure 5.11b). A more remarkable observation was the clear improvement in the RTT-like aggregate severity score in the 2nd generation vector treated group (RTT-like aggregate severity score at 11 weeks = 2.07 ± 2.01) compared to vehicle-treated *Mecp2*-

null mice (RTT-like aggregate severity score at 11 weeks = 6.17 ± 1.23) ($p < 0.01$ at 11 weeks, one-way ANOVA, with Tukey post hoc pairwise comparison) (Figure 5.11c). However, some WT treated with the 2nd generation vector found unexpected adverse effect showed as a mild hind-limb abnormality phenotype. (RTT-like aggregate severity score at 11 weeks = 1.87 ± 1.80)

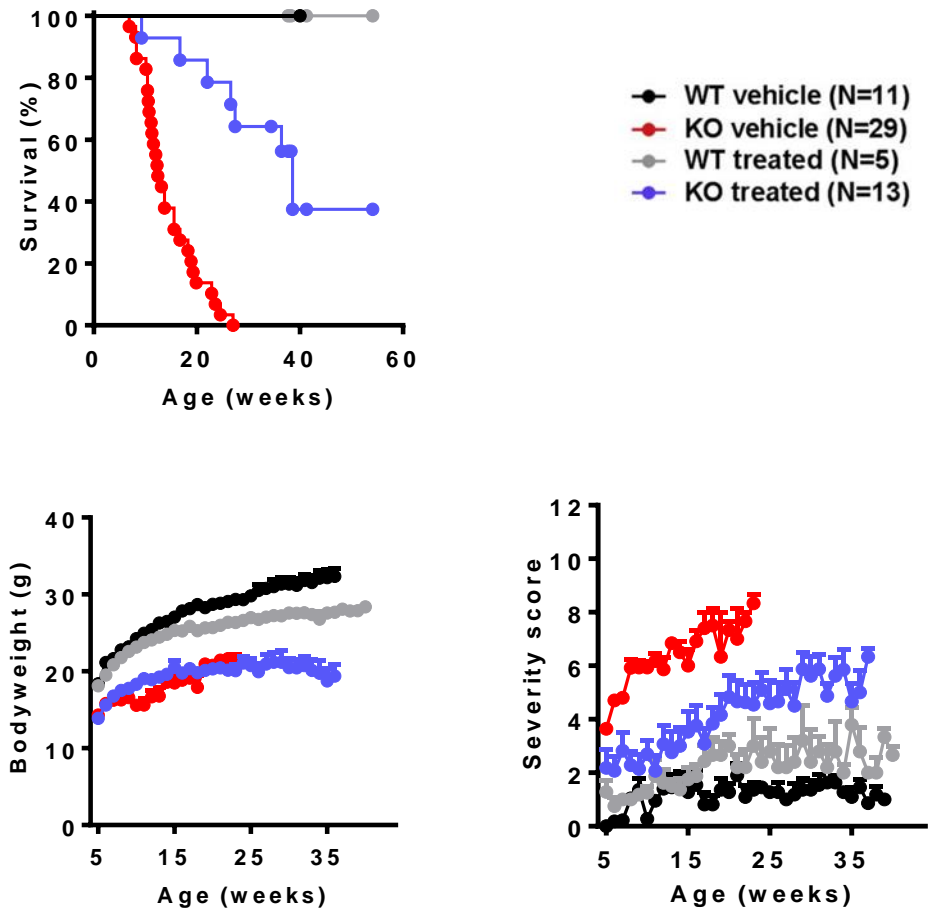


Figure 5.11 Survival plot, bodyweight measurements and bodyweight measurements of *Mecp2*^{-/-} and WT neonatal mice treated with the 426-vector 1×10^{11} vg/ mouse and *Mecp2*^{-/-} and WT mice treated with vehicle by direct brain injection.

(a) Survival plot showing extended survival of neonatally treated *Mecp2*^{-/-} mice (median survival = 38.6 weeks; $p < 0.0001$, Mantel-Cox test) compared with vehicle-treated animals (median survival = 12.4 weeks). (b and c) Plots showing mean (b) body weight. Statistical test results at 6 weeks: ANOVA test, $F(3, 46) = 38.57$, $p < 0.0001$. Tukey's post-hoc tests: ** = $P < 0.01$ between *Mecp2*^{-/-} mice treated with vehicle and *Mecp2*^{-/-} mice treated with 426 vector (c) aggregate severity scores. Statistical test results at 6 weeks: ANOVA test, $F(3, 43) = 38.24$, $p < 0.0001$. Tukey's post-hoc tests: ** = $P < 0.01$ between *Mecp2*^{-/-} mice treated with vehicle and *Mecp2*^{-/-} mice treated with 426 vector. Tukey's post-hoc tests: **** = $P < 0.001$ between WT and *Mecp2*^{-/-} mice)

To confirm that the improvement of the survival and RTT-like phenotype in *Mecp2*^{-y} mice treated with the 426-vector may involve an increase of the proportion of MeCP2-expressing cells in the brain, brain tissue from three mice in each group were analyzed for Vector-derived MeCP2 (revealed by anti-Myc tag immunolabelling). The result showed that the vector-derived MeCP2 was detectable in all brain regions, with transduction efficiencies across brain regions ranging from ~10-40% (Figure 5.12).

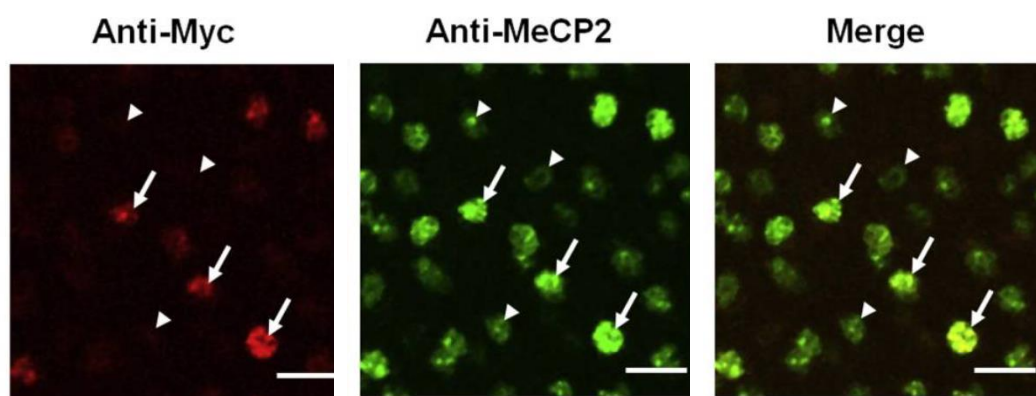


Figure 5.12 Direct Brain Delivery of Second-Generation Vector to Neonatal *Mecp2*^{-y} Mice Revealed Therapeutic Efficacy Representative confocal images from the cortex of injected wild-type mice. White arrows indicate transduced cells; arrowheads indicate non-transduced cells; scale bars indicate 20 μ m.

Moreover, the distribution analysis revealed that the modal cellular MeCP2 level in transduced cells in cortex was approx. twice that of endogenous MeCP2 (consistent with an exogenous expression level equal to the endogenous level), with some cells expressing higher levels of exogenous MeCP2 (Figure 5.13).

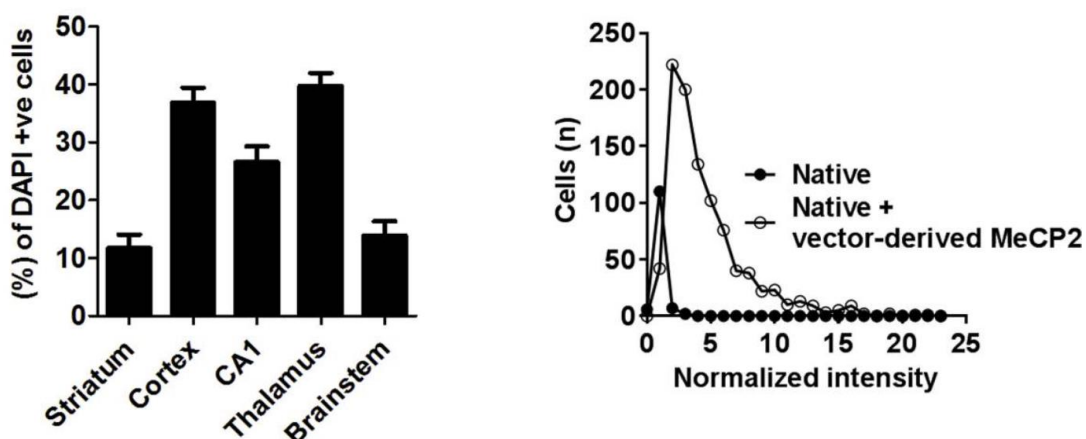


Figure 5.13 Distribution analysis of 2nd generation vector delivered MeCP2 in mouse brain by direct brain injection method. (a) Graph showing transduction efficiency in different brain regions (n = 3 mice). Statistical test results: ANOVA test, $F(3, 43) = 38.24$, $p < 0.0001$. Tukey's post-hoc tests: **** = $P < 0.0001$ (Striatum vs. Cortex, Striatum vs. Thalamus, Cortex vs. Brainstem, and Thalamus vs. Brainstem), *** = $P < 0.001$ (Striatum vs. CA1), ** = $P < 0.01$ (CA1 vs. Thalamus, CA1 vs. Brainstem), * = $P < 0.05$ (Cortex vs. CA1) (b) Frequency distribution of MeCP2 levels in transduced and non-transduced (“native”) cells in the mouse cortex (n = 3 mice; 954 transduced cells) data presented as mean \pm SEM.

5.4 Discussion

The monogenicity of RTT and the demonstrated reversibility of the RTT-like phenotype after delayed activation of silent *Mecp2* in mice (Robinson et al., 2012) suggest gene therapy as a potential avenue to treat RTT. Several attempts have been conducted at the preclinical level to deliver *MECP2* exogenously in RTT-mouse models (Gadalla et al., 2013; Matagne et al., 2013; Matagne et al., 2017), they showed promising outcomes either when *MECP2* was delivered intracranially to mouse neonates (Gadalla et al., 2013) or intravenously to young adult and adult mice (Gadalla et al., 2013; Garg et al., 2013; Matagne et al., 2017). However, the differences in vector design and dosage adopted in both experiments highlight the importance of conducting dose escalation and vector comparison studies to determine the most efficacious/safe vector to move forward to testing in higher primates and eventually in clinical trials.

In this chapter, a first attempt to reduce toxic MeCP2 expression and liver pathology involved construction of the expression cassette and capsid. However, vector modifications to reduce liver transduction and hence toxicity through using putative weaker synthetic promoters and polyadenylation signals was not

sufficient to avoid liver toxicity and AAV9.47 capsid that was shown to de-target the liver relative to AAV9 (Karumuthil-Melethil et al., 2016; Pulicherla et al., 2011), showed no advantage over AAV9 in terms of liver pathology. The mice that were treated with 9.47 vector also present vacuolation of hepatocytes as well as mice that were treated with the 1st generation at the same dose. This proved to be contrary to my predictions of no toxicity.

Consequently, I focused my efforts on the second-generation vector which includes endogenous regulatory elements that may better regulate vector-derived MeCP2 levels in transduced cells. This included the incorporation of both an extended endogenous promoter and an endogenous 3'-UTR fragment.

Our 426 extended promoter is based on several studies which assessed the well-conserved human *MECP2* and mouse *Mecp2* promoter regions and identified the presence of some putative regulatory elements within a 1-kb window immediately upstream of the transcription start site (Adachi et al., 2005; Liu and Francke, 2006; Liyanage et al., 2013). Subsequently, the extended endogenous promoter (426 bp) in the 2nd generation vector included a putative silencer element at position -274 to -335 relative to the RefSeq transcription start site (Figure 5.8).

The significantly reduced MeCP2 expression in the liver, with subsequent reduction of the hepatotoxicity encountered with the 1st generation vector, also presumably involved the regulatory site combination deployed in the 3'-UTR, which contained a non-consensus distal *MECP2* polyadenylation signal (TATAAA), as well as a number of clustered putative 3'UTR regulatory elements (Bagga and D'Antonio, 2013; Coy et al., 1999; Newnham et al., 2010) and a number of miRNA binding sites (predicted using bioinformatic tools; Lewis et al., 2005; Rehmsmeier et al., 2004; Vorozheykin and Titov, 2015) for three highly conserved miRNAs known to be involved in regulation of MeCP2 in the brain and liver; miR-22, (Feng et al., 2014) miR-19, (Jovičić et al., 2013) and miR-132 (Klein et al., 2007). As predicted, these regulatory elements, combined, decreased the expression of MeCP2 in the liver. The relative importance of different modifications (elements within the extended promoter and novel 3'-UTR) was not investigated. However, the efficacy of 1st generation vector and 426-vector 2nd generation vector after IV tail injection of 10^{12} vg per mouse was not

significantly different. The RTT-like severity score in both 1st and 2nd generation groups was the same as the vehicle group. The most important finding with the 426-vector, therefore, is the lack of prominent liver pathology at a dose where this was observed with other cassette designs. The possible reason for this improvement after systemic injection, despite low brain transduction efficiency, could be to do with the restoration of MeCP2 levels in sufficiently numerous critical cells in the brain (for instance the brainstem) or to restoration in critical peripheral tissues. One of the previous studies in peripheral *Mecp2* KO mice reported that the expression of MeCP2 in peripheral organs involved the increase of survival and body weight (Ross et al., 2016). In my study, I also looked at heart and kidney, but the expression was not as high as in the liver. I decided to focus on the liver. To explain the increase in survival and body weight in my experiment, perhaps the 2% brain transduction may be enough to enhance survival and body weight if it happens to hit the most important cell type. Direct brain injection in neonatal mouse, along with potentially more significant impact via earlier intervention, benefit to target more cells in the brain as shown in the previous study (Gadalla et al., 2013) at dose 4.8×10^{10} . In my study I used (1×10^{11} vg per mouse) approximately equivalent to the 10^{12} systemic treatment dose and led to pronounced survival enhancement. Direct brain injection in neonatal mice was associated with an improvement in body weight but, importantly, also with an improvement in RTT-like phenotype score after 6 weeks. This improvement from the direct brain injection at 10^{11} vg/mice (5 μ l per hemisphere) was not as complete as that reported in genetic reversal experiments, (Robinson et al., 2012) and this is likely to be caused by the combined effects of (1) the percentage of relative inefficiency of MeCP2 re-expression across the brain (10%-40%), compared to genetic reversal experiments (up to 90%), and (2) the possible deleterious counteracting effects of overexpressing MeCP2 in a proportion of transduced cells. A significant pool of cells overexpressing MeCP2 were apparently transduced with multiple copies of vector delivering *MECP2*. This may also account for the slightly elevated severity score in vector-treated WT mice (Figure 5.11c) in the form of mild hindlimb clasping. I cannot rule out very subtle consequences of MeCP2 overexpression that may be revealed by fine-grained behavioral testing. Overall, the proof-of-concept experiments involving direct brain delivery in neonatal mice suggest that, if transduction efficiency across the brain can reach sufficiently high

levels, then a behavioral improvement is conferred by this vector design. For example, direct injection into CFS.

The next step is to prove that the 2nd generation vector is effective and suitable for long-term use. I observed as a pilot study in 6-8 months heterozygous KI female mice injected directly into the brain with dose 10^{11} vg/mouse. However, some mice in the viral treated group presented severe eye lesions and I had to halt the experiment. The lesions were likely to result from the effect of the viral vector, however further experimentation is required as I was unable to fully clarify the cause of the eye lesions. Future experiments must be aware of this adverse effect from the brain injection.

Chapter 6 General discussion

The principal aim of this thesis was to investigate the therapeutic potential of delivering an *MECP2* exogenously, via a viral vector, to a mouse model of Rett syndrome. It was anticipated that such a study would provide fundamental information about the pattern and levels of exogenous MeCP2 expression and give an insight into the vector and promoter combinations most capable of delivering therapeutic benefits. This study was further extended to investigate the effect of both global and brain-specific delivery of *MECP2*, via an AAV2/9-based vector system, on the prevention/improvement of the RTT-like phenotype in a mouse model of Rett syndrome. This chapter will integrate the major findings and significant discoveries of this thesis and will evaluate the importance of these findings in relation to gene therapy and neuroscience research, and, to the evolving field of recent gene therapy in RTT. In addition, I will discuss the technical difficulties experienced during this work, the limitations of the methodology, and suggest possible ways to overcome these limitations. Finally, I will discuss possible future experiments to extend this work and derive the maximum benefits from the results I obtained in this study.

6.1 Major findings

The major findings/discoveries reported in this thesis are as follows:

1. Concerning the determination of the characteristic baseline RTT-like phenotypes in male and female mice of different genotypes in KO and KI lines:
 - I. In male mice, the *Mecp2* knockout mouse model differed significantly from their wild-type cage mates in terms of survival, body weight and a range of behavioural tests while, the T158M *Mecp2* knock-in model presents with a milder phenotype compare with *Mecp2* knockout model
 - II. In female mice, the knockout and knock-in heterozygotes show the same severity of the RTT-like phenotype in the behavioural tests
2. Concerning the behavioural testing of two RTT mouse models and modification of the tests to render them less sensitive to impaired mobility:

I. RTT mouse models motor ability showed improvement with the addition of their own bedding into the testing arena (distance moved in open field arena with bedding increased around 60% in male knockout mice).

II. Locomotor assessment in open field test demonstrated that male knockout mice had locomotor ability significantly lower than the knock-in and WT both in male and female, whereas the groups were affected to different degrees in the treadmill motor challenge test and rotarod test.

III. In learning tests, the RTT mouse model didn't present learning ability in the novel object recognition test, while there were some learning capability show on rotarod motor learning tests.

IV. Reducing the size of the three-chamber arena in the social interaction test demonstrated that RTT mice did not engage preferentially with a stranger mouse, as is the case for WT mice.

V. In both anxiety tests, the light-dark test and splash test, the RTT mouse models did not present anxiety.

VI. The breathing test for apneas using the whole-body plethysmography apparatus presented significantly different levels of breathing abnormality in knockout and knock-in mice.

3. Concerning systemic administration of first generation vector to *Mecp2*^{-/y} mice:

I. Dose escalation in first generation vector revealed a narrow therapeutic window following systemic administration.

II. Systemic delivery of first-generation vector resulted in liver toxicity.

4. Systemic administration of First-Generation Vector Improves Survival in *Mecp2*^{T158M/y} Knock-in Mice.

5. newer cassette design vectors scAAV9/JeT/MECP2, scAAV9/sPA (sPA), and scAAV9.47/MECP2 (9.47) are no better in terms of efficiency and toxicity than the first-generation vector.

6. Development of a Second-Generation Vector that Reduced Liver Toxicity after Systemic Administration.

7. Neonatal Cerebroventricular Injection of the Second-Generation Vector Improved the RTT-like Aggregate Severity Score.

6.1.1 Phenotypic characteristics and behavioural test results in the RTT mouse models.

RTT mouse models have been generated by deletion of portions of *Mecp2* (Chen et al., 2001; Guy et al., 2001; Shahbazian et al., 2002) or by knocking-in human mutations (Brown et al., 2016; Goffin et al., 2011; Lyst et al., 2013; Pitcher et al., 2015). Many of these models have been used for studying the principal features that characterize RTT in humans, although there are differences that reflect the phenotypic variability seen in patients (Archer et al., 2007; Ghosh et al., 2008; Leonard et al., 2017). Despite the severity of RTT-like phenotypes, genetic reactivation of silenced *Mecp2* in conditional knockout mice resulted in a robust and enduring reversal of phenotypes on the targeting in pharmacological therapeutic action (Guy et al., 2007; Jugloff et al., 2008; Robinson et al., 2012). In this study the male KO mice present early onset and severe phenotypes agreeing with the previous literature in term of movement disability, gait abnormality breathing abnormality and weight loss (Chen et al., 2001; Guy et al., 2001; Shahbazian et al., 2002) comparing with the WT, although male T158M KI mice, modelling a common *MECP2* missense mutation, show milder phenotype including hypoactivity, gait impairment, weight loss and breathing irregularities (Brown et al., 2016; Goffin et al., 2011; Lyst et al., 2013; Pitcher et al., 2015). However, the severity of RTT-like phenotypes, genetic reactivation of silenced *Mecp2* in conditional knockout mice resulted in a robust and enduring reversal of phenotypes on the targeting in pharmacological therapeutic action (Guy et al., 2007; Jugloff et al., 2008; Robinson et al., 2012). From this information, I suggest that hemizygous *Mecp2* KO mice are a more suitable model to use for screening tests than hemizygous *Mecp2* T158M KI mice, which present the RTT phenotype more mildly and gradually.

In my study, mobility impairments were ameliorated by adding the mutant mouse's own bedding in the testing arena. This finding partly agrees with the previous literature suggests that mobility is affected by the surface of the floor, not due to its own intrinsic mobility impairment (Orefice et al., 2016). The application with this information into some of my experiments, for example

light-dark anxiety test and novel object recognition test made my result robust that the main responsiveness does not interfere with the hypoactivity of the RTT mouse. In addition, adding extra time in an open-field test, tests of mobility function, benefit encounter more difference between mouse lines. While other groups study the mobility function in the open field test (Gadalla et al., 2013; Matagne et al., 2013; Matagne et al., 2017; Ross et al., 2016; Sztainberg et al., 2015), rotarod test (Matagne et al., 2017; Ross et al., 2016; Sztainberg et al., 2015) and gait analysis (Gadalla et al., 2014; Ross et al., 2016). My result presents that the Treadmill motor challenge test is the best test for detecting therapeutic actions in both male and female mouse in term of mobility, balance and locomotion function due to the clarity of the different degree presenting between *Mecp2* mutant mice and WT.

The other major aspect of the RTT-like phenotype in the mouse model is the learning retardation. I found that the result of motor learning on rotarod and novel object recognition test presents the significant difference between WT and KO agreeing with the previous study, but the result of the newer *Mecp2* T158M KI group is not a significant difference from other groups. I would like to test the learning in other experiment but there was a limited time on my PhD. The re-sized the three-chamber arena in my study presented the difference between the WT and the mutant in both males and females was indicated. The smaller arena can present the time of interaction and time of non-interaction much more clearly and make me result robust to presenting that my result and another report on the RTT mouse (Moretti et al., 2006) showing the RTT mouse model spending significantly more time away from the stranger. I also apply the splash test testing and anxiety in RTT mouse due to this test does not much more require the movement of the mouse. The result showed that all experimental mice had no anxiety as the same as the result in the standard anxiety test, light-dark test. (Castro et al., 2014; Samaco et al., 2013)

6.1.2 Dose escalation with AAV/MECP2 revealed a narrow therapeutic window following systemic administration and resulted in liver toxicity

In order to explore the relationship between vector dose and therapeutic benefits, I examined the effectiveness of peripheral administration of the first-generation vector first in three different doses. First, the low dose 10^{11} vg/kg in mouse, 4×10^{12} vg/kg for human, had no therapeutic effectiveness. The result of survival severity score and body weight showed similarities to the control group. This is an unexpected result because Gadalla et al (2013) showed survival benefits after injecting the same dose. In addition, there was a low transduction efficiency after administration of a low dose of vector (less than 5% in the brain). Second, the result in post-administration of moderate dose, 10^{12} vg/kg in mouse, showed that only the body weight increased. Severity score showed little change from that of the control group. However, there showed a significant increase in survival and transduction efficiency is low, like that of the low dose. This can explain the extension of survival - it might be due to peripheral expression or hitting important cells in the brain. It is likely that to fix RTT, any molecular therapy (in this case, vector-derived MeCP2 expression) will need to hit a high percentage of neurons to prevent or cure RTT. Moreover, moderate dose showed signs of liver damage, vacuolation and loss of hepatocytes, confirming the toxicity involved with MeCP2 overexpression. The liver damage could be tolerated as these mice survived for a long time, but it is likely that there is a threshold for gene expression. Too much expression is toxic and so little will not affect the progression of the phenotype. It needs to be expressed within the physiological limit (Robinson et al., 2012). Administration of a high dose, 10^{13} vg/kg, showed greatly increased lethality with mortality within 5 days, preventing body weight and severity score from being tracked. After death, I sampled brain tissue for transduction (around 10-20%), but this is perhaps not as high as would be needed for a successful RTT therapy. However, high transduction efficiency in the liver was observed. This information agrees that this vector had a low safety margin. If high transduction efficiency in the brain is required, different route of administration or other capsids design that able to express in the brain and increase the number of transduction efficiency. The challenges are using the same vector to get enough cells in the brain without overexpressing mecp2 in the brain and peripheral tissues.

To transfer therapeutic gene in RTT is whether the presence of endogenous mutant MeCP2 might reduce the therapeutic effect of vector-derived wild-type

MeCP2. Male mice expressing native MeCP2 tagged with GFP as a fusion protein and harbouring the common RTT-causing p.T158M mutation, *Mecp2*^{T158M/y}, display a phenotype very similar to that of *Mecp2* null mice.

6.1.3 Development of a second-generation vector that reduced liver toxicity after systemic administration and the efficiency of the second-generation vector improved the RTT-like aggregate severity score via neonatal cerebroventricular injection

In chapter 5, I was aiming to reduce the liver toxicity from the first-generation vector. Newer cassette design vectors with a weaker synthetic promoter (scAAV9/JeT/MECP2), a synthetic short poly A (scAAV9/sPA), and a liver de-target vector (scAAV9.47/MECP2 (9.47) (Karumuthil-Melethil et al., 2016; Pulicherla et al., 2011) were predicted to reduce liver toxicity. However, those three vectors result in the hepatotoxicity similar to the first-generation vector. Only a second-generation vector, incorporating additional promoter regulatory elements and a putative silencer element, showed significantly reduced hepatotoxicity comparing with the first-generation vector also in survival and body weight in *Mecp2*^{-/y}. However, the aggregate severity score showed a minimal decrease. The transduction efficiency in the brain, using systemic injection is still low. The neonatal brain injection study demonstrated that the phenotype by increasing the transduction efficiency in the brain. The histology from the second-generation vector showed the transduction efficiencies across brain regions ranging from 10-40%. This might be related to the combined effects of enough of transduction efficiency in trigger cell. The unexpected adverse effect is the mild hindlimb claspings in vector-treated WT mice that may originate from significant pool of cells overexpressing MeCP2 was apparently transduced with multiple copies of vector delivering *MECP2*. This issue is remarkable, and it should receive more information using additional behavioural testing.

6.2 Technical considerations

Most of the technical problems in this study were related to the *MECP2* RTT model. Hemizygous male *Mecp2* KO/KI mice are infertile therefore heterozygous female must be mated with WT males to generate hemizygous male mice and

heterozygous female mice (the genotype I was interested in). This breeding scheme means that the segregation ratio of hemizygous and heterozygous is 25%. This low percentage is further complicated by the small litter size (3-5 pups) in *Mecp2* KO lines which further reduces the chances of getting the desired genotype. Moreover, the numbers of pups that reach weaning age and the inclusion criteria of body weight (> 9 grams) are also limited, either because of failure to compete with the WT or due to the increased incidence of infanticide (Jugloff et al., 2006). Many steps were taken to improve the breeding such as doubling the number of heterozygous females in each age group, minimizing cage disturbance and decreasing environmental noise, especially around the delivery time, and avoiding unnecessary handling of the pups to prevent infanticide. Moreover, symptomatic RTT mouse needed the special emphasis, for example when the mouse loses weight or the RTT-like phenotype score was more than five, close monitoring, baby food or moving to a warm chamber was supplied. However, when the mouse presents body weight below 20 per cent from the peak body weight or got a scoring for tremor or breathing abnormality as two, I had to euthanize them humanely. This sometimes affected the number of mice in the experiment and may affect the study of mouse behavioural tests or the group of control mice in the study of the effectiveness of the viral vector. This problem is very common in the study in KO mouse because it has an onset of disease and the progress very quickly (6-8 weeks old) (Brown et al., 2016; Chen et al., 2001; Guy et al., 2001; Shahbazian et al., 2002). The preparation of spare hemizygous mice needs to be considered in the future.

Another problem originated in the *Mecp2* knockout mice had tail lesions around the age of 7-8 weeks. This problem usually began as small lesions around the tail-base which then progress to skin ulcers and eventually complete necrosis and loss of the tail. This condition is usually accompanied by a perianal infection which necessitates culling the affected mice. In my study attempts were made to the application of topical antibiotics but this showed very limited benefit. One possible reason was that this lesion was due to animals fighting with each other, however caging mice individually did not prevent or improve this phenotype. Interestingly, this tail problem has been not observed in the cohort of mice using in the RTT mouse characteristic and validation of behavioural

study (chapter 3). Further investigations are required to identify the underlying cause of this problem.

In the setting of the suitable behavioural test, the difficulty occurring in RTT mouse model, apart from the limitation of mobility, is that all of the mutant mice refuse the mouse treat-reward in experimental arena although they fasted for food and water for 6 hours. Under my observation, the RTT mouse, although starving, will only take the treat when I put it back to its own cage and saw the cage-mate eats a treat. This is why I could not set the test using mouse treat-reward as the endpoint target of the tests, for example, T-maze or touch screen memory test. The difficulty issue on the learning test, novel object recognition test, is that the test object must appeal to the mouse and the size cannot be too small so the mouse can play with it and also easy to clean. In my study, there were more than ten objected that I tested with the RTT mouse model.

6.3 Significance of this study

Rett syndrome was considered for decades a neurodevelopmental disorder and was thought to be incurable. Although MeCP2 function is still incompletely understood, enough is known about it that it is considered unlikely that drug molecules can be found to replace its function directly. In contemplating the basis for rational therapies in RTT, there have been many attempts to identify appropriate factors downstream of MeCP2 function and target those pharmacologically. The previous study showed that MeCP2 is target genes whose expression becomes significantly aberrant in the absence of functional MeCP2 has a few support in terms of the functions to interpret the DNA methylation signal, and ubiquity of DNA methylation suggests that candidates for targeting its core chromatin-binding function therapeutically will be multiple and diverse (Skene et al., 2010). Many attempts with the pharmacological treatment in pre-clinical study, For example IGF-1 was studied in Rett mice in parallel with the clinical trials and efficacy reported on several assays including locomotor activity, heart rate, respiration patterns, and social and anxiety behaviour(Castro et al., 2014). However, it did not produce clinically meaningful efficacy in humans. The pre-clinical study also examined Statins which is a class

of lipid-lowering medications approved to prevent cardiovascular disease. Statins improved motor function and prolonged survival (by 15 days) in a single trial performed in Rett mice (Buchovecky et al., 2013). A single study reported improvements in motor function and survival in Rett mice. But there is no clinically meaningful benefit was observed in clinical trial. These also presented the same result in Ketamine (Katz et al., 2016; Kron et al., 2012; Patrizi et al., 2016) and . Desipramine (Roux et al., 2007) which no clinical benefit was observed in clinical studies. The trials and studies above support the argument that the existing pharmacological approaches could not be the best way to treatment for RTT in the human. The main reason is those pharmacological attempts action on the 2nd downstream not from the whole phenotype. Gene therapy can treatment directly at the early state.

Research study on RTT using RTT KO mouse model made more explanation about the mechanism on *MECP2* and the study in KI mouse model, for example, *MeCP2 T158M* mice, which models the human disease as meticulously as possible can interpret the function of *MECP2* mutation occurring in patients. However, the study in *MECP2 T158M* mice still has few publications and the validation of the suitable behavioural tests for RTT mouse model are needed to apply for the validation therapeutic study in the future. The reversal studies have shown the potential reversibility of RTT-like phenotypes in mice models. In this study I compared characteristics of two mouse lines, KO and KI, to ascertain the most suitable model for the study of RTT. In addition, I provide the safe therapeutic dose using in RTT mouse model and highlight the adverse effect liver of this approach. I also highlight the potential new cassette, the second-generation vector, that reduced the liver toxicity and can have a possible efficiency to reducing the RTT-like phenotype when delivery by direct brain injection increasing high brain transduction efficiency. These data however at the proof of concept level should have an impact on the future therapeutic approaches not only for RTT but also for other related neurological disorders. The importance of this study is listed in the following key points;

1. In this thesis I provide a comprehensive study investigating the two important RTT mouse lines with the standard test for RTT-like phenotype tests showing the same validation of my test and then extended to validate additional behavioural

tests in order to properly design a therapeutic evaluation in term of the best mouse model and the best suitable test.

2. In this thesis, I showed the first proof-of-concept demonstration that impaired mobility in RTT mouse models can be improved by adding the mouse's own bedding. This may be a valuable tool for other behavioural studies of RTT mouse models involving mobility.

3. My thesis provides the therapeutic dose in a mouse model of RTT delivered by scAAV9/MeP-mediated MeCP2 by systemic injection in young adult mice. This data, along with the observed lack of overt adverse effects of this vector in mouse hepatocyte and confirmed that the cause from exogenous MeCP2 overexpression.

4. My thesis shows that the presence of the mutant protein does not impede the functionality of vector-derived MeCP2. This finding was supported by the delivery of scAAV9/MeP-mediated MeCP2 in male KI RTT mouse model. This result indicated the potential translational application of augmentation gene therapy in patients with missense *MECP2* mutations.

5. My thesis provides evidence that the new modified vector, the second-generation vector, designed to include an extended *Mecp2* promoter and additional regulatory 3'-UTR elements, significantly reduced hepatic toxicity after systemic administration. This show that controlling levels of MeCP2 expression in the liver is achievable through modification of the expression cassette. Moreover, direct brain injection of this vector reducing the physical barrier to the brain, into neonatal KO male mice present the improvement of RTT-like phenotype. These considerations are essential for the field of RTT gene therapy in order to properly design a therapeutic vector and route.

6.4 Future studies

This project examined various gene delivery doses and then refined vector design and delivery strategies, moving to proof of concept studies in RTT mice. This series of studies formed a logical course in reaching the goal of developing translational strategies in treating RTT in patients. The results shown in my thesis suggest important future experiments in various directions.

1. Following the success of the second-generation vector in producing therapeutic benefits after direct brain injection in neonates, I would recommend several more experiments to further investigate the potential for future human translation:

I. The vast majority of RTT patients are females with a mosaic network of cells either expressing normal MeCP2 or lacking functional MeCP2. Therefore, the next experiment should be to consider injecting adult heterozygous female mice with the second generation. Female mice are the most relevant genetically to a human patient and the RTT progress in females is gradual (Guy et al 2007).

II. Optimising viral delivery methods to increase transduction efficiency in adult mice brain for example administration the second generation vector via intrathecal or intra cisterna Magna injection (Sinnott, 2017) to reduce the amount of virus particles and also decrease peripheral expression because the direct brain delivery of exogenous *MECP2* is difficult to apply in human.

III. Optimising the vector construct to enable targeting of exogenous *MECP2* to null cells aiming to increase brain transduction through the new design of AAV9PHP.B and AAV9PHP.eB (Deverman et. al., 2016, György et. al., 2018, Hordeaux et.al., 2018, Rincon et. al., 2018) has been reported to have a higher transduction efficiency to the effect of 40 times more than AAV9. Using this new vector to deliver *MECP2* may increase the therapeutic effect from the systemic injection.

2. Other potential avenues to explore include *MECP2* reactivation from the inactive X and genome or base editing approaches. A rapid increase of work in this area over the last few years has enabled the development of such approaches. Currently, many editing agents are in development including CRISPR/Cas9 and the TALEN system.

The emergence of the former as the genome editing system of choice is because of its efficiency, ease of synthesis and targeting ability of simultaneous multiple loci. The CRISPR system, in bacteria, with its Cas (CRISPR-associated) nuclease proteins have provision of an adaptive immunity form by targeting nucleases against invading viral DNA (Horvath and Barrangou, 2010).

In a study conducted recently, Maresca and colleagues (Maresca et al., 2013) provided a demonstration that large sequences of DNA may be captured at nuclease-induced double stranded breaks when the DNA is flanked by targeting identical sequences to the chromosomal DNA. This process has been found to be dependent on NHEJ and the provision of a robust way in ligating DNA constructs in the genome's precise locations.

One therapeutic strategy would be the use of this process in inserting a WT copy of *MECP2* into the *AAVS1* safe harbour locus. This allows for stability of transgene expression in the human genome (Tiyaboonchai et al., 2014). Like the approaches of current gene therapy, this strategy enables the cell to express functional proteins without damaging the WT copy in cells expressing the non-mutant allele.

This approach has a potential advantage over the current strategies pertaining to gene therapy - it could allow dividing cells, such as microglia and astrocytes, and neuronal stem cells in passing the WT transgene to daughter cells. The targeted nature of the insertion will help to avoid the potential consequences of insertional mutagenesis at the endogenous *MECP2* locus or at other insertion loci in the case of lentiviral delivery of transgenes.

3. Since most of learning and memory tests depend on the mobility ability and mouse treat-reward, the following experiments could help determine the reasons for this problem:

I. the novel object recognition test arena needs to be reduced in area.

II. Provide a smell that is attractive to mice as a treat-reward after weaning, aiming to increase the familiarity of the treat-reward.

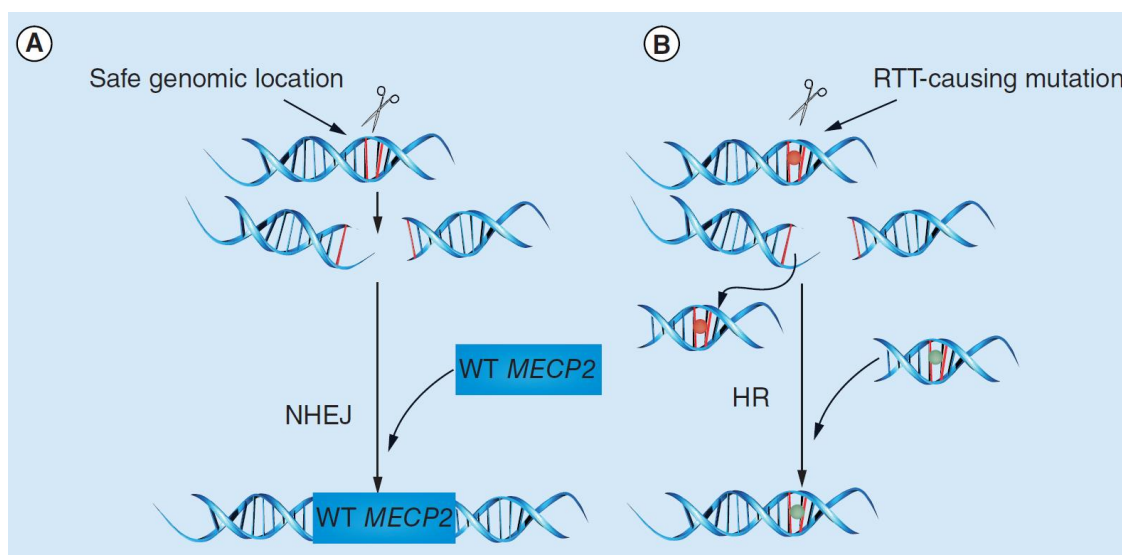


Figure 1.6 Mechanism of action of CRISPR/Cas system. In the CRISPR/Cas9 genome editing system a guide RNA (gRNA) binds to a target sequence and creates a template for the Cas9 nuclease to make a targeted, double-stranded break in the DNA, leading to activation of one of the two major repair pathways that can be exploited for therapy. (A) When the NHEJ pathway is activated, DNA ends are ligated together without the need for a homologous DNA template. This pathway could be used to ligate a WT copy of the *MECP2* gene into a safe harbour in the genome. (B) In the presence of the HR machinery in dividing cells, homology-directed repair occurs and an exogenously provided WT template can be inserted accurately into the genome in place of a region containing a disease-causing mutation, thus editing the mutant allele (red) and causing WT MeCP2 to be expressed instead (green). HR: Homologous. This figure was adapted from (Gadalla, 2015).

6.5 Summary

The aim of this thesis was an exploration of viral-mediated exogenous *MECP2* delivery to RTT mouse model, and then to use this information to design therapies suitable for future clinical translation. This investigation was extremely productive in several respects. First, phenotyping of a novel knock-in mouse model, in which the *Mecp2* T158M missense mutation occurring in human patients was recreated, revealed that the majority of the RTT phenotype and other additional behavioural tests was milder phenotype than the *Mecp2* knockout mice in both sexes. Thus, hemizygous T158M knock-in mice may be used for the therapy screening tests, but phenotypic reversal may not be as clear as in the *Mecp2* knockout line. Second, this study demonstrates beyond doubt that our first generation vector has a narrow therapeutic window following systemic administration and that toxicity occurs in liver cells, probably due to exogenous vector-derived MeCP2 overexpression. Finally, my study is the

first to report results using a new modified vector design, the second generation vector, by incorporating an extended *Mecp2* promoter and additional regulatory 3' UTR elements significantly reduced hepatic toxicity after systemic administration and also ameliorates RTT-like phenotypes after direct brain injection in mouse neonates. I believe that this study provides the groundwork for further studies to identify the newer potential cassette design having more efficiency and the potential of achieving therapeutic benefits in long term studies in the heterozygous female *Mecp2* mouse model, a more accurate model of human RTT, and also for studies to investigate the underlying pathology of the hindlimb motor deficit to enable avoiding this problem in future clinical studies.

References

- Abdala, A. P., M. Dutschmann, J. M. Bissonnette, and J. F. Paton, 2010, Correction of respiratory disorders in a mouse model of Rett syndrome: *Proc Natl Acad Sci U S A*, v. 107, p. 18208-13.
- Adachi, M., E. W. Keefer, and F. S. Jones, 2005, A segment of the *Mecp2* promoter is sufficient to drive expression in neurons: *Hum Mol Genet*, v. 14, p. 3709-22.
- Amir, R. E., I. B. Van den Veyver, M. Wan, C. Q. Tran, U. Francke, and H. Y. Zoghbi, 1999, Rett syndrome is caused by mutations in X-linked *MECP2*, encoding methyl-CpG-binding protein 2: *Nat Genet*, v. 23, p. 185-8.
- Antunes, M., and G. Biala, 2012, The novel object recognition memory: neurobiology, test procedure, and its modifications: *Cogn Process*, v. 13, p. 93-110.
- Archer, H., J. Evans, H. Leonard, L. Colvin, D. Ravine, J. Christodoulou, S. Williamson, T. Charman, M. E. Bailey, J. Sampson, N. de Klerk, and A. Clarke, 2007, Correlation between clinical severity in patients with Rett syndrome with a p.R168X or p.T158M *MECP2* mutation, and the direction and degree of skewing of X-chromosome inactivation: *J Med Genet*, v. 44, p. 148-52.
- Arime, Y., and K. Akiyama, 2017, Abnormal neural activation patterns underlying working memory impairment in chronic phencyclidine-treated mice: *PLoS One*, v. 12, p. e0189287.
- Armstrong, D. D., 2002, Neuropathology of Rett syndrome: *Ment Retard Dev Disabil Res Rev*, v. 8, p. 72-6.
- Arruda, V. R., H. H. Stedman, T. C. Nichols, M. E. Haskins, M. Nicholson, R. W. Herzog, L. B. Couto, and K. A. High, 2005, Regional intravascular delivery of AAV-2-F.IX to skeletal muscle achieves long-term correction of hemophilia B in a large animal model: *Blood*, v. 105, p. 3458-64.
- Azzouz, M., A. Hottinger, J. C. Paterna, A. D. Zurn, P. Aebischer, and H. Büeler, 2000, Increased motoneuron survival and improved neuromuscular function in transgenic ALS mice after intraspinal injection of an adeno-associated virus encoding *Bcl-2*: *Hum Mol Genet*, v. 9, p. 803-11.
- Bagga, J. S., and L. A. D'Antonio, 2013, Role of conserved cis-regulatory elements in the post-transcriptional regulation of the human *MECP2* gene involved in autism: *Hum Genomics*, v. 7, p. 19.
- Ballestar, E., T. M. Yusufzai, and A. P. Wolffe, 2000, Effects of Rett syndrome mutations of the methyl-CpG binding domain of the transcriptional repressor *MeCP2* on selectivity for association with methylated DNA: *Biochemistry*, v. 39, p. 7100-6.
- Berns, K. I., 1990, Parvovirus replication: *Microbiol Rev*, v. 54, p. 316-29.
- Bhatnagar, S., X. Zhu, J. Ou, L. Lin, L. Chamberlain, L. J. Zhu, N. Wajapeyee, and M. R. Green, 2014, Genetic and pharmacological reactivation of the mammalian inactive X chromosome: *Proc Natl Acad Sci U S A*, v. 111, p. 12591-8.
- Bienvenu, T., and J. Chelly, 2006, Molecular genetics of Rett syndrome: when DNA methylation goes unrecognized: *Nat Rev Genet*, v. 7, p. 415-26.
- Bourin, M., and M. Hascoët, 2003, The mouse light/dark box test: *Eur J Pharmacol*, v. 463, p. 55-65.
- Brendel, C., E. Klahold, J. Gärtner, and P. Huppke, 2009, Suppression of nonsense mutations in Rett syndrome by aminoglycoside antibiotics: *Pediatr Res*, v. 65, p. 520-3.
- Brielmaier, J., P. G. Matteson, J. L. Silverman, J. M. Senerth, S. Kelly, M. Genestine, J. H. Millonig, E. DiCicco-Bloom, and J. N. Crawley, 2012, Autism-relevant social abnormalities and cognitive deficits in engrailed-2 knockout mice: *PLoS One*, v. 7, p. e40914.
- Brooks, A. I., C. S. Stein, S. M. Hughes, J. Heth, P. M. McCray, S. L. Sauter, J. C. Johnston, D. A. Cory-Slechta, H. J. Federoff, and B. L. Davidson, 2002, Functional correction of established

- central nervous system deficits in an animal model of lysosomal storage disease with feline immunodeficiency virus-based vectors: *Proc Natl Acad Sci U S A*, v. 99, p. 6216-21.
- Brown, K., J. Selfridge, S. Lagger, J. Connelly, D. De Sousa, A. Kerr, S. Webb, J. Guy, C. Merusi, M. V. Koerner, and A. Bird, 2016, The molecular basis of variable phenotypic severity among common missense mutations causing Rett syndrome: *Hum Mol Genet*, v. 25, p. 558-70.
- Campos, A. C., M. V. Fogaça, D. C. Aguiar, and F. S. Guimarães, 2013, Animal models of anxiety disorders and stress: *Braz J Psychiatry*, v. 35 Suppl 2, p. S101-11.
- Carter, B. J., and J. A. Rose, 1972, Adenovirus-associated virus multiplication. 8. Analysis of in vivo transcription induced by complete or partial helper viruses: *J Virol*, v. 10, p. 9-16.
- Castro, J., R. I. Garcia, S. Kwok, A. Banerjee, J. Petravicz, J. Woodson, N. Mellios, D. Tropea, and M. Sur, 2014, Functional recovery with recombinant human IGF1 treatment in a mouse model of Rett Syndrome: *Proc Natl Acad Sci U S A*, v. 111, p. 9941-6.
- Chahrour, M., and H. Y. Zoghbi, 2007, The story of Rett syndrome: from clinic to neurobiology: *Neuron*, v. 56, p. 422-37.
- Chao, H. T., H. Chen, R. C. Samaco, M. Xue, M. Chahrour, J. Yoo, J. L. Neul, S. Gong, H. C. Lu, N. Heintz, M. Ekker, J. L. Rubenstein, J. L. Noebels, C. Rosenmund, and H. Y. Zoghbi, 2010, Dysfunction in GABA signalling mediates autism-like stereotypies and Rett syndrome phenotypes: *Nature*, v. 468, p. 263-9.
- Chao, H. T., and H. Y. Zoghbi, 2012, MeCP2: only 100% will do: *Nat Neurosci*, v. 15, p. 176-7.
- Chen, R. Z., S. Akbarian, M. Tudor, and R. Jaenisch, 2001, Deficiency of methyl-CpG binding protein-2 in CNS neurons results in a Rett-like phenotype in mice: *Nat Genet*, v. 27, p. 327-31.
- Chin, E. W. M., W. M. Lim, D. Ma, F. J. Rosales, and E. L. K. Goh, 2018, Choline Rescues Behavioural Deficits in a Mouse Model of Rett Syndrome by Modulating Neuronal Plasticity: *Mol Neurobiol*.
- Choleris, E., A. W. Thomas, M. Kavaliers, and F. S. Prato, 2001, A detailed ethological analysis of the mouse open field test: effects of diazepam, chlordiazepoxide and an extremely low frequency pulsed magnetic field: *Neurosci Biobehav Rev*, v. 25, p. 235-60.
- Clément, N., and J. C. Grieger, 2016, Manufacturing of recombinant adeno-associated viral vectors for clinical trials: *Mol Ther Methods Clin Dev*, v. 3, p. 16002.
- Cohen, S., H. W. Gabel, M. Hemberg, A. N. Hutchinson, L. A. Sadacca, D. H. Ebert, D. A. Harmin, R. S. Greenberg, V. K. Verdine, Z. Zhou, W. C. Wetsel, A. E. West, and M. E. Greenberg, 2011, Genome-wide activity-dependent MeCP2 phosphorylation regulates nervous system development and function: *Neuron*, v. 72, p. 72-85.
- Collins, A. L., J. M. Levenson, A. P. Vilaythong, R. Richman, D. L. Armstrong, J. L. Noebels, J. David Sweatt, and H. Y. Zoghbi, 2004, Mild overexpression of MeCP2 causes a progressive neurological disorder in mice: *Hum Mol Genet*, v. 13, p. 2679-89.
- Costa, R. M., N. B. Federov, J. H. Kogan, G. G. Murphy, J. Stern, M. Ohno, R. Kucherlapati, T. Jacks, and A. J. Silva, 2002, Mechanism for the learning deficits in a mouse model of neurofibromatosis type 1: *Nature*, v. 415, p. 526-30.
- Coy, J. F., Z. Sedlacek, D. Bächner, H. Delius, and A. Poustka, 1999, A complex pattern of evolutionary conservation and alternative polyadenylation within the long 3'-untranslated region of the methyl-CpG-binding protein 2 gene (MeCP2) suggests a regulatory role in gene expression: *Hum Mol Genet*, v. 8, p. 1253-62.
- Dastidar, R. G., J. Hooda, A. Shah, T. M. Cao, R. M. Henke, and L. Zhang, 2012, The nuclear localization of SWI/SNF proteins is subjected to oxygen regulation: *Cell Biosci*, v. 2, p. 30.
- Daya, S., and K. I. Berns, 2008, Gene therapy using adeno-associated virus vectors: *Clin Microbiol Rev*, v. 21, p. 583-93.
- De Felice, C., M. Rossi, S. Leoncini, G. Chisci, C. Signorini, G. Lonetti, L. Vannuccini, D. Spina, A. Ginori, I. Iacona, A. Cortelazzo, A. Pecorelli, G. Valacchi, L. Ciccoli, T. Pizzorusso, and J. Hayek, 2014, Inflammatory lung disease in Rett syndrome: *Mediators Inflamm*, v. 2014, p. 560120.
- De Filippis, B., A. Fabbri, D. Simone, R. Canese, L. Ricceri, F. Malchiodi-Albedi, G. Laviola, and C. Fiorentini, 2012, Modulation of RhoGTPases improves the behavioral phenotype and

- reverses astrocytic deficits in a mouse model of Rett syndrome: *Neuropsychopharmacology*, v. 37, p. 1152-63.
- De Filippis, B., L. Ricceri, and G. Laviola, 2010, Early postnatal behavioral changes in the *Mecp2*-308 truncation mouse model of Rett syndrome: *Genes Brain Behav*, v. 9, p. 213-23.
- del Gaudio, D., P. Fang, F. Scaglia, P. A. Ward, W. J. Craigen, D. G. Glaze, J. L. Neul, A. Patel, J. A. Lee, M. Irons, S. A. Berry, A. A. Pursley, T. A. Grebe, D. Freedenberg, R. A. Martin, G. E. Hsich, J. R. Khera, N. R. Friedman, H. Y. Zoghbi, C. M. Eng, J. R. Lupski, A. L. Beaudet, S. W. Cheung, and B. B. Roa, 2006, Increased *MECP2* gene copy number as the result of genomic duplication in neurodevelopmentally delayed males: *Genet Med*, v. 8, p. 784-92.
- Derecki, N. C., J. C. Cronk, Z. Lu, E. Xu, S. B. Abbott, P. G. Guyenet, and J. Kipnis, 2012, Wild-type microglia arrest pathology in a mouse model of Rett syndrome: *Nature*, v. 484, p. 105-9.
- Duan, Y., and P. A. Kollman, 1998, Pathways to a protein folding intermediate observed in a 1-microsecond simulation in aqueous solution: *Science*, v. 282, p. 740-4.
- Duque, S., B. Joussemet, C. Riviere, T. Marais, L. Dubreil, A. M. Douar, J. Fyfe, P. Moullier, M. A. Colle, and M. Barkats, 2009, Intravenous administration of self-complementary AAV9 enables transgene delivery to adult motor neurons: *Mol Ther*, v. 17, p. 1187-96.
- Elian, M., and N. D. Rudolf, 1991, EEG and respiration in Rett syndrome: *Acta Neurol Scand*, v. 83, p. 123-8.
- Eslamboli, A., B. Georgievska, R. M. Ridley, H. F. Baker, N. Muzyczka, C. Burger, R. J. Mandel, L. Annett, and D. Kirik, 2005, Continuous low-level glial cell line-derived neurotrophic factor delivery using recombinant adeno-associated viral vectors provides neuroprotection and induces behavioral recovery in a primate model of Parkinson's disease: *J Neurosci*, v. 25, p. 769-77.
- Feigin, A., M. G. Kaplitt, C. Tang, T. Lin, P. Mattis, V. Dhawan, M. J. During, and D. Eidelberg, 2007, Modulation of metabolic brain networks after subthalamic gene therapy for Parkinson's disease: *Proc Natl Acad Sci U S A*, v. 104, p. 19559-64.
- Feng, Y., W. Huang, M. Wani, X. Yu, and M. Ashraf, 2014, Ischemic preconditioning potentiates the protective effect of stem cells through secretion of exosomes by targeting *Mecp2* via miR-22: *PLoS One*, v. 9, p. e88685.
- Ferrari, F. K., T. Samulski, T. Shenk, and R. J. Samulski, 1996, Second-strand synthesis is a rate-limiting step for efficient transduction by recombinant adeno-associated virus vectors: *J Virol*, v. 70, p. 3227-34.
- Foust, K. D., E. Nurre, C. L. Montgomery, A. Hernandez, C. M. Chan, and B. K. Kaspar, 2009, Intravascular AAV9 preferentially targets neonatal neurons and adult astrocytes: *Nat Biotechnol*, v. 27, p. 59-65.
- Friez, M. J., J. R. Jones, K. Clarkson, H. Lubs, D. Abuelo, J. A. Bier, S. Pai, R. Simensen, C. Williams, P. F. Giampietro, C. E. Schwartz, and R. E. Stevenson, 2006, Recurrent infections, hypotonia, and mental retardation caused by duplication of *MECP2* and adjacent region in *Xq28*: *Pediatrics*, v. 118, p. e1687-95.
- Gadalla, K. K., M. E. Bailey, and S. R. Cobb, 2011, *MeCP2* and Rett syndrome: reversibility and potential avenues for therapy: *Biochem J*, v. 439, p. 1-14.
- Gadalla, K. K., M. E. Bailey, R. C. Spike, P. D. Ross, K. T. Woodard, S. N. Kalburgi, L. Bachaboina, J. V. Deng, A. E. West, R. J. Samulski, S. J. Gray, and S. R. Cobb, 2013, Improved survival and reduced phenotypic severity following AAV9/*MECP2* gene transfer to neonatal and juvenile male *Mecp2* knockout mice: *Mol Ther*, v. 21, p. 18-30.
- Gadalla, K. K., P. D. Ross, J. S. Riddell, M. E. Bailey, and S. R. Cobb, 2014, Gait analysis in a *Mecp2* knockout mouse model of Rett syndrome reveals early-onset and progressive motor deficits: *PLoS One*, v. 9, p. e112889.
- Gadalla, K. K. E., Ross, P. D., Hector, R. D., Bahey, N. G., Bailey, M. E.S. and Cobb, S. R., 2015, Gene therapy for Rett syndrome: prospects and challenges: *Future Neurology*, v. 10(5), p. 18.
- Gadalla, K. K. E., T. Vudhironarit, R. D. Hector, S. Sinnett, N. G. Bahey, M. E. S. Bailey, S. J. Gray, and S. R. Cobb, 2017, Development of a Novel AAV Gene Therapy Cassette with Improved Safety Features and Efficacy in a Mouse Model of Rett Syndrome: *Mol Ther Methods Clin Dev*, v. 5, p. 180-190.

- Gandaglia, A., E. Brivio, S. Carli, M. Palmieri, F. Bedogni, G. Stefanelli, A. Bergo, B. Leva, C. Cattaneo, L. Pizzamiglio, M. Cicerone, V. Bianchi, C. Kilstrup-Nielsen, I. D'Annessa, D. Di Marino, P. D'Adamo, F. Antonucci, A. Frasca, and N. Landsberger, 2018, A Novel Mecp2: *Mol Neurobiol*.
- Garg, S. K., D. T. Lioy, H. Cheval, J. C. McGann, J. M. Bissonnette, M. J. Murtha, K. D. Foust, B. K. Kaspar, A. Bird, and G. Mandel, 2013, Systemic delivery of MeCP2 rescues behavioral and cellular deficits in female mouse models of Rett syndrome: *J Neurosci*, v. 33, p. 13612-20.
- Gemelli, T., O. Berton, E. D. Nelson, L. I. Perrotti, R. Jaenisch, and L. M. Monteggia, 2006, Postnatal loss of methyl-CpG binding protein 2 in the forebrain is sufficient to mediate behavioral aspects of Rett syndrome in mice: *Biol Psychiatry*, v. 59, p. 468-76.
- Ghosh, R. P., R. A. Horowitz-Scherer, T. Nikitina, L. M. Gierasch, and C. L. Woodcock, 2008, Rett syndrome-causing mutations in human MeCP2 result in diverse structural changes that impact folding and DNA interactions: *J Biol Chem*, v. 283, p. 20523-34.
- Giacometti, E., S. Luikenhuis, C. Beard, and R. Jaenisch, 2007, Partial rescue of MeCP2 deficiency by postnatal activation of MeCP2: *Proc Natl Acad Sci U S A*, v. 104, p. 1931-6.
- Gigout, L., P. Rebollo, N. Clement, K. H. Warrington, N. Muzyczka, R. M. Linden, and T. Weber, 2005, Altering AAV tropism with mosaic viral capsids: *Mol Ther*, v. 11, p. 856-65.
- Goffin, D., M. Allen, L. Zhang, M. Amorim, I. T. Wang, A. R. Reyes, A. Mercado-Berton, C. Ong, S. Cohen, L. Hu, J. A. Blendy, G. C. Carlson, S. J. Siegel, M. E. Greenberg, and Z. Zhou, 2011, Rett syndrome mutation MeCP2 T158A disrupts DNA binding, protein stability and ERP responses: *Nat Neurosci*, v. 15, p. 274-83.
- Goffin, D., M. Allen, L. Zhang, M. Amorim, I. T. Wang, A. R. Reyes, A. Mercado-Berton, C. Ong, S. Cohen, L. Hu, J. A. Blendy, G. C. Carlson, S. J. Siegel, M. E. Greenberg, and Z. Zhou, 2012, Rett syndrome mutation MeCP2 T158A disrupts DNA binding, protein stability and ERP responses: *Nat Neurosci*, v. 15, p. 274-83.
- Goffin, D., E. S. Brodtkin, J. A. Blendy, S. J. Siegel, and Z. Zhou, 2014, Cellular origins of auditory event-related potential deficits in Rett syndrome: *Nat Neurosci*, v. 17, p. 804-6.
- Gogliotti, R. G., R. K. Senter, J. M. Rook, A. Ghoshal, R. Zamorano, C. Malosh, S. R. Stauffer, T. M. Bridges, J. M. Bartolome, J. S. Daniels, C. K. Jones, C. W. Lindsley, P. J. Conn, and C. M. Niswender, 2016, mGlu5 positive allosteric modulation normalizes synaptic plasticity defects and motor phenotypes in a mouse model of Rett syndrome: *Hum Mol Genet*, v. 25, p. 1990-2004.
- Gray, S. J., S. B. Foti, J. W. Schwartz, L. Bachaboina, B. Taylor-Blake, J. Coleman, M. D. Ehlers, M. J. Zylka, T. J. McCown, and R. J. Samulski, 2011a, Optimizing promoters for recombinant adeno-associated virus-mediated gene expression in the peripheral and central nervous system using self-complementary vectors: *Hum Gene Ther*, v. 22, p. 1143-53.
- Gray, S. J., V. Matagne, L. Bachaboina, S. Yadav, S. R. Ojeda, and R. J. Samulski, 2011b, Preclinical differences of intravascular AAV9 delivery to neurons and glia: a comparative study of adult mice and nonhuman primates: *Mol Ther*, v. 19, p. 1058-69.
- Gray, S. J., S. Nagabhushan Kalburgi, T. J. McCown, and R. Jude Samulski, 2013, Global CNS gene delivery and evasion of anti-AAV-neutralizing antibodies by intrathecal AAV administration in non-human primates: *Gene Ther*, v. 20, p. 450-9.
- Grayson, B., M. Leger, C. Piercy, L. Adamson, M. Harte, and J. C. Neill, 2015, Assessment of disease-related cognitive impairments using the novel object recognition (NOR) task in rodents: *Behav Brain Res*, v. 285, p. 176-93.
- Grieger, J. C., and R. J. Samulski, 2005, Adeno-associated virus as a gene therapy vector: vector development, production and clinical applications: *Adv Biochem Eng Biotechnol*, v. 99, p. 119-45.
- Guy, J., J. Gan, J. Selfridge, S. Cobb, and A. Bird, 2007, Reversal of neurological defects in a mouse model of Rett syndrome: *Science*, v. 315, p. 1143-7.
- Guy, J., B. Hendrich, M. Holmes, J. E. Martin, and A. Bird, 2001, A mouse Mecp2-null mutation causes neurological symptoms that mimic Rett syndrome: *Nat Genet*, v. 27, p. 322-6.
- Hagberg, B., 2002, Clinical manifestations and stages of Rett syndrome: *Ment Retard Dev Disabil Res Rev*, v. 8, p. 61-5.

- Hagberg, B., J. Aicardi, K. Dias, and O. Ramos, 1983, A progressive syndrome of autism, dementia, ataxia, and loss of purposeful hand use in girls: Rett's syndrome: report of 35 cases: *Ann Neurol*, v. 14, p. 471-9.
- Herzog, R. W., J. N. Hagstrom, S. H. Kung, S. J. Tai, J. M. Wilson, K. J. Fisher, and K. A. High, 1997, Stable gene transfer and expression of human blood coagulation factor IX after intramuscular injection of recombinant adeno-associated virus: *Proc Natl Acad Sci U S A*, v. 94, p. 5804-9.
- Horvath, P., and R. Barrangou, 2010, CRISPR/Cas, the immune system of bacteria and archaea: *Science*, v. 327, p. 167-70.
- Inagaki, K., S. Fuess, T. A. Storm, G. A. Gibson, C. F. Mctiernan, M. A. Kay, and H. Nakai, 2006, Robust systemic transduction with AAV9 vectors in mice: efficient global cardiac gene transfer superior to that of AAV8: *Mol Ther*, v. 14, p. 45-53.
- Jiang, H., G. F. Pierce, M. C. Ozelo, E. V. de Paula, J. A. Vargas, P. Smith, J. Sommer, A. Luk, C. S. Manno, K. A. High, and V. R. Arruda, 2006, Evidence of multiyear factor IX expression by AAV-mediated gene transfer to skeletal muscle in an individual with severe hemophilia B: *Mol Ther*, v. 14, p. 452-5.
- Johnson, C. M., W. Zhong, N. Cui, Y. Wu, H. Xing, S. Zhang, and C. Jiang, 2016, Defects in brainstem neurons associated with breathing and motor function in the *Mecp2*^{R168X/Y} mouse model of Rett syndrome: *Am J Physiol Cell Physiol*, v. 311, p. C895-C909.
- Jovicic, A., R. Roshan, N. Moisoj, S. Pradervand, R. Moser, B. Pillai, and R. Luthi-Carter, 2013, Comprehensive expression analyses of neural cell-type-specific miRNAs identify new determinants of the specification and maintenance of neuronal phenotypes: *J Neurosci*, v. 33, p. 5127-37.
- Jovičić, A., R. Roshan, N. Moisoj, S. Pradervand, R. Moser, B. Pillai, and R. Luthi-Carter, 2013, Comprehensive expression analyses of neural cell-type-specific miRNAs identify new determinants of the specification and maintenance of neuronal phenotypes: *J Neurosci*, v. 33, p. 5127-37.
- Jugloff, D. G., K. Vandamme, R. Logan, N. P. Visanji, J. M. Brotchie, and J. H. Eubanks, 2008, Targeted delivery of an *Mecp2* transgene to forebrain neurons improves the behavior of female *Mecp2*-deficient mice: *Hum Mol Genet*, v. 17, p. 1386-96.
- Julu, P. O., A. M. Kerr, F. Apartopoulos, S. Al-Rawas, I. W. Engerström, L. Engerström, G. A. Jamal, and S. Hansen, 2001, Characterisation of breathing and associated central autonomic dysfunction in the Rett disorder: *Arch Dis Child*, v. 85, p. 29-37.
- Julu, P. O., and I. Witt Engerström, 2005, Assessment of the maturity-related brainstem functions reveals the heterogeneous phenotypes and facilitates clinical management of Rett syndrome: *Brain Dev*, v. 27 Suppl 1, p. S43-S53.
- Jung, B. P., D. G. Jugloff, G. Zhang, R. Logan, S. Brown, and J. H. Eubanks, 2003, The expression of methyl CpG binding factor MeCP2 correlates with cellular differentiation in the developing rat brain and in cultured cells: *J Neurobiol*, v. 55, p. 86-96.
- Karumuthil-Melethil, S., S. Nagabhushan Kalburgi, P. Thompson, M. Tropak, M. D. Kaytor, J. G. Keimel, B. L. Mark, D. Mahuran, J. S. Walia, and S. J. Gray, 2016, Novel Vector Design and Hexosaminidase Variant Enabling Self-Complementary Adeno-Associated Virus for the Treatment of Tay-Sachs Disease: *Hum Gene Ther*, v. 27, p. 509-21.
- Kaspar, B. K., L. M. Frost, L. Christian, P. Umapathi, and F. H. Gage, 2005, Synergy of insulin-like growth factor-1 and exercise in amyotrophic lateral sclerosis: *Ann Neurol*, v. 57, p. 649-55.
- Katz, D. M., A. Bird, M. Coenraads, S. J. Gray, D. U. Menon, B. D. Philpot, and D. C. Tarquinio, 2016, Rett Syndrome: Crossing the Threshold to Clinical Translation: *Trends Neurosci*, v. 39, p. 100-13.
- Kay, M. A., J. C. Glorioso, and L. Naldini, 2001, Viral vectors for gene therapy: the art of turning infectious agents into vehicles of therapeutics: *Nat Med*, v. 7, p. 33-40.
- Kay, M. A., C. S. Manno, M. V. Ragni, P. J. Larson, L. B. Couto, A. McClelland, B. Glader, A. J. Chew, S. J. Tai, R. W. Herzog, V. Arruda, F. Johnson, C. Scallan, E. Skarsgard, A. W. Flake, and K. A. High, 2000, Evidence for gene transfer and expression of factor IX in haemophilia B patients treated with an AAV vector: *Nat Genet*, v. 24, p. 257-61.

- Kells, A. P., D. M. Fong, M. Dragunow, M. J. During, D. Young, and B. Connor, 2004, AAV-mediated gene delivery of BDNF or GDNF is neuroprotective in a model of Huntington disease: *Mol Ther*, v. 9, p. 682-8.
- Kemi, O. J., P. M. Haram, U. Wisløff, and Ø. Ellingsen, 2004, Aerobic fitness is associated with cardiomyocyte contractile capacity and endothelial function in exercise training and detraining: *Circulation*, v. 109, p. 2897-904.
- Kerr, B., J. Soto C, M. Saez, A. Abrams, K. Walz, and J. I. Young, 2012, Transgenic complementation of MeCP2 deficiency: phenotypic rescue of *Mecp2*-null mice by isoform-specific transgenes: *Eur J Hum Genet*, v. 20, p. 69-76.
- Kim, C. H., M. Hvoslef-Eide, S. R. Nilsson, M. R. Johnson, B. R. Herbert, T. W. Robbins, L. M. Saksida, T. J. Bussey, and A. C. Mar, 2015, The continuous performance test (rCPT) for mice: a novel operant touchscreen test of attentional function: *Psychopharmacology (Berl)*, v. 232, p. 3947-66.
- Kishi, N., and J. D. Macklis, 2004, MECP2 is progressively expressed in post-migratory neurons and is involved in neuronal maturation rather than cell fate decisions: *Mol Cell Neurosci*, v. 27, p. 306-21.
- Klein, M. E., D. T. Lioy, L. Ma, S. Impey, G. Mandel, and R. H. Goodman, 2007, Homeostatic regulation of MeCP2 expression by a CREB-induced microRNA: *Nat Neurosci*, v. 10, p. 1513-4.
- Klose, R. J., and A. P. Bird, 2006, Genomic DNA methylation: the mark and its mediators: *Trends Biochem Sci*, v. 31, p. 89-97.
- Klugmann, M., C. B. Leichtlein, C. W. Symes, T. Serikawa, D. Young, and M. J. During, 2005, Restoration of aspartoacylase activity in CNS neurons does not ameliorate motor deficits and demyelination in a model of Canavan disease: *Mol Ther*, v. 11, p. 745-53.
- Kotin, R. M., R. M. Linden, and K. I. Berns, 1992, Characterization of a preferred site on human chromosome 19q for integration of adeno-associated virus DNA by non-homologous recombination: *EMBO J*, v. 11, p. 5071-8.
- Kriaucionis, S., and A. Bird, 2004, The major form of MeCP2 has a novel N-terminus generated by alternative splicing: *Nucleic Acids Res*, v. 32, p. 1818-23.
- Lamonica, J. M., D. Y. Kwon, D. Goffin, P. Fenik, B. S. Johnson, Y. Cui, H. Guo, S. Veasey, and Z. Zhou, 2017, Elevating expression of MeCP2 T158M rescues DNA binding and Rett syndrome-like phenotypes: *J Clin Invest*, v. 127, p. 1889-1904.
- LaSalle, J. M., J. Goldstine, D. Balmer, and C. M. Greco, 2001, Quantitative localization of heterogeneous methyl-CpG-binding protein 2 (MeCP2) expression phenotypes in normal and Rett syndrome brain by laser scanning cytometry: *Hum Mol Genet*, v. 10, p. 1729-40.
- Leach, P. T., and J. N. Crawley, 2018, Touchscreen learning deficits in *Ube3a*, *Ts65Dn* and *Mecp2* mouse models of neurodevelopmental disorders with intellectual disabilities: *Genes Brain Behav*, v. 17, p. e12452.
- Leonard, H., and C. Bower, 1998, Is the girl with Rett syndrome normal at birth?: *Dev Med Child Neurol*, v. 40, p. 115-21.
- Leonard, H., S. Cobb, and J. Downs, 2017, Clinical and biological progress over 50 years in Rett syndrome: *Nat Rev Neurol*, v. 13, p. 37-51.
- Leone, P., D. Shera, S. W. McPhee, J. S. Francis, E. H. Kolodny, L. T. Bilaniuk, D. J. Wang, M. Assadi, O. Goldfarb, H. W. Goldman, A. Freese, D. Young, M. J. During, R. J. Samulski, and C. G. Janson, 2012, Long-term follow-up after gene therapy for canavan disease: *Sci Transl Med*, v. 4, p. 165ra163.
- Levitt, N., D. Briggs, A. Gil, and N. J. Proudfoot, 1989, Definition of an efficient synthetic poly(A) site: *Genes Dev*, v. 3, p. 1019-25.
- Lewis, B. P., C. B. Burge, and D. P. Bartel, 2005, Conserved seed pairing, often flanked by adenosines, indicates that thousands of human genes are microRNA targets: *Cell*, v. 120, p. 15-20.
- Li, M., H. Zhang, J. X. Wang, and Y. Pan, 2012, A new essential protein discovery method based on the integration of protein-protein interaction and gene expression data: *BMC Syst Biol*, v. 6, p. 15.

- Li, Q., D. H. Loh, T. Kudo, D. Truong, M. Derakhshesh, Z. M. Kaswan, C. A. Ghiani, R. Tsoa, Y. Cheng, Y. E. Sun, and C. S. Colwell, 2015, Circadian rhythm disruption in a mouse model of Rett syndrome circadian disruption in RTT: *Neurobiol Dis*, v. 77, p. 155-64.
- Li, W., A. Asokan, Z. Wu, T. Van Dyke, N. DiPrimio, J. S. Johnson, L. Govindaswamy, M. Agbandje-McKenna, S. Leichtle, D. Eugene Redmond, T. J. McCown, K. B. Petermann, N. E. Sharpless, and R. J. Samulski, 2008, Engineering and Selection of Shuffled AAV Genomes: A New Strategy for Producing Targeted Biological Nanoparticles: *Mol Ther*, v. 16, p. 1252-1260.
- Lioy, D. T., S. K. Garg, C. E. Monaghan, J. Raber, K. D. Foust, B. K. Kaspar, P. G. Hirrlinger, F. Kirchhoff, J. M. Bissonnette, N. Ballas, and G. Mandel, 2011, A role for glia in the progression of Rett's syndrome: *Nature*, v. 475, p. 497-500.
- Liu, J., and U. Francke, 2006, Identification of cis-regulatory elements for MECP2 expression: *Hum Mol Genet*, v. 15, p. 1769-82.
- Liyanage, V. R., R. M. Zachariah, and M. Rastegar, 2013, Decitabine alters the expression of Mecp2 isoforms via dynamic DNA methylation at the Mecp2 regulatory elements in neural stem cells: *Mol Autism*, v. 4, p. 46.
- Lonetti, G., A. Angelucci, L. Morando, E. M. Boggio, M. Giustetto, and T. Pizzorusso, 2010, Early environmental enrichment moderates the behavioral and synaptic phenotype of MeCP2 null mice: *Biol Psychiatry*, v. 67, p. 657-65.
- Luikenhuis, S., E. Giacometti, C. F. Beard, and R. Jaenisch, 2004, Expression of MeCP2 in postmitotic neurons rescues Rett syndrome in mice: *Proc Natl Acad Sci U S A*, v. 101, p. 6033-8.
- Lyst, M. J., and A. Bird, 2015, Rett syndrome: a complex disorder with simple roots: *Nat Rev Genet*, v. 16, p. 261-75.
- Lyst, M. J., R. Ekiert, D. H. Ebert, C. Merusi, J. Nowak, J. Selfridge, J. Guy, N. R. Kastan, N. D. Robinson, F. de Lima Alves, J. Rappsilber, M. E. Greenberg, and A. Bird, 2013, Rett syndrome mutations abolish the interaction of MeCP2 with the NCoR/SMRT co-repressor: *Nat Neurosci*, v. 16, p. 898-902.
- Manno, C. S., A. J. Chew, S. Hutchison, P. J. Larson, R. W. Herzog, V. R. Arruda, S. J. Tai, M. V. Ragni, A. Thompson, M. Ozelo, L. B. Couto, D. G. Leonard, F. A. Johnson, A. McClelland, C. Scallan, E. Skarsgard, A. W. Flake, M. A. Kay, K. A. High, and B. Glader, 2003, AAV-mediated factor IX gene transfer to skeletal muscle in patients with severe hemophilia B: *Blood*, v. 101, p. 2963-72.
- Mantis, J. G., C. L. Fritz, J. Marsh, S. C. Heinrichs, and T. N. Seyfried, 2009, Improvement in motor and exploratory behavior in Rett syndrome mice with restricted ketogenic and standard diets: *Epilepsy Behav*, v. 15, p. 133-41.
- Manuvakhova, M., K. Keeling, and D. M. Bedwell, 2000, Aminoglycoside antibiotics mediate context-dependent suppression of termination codons in a mammalian translation system: *RNA*, v. 6, p. 1044-55.
- Marcus, C. L., J. L. Carroll, S. A. McColley, G. M. Loughlin, S. Curtis, P. Pyzik, and S. Naidu, 1994, Polysomnographic characteristics of patients with Rett syndrome: *J Pediatr*, v. 125, p. 218-24.
- Maresca, M., V. G. Lin, N. Guo, and Y. Yang, 2013, Obligate ligation-gated recombination (ObLiGaRe): custom-designed nuclease-mediated targeted integration through nonhomologous end joining: *Genome Res*, v. 23, p. 539-46.
- Matagne, V., S. Budden, S. R. Ojeda, and J. Raber, 2013, Correcting deregulated Fxyd1 expression ameliorates a behavioral impairment in a mouse model of Rett syndrome: *Brain Res*, v. 1496, p. 104-14.
- Matagne, V., Y. Ehinger, L. Saidi, A. Borges-Correia, M. Barkats, M. Bartoli, L. Villard, and J. C. Roux, 2016, A codon-optimized Mecp2 transgene corrects breathing deficits and improves survival in a mouse model of Rett syndrome: *Neurobiol Dis*, v. 99, p. 1-11.
- Matagne, V., Y. Ehinger, L. Saidi, A. Borges-Correia, M. Barkats, M. Bartoli, L. Villard, and J. C. Roux, 2017, A codon-optimized Mecp2 transgene corrects breathing deficits and improves survival in a mouse model of Rett syndrome: *Neurobiol Dis*, v. 99, p. 1-11.

- McBride, J. L., M. J. During, J. Wu, E. Y. Chen, S. E. Leurgans, and J. H. Kordower, 2003, Structural and functional neuroprotection in a rat model of Huntington's disease by viral gene transfer of GDNF: *Exp Neurol*, v. 181, p. 213-23.
- McCarty, D. M., J. DiRosario, K. Gulaid, J. Muenzer, and H. Fu, 2009, Mannitol-facilitated CNS entry of rAAV2 vector significantly delayed the neurological disease progression in MPS IIIB mice: *Gene Ther*, v. 16, p. 1340-52.
- McCarty, D. M., P. E. Monahan, and R. J. Samulski, 2001, Self-complementary recombinant adeno-associated virus (scAAV) vectors promote efficient transduction independently of DNA synthesis: *Gene Ther*, v. 8, p. 1248-54.
- McCarty, M. F., J. Wey, O. Stoeltzing, W. Liu, F. Fan, C. Bucana, P. F. Mansfield, A. J. Ryan, and L. M. Ellis, 2004, ZD6474, a vascular endothelial growth factor receptor tyrosine kinase inhibitor with additional activity against epidermal growth factor receptor tyrosine kinase, inhibits orthotopic growth and angiogenesis of gastric cancer: *Mol Cancer Ther*, v. 3, p. 1041-8.
- McGill, B. E., S. F. Bundle, M. B. Yaylaoglu, J. P. Carson, C. Thaller, and H. Y. Zoghbi, 2006, Enhanced anxiety and stress-induced corticosterone release are associated with increased Crh expression in a mouse model of Rett syndrome: *Proc Natl Acad Sci U S A*, v. 103, p. 18267-72.
- McGraw, C. M., R. C. Samaco, and H. Y. Zoghbi, 2011, Adult neural function requires MeCP2: *Science*, v. 333, p. 186.
- McIntyre, C., A. L. Derrick Roberts, E. Ranieri, P. R. Clements, S. Byers, and D. S. Anson, 2008, Lentiviral-mediated gene therapy for murine mucopolysaccharidosis type IIIA: *Mol Genet Metab*, v. 93, p. 411-8.
- Meins, M., J. Lehmann, F. Gerresheim, J. Herchenbach, M. Hagedorn, K. Hameister, and J. T. Epplen, 2005, Submicroscopic duplication in Xq28 causes increased expression of the MECP2 gene in a boy with severe mental retardation and features of Rett syndrome: *J Med Genet*, v. 42, p. e12.
- Miao, C. H., K. Ohashi, G. A. Patijn, L. Meuse, X. Ye, A. R. Thompson, and M. A. Kay, 2000, Inclusion of the hepatic locus control region, an intron, and untranslated region increases and stabilizes hepatic factor IX gene expression in vivo but not in vitro: *Mol Ther*, v. 1, p. 522-32.
- Mnatzakanian, G. N., H. Lohi, I. Munteanu, S. E. Alfred, T. Yamada, P. J. MacLeod, J. R. Jones, S. W. Scherer, N. C. Schanen, M. J. Friez, J. B. Vincent, and B. A. Minassian, 2004, A previously unidentified MECP2 open reading frame defines a new protein isoform relevant to Rett syndrome: *Nat Genet*, v. 36, p. 339-41.
- Mohandas, T., R. S. Sparkes, and L. J. Shapiro, 1981, Reactivation of an inactive human X chromosome: evidence for X inactivation by DNA methylation: *Science*, v. 211, p. 393-6.
- Moretti, P., J. A. Bouwknecht, R. Teague, R. Paylor, and H. Y. Zoghbi, 2005, Abnormalities of social interactions and home-cage behavior in a mouse model of Rett syndrome: *Hum Mol Genet*, v. 14, p. 205-20.
- Moretti, P., J. M. Levenson, F. Battaglia, R. Atkinson, R. Teague, B. Antalffy, D. Armstrong, O. Arancio, J. D. Sweatt, and H. Y. Zoghbi, 2006, Learning and memory and synaptic plasticity are impaired in a mouse model of Rett syndrome: *J Neurosci*, v. 26, p. 319-27.
- Moss, R. B., D. Rodman, L. T. Spencer, M. L. Aitken, P. L. Zeitlin, D. Waltz, C. Milla, A. S. Brody, J. P. Clancy, B. Ramsey, N. Hamblett, and A. E. Heald, 2004, Repeated adeno-associated virus serotype 2 aerosol-mediated cystic fibrosis transmembrane regulator gene transfer to the lungs of patients with cystic fibrosis: a multicenter, double-blind, placebo-controlled trial: *Chest*, v. 125, p. 509-21.
- Moy, S. S., J. J. Nadler, N. B. Young, A. Perez, L. P. Holloway, R. P. Barbaro, J. R. Barbaro, L. M. Wilson, D. W. Threadgill, J. M. Lauder, T. R. Magnuson, and J. N. Crawley, 2007, Mouse behavioral tasks relevant to autism: phenotypes of 10 inbred strains: *Behav Brain Res*, v. 176, p. 4-20.

- Nadler, J. J., S. S. Moy, G. Dold, D. Trang, N. Simmons, A. Perez, N. B. Young, R. P. Barbaro, J. Piven, T. R. Magnuson, and J. N. Crawley, 2004, Automated apparatus for quantitation of social approach behaviors in mice: *Genes Brain Behav*, v. 3, p. 303-14.
- Nakai, J., M. Ohkura, and K. Imoto, 2001, A high signal-to-noise Ca²⁺ probe composed of a single green fluorescent protein: *Nat Biotechnol*, v. 19, p. 137-41.
- Nan, X., F. J. Campoy, and A. Bird, 1997, MeCP2 is a transcriptional repressor with abundant binding sites in genomic chromatin: *Cell*, v. 88, p. 471-81.
- Nan, X., H. H. Ng, C. A. Johnson, C. D. Laherty, B. M. Turner, R. N. Eisenman, and A. Bird, 1998, Transcriptional repression by the methyl-CpG-binding protein MeCP2 involves a histone deacetylase complex: *Nature*, v. 393, p. 386-9.
- Nan, X., P. Tate, E. Li, and A. Bird, 1996, DNA methylation specifies chromosomal localization of MeCP2: *Mol Cell Biol*, v. 16, p. 414-21.
- Neul, J. L., P. Fang, J. Barrish, J. Lane, E. B. Caeg, E. O. Smith, H. Zoghbi, A. Percy, and D. G. Glaze, 2008, Specific mutations in methyl-CpG-binding protein 2 confer different severity in Rett syndrome: *Neurology*, v. 70, p. 1313-21.
- Neul, J. L., W. E. Kaufmann, D. G. Glaze, J. Christodoulou, A. J. Clarke, N. Bahi-Buisson, H. Leonard, M. E. Bailey, N. C. Schanen, M. Zappella, A. Renieri, P. Huppke, A. K. Percy, and R. Consortium, 2010, Rett syndrome: revised diagnostic criteria and nomenclature: *Ann Neurol*, v. 68, p. 944-50.
- Neul, J. L., and H. Y. Zoghbi, 2004, Rett syndrome: a prototypical neurodevelopmental disorder: *Neuroscientist*, v. 10, p. 118-28.
- Newnham, C. M., T. Hall-Pogar, S. Liang, J. Wu, B. Tian, J. Hu, and C. S. Lutz, 2010, Alternative polyadenylation of MeCP2: Influence of cis-acting elements and trans-acting factors: *RNA Biol*, v. 7, p. 361-72.
- Nichols, J. N., K. L. Hagan, and C. L. Floyd, 2017, Evaluation of Touchscreen Chambers To Assess Cognition in Adult Mice: Effect of Training and Mild Traumatic Brain Injury: *J Neurotrauma*, v. 34, p. 2481-2494.
- Nightingale, S. J., R. P. Hollis, K. A. Pepper, D. Petersen, X. J. Yu, C. Yang, I. Bahner, and D. B. Kohn, 2006, Transient gene expression by nonintegrating lentiviral vectors: *Mol Ther*, v. 13, p. 1121-32.
- Nikitina, T., R. P. Ghosh, R. A. Horowitz-Scherer, J. C. Hansen, S. A. Grigoryev, and C. L. Woodcock, 2007, MeCP2-chromatin interactions include the formation of chromatosome-like structures and are altered in mutations causing Rett syndrome: *J Biol Chem*, v. 282, p. 28237-45.
- Ogier, M., H. Wang, E. Hong, Q. Wang, M. E. Greenberg, and D. M. Katz, 2007, Brain-derived neurotrophic factor expression and respiratory function improve after ampakine treatment in a mouse model of Rett syndrome: *J Neurosci*, v. 27, p. 10912-7.
- Orefice, L. L., A. L. Zimmerman, A. M. Chirila, S. J. Sleboda, J. P. Head, and D. D. Ginty, 2016, Peripheral Mechanosensory Neuron Dysfunction Underlies Tactile and Behavioral Deficits in Mouse Models of ASDs: *Cell*, v. 166, p. 299-313.
- Owens, G. C., S. Mistry, G. M. Edelman, and K. L. Crossin, 2002, Efficient marking of neural stem cell-derived neurons with a modified murine embryonic stem cell virus, MESV2: *Gene Ther*, v. 9, p. 1044-8.
- Pelka, G. J., C. M. Watson, T. Radziewicz, M. Hayward, H. Lahooti, J. Christodoulou, and P. P. Tam, 2006, *Mecp2* deficiency is associated with learning and cognitive deficits and altered gene activity in the hippocampal region of mice: *Brain*, v. 129, p. 887-98.
- Pereira, D. J., and N. Muzyczka, 1997, The cellular transcription factor SP1 and an unknown cellular protein are required to mediate Rep protein activation of the adeno-associated virus p19 promoter: *J Virol*, v. 71, p. 1747-56.
- Piato, A. L., B. C. Detanico, J. F. Jesus, F. L. Lhullier, D. S. Nunes, and E. Elisabetsky, 2008, Effects of Marapuama in the chronic mild stress model: further indication of antidepressant properties: *J Ethnopharmacol*, v. 118, p. 300-4.
- Pitcher, M. R., J. A. Herrera, S. A. Buffington, M. Y. Kochukov, J. K. Merritt, A. R. Fisher, N. C. Schanen, M. Costa-Mattioli, and J. L. Neul, 2015, Rett syndrome like phenotypes in the

- R255X Mecp2 mutant mouse are rescued by MECP2 transgene: *Hum Mol Genet*, v. 24, p. 2662-72.
- Pulicherla, N., S. Shen, S. Yadav, K. Debbink, L. Govindasamy, M. Agbandje-McKenna, and A. Asokan, 2011, Engineering liver-detargeted AAV9 vectors for cardiac and musculoskeletal gene transfer: *Mol Ther*, v. 19, p. 1070-8.
- Ramirez, J. M., C. S. Ward, and J. L. Neul, 2013, Breathing challenges in Rett syndrome: lessons learned from humans and animal models: *Respir Physiol Neurobiol*, v. 189, p. 280-7.
- Rastegar, M., A. Hotta, P. Pasceri, M. Makarem, A. Y. Cheung, S. Elliott, K. J. Park, M. Adachi, F. S. Jones, I. D. Clarke, P. Dirks, and J. Ellis, 2009, MECP2 isoform-specific vectors with regulated expression for Rett syndrome gene therapy: *PLoS One*, v. 4, p. e6810.
- Rehmsmeier, M., P. Steffen, M. Hochsmann, and R. Giegerich, 2004, Fast and effective prediction of microRNA/target duplexes: *RNA*, v. 10, p. 1507-17.
- Ren, C., S. Kumar, D. R. Shaw, and S. Ponnazhagan, 2005, Genomic stability of self-complementary adeno-associated virus 2 during early stages of transduction in mouse muscle in vivo: *Hum Gene Ther*, v. 16, p. 1047-57.
- Rett, A., 1966, [On a unusual brain atrophy syndrome in hyperammonemia in childhood]: *Wien Med Wochenschr*, v. 116, p. 723-6.
- Robinson, L., J. Guy, L. McKay, E. Brockett, R. C. Spike, J. Selfridge, D. De Sousa, C. Merusi, G. Riedel, A. Bird, and S. R. Cobb, 2012, Morphological and functional reversal of phenotypes in a mouse model of Rett syndrome: *Brain*, v. 135, p. 2699-710.
- Ross, P. D., J. Guy, J. Selfridge, B. Kamal, N. Bahey, K. E. Tanner, T. H. Gillingwater, R. A. Jones, C. M. Loughrey, C. S. McCarroll, M. E. Bailey, A. Bird, and S. Cobb, 2016, Exclusive expression of MeCP2 in the nervous system distinguishes between brain and peripheral Rett syndrome-like phenotypes: *Hum Mol Genet*.
- Sakai, K., H. Shoji, T. Kohno, T. Miyakawa, and M. Hattori, 2016, Mice that lack the C-terminal region of Reelin exhibit behavioral abnormalities related to neuropsychiatric disorders: *Sci Rep*, v. 6, p. 28636.
- Samaco, R. C., C. Mandel-Brehm, H. T. Chao, C. S. Ward, S. L. Fyffe-Maricich, J. Ren, K. Hyland, C. Thaller, S. M. Maricich, P. Humphreys, J. J. Greer, A. Percy, D. G. Glaze, H. Y. Zoghbi, and J. L. Neul, 2009, Loss of MeCP2 in aminergic neurons causes cell-autonomous defects in neurotransmitter synthesis and specific behavioral abnormalities: *Proc Natl Acad Sci U S A*, v. 106, p. 21966-71.
- Samaco, R. C., C. Mandel-Brehm, C. M. McGraw, C. A. Shaw, B. E. McGill, and H. Y. Zoghbi, 2012, Crh and Oprm1 mediate anxiety-related behavior and social approach in a mouse model of MECP2 duplication syndrome: *Nat Genet*, v. 44, p. 206-11.
- Samaco, R. C., C. M. McGraw, C. S. Ward, Y. Sun, J. L. Neul, and H. Y. Zoghbi, 2013, Female Mecp2(+/-) mice display robust behavioral deficits on two different genetic backgrounds providing a framework for pre-clinical studies: *Hum Mol Genet*, v. 22, p. 96-109.
- Samulski, R. J., K. I. Berns, M. Tan, and N. Muzyczka, 1982, Cloning of adeno-associated virus into pBR322: rescue of intact virus from the recombinant plasmid in human cells: *Proc Natl Acad Sci U S A*, v. 79, p. 2077-81.
- Samulski, R. J., and N. Muzyczka, 2014, AAV-Mediated Gene Therapy for Research and Therapeutic Purposes: *Annu Rev Virol*, v. 1, p. 427-51.
- Saunders, N. R., C. Joakim Ek, and K. M. Dziegielewska, 2009, The neonatal blood-brain barrier is functionally effective, and immaturity does not explain differential targeting of AAV9: *Nat Biotechnol*, v. 27, p. 804-5; author reply 805.
- Schaevitz, L. R., N. B. Gómez, D. P. Zhen, and J. E. Berger-Sweeney, 2013, MeCP2 R168X male and female mutant mice exhibit Rett-like behavioral deficits: *Genes Brain Behav*, v. 12, p. 732-40.
- Schaevitz, L. R., J. M. Moriuchi, N. Nag, T. J. Mellot, and J. Berger-Sweeney, 2010, Cognitive and social functions and growth factors in a mouse model of Rett syndrome: *Physiol Behav*, v. 100, p. 255-63.

- Scherr, M., K. Battmer, U. Blömer, A. Ganser, and M. Grez, 2001, Quantitative determination of lentiviral vector particle numbers by real-time PCR: *Biotechniques*, v. 31, p. 520, 522, 524, passim.
- Schnepp, B. C., R. L. Jensen, C. L. Chen, P. R. Johnson, and K. R. Clark, 2005, Characterization of adeno-associated virus genomes isolated from human tissues: *J Virol*, v. 79, p. 14793-803.
- Sferra, T. J., K. Backstrom, C. Wang, R. Rennard, M. Miller, and Y. Hu, 2004, Widespread correction of lysosomal storage following intrahepatic injection of a recombinant adeno-associated virus in the adult MPS VII mouse: *Mol Ther*, v. 10, p. 478-91.
- Shahbazian, M., J. Young, L. Yuva-Paylor, C. Spencer, B. Antalffy, J. Noebels, D. Armstrong, R. Paylor, and H. Zoghbi, 2002, Mice with truncated MeCP2 recapitulate many Rett syndrome features and display hyperacetylation of histone H3: *Neuron*, v. 35, p. 243-54.
- Shiotsuki, H., K. Yoshimi, Y. Shimo, M. Funayama, Y. Takamatsu, K. Ikeda, R. Takahashi, S. Kitazawa, and N. Hattori, 2010, A rotarod test for evaluation of motor skill learning: *J Neurosci Methods*, v. 189, p. 180-5.
- Sinnett, S. E., and S. J. Gray, 2017, Recent endeavors in MECP2 gene transfer for gene therapy of Rett syndrome: *Discov Med*, v. 24, p. 153-159.
- Sinnett, S. E., R. D. Hector, K. K. E. Gadalla, C. Heindel, D. Chen, V. Zaric, M. E. S. Bailey, S. R. Cobb, and S. J. Gray, 2017, Improved: *Mol Ther Methods Clin Dev*, v. 5, p. 106-115.
- Skene, P. J., R. S. Illingworth, S. Webb, A. R. Kerr, K. D. James, D. J. Turner, R. Andrews, and A. P. Bird, 2010, Neuronal MeCP2 is expressed at near histone-octamer levels and globally alters the chromatin state: *Mol Cell*, v. 37, p. 457-68.
- Srivastava, A., E. W. Lusby, and K. I. Berns, 1983, Nucleotide sequence and organization of the adeno-associated virus 2 genome: *J Virol*, v. 45, p. 555-64.
- Stearns, N. A., L. R. Schaevitz, H. Bowling, N. Nag, U. V. Berger, and J. Berger-Sweeney, 2007, Behavioral and anatomical abnormalities in *Mecp2* mutant mice: a model for Rett syndrome: *Neuroscience*, v. 146, p. 907-21.
- Stieger, K., J. Schroeder, N. Provost, A. Mendes-Madeira, B. Belbellaa, G. L. Meur, M. Weber, J. Y. Deschamps, B. Lorenz, P. Moullier, and F. Rolling, 2009, Detection of Intact rAAV Particles up to 6 Years After Successful Gene Transfer in the Retina of Dogs and Primates: *Mol Ther*, v. 17, p. 516-523.
- Sztainberg, Y., H. M. Chen, J. W. Swann, S. Hao, B. Tang, Z. Wu, J. Tang, Y. W. Wan, Z. Liu, F. Rigo, and H. Y. Zoghbi, 2015, Reversal of phenotypes in MECP2 duplication mice using genetic rescue or antisense oligonucleotides: *Nature*, v. 528, p. 123-6.
- Tillotson, R., J. Selfridge, M. V. Koerner, K. K. E. Gadalla, J. Guy, D. De Sousa, R. D. Hector, S. R. Cobb, and A. Bird, 2017, Radically truncated MeCP2 rescues Rett syndrome-like neurological defects: *Nature*, v. 550, p. 398-401.
- Tiyaboonchai, A., H. Mac, R. Shamsedeen, J. A. Mills, S. Kishore, D. L. French, and P. Gadue, 2014, Utilization of the AAVS1 safe harbor locus for hematopoietic specific transgene expression and gene knockdown in human ES cells: *Stem Cell Res*, v. 12, p. 630-7.
- Tornøe, J., P. Kusk, T. E. Johansen, and P. R. Jensen, 2002, Generation of a synthetic mammalian promoter library by modification of sequences spacing transcription factor binding sites: *Gene*, v. 297, p. 21-32.
- Valori, C. F., K. Ning, M. Wyles, R. J. Mead, A. J. Grierson, P. J. Shaw, and M. Azzouz, 2010, Systemic delivery of scAAV9 expressing SMN prolongs survival in a model of spinal muscular atrophy: *Sci Transl Med*, v. 2, p. 35ra42.
- Viemari, J. C., J. C. Roux, A. K. Tryba, V. Saywell, H. Burnet, F. Peña, S. Zanella, M. Bévangut, M. Barthelemy-Requin, L. B. Herzing, A. Moncla, J. Mancini, J. M. Ramirez, L. Villard, and G. Hilaire, 2005, *Mecp2* deficiency disrupts norepinephrine and respiratory systems in mice: *J Neurosci*, v. 25, p. 11521-30.
- Vigli, D., L. Cosentino, C. Raggi, G. Laviola, M. Woolley-Roberts, and B. De Filippis, 2018, Chronic treatment with the phytocannabinoid Cannabidivarin (CBDV) rescues behavioural alterations and brain atrophy in a mouse model of Rett syndrome: *Neuropharmacology*, v. 140, p. 121-129.

- Vogel Ciernia, A., M. C. Pride, B. Durbin-Johnson, A. Noronha, A. Chang, D. H. Yasui, J. N. Crawley, and J. M. LaSalle, 2017, Early motor phenotype detection in a female mouse model of Rett syndrome is improved by cross-fostering: *Hum Mol Genet*, v. 26, p. 1839-1854.
- Vogel-Ciernia, A., D. P. Matheos, R. M. Barrett, E. A. Kramár, S. Azzawi, Y. Chen, C. N. Magnan, M. Zeller, A. Sylvain, J. Haettig, Y. Jia, A. Tran, R. Dang, R. J. Post, M. Chabrier, A. H. Babayan, J. I. Wu, G. R. Crabtree, P. Baldi, T. Z. Baram, G. Lynch, and M. A. Wood, 2013, The neuron-specific chromatin regulatory subunit BAF53b is necessary for synaptic plasticity and memory: *Nat Neurosci*, v. 16, p. 552-61.
- Vogel-Ciernia, A., and M. A. Wood, 2014, Examining object location and object recognition memory in mice: *Curr Protoc Neurosci*, v. 69, p. 8.31.1-17.
- Voituron, N., and G. Hilaire, 2011, The benzodiazepine Midazolam mitigates the breathing defects of Mecp2-deficient mice: *Respir Physiol Neurobiol*, v. 177, p. 56-60.
- Voituron, N., S. Zanella, C. Menuet, A. M. Lajard, M. Dutschmann, and G. Hilaire, 2010, Early abnormalities of post-sigh breathing in a mouse model of Rett syndrome: *Respir Physiol Neurobiol*, v. 170, p. 173-82.
- Vorozheykin, P. S., and I. I. Titov, 2015, [Web server for prediction of miRNAs and their precursors and binding sites]: *Mol Biol (Mosk)*, v. 49, p. 846-53.
- Wagner, J. A., T. Reynolds, M. L. Moran, R. B. Moss, J. J. Wine, T. R. Flotte, and P. Gardner, 1998, Efficient and persistent gene transfer of AAV-CFTR in maxillary sinus: *Lancet*, v. 351, p. 1702-3.
- Wang, Q., G. M. Garrity, J. M. Tiedje, and J. R. Cole, 2007, Naive Bayesian classifier for rapid assignment of rRNA sequences into the new bacterial taxonomy: *Appl Environ Microbiol*, v. 73, p. 5261-7.
- Warrington, K. H., and R. W. Herzog, 2006, Treatment of human disease by adeno-associated viral gene transfer: *Hum Genet*, v. 119, p. 571-603.
- Weese-Mayer, D. E., S. P. Lieske, C. M. Boothby, A. S. Kenny, H. L. Bennett, and J. M. Ramirez, 2008, Autonomic dysregulation in young girls with Rett Syndrome during nighttime in-home recordings: *Pediatr Pulmonol*, v. 43, p. 1045-1060.
- Weese-Mayer, D. E., S. P. Lieske, C. M. Boothby, A. S. Kenny, H. L. Bennett, J. M. Silvestri, and J. M. Ramirez, 2006, Autonomic nervous system dysregulation: breathing and heart rate perturbation during wakefulness in young girls with Rett syndrome: *Pediatr Res*, v. 60, p. 443-9.
- Welch, E. M., E. R. Barton, J. Zhuo, Y. Tomizawa, W. J. Friesen, P. Trifillis, S. Paushkin, M. Patel, C. R. Trotta, S. Hwang, R. G. Wilde, G. Karp, J. Takasugi, G. Chen, S. Jones, H. Ren, Y. C. Moon, D. Corson, A. A. Turpoff, J. A. Campbell, M. M. Conn, A. Khan, N. G. Almstead, J. Hedrick, A. Mollin, N. Risher, M. Weetall, S. Yeh, A. A. Branstrom, J. M. Colacino, J. Babiak, W. D. Ju, S. Hirawat, V. J. Northcutt, L. L. Miller, P. Spatrick, F. He, M. Kawana, H. Feng, A. Jacobson, S. W. Peltz, and H. L. Sweeney, 2007, PTC124 targets genetic disorders caused by nonsense mutations: *Nature*, v. 447, p. 87-91.
- Weng, S. M., F. McLeod, M. E. Bailey, and S. R. Cobb, 2011, Synaptic plasticity deficits in an experimental model of rett syndrome: long-term potentiation saturation and its pharmacological reversal: *Neuroscience*, v. 180, p. 314-21.
- Xu, K., G. Zhong, and X. Zhuang, 2013, Actin, spectrin, and associated proteins form a periodic cytoskeletal structure in axons: *Science*, v. 339, p. 452-6.
- Yalcin, I., F. Aksu, and C. Belzung, 2005, Effects of desipramine and tramadol in a chronic mild stress model in mice are altered by yohimbine but not by pindolol: *Eur J Pharmacol*, v. 514, p. 165-74.
- Yalcin, I., F. Aksu, S. Bodard, S. Chalon, and C. Belzung, 2007, Antidepressant-like effect of tramadol in the unpredictable chronic mild stress procedure: possible involvement of the noradrenergic system: *Behav Pharmacol*, v. 18, p. 623-31.
- Yang, B., S. Li, H. Wang, Y. Guo, D. J. Gessler, C. Cao, Q. Su, J. Kramer, L. Zhong, S. S. Ahmed, H. Zhang, R. He, R. C. Desrosiers, R. Brown, Z. Xu, and G. Gao, 2014, Global CNS transduction of adult mice by intravenously delivered rAAVrh.8 and rAAVrh.10 and nonhuman primates by rAAVrh.10: *Mol Ther*, v. 22, p. 1299-309.

- Yang, M., O. Bozdagi, M. L. Scattoni, M. Wöhr, F. I. Roulet, A. M. Katz, D. N. Abrams, D. Kalikhman, H. Simon, L. Woldeyohannes, J. Y. Zhang, M. J. Harris, R. Saxena, J. L. Silverman, J. D. Buxbaum, and J. N. Crawley, 2012, Reduced excitatory neurotransmission and mild autism-relevant phenotypes in adolescent Shank3 null mutant mice: *J Neurosci*, v. 32, p. 6525-41.
- Yang, M., J. L. Silverman, and J. N. Crawley, 2011, Automated three-chambered social approach task for mice: *Curr Protoc Neurosci*, v. Chapter 8, p. Unit 8.26.
- Yang, S.-S., C.-L. Huang, H.-E. Chen, C.-S. Tung, H.-P. Shih, and Y.-P. Liu, 2015, Effects of SPAK knockout on sensorimotor gating, novelty exploration, and brain area-dependent expressions of NKCC1 and KCC2 in a mouse model of schizophrenia: *Progress in Neuro-Psychopharmacology and Biological Psychiatry*, v. 61, p. 30-36.
- Young, J. I., E. P. Hong, J. C. Castle, J. Crespo-Barreto, A. B. Bowman, M. F. Rose, D. Kang, R. Richman, J. M. Johnson, S. Berget, and H. Y. Zoghbi, 2005, Regulation of RNA splicing by the methylation-dependent transcriptional repressor methyl-CpG binding protein 2: *Proc Natl Acad Sci U S A*, v. 102, p. 17551-8.
- Yusufzai, T. M., and A. P. Wolffe, 2000, Functional consequences of Rett syndrome mutations on human MeCP2: *Nucleic Acids Res*, v. 28, p. 4172-9.
- Zeleznikow-Johnston, A. M., T. Renoir, L. Churilov, S. Li, E. L. Burrows, and A. J. Hannan, 2018, Touchscreen testing reveals clinically relevant cognitive abnormalities in a mouse model of schizophrenia lacking metabotropic glutamate receptor 5: *Sci Rep*, v. 8, p. 16412.
- Zhang, H., B. Yang, X. Mu, S. S. Ahmed, Q. Su, R. He, H. Wang, C. Mueller, M. Sena-Esteves, R. Brown, Z. Xu, and G. Gao, 2011, Several rAAV vectors efficiently cross the blood-brain barrier and transduce neurons and astrocytes in the neonatal mouse central nervous system: *Mol Ther*, v. 19, p. 1440-8.
- Zhong, W., C. M. Johnson, Y. Wu, N. Cui, H. Xing, S. Zhang, and C. Jiang, 2016, Effects of early-life exposure to THIP on phenotype development in a mouse model of Rett syndrome: *J Neurodev Disord*, v. 8, p. 37.
- Zhou, H., W. Wu, Y. Zhang, H. He, Z. Yuan, Z. Zhu, and Z. Zhao, 2017, Selective preservation of cholinergic MeCP2 rescues specific Rett-syndrome-like phenotypes in MeCP2: *Behav Brain Res*, v. 322, p. 51-59.
- Zincarelli, C., S. Soltys, G. Rengo, and J. E. Rabinowitz, 2008, Analysis of AAV serotypes 1-9 mediated gene expression and tropism in mice after systemic injection: *Mol Ther*, v. 16, p. 1073-80.